# A New Optimisation Procedure for Uncertainty Reduction by Intelligent Wells during Field Development Planning

**Ivan Mikhailovich Grebenkin**

*A thesis submitted for the Degree of Doctor of Philosophy*
*Institute of Petroleum Engineering*
*Heriot-Watt University*
*Edinburgh, Scotland, UK*

**October, 2013**

# Abstract

The uncertainty in the produced oil volume can be minimised by substituting intelligent wells (IWs) for conventional wells. A previous study showed that IWs reduce the impact of geological uncertainty on the production forecast (Birchenko, Demyanov et al. 2008). This investigation has now been extended to the "dynamic" parameters (fluid contacts, relative permeabilities, aquifer strength and zonal skin). The efficiency of the IWs in reducing the total production uncertainty due to the reservoir's dynamic parameters was found to be comparable to that reported for the static parameters.

However, this later study identified that the result was strongly dependent on the strategy employed to optimise the field's performance. Experience has shown that challenges arise while using commercial software for optimisation of a typical, modern field with multiple reservoirs and a complex surface production network. Inclusion of the optimisation algorithm dramatically increases the calculation time in addition to showing stability and convergence problems.

This thesis describes the development of a novel method of a reactive control strategy for ICVs that is both robust and computationally fast. The developed method identifies the critical water cut threshold at which a well will operate optimally when on/off valves are used. This method is not affected by the convergence problems which have lead to many of the difficulties associated with previous efforts to solve our non-linear optimisation problem. Run times similar to the (non-optimised) base case are now potentially possible and, equally importantly, the optimal value calculated is similar to the result from the various optimisation software referred to above.

The approach is particularly valuable when analysing the impact of uncertainty on the reservoir's dynamic and static parameters, the method being convergent and independent of the point used to initiate the optimization process. "Tuning" the algorithm's optimisation parameters in the middle of the calculation is no longer required; thus ensuring the results from the many realisations are comparable.

## Acknowledgment

I would like to express my sincere appreciation to all those who supported and helped me during my study.

I owe a special gratitude to my supervisor Prof. David Davies who provided a great support and invaluable help during this long period of my PhD study.

My sincere gratitude to my colleagues: Dr. Khafiz Muradov, Yousef Rafiei, Dr. Vasily Birchenko, Morteza Haghighat and other members of IWFsT JIP project for their moral support and invaluable discussions.

I also thank Dr. Vasily Demyanov for the valuable advice and support in the reservoir uncertainty study.

Furthermore I would also like to acknowledge with much appreciation the crucial role of the IPE staff.

I would like to thank all sponsors of IWFsT JIP project for the financial support and data provided for my study, as well as valuable discussions and suggestions during JIP meetings.

My special thanks to Ross Waterhouse and Jeremy Rhodes from Nexen for the data, help and useful discussions during the N-Field project.

My great gratitude to PETEX for their excellent software, especially open server option, which helped me to accomplish most of my algorithms. I also wish to thank Steve Todman for the help with the software and valuable recommendations.

In addition I gratefully acknowledge Dr. Alexander Kuznetsov from Weatherford for his great support in optimisation methods.

Schlumberger Information Systems are gratefully acknowledged for their generous provision of software.

I wish to thank the examiners Prof. Matthew Jackson and Prof. Eric Mackay for spending their valuable time in reading this thesis and for examination.

My final and deepest gratitude to my parents who have played a major role in my success, and my siblings- brother Alexander and sister Julia for their moral support.

ACADEMIC REGISTRY
**Research Thesis Submission**

| | | | |
|---|---|---|---|
| Name*:* | IVAN MIKHAILOVICH GREBENKIN | | |
| School/PGI: | INSTITUTE OF PETROLEUM ENGINEERING | | |
| Version: *(i.e. First, Resubmission, Final)* | Final | Degree Sought (Award **and** Subject area) | PhD IN PETROLEUM ENGINEERING |

## Declaration

In accordance with the appropriate regulations I hereby submit my thesis and I declare that:

1) the thesis embodies the results of my own work and has been composed by myself
2) where appropriate, I have made acknowledgement of the work of others and have made reference to work carried out in collaboration with other persons
3) the thesis is the correct version of the thesis for submission and is the same version as any electronic versions submitted*.
4) my thesis for the award referred to, deposited in the Heriot-Watt University Library, should be made available for loan or photocopying and be available via the Institutional Repository, subject to such conditions as the Librarian may require
5) I understand that as a student of the University I am required to abide by the Regulations of the University and to conform to its discipline.

* *Please note that it is the responsibility of the candidate to ensure that the correct version of the thesis is submitted.*

| | | | |
|---|---|---|---|
| Signature of Candidate*:* | | Date: | |

## Submission

| | |
|---|---|
| Submitted By *(name in capitals):* | IVAN GREBENKIN |
| Signature of Individual Submitting: | |
| Date Submitted: | |

## For Completion in the Student Service Centre (SSC)

| | |
|---|---|
| Received in the SSC by *(name in capitals):* | |

# Table of Contents

## List of Figures

## List of Tables

## Glossary

$\cup$ - union of sets

$\epsilon$ - contained in

| | - absolute value

|| || - Euclidean norm

$\nabla$ - gradient

■ – end of proof

” – inch

$ -US dollar

$\rho$ – density

API - American Petroleum Institute units of density

AQUIPerm – aquifer permeability

AQUIPoro – aquifer porosity

arg – argument

bbl – barrels

$B_g$ – gas formation volume factor

BHP – Bottom Hole Pressure

$B_o$ – oil formation volume factor

$B_w$ – water formation volume factor

CAPEX –capital cost

CCD - Central Composite Design

CF - Cash Flow

CH – Choke

CW - Conventional Well

CWC - Critical Water Cut

DC - Direct Check

deg C – Celsius degree

DS - Direct Search

DTS - Distributed Temperature Sensing system

EnKF - Ensemble Kalman Filter

EnOpt - Ensemble Optimisation

ESP - Electric Submersible Pump

FOIP – Field Oil in Place

FT – Failure Time

GA - Genetic Algorithms

GOC – gas-oil contact

GOR – gas oil ratio

hh:mm:ss – hours:minutes:seconds

ICD - Inflow Control Device

ICV - Interval Control Valves

IPM - Integrated Production Modelling

IW – intelligent well

J – productivity index

km –kilometre

LHCD - Latin Hypercube Design

m –metre

$m^3$- cubic metre

max – maximum

MD – measured depth

mD – milidarcy

min – minimum

MM – million

MPC - Model Predictive Control

NPV – Net Present Value

OF – Objective Function

OPEX –operational cost

OWC – oil-water contact

PE – Petroleum Engineering

PI – Productivity Index

Pres – reservoir pressure

PVT - Pressure-Volume-Temperature

$Q_{liq}$ – liquid production rate

$Q_{oil}$ – oil production rate

RC -Reduction Coefficient

ROV - Real Option Valuation

$R_s$ – dissolved gas oil ratio

RS - Response Surface

RSM - Response Surface Methodology

SA- Steepest Ascent

SC - Smoothness Coefficient

Scf – standard cubic feet

sec – second

Sep – Separator

SFCCD - Small Face Centred Composite Design

SLP - Sequential Linear Programming

SPSA - Simultaneous Perturbation Stochastic Approximation

SQP - Sequential Quadratic Programming

Stb – stock tank barrel

THP – Tubing Head Pressure

TVD – True Vertical Depth

VBA - Visual Basic for Applications

WC, WCT – Water Cut

$\Delta P$ – pressure drop

# Chapter 1 – Introduction

Intelligent wells have become a popular well completion option. Such wells are equipped with various kinds of sensors that allow a better understanding of the zonal reservoir properties and help to reduce uncertainty. Passive Inflow Control Devices (ICDs) allow equalization of the production from different zones, reduce the horizontal well's "heel-toe" effect and, as a result, increase the sweep efficiency (Birchenko, Bejan et al. 2011). By contrast, "active" devices – Interval Control Valves (ICVs) - are controlled from the surface in order to reduce undesired fluid production, improve the recovery factor, avoid costly well interventions and reduce production uncertainty (Grebenkin and Davies 2010). However, many oil companies today still do not feel confident in investing in the latter, more expensive, technology. For example, verbal reports at industry gatherings have indicated that, even when this technology has been installed in the wells, it is not always being fully utilised because field operators do not have an "easy to use" tool that allows them to determine when, and how much, the setting of a particular ICV should be changed.

A further difficulty is that the benefit of Intelligent Well (IW) technology is still not always clear at the field development design stage. Partly this is because the standard simulation tools and workflows used by reservoir engineers only identify some of the IW benefits. They do not have an "easy-to-use" tool that allows them to consider the full range of possible uncertainties present in the field. Further, the standard reservoir development strategy is to place the wells in their optimal location within a chosen reservoir model. This reduces the potential benefit of IWs in that model, making them less, or even, un-profitable. However, the real reservoir will always differ from this chosen model since high levels of uncertainty always exists in the reservoir properties. This is especially true during the initial field development stages when there is insufficient information to identify the full range of uncertainties in the reservoir data. In practice these difficulties result in wells being drilled in non-optimum locations, followed by water or gas unexpectedly coning into the well. Such problems can be solved employing the capabilities of IWs, if they have been installed. By contrast, the production performance of a lower cost conventional well (CW) option would have been disappointing with the actual production possibly being far below the expected value.

One of the benefits of IWs is reduced reservoir and production uncertainty through a better understanding of a well and field performance.

Data produced by the multiple sensors which are installed as standard in smart wells makes it possible to identify any mismatch of reservoir properties with the current reservoir model. The inherent flexibility and the extra level of control provided by ICVs, when compared to conventional wells, allows a higher level of management of the field development delivering a reduced level of production uncertainty. Thus, Birchenko et all (Birchenko, Demyanov et al. 2008) showed that an intelligent well completed with ICVs can reduce the production uncertainty by 50%. Addiego-Guevara and others (Addiego-Guevara, Jackson et al. 2008) also found that even a simple reactive control strategy may significantly reduce the risk and provide insurance against reservoir uncertainty.

One of the approaches to quantify this benefit is the Real Option Valuation Theory (ROV) (Dezen and Morooka 2001; Faiz 2001; Dezen and Morooka 2002; Han, Rajagopalan et al. 2002; Sharma, Chorn et al. 2002; Han 2003; Lima, Suslick et al. 2007). The advantage of this method is that it allows the quantification and the comparison of a whole range of possible scenarios that reflect the uncertainty in reservoir properties. For example, Sharma and others (Sharma, Chorn et al. 2002) showed how to compare intelligent and conventional wells using four example problems. The disadvantage of ROV is that the parameters required for this method, such as stock price, future revenue, standard deviation, reliability etc. are not certain and often a subject of expert's judgment. Moreover, even in theory this mathematically sophisticated method does not guarantee an accurate solution (Gai 2002). Many authors (Yeten, Castellini et al. 2005; Ajayi and Konopczynski 2007; Addiego-Guevara, Jackson et al. 2008; Alhuthali, Datta-Gupta et al. 2008; Birchenko, Demyanov et al. 2008; Hasan, Ciaurri et al. 2009; Cullick and Sukkestad 2010; Dilib and Jackson 2012; Pinto, Barreto et al. 2012) have, therefore, used a simpler approach to compare conventional and intelligent completions. They compared the mean value of oil production, the recovery factor or NPV and their distribution for both IW and conventional scenarios.

Most of the authors used a deterministic approach for modelling uncertainty. Optimistic (P10), the most probable (P50) and pessimistic (P90) values for each input parameter were specified based on the author's expert opinion. Others, such as Birchenko (Birchenko, Demyanov et al. 2008) and Alhuthali (Alhuthali, Datta-Gupta et al. 2008),

added use of stochastic approach. The stochastic approach is more accurate, since the result relies on the input data only and does not depend on an expert opinion. Moreover, this approach calculates a distribution and provides an estimate of the risk for each scenario. However, this method suffers from high computational demands with the running of many reservoir simulator realisations being required. This not only significantly increases the computational time, but also put certain requirements on the optimisation algorithm for intelligent wells. It should be fast, stable, reliable and not dependant on the input parameters.

A number of different strategies were analysed and described in the literature over the last decade and some of them are realised in commercial petroleum engineering software. However, not of them satisfies all the conditions specified above. The stochastic algorithms often are very time consuming. The gradient-based algorithms are normally sufficiently fast, but often suffer from oscillations and instability. An *Adjoint* algorithm realised in *ECLIPSE* software demonstrated a high dependence from the initial point and non stable results. Moreover, most of the control strategies are designed for infinitely variable ICVs, while more than 95% of the IWs are actually completed with On/Off or discrete position valves (Tirado 2009).

### 1.1 Thesis Objectives

The main objectives of this research are:

1. Find an IW optimisation method considering reservoir uncertainty represented by multiple realisations. Therefore, the algorithm should be robust, stable and relatively fast.
2. Compare different types of ICVs based on the provided value, equipment cost and reliability.
3. Define the application area of the proposed method.

This thesis proposes a new optimisation strategy which satisfies all of the above conditions and is applicable to On/Off and discrete position ICVs. Application of this control strategy allows the impact of the IWs on the production uncertainty to be analysed in a more complete manner that was often not possible in the past.

The thesis demonstrates that On/Off ICVs have a wide application area, where they provide maximum oil rate or very close to maximum value. It defines the Critical Water Cut criterion – a simple and efficient method of the On/Off ICVs optimisation.

It also shows that the decision about the well completion and development strategy type is more accurate if the reservoir and dynamic uncertainty is considered than in the only one “most likely” realisation based approach.

## 1.2 Chapters Outline

***Chapter 2*** summarises control strategies for IWs described in the literature. Two types of the strategy are specified: *reactive* for short term optimisation and *proactive* for long term. The requirements to the optimisation algorithm which can be used to investigate an impact of the IWs on uncertainty are also specified. It should be fast, convergent and independent of the input parameters. The strategies were ranked based on these criteria.

***Chapter 3*** describes a workflow analysing the impact of an intelligent completion controlled by a simple WC threshold algorithm on the production uncertainty. The IW increased the oil production and reduced its uncertainty in liquid constrained scenarios. However, the cumulative oil production was decreased in the IW case in comparison with conventional completion for the pressure constrained scenario. An efficient control strategy of IWs is required thus for the pressure constrained scenarios.

***Chapter 4*** compares the results of three algorithms: *Sequential Linear Programming (SLP), Sequential Quadratic Programming (SQP) and Adjoint-based algorithm* which are already available in PE software in two example models**.**

***Chapter 5*** describes the novel optimisation strategies for intelligent wells. First, a *Direct Search (DS)* optimisation method which received the highest score among the other methods are described in chapter 2. The method was implemented in PETEX Integrated Production Modelling (IPM) software using a user supplied script. The results have been compared with the other methods. The *Direct Search* method can be used for discrete valve position and On/Off ICVs optimisation.

Secondly, the novel proactive control strategy for an initial production period with an oil plateau has been proposed in this chapter. This method can be used as an alternative to the Adjoint algorithm, which demonstrated convergence problem and dependence from the input point.

Different types of ICV not only require different optimisation algorithms, but also have a different reliability and cost. From one side, the infinitely variable ICVs have the highest flexibility and the greatest ability to optimise the oil production. On another side, the risk of failure and the cost increase with the complexity of the devices. ***Chapter 6*** compares infinitely variable, discrete position and On/Off ICVs in terms of cost and reliability.

Intelligent wells completed with On/Off ICVs demonstrated similar technical and higher economic value than the infinitely variable ICVs. ***Chapter 7*** investigates the fundamental reasons for this. It discusses theoretical aspects of downhole flow reactive control with tubing head pressure constraint**.** It was shown that On/Off ICVs are sufficient for the optimal performance at certain conditions. The *Critical Water Cut Criterion* which can be used for the optimisation is defined in this chapter.

***Chapter 8*** allocates the application area of On/Off control strategy. It shows that the On/Off control strategy has a wide application area, where it provides maximum oil rate or very close to maximum value. The workflow is proposed to identify if On/Off completion is sufficient for a particular case.

***Chapter 9*** demonstrates the application of novel CWC and DS control strategies. First, the control algorithm based on the zonal critical water cuts (CWC) is illustrated for three cases. The first case demonstrates how to calculate CWC. In the second example the CWC was used to optimise instant oil rate in a four layer vertical well. The third case is a full-scale, simulation and optimisation study of a real-field where the CWC algorithm was compared with the Direct Search and commercial software optimisers. Finally, Chapter 9 provides the uncertainty analysis performed employing different optimisation methods. It shows the importance of the multiple realisation analysis for a decision making about intelligent or conventional completion.

***Chapter 10*** presents the thesis conclusions and recommendations for the further work.

# Chapter 2 - Choice of an IW Optimisation Strategy

This chapter provides a literature review of a history of intelligent well technology, describes factors and real field situation where IWs provided a greater value than a standard technology and overviews currently available IW control strategies. Further, the criteria for the optimisation algorithm which are necessary for a successful uncertainty analysis will be specified. The available strategies will be ranked based on these criteria and the highest score strategies will be selected for the further detailed analysis.

## 2.1 Literature Review

### *2.1.1 History of Intelligent Well Technology*

The Intelligent Well technology is a relatively new and quickly developing area of oil industry. The first intelligent well was successfully installed in 1997 in Snorre Field located in Norwegian part of the North Sea (Gao, Rajeswaran et al. 2007). Initially the flow control was performed by conventional sliding sleeve valves (Robinson 2003) which had 2 positions for on/off control or 4 positions for discrete inflow control (Williamson, Bouldin et al. 2000). Line T. Skarsholt and others (Skarsholt, Mitchell et al. 2005) describe the experience of installation of intelligent wells in Snorre field over a 7 year period. They conclude that despite of the challenges "the installation and active use of advanced completion solutions gave increased production and a considerable economic advantage to both routine operations and production and reservoir management."

One of the challenges mentioned by Skarsholt and other authors (Williamson, Bouldin et al. 2000; Drakeley, Douglas et al. 2003; Hother 2003; Ajayi, Mathieson et al. 2005; Gao, Rajeswaran et al. 2007; Khrulenko and Zolotukhin 2011) is the lower reliability of the intelligent wells completion when compared with equivalent conventional wells. Thus, of the Snorre Field's 55 intelligent completions, only 41 of them were still operational in 2004 (Skarsholt, Mitchell et al. 2005); an almost 30% rate of failure. The identified reasons for the failure include not only non-operational control valves, but also packer failures or poor cement quality behind the liner. However, the question of the reliability is always an important consideration for oil companies, particularly when considering the early use of new technologies. Further developments such as erosion resistance of control valves when combined with new technologies such as fibre-optic

systems (Wright and Womack 2006) have increased the attractiveness of IWs. The latest reports shows that reliability of intelligent completion has increased up to 95% (WellDynamics and Halliburton 2009).

Another serious challenge faced the operators is data overload. The intelligent wells are completed with multiple gauges containing pressure and temperature sensors, providing data that can be transformed into useful information about the reservoir and fluid properties as well as the production intervals' flow rates. This data stream must be transmitted and analysed in real time to correct control of ICVs for delivering maximum value. Operating a smart field requires a new workflow to handle this new data flow and to take a full advantage of the field's operation flexibility. A number of workflows and data management systems have been developed to solve this problem.

One of the examples of such systems is the *i-field*™ (Burda, Crompton et al. 2007; Hauser and Gilman 2008; Berg, Perrons et al. 2010) which has been implemented around a world. According to the Sankaran et al report (Sankaran, Olise et al. 2010), the application of the *i-field* system in one of the offshore fields in Nigeria:

1. Significantly increased the well's availability and the facility's uptime during the first 6 month of production.
2. Avoided the lost production due to quick and regular access to the data. Actual savings during the first year was estimated at more than $10 MM.
3. Reduced the engineers' non-productive time associated with data gathering, sorting, analysis and reporting by up to 98%.
4. Captured knowledge and reduced the loss of expertise when the members of the team were relocated or new employees recruited in the project.
5. Eliminated data duplication and avoided the resulting confusion, minimised unnecessary rework, improved efficiency and the quality of the data, resulting in increased confidence of the results.
6. Provided effective collaboration and communication between different teams.

Other manifestations of this approach, such as "Smart Fields" (Berg, Perrons et al. 2010), Well-Reservoir Monitoring System (WRMS) (Vilanova and Alvarez 2010) or Real-time production optimization (RTPO) (Omolev, Saputelli et al. 2011) all showed similar benefits resulting from the higher well availability and the improved efficiency of IW systems.

The number of IWs significantly increased as a result of improving and developing new equipment and information systems. The number of intelligent completion installations

is thought to have increased annually by 27% for the first 5 years after the first IW was installed (Figure 2-1) (Gao, Rajeswaran et al. 2007). The number of intelligent wells is greater than 1000 according to current estimates (Sun, Constantine et al. 2009; Mazerov 2012). This number is growing quickly and the smart field approach has become popular in the oil industry; although the percentage of IWs is still small in comparison to the number of conventional wells.

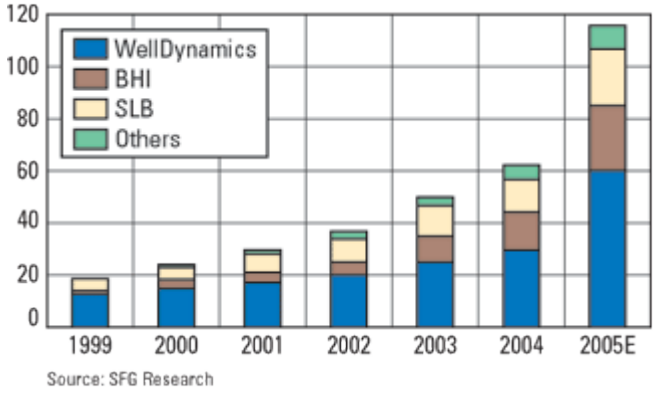


*Figure 2-1 Number of intelligent completion installations (after SFG)*

### *2.1.2 IW Value*

There are three key elements which make IWs more valuable than conventional wells (Konopczynski and Ajayi 2008):

1. **Zonal Flow Monitoring** makes available real-time data about key reservoir parameters such as pressure, temperature, flow rate and fluid composition. This information can be used to develop a better understanding of both the well and the reservoir performance; parameters which are often uncertain, especially during the initial stages of reservoir development.
2. **Flow Control** allows segmenting the wellbore into individual zones and controlling the inflow or outflow of each zone separately. This ability helps to reduce the recycling of unwanted fluid such as water or gas, make movement of the displacement front more uniform and avoid well interventions.
3. **Flow Optimisation:** the ability to use the information collected from the downhole sensors and zonal control devices to improve the overall well performance. This improved performance can achieve an increased oil rate, recovery and Net Present Value (NPV), reduce the operating costs and the volumes of unwanted fluid production. Others objectives may also be improved specified by the operating company for a particular field.

Many of the benefits of using IWs have been described by various authors based on their application in real fields (Gai 2002; Sharma, Chorn et al. 2002; Han 2003;

Robinson 2003; Glandt 2005; Sakowski, Anderson et al. 2005; Mubarak, Dawood et al. 2009; Sun, Constantine et al. 2009; Berg, Perrons et al. 2010; Vilanova and Alvarez 2010; Nagib, Ezuka et al. 2011; Yadav and Surya 2012). For example, Glandt published a complete review (Glandt 2005) summarising the use of smart wells in more than 80 projects. He found that the value of IWs can be divided into 2 groups: "quantifiable (hard)" and "difficult to quantify (soft)". The **quantifiable** benefits include:

- Reduction in well count.
- Savings on intervention cost.
- Well's ability to respond immediately to (un)expected changes which transfers into intervention-cost savings and a minimal production deferment.
- Increased recovery or NPV.

The values which are **difficult to quantify** include:

- Early data acquisition to improve the infill drilling.
- Identification of key variables that need to be measured.
- Mitigation of the downside risks.
- Health, safety and environmental dividends from unmanned operations.
- Smaller environmental footprint due to reduction of the number of wells and production of unwanted fluid.
- Opportunity to acquire relevant data in wells to be abandoned.

The examples of benefits from IWs usage were achieved in practice in the following situations:

1. ***Optimal Sequential Production.*** The use of IW prolonged the production from one of the reservoirs and increased the overall oil production more than 85,000 bbl, while the intervention cost was reduced (Akram, Hicking et al. 2001; Glandt 2005).
2. ***Commingled Production*** increased the production at the Fourier 3 well of the Na Kika development in the Gulf of Mexico by 28% (Jackson-Nielsen, Piedras et al. 2001; Glandt 2005).
3. ***Fluid Transfer for Sweep or Pressurization.*** The controlled gas crossflow from the deep reservoir into a gas cap helped to maintain the reservoir pressure and increase the production rate by more than 2,500 STB/day. Using of advanced technology lowered the risk and avoided well interventions. Moreover, this

scheme reduced the capital required for gas and injection facilities (Lau, Deutman et al. 2001; Glandt 2005).

4. ***Oil Rims in Single Reservoir.*** A horizontal well is the most effective solution for producing oil from a thin oil rim between gas and water containing formations. One of the problems is that the pressure distribution is not uniform along the horizontal completion's length. The resulting early gas or water breakthrough may significantly reduce oil production. Any reservoir heterogeneity along the length of the well will accelerate this effect. Intelligent completion helps to reduce such risks, delay the production of unwanted fluids, increase the oil production and prolong the well's producing life (Sinha, Kumar et al. 2001; Jansen, Wagenvoort et al. 2002; Glandt 2005).
5. ***Oil Rims in Compartmentalized Reservoirs.*** The zonal control has even higher benefit if a horizontal well drains several compartments simultaneously. The estimated increase in the cumulative production due to the installation of smart well in Iron Duke field was estimated at being 38% compared with that expected from conventional completion (Skilbrei, Chia et al. 2003; Glandt 2005). It is also interesting in the context of the research reported in this thesis that in this situation such good results were achieved with using hydraulic operating system and On/Off ICVs.
6. ***Sweep Efficiency Improvement.*** The displacement front is often non-uniform in heterogeneous reservoirs with a high contrast of rock properties along the well trajectory. As a result part of oil remains unswept and further measures such as secondary, tertiary methods and well sidetracking are required to recover this oil. IWs allow controlling injection and production of different zones, flattening the displacement front and improving the sweep efficiency as observed, for example, in the Oseberg field (Sigurd 2000; Glandt 2005). Fractured carbonate reservoirs are another example where a smart completion has helped significantly improve the sweep efficiency and increase the oil production (Arenas and Dolle 2003; Abduldayem, Shafiq et al. 2007).
7. ***Swing production.*** The production requirements may vary during the year. For example, the volumes of gas required may be different during the winter compared to the summer time. An intelligent well flexibly provided the gas requirements of the Brent-Charlie platform in the North Sea, avoiding the need

for capital investments to upgrade the production facilities (Akram, Hicking et al. 2001; Glandt 2005).

8. ***Auto gas lift*** employing downhole flow control significantly increased the production in Oman field (Peringod, Al-Ruheili et al. 2011) by use of an intelligent completion. A significant reduction in the cost of the surface equipment was also achived. The authors also mentioned that this approach was safer, more efficient and had reduced environmental impact compared to the normal gas lift system.
9. ***Downhole Flow profiling.*** The inflow profile along the well is normally based on the formation's permeability-height (*kh*) thickness, calculated from well logs. The production profile frequently does not match this initial expectation. Analysis of the data provided by the downhole sensors and gauges, such as Permanent Downhole Gauges (PDG) and Distributed Temperature Sensing system (DTS) allows the actual well performance to be determined and modified, improving the understanding of the reservoir and reducing uncertainty. Thus, use of DTS in a steam injection project allowed identification of breakthrough zones and improved the well injection performance (Batocchio, Triques et al. 2010). A second example showed how DTS could recognise a cross-flow during a well shut-in (Brown, Kennedy et al. 2000).

It was claimed that the implementation of Smart Field technologies in 50 assets for a 7 year period resulted in an estimated US$ $5*10^9$ of quantified benefits. This figure was calculated based on the improved production and reduced capital and operational cost. As was mentioned earlier, there are also "soft" benefits which cannot be quantified directly. One such benefit is reduced reservoir and production uncertainty through a better understanding of well and field performance.

## 2.2 Overview of IW Control Strategies

Choice of an efficient control strategy is a difficult problem. All optimization strategies can be divided into two main types: "proactive" and "reactive" (Ebadi and Davies 2006). "Reactive" optimization requires the IW to responds to the current inflows into the well; either flow rates, WC or GOR in our case. By contrast, a "proactive" strategy can change the invading front's behaviour; delaying the unwanted fluid's breakthrough and increasing the sweep efficiency.

Further, the ICVs can be also divided into three types:

1. On/Off valves with only two positions, fully open or fully closed.
2. Discrete vales with a fixed, normally 10 or fewer, number of positions.
3. Infinitely variable valves which can have any position between fully open and closed. These valves provide the most flexible control.

A number of different strategies have been published in the literature over the last decade. The main strategies, and the results for their application to optimise intelligent wells, are summarised below.

### *2.2.1 Reactive Strategies*

The simplest approach to control the valve is to use a ***water-cut threshold*** to close the operating valve or choke it down to the next position. This threshold can be fixed, e.g. at 80%, or it can change with time. Cullick and Sukkestad used this approach to control an intelligent well in their work (Cullick and Sukkestad 2010). Their fixed policy example used a water cut threshold fraction of 0.8 value; the ICV being closed once the zonal water cut reached this value. Their flexible policy example employed a threshold that increases monotonically from a value of 0.1 to 0.9. The flexible policy showed significantly better results than the fixed one, increasing the total cumulative oil production by 67% and reducing the cumulative water production by 47% for one of the studied cases. In all cases, IWs demonstrated a significant advantage over the conventional scenario with added cumulative oil production varying from 7.4% to 57% even when the fixed control policy was employed. Such impressive results for this simple strategy can be explained if we look at the constraints used in this work. As in the previous chapter, the well was constrained by liquid rate, which is advantageous for an IW. The advantage of this method is that it is simple, fast and can therefore be used for optimising large fields.

Using a ***function containing the WC*** as the criterion for choking the ICV is a slightly more complex strategy. This strategy is more suited to infinitely variable valves, which can be adjusted on the basis of this function. Addiego-Guevara and Jackson demonstrated this approach (Addiego-Guevara, Jackson et al. 2008) with the following function to control infinitely variable ICVs:

$$\Delta P_C = \Delta P_O \cdot \max\left[ A + B \cdot \left( \frac{WCT}{1 - WCT} \right)^C, 1 \right] \qquad (2\text{-}1)$$

where $\Delta P_c$ is the pressure drop across the ICV for a given choke setting, $\Delta P_o$ is the pressure drop when the ICV is fully open, *WC* is the completion water cut and *A*, *B* and

*C* are constants. The values of these constants are specific for each production case and can be optimised based on the model.

The approach in this method was superior to the fixed control strategy. The well was constrained by both liquid rate and BHP. Unfortunately, it is not clear from the paper whether or not the liquid rate was restricted for the major part of the production period. Moreover, a relatively low economic WC value of 25% was used, the production being terminated once the wells WC reached this threshold. This condition is advantageous for IWs since they can normally efficiently reduce the WC and extend the production time. Despite these caveats, this method is simple and fast, allowing this strategy to be used for uncertainty investigations as demonstrated in (Addiego-Guevara, Jackson et al. 2008) and extended by Dilib and Jackson (Dilib and Jackson 2012).

The previous methods are able to improve the objective function (e.g. cumulative oil production or NPV) but they do not provide the optimum value. The ***gradient-based*** technique is a more complex approach for controlling the ICVs to find a local optimum. It uses the first order derivative of the objective function with respect to the control parameters, such as ICV choke diameter or pressure drop. The advantage of these methods is that they are still easy to implement and relatively fast, providing there is no problem with convergence. However, the objective function is normally complex and non-linear; hence, it is usually found via the output a black-box simulator. The accuracy of this derivative value is often poor, especially when the model has several control parameters which may interact with each other.

Yeten and others used a ***nonlinear conjugant gradient*** method for production optimisation (Yeten, Durlofsky et al. 2002). In one of the cases they run five realisations to compare a multilateral well with conventional and intelligent completion. The IW scenario showed a high range of additional cumulative oil production varying from 1.8% to 64.9% for different realisations. However, the advantage of IW in this particular example may be not clear. The liquid rate and GOR constraints were used in this model and, although the BHP limit was also specified, it was not reached. Moreover, an 80% WC economic limit was used as the termination condition. This increased the producing period and the resulting cumulative oil production for the IW case, even though the initial oil production was less than for the conventional case (Fig.2-2).

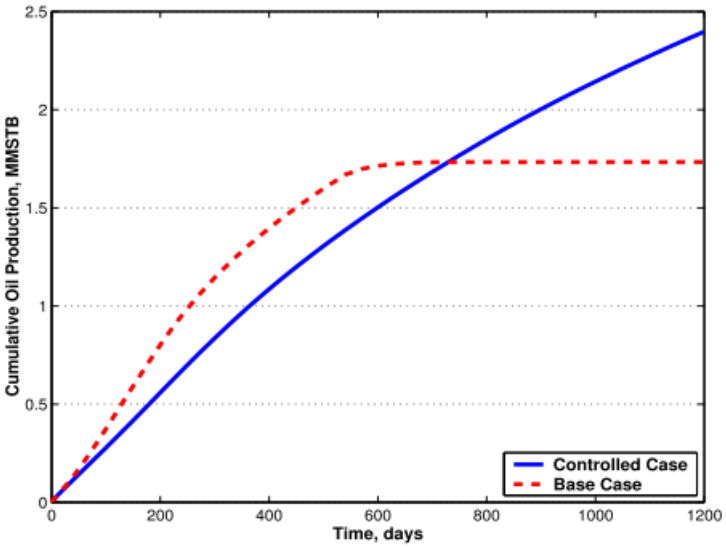


*Figure 2-2 Cumulative Oil Production Comparision (after Yeten(Yeten, Durlofsky et al. 2002))*

Wang et al. (Wang, Li et al. 2009) used a ***Steepest Ascent (SA)*** algorithm for production and NPV optimisation. Similar to the previous work, it uses the first order derivative which was calculated by perturbing the model. The authors noted that this method is time consuming since each perturbation of each parameter requires at least one simulation run. They suggested comparing it with two other methods. One of them is ***Simultaneous Perturbation Stochastic Approximation (SPSA).*** In this method all parameters are perturbed stochastically at the same time, therefore it only requires two simulation runs for finding all derivatives. However, SPSA showed much slower convergence in the two cases they investigated. Figure 2-3 shows that SA algorithm required only 20 simulation runs for converging to an optimal value, while SPSA needed about 1000 simulations to reach the same result.

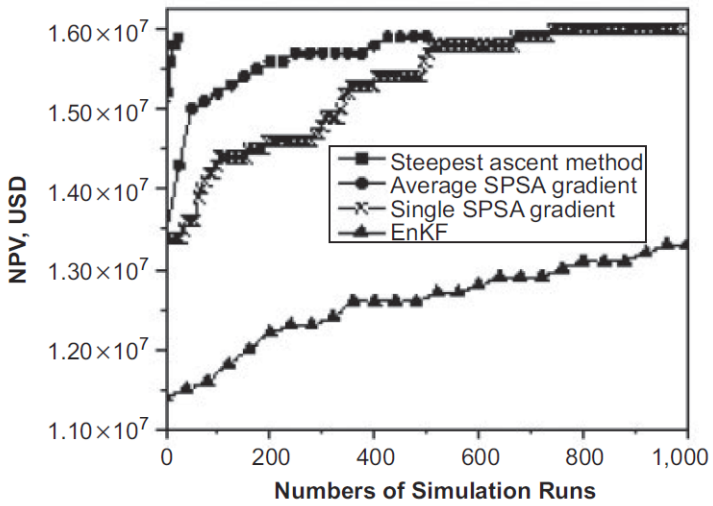


*Figure 2-3 Number of simulation runs for Steepest Ascent, SPSA and Ensemble Kalman Filter methods (after Wang(Wang, Li et al. 2009))*

Dilib and Jackson used gradient-based method implemented in MathLab software for maximising NPV (Dilib and Jackson 2012). Unlike the previous work in which valve settings update at fixed time steps, the authors propose to use time steps dependant on the well's water cut increment. They suggest that this approach can help to reduce the computational time by avoiding unnecessary optimisation when the systems conditions do not change. Moreover, it can help to unify the optimisation process for different realisations which can have a significant difference in production timescale. Therefore, such an approach can be used for uncertainty investigation.

Dilib and Jackson (Dilib and Jackson 2012) compared four different methods:

- Fixed control, employing ICD;
- On/Off control, based on the WC threshold;
- Variable flow control based on an equation containing the WC;
- Model-based optimisation using a gradient-based method.

The gradient method showed the best result for the initial case. However, the authors noticed that it provides a lower initial oil production rate than the other cases; the higher cumulative oil production resulted from a longer production lifetime. This difference in total production time for different cases is caused by the well's WC limit, set at 25% for the analysed scenario. In addition, the authors mentioned that the IW did not provide any significant benefits once the WC limit is greater than 90%.

The impact of reservoir uncertainty to the result of different optimisation strategies was also investigated. As expected, the closed-loop strategies with flexible ICV control gave better results than fixed-control methods employing ICDs. The ICD strategy can even provide a worse result if the reservoir behaviour is different from that predicted initially; since the control device cannot be changed or adjusted based on the reservoir response. Surprisingly, the On/Off and variable control strategies showed similar results to the more complex model-based method; even though they were optimised and calibrated only for the base case. In addition, the On/Off strategy showed better economic results due to its lower completion cost.

In addition to the other results, Dilib and Jackson mentioned that the later control is likely to be more attractive in situations where the well is constrained by pressure. Early control may reduce the oil production significantly since the resulting loss in value may not be compensated by later production of extra oil due to the discount coefficient. We will be returning to this observation in a Section 2.3 when comparing reactive and proactive strategies.

The gradient-based methods require continuity of the control parameters. A ***direct search*** is a modification of the gradient-based approach allowing them to be applied in a discrete space. This method allows optimising On/Off valves and chokes with a fixed number of positions. The application of this method in two real-field cases was demonstrated by Emerick and Portella (Emerick and Portella 2007). Their optimisation procedure developed for this method is demonstrated in figure 2-4.

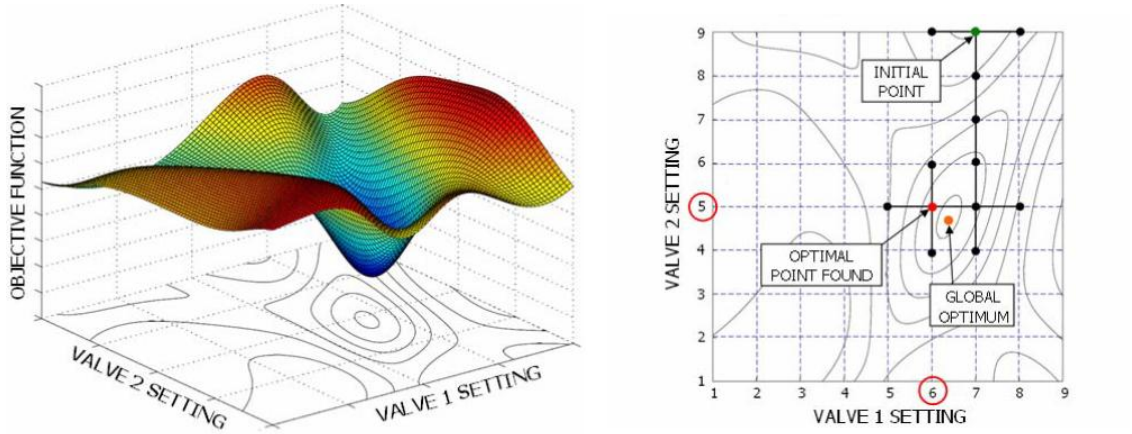


*Figure 2-4 Optimisation procedure of Direct Search method (after Emeric(Emerick and Portella 2007))*

The solution area is divided into a discrete space. The algorithm procedure starts with an exploratory search in the neighbourhood of the initial point, searching the direction with the highest rate of increase in the objective function for the maximisation problem. This direction is followed until the objective function ceases to increase. After that, a new exploratory search is performed. The algorithm stops when there is no direction where the objective function increases.

The advantage of this algorithm is that it is simple and easy to implement and can also be used for discrete ICVs. It does not require calculation of the first derivative, which is usually difficult task for a complex full-field model. The disadvantage is that the solution and convergence time depend on the initial point; hence they may vary depending on the initial value chosen. Moreover, each exploratory movement implies that a simulation model must be run. This method thus becomes progressively more computationally expensive especially as the number of control parameters increases. However, as was correctly mentioned by Emerick and Portella, these calculations can be easily performed in parallel.

Nine different cases with producers and injectors completed with On/Off, six and ten position valves were investigated. Cases with only production wells completed with ICVs showed similar results (a 9% of increase of cumulative oil production). That was independent of the number of ICV positions. Cases with injection wells completed with

ICVs showed a slightly higher cumulative oil production; but were rejected because the oil production rate was slower, making them less financially attractive.

A WC constraint equal 90% increased attractiveness of IWs because the production period was approximately twice that of the base case (20 years). Also, some of the ICV cases showed a higher oil production prior to this time.

Khrulenko and Zolotukhin used the direct search method for optimising the oil production for a 10 position, discrete ICV in a real-field model (Khrulenko and Zolotukhin 2011). They reduced the computational time by specifying several sectors which included only near wellbore area and optimised the production of each sector individually at each time step. The flux option was then be used to join all sectors together and find a solution for a whole model. Five realisations of the model were analysed to provide an idea of the impact of production uncertainty.

***Sequential Linear Programming (SLP)*** is a more complex approach to production optimisation. Similar to the gradient-based methods, SLP uses first order derivatives for optimising the objective function. However, it employs a linear programming Simplex method instead of searching for the optimum directly. Solving a linear optimisation problem is a much easier task than looking for the optimum of a non-linear task. However, the original problem is non-linear; with several Simplex solutions being required to find a solution of the original problem.

Naus and others made a detailed description of SLP method and applied it to ICV optimisation (Naus, Dolle et al. 2006). Their optimisation procedure is shown in Fig. 2-5.

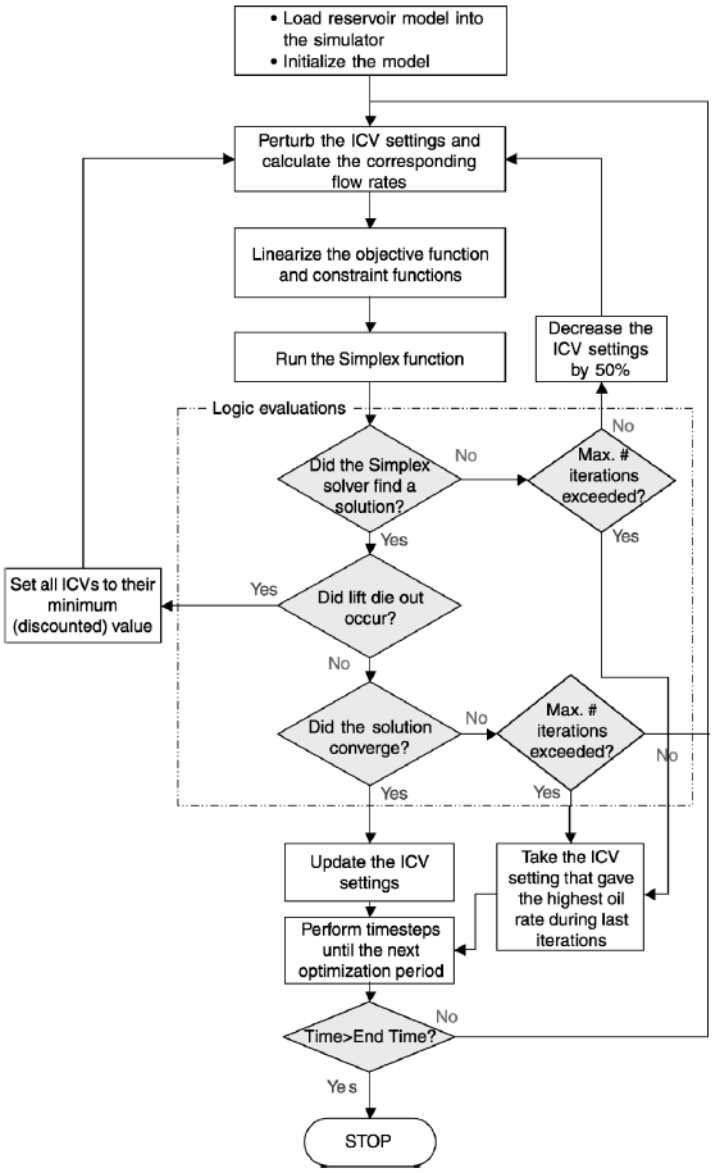


*Figure 2-5 SLP optimisation procedure(after Naus(Naus, Dolle et al. 2006))*

The method increased oil production in both water and gas constrained situations. The individual calculation steps are relatively fast and, in general, the algorithm converged within 5 to 10 iterations. However, the authors noticed that sometimes the method suffered from convergence problems caused by nonlinearities and oscillations. There are two main possible reasons for this behaviour.

The first one is the inaccuracy of the derivatives. The derivatives are normally found from perturbation of the control parameters, such as the downhole valve area, and observation of the resulting response of a "black-box" simulation model. The observation covers only transient time regime if the time of observation is relatively small. A longer time window is required to find a steady–state solution, slowing down the optimisation process. These two parameters should be balanced against each other.

The second possible reason for a convergence problem is linearization of the original model and constraints, especially when both reservoir model and production systems are considered together as a single optimisation task. The solution of the linear task may be far from the optimum of the original problem and the method is not always able to converge.

***Sequential Quadratic Programming (SQP)*** method may reduce the effect of the mismatch of the original model and its approximation because it uses a quadratic approximation of the original task which is more accurate than a linear one. The detailed description of this algorithm can be found in a paper by Dehdari and Oliver (Dehdari and Oliver 2011). They mention that the method can be computationally expensive; especially when the number of inequality constraints is high. Modifications of the algorithm proposed by Dehdari and Oliver, including parallel computation, reduced the run time by up to a factor of 7. They also compared SQP with Steepest Ascent method; with SQP providing a higher NPV value (Fig. 2-6).

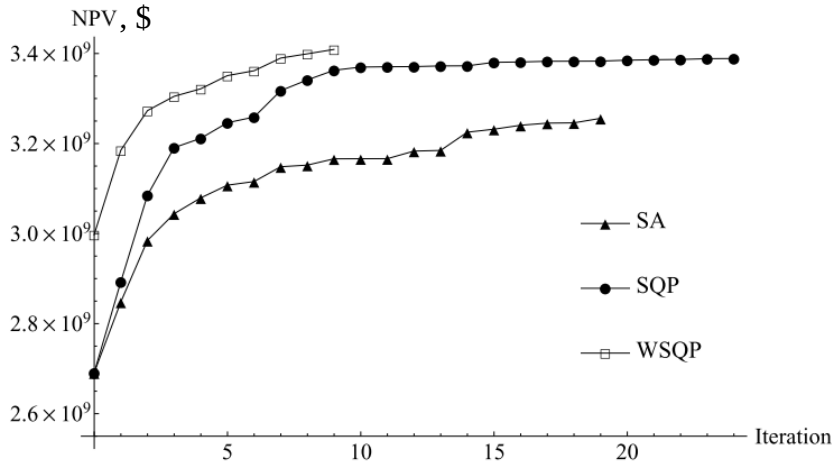


*Figure 2-6 An NPV based Comparison of SA and SQP methods before and after WC constraint (after Dehdari (Dehdari and Oliver 2011))*

Lorentzen et al. (Lorentzen, Shafieirad et al. 2009) demonstrated the successful application of the SQP method for optimising the benchmark Brugge model (Peters, Arts et al. 2010). They also investigated uncertainty, mentioning that "the reduction of computation time is a crucial issue" in addition to this optimisation.

The SQP algorithm was also used for optimisation of an integrated model coupling a dynamic reservoir and facility network (Davidson and Beckner 2003; Elmsallati and Davies 2005). This is a challenging problem for the SQP method because of the increasing number of constraints; since the convergence of this method is known to be very sensitive to the number of constraints. Moreover, SQP needs second-order

derivatives for the model approximation, which sometimes are quite inaccurate because the fluid flow in a production system is described by complex, non-linear correlations. The correlations may change depending on the flow regimes, sometimes showing discontinuities when the correlation changes due to entering the area of a different flow regime. The method can thus suffer from convergence problems resulting in unstable or oscillating production rates, increasing the run time and delivering poor optimisation results (Elmsallati and Davies 2005; Al-Khelaiwi, Davies et al. 2007).

***Ensemble Kalman Filter (EnKF)*** is a stochastic method used by some authors (Chen, Oliver et al. 2009; Lorentzen, Shafieirad et al. 2009; Wang, Li et al. 2009; Su and Oliver 2010; Dehdari and Oliver 2011) for ICV optimisation. EnKF became popular in the oil industry due to the good results it achieved in data assimilation and history matching problems (Evensen, Hove et al. 2007; Schulze-Riegert, Krosche et al. 2009; Emerick and Reynolds 2010; He, Sarma et al. 2011). A theoretical description of this method can be found in Evensen (Evensen 2003).

The ensemble optimisation (EnOpt) approach is based on the covariance between the control variables and objective function (Su and Oliver 2010). The ensemble of random perturbations of control variables is used to find which control parameters can increase the objective function. The EnOpt procedure does not need to calculate gradients, unlike gradient-based method, enabling each iteration to be completed faster. However, the convergence to the optimal solution may be slower than with gradient-based methods.

The advantage of EnKF is that it is suitable for a large number of variables, is very flexible and can be combined with any reservoir simulator. It also can be used for situations where the model has uncertain parameters.

Chen et al (Chen, Oliver et al. 2009) showed that the algorithm employing EnKF provides better results than reactive optimisation based on the WC threshold. However, Wang (Wang, Li et al. 2009) showed that SA and SPSA methods converge faster and provide a higher value of objective function than algorithms based on the Kalman Filter. The production was optimised at every time step, an appropriate approach for a reactive strategy, despite most of the papers referred to above using the label cumulative oil production or NPV at the end of a field life as a result function. By contrast, proactive strategies consider the optimal control values for all time steps for the whole production period.

### *2.2.2 Proactive Strategies*

The simplest proactive control strategy uses passive control employing Inflow Control Devices (ICDs). They are usually used for equalising the inflow rate per unit length of completion along the horizontal well's length. Such inflow heterogeneity in different parts of the well can be caused, for example, by differences in the reservoir's permeability or the horizontal well's "heel-toe" effect. ICD completions employ a fixed flow restriction installed at each completion joint. The inflow from high-permeability reservoir zones into the well is restricted. By contrast, an ICV is controlled from the surface by an operator in order to restrict the inflow into specific intervals. Al-Khelaiwi and Birchenko have made a detailed analysis comparing the application area for both devices (Al-Khelaiwi, Birchenko et al. 2008; Birchenko, Al-Khelaiwi et al. 2008). "Passive" control has a low installation cost and risk. However, installation of such devices requires good knowledge about a reservoir, which is often uncertain. An incorrect prediction of reservoir behaviour may result in loss of production, which cannot be recovered in the future. Therefore, "active" control devices are often preferred in heterogeneous reservoirs due to the higher levels of uncertainty present in this type of reservoir. The flexibility of "active" IW control allows changes to be made at any time to the well's production strategy, reducing the risk caused by reservoir uncertainty.

The "active" proactive strategies can be divided into two large groups: gradient-based and stochastic methods.

***Adjoint*** method is one of the most popular gradient-based optimisation approaches in oil industry. Zakirov(Zakirov, Aanonsen et al. 1996) and Brouwer(Brouwer and Jansen 2002) used this method for water flooding optimisation, Sarma et al. (Sarma, Chen et al. 2008) applied the adjoint method for optimising an intelligent horizontal well.

The adjoint method is not easily implemented. It uses an adjoint model which must be solved backward in time. Access to the internal parameters of the reservoir simulator is required for the most effective application and the fastest converge the. The detailed description of the algorithm can be found in Sarma et al (Sarma, Chen et al. 2008). Solving the adjoint model requires approximately the same calculation time as for solving a simulation model. The convergence depends on the model, the initial point and the accuracy of the derivatives. The number of simulations depends on the number of control parameters, the complexity of the model and the number of control steps. Sarma reported that 15 simulations were required for reaching the optimal solution for a simple model with one horizontal producer and one injector. A slightly more complex

model containing a tri-lateral well completed with ICVs (Fig.2-7) required 68 simulations.

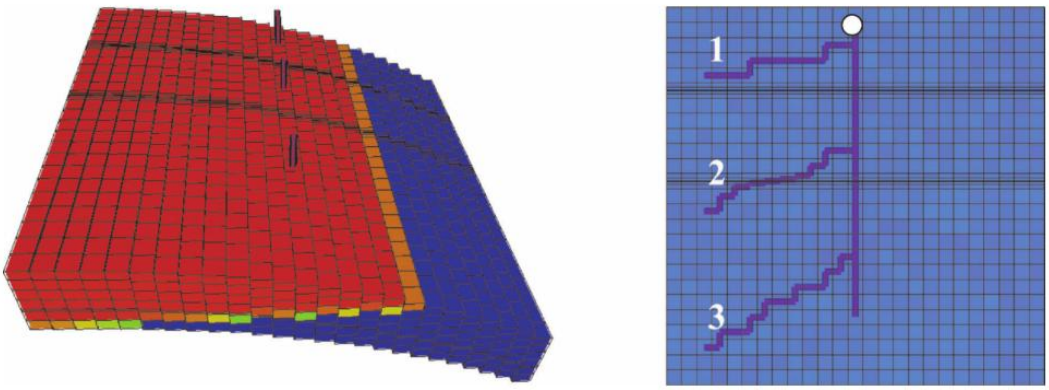


*Figure 2-7 3D simulation model (left) and the trilateral well(right) (after Sarma(Sarma, Chen et al. 2008))*

The method based on an ***Augmented Lagrangian*** function with the Karush-Kuhn-Tucker conditions was investigated by Doublet et al (Doublet, Aanonsen et al. 2009) for a simple model containing one horizontal producer and one injector. The example also assumed that the liquid production and injection were equal at every time step. The authors found that their method provides approximately the same NPV value as the adjoint method, but required less computational effort.

Stochastic methods are usually represented by ***Genetic Algorithms (GA)***. GA are heuristic search methods which generate solutions to optimization problems using techniques inspired by natural evolution, such as inheritance, mutation, selection, and crossover. Each of these actions is very simple and very fast. The method does not require the difficult and time consuming procedures required to find the derivative. GAs are easy to implement and do not require any specific data from the simulation. They have been applied in many areas, including petroleum engineering. Similar to the EnKF, GAs found a broad application in history matching. Increased computer power and availability of parallel calculation has resulted in greater attention being given to genetic algorithms for production optimisation purposes.

Almeida et al. (Almeida, Tupac et al. 2007) employed GA for proactive optimisation of a vertical well completed with an ICV in a simple synthetic model. They investigated both On/Off and multiple-position valves. The multiple-position scenario showed slightly better results than the On/Off case, although as the authors noted, the On/Off scenario was able to find a better result. The probability of valve failure was also analysed. A higher average NPV than in the base case was delivered when the technical uncertainty of the valve failure was included, justifying use of ICVs. Alghareeb et al.

(Alghareeb, Horne et al. 2009) used GA for multilateral well optimisation. Different types of objective functions were improved in this study: minimising of water cut, extending a production plateau and maximising the NPV. Uncertainty in a fractured model was also investigated. The proactive control of a simple waterflooding model under economic uncertainty was investigated by Sampaio and others (Pinto, Barreto et al. 2012).

The advantage of GAs over the gradient-based methods is that they can theoretically find the global optimum. However, the convergence of these methods is much slower than gradient-based algorithms. The number of simulations is often higher than 1,000, even for simple models. For example, this number reached 20,000 in Sampaio's work. Therefore, using GAs for optimising IWs in complex real field cases, where each simulation may take more than one hour, can be very time-consuming.

To avoid this problem and decrease run time some authors (Talavera, Tupac et al. 2010; Qing and Davies 2011) used ***Model Predictive Control (MPC)*** and built a proxy model of the reservoir. The optimisation process can be significantly speeded-up in this case. However, MPC is not a good predictive model for a complex heterogeneous reservoir with a high number of control parameters.

All the control methods discussed in this chapter are summarised in Figure 2-8.

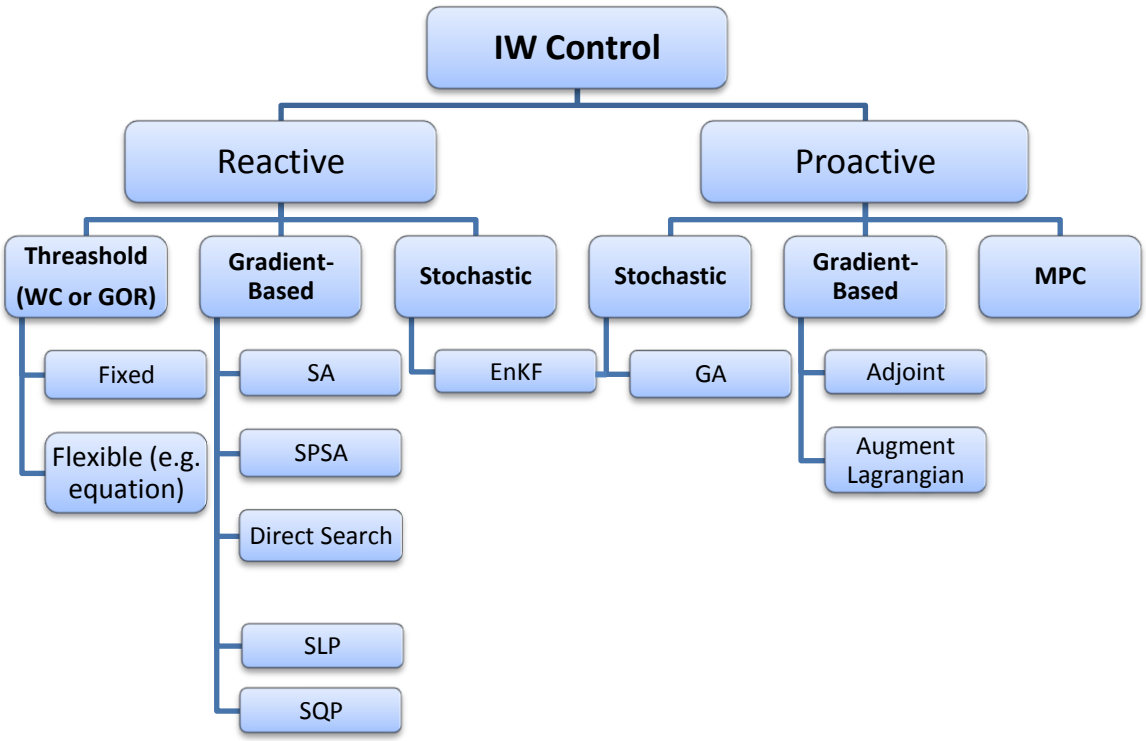


*Figure 2-8 Main IW control methods from literature*

## 2.3 Comparison of the Reactive and Proactive Production Strategies

Reactive control ICVs respond to the current inflow conditions in each zone, reducing the current water or gas production and increasing oil rate or NPV. The advantage of this approach is that it requires only the instantaneous production data and does not require knowledge of the inter-well geological properties. Reactive control algorithms therefore are usually fast, except when convergence is a problem. However, it does little to affect the global position of the water or gas front that is advancing across the reservoir.

Choking an ICV may not be an efficient procedure to control unwanted fluid since it may flow towards neighbouring zones (Fig. 2-9) unless low permeability layers are present in the reservoir in conjunction with packers in the annulus.

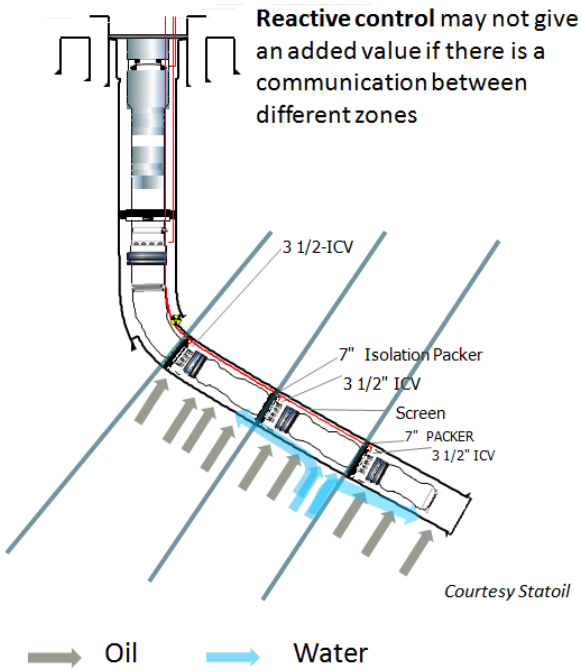


*Figure 2-9 Water flow into neighbouring zones*

A "proactive" strategy can thus be more beneficial than a "reactive" one, giving an increased total oil production. However, most published reports on the use of proactive strategies refer to it being employed in the optimisation of a synthetic reservoir model rather than it being used on a real, full-field model. This is not surprising since the computational time required for a "proactive" method is much higher than their "reactive" equivalent, making them difficult to use when analysing reservoir simulation models that are either big or very detailed.

Reservoir uncertainty is a second challenge for the "proactive" optimisation strategy. This strategy requires selective choking to start early in a well's or field's productive life. If effective, this choking will delay the breakthrough time of unwanted fluids; but it

will also, of necessity, lead to a decreased early oil production unless the well has a higher zonal flow capacity than the well's allowable production rate.

The accuracy of the initial reservoir simulation model will also strongly influence the total oil production achieved. For example, an inappropriate (early) choking strategy based on an inaccurate model can lead to a decreased oil production and an earlier breakthrough of an (unwanted) fluid front. A control strategy based on a model which is different from the real field will give a non-optimum production strategy for the real case. Some authors overcome this problem by periodically updating their models based on "real-time", measured well data (Aitokhuehi and Durlofsky 2005). However, the initial control strategy still has, of necessity, a high degree of uncertainty associated with it. It is not possible to precisely predict the breakthrough time or the initial water and/or gas production profile of a real field during this early production period since the well is usually producing 100% oil at this time. By contrast, this information is always available from a reservoir simulation model. Hence it can be actively used, even during early, times by "proactive" optimisation methods.

The discount coefficient used in NPV calculations reduces economic benefit of the proactive strategy. The later extra oil produced may be worth less than the early-time production loss; even if the proactive control increases the recovery factor. Therefore, proactive control is most suitable for the plateau period only, if a significantly discounted NPV is the objective of the optimisation, since it will not reduce an oil production (Fig 2-10). Reactive strategy can be applied once the production of unwanted fluid has started. This type of strategy is often the most beneficial, because it provides the maximum value today which does not require any discounting. Moreover, reactive control is less risky than proactive control, since it does not depend on either reservoir uncertainty or the accuracy of the model.

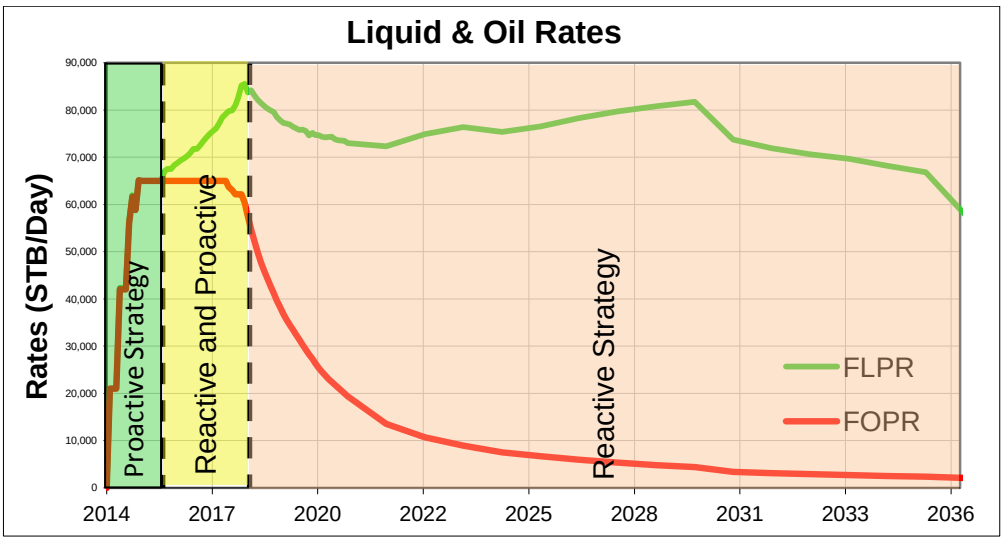


*Figure 2-10 Areas most suited for Reactive & Proactive Control*

Table 2-1 summarises the difference between the proactive and reactive approaches. Consideration of all these arguments leads to the conclusion that the reactive control is more situated to our purpose – uncertainty investigation.

*Table 2-1 Comparison Proactive and Reactive approaches*

| Parameter to Compare | Proactive Control | Reactive Control |
|---|---|---|
| **Objective Function** | Maximises Recovery Factor /Sweep Efficiency | Maximises Instant Oil Rate or NPV |
| **When applicable** | Most effective at plateau period when oil/liquid production is constrained | Applicable after plateau |
| **Data requirements** | Requires inter-well data | Does not require inter-well reservoir data |
| **Implementation** | Difficult to implement | Easy to implement |
| **Run time** | Very significant increase in Run Time | Normally much faster than proactive approach |
| **Dependence from uncertainty** | Algorithm is very sensitive to uncertainty in reservoir parameters | Algorithm does not depend on uncertainty |

## 2.4 Choice of Control Strategy

The ideal optimisation strategy for uncertainty investigation should be fast, robust and relatively easy to implement. Running multiple realisations of a real field model can be time-consuming in itself; hence the optimisation process should not slow down the calculations significantly. The algorithm should provide a stable result with fast convergence for any situation. It should be easy to implement since we are going to test it on several cases, including a real-field. Moreover, optimisation of On/Off and discrete-position valves would be highly beneficial because they are cheaper and more reliable, and hence more frequently employed by oil companies than infinitely variable valves.

Table 2-2 summarises compatibility of each algorithm to each of the criteria mentioned above. If the algorithm is compatible the cell has a green colour and gives one point in the overall column. If the compatibility is medium or unknown, the colour is yellow, adding 0.5 points. Red colour means that the algorithm does not meet the criteria and does not add any points to a total value.

*Table 2-2 Choice of Control Algorithm for Uncertainty Investigation (green- good, yellow – medium, red – unsatisfied)*

| Algorithm | Speed | Stable | Available in PE Software | Easy to Implement | Discrete Valves | Total Points |
|---|---|---|---|---|---|---|
| Threshold | Very Fast | Yes | No | Yes | Yes | 4.5 |
| SA | Fast | ? | No | Medium | No | 2.5 |
| SPSA | Fast | ? | No | Medium | No | 2.5 |
| Direct Search | Fast | Yes | No | Yes | Yes | 4.5 |
| SLP | Medium | No | Yes | No | No | 1.5 |
| SQP | Medium | No | Yes | No | No | 1.5 |
| EnKF | Very Slow | Yes | No | Yes | Yes | 3.5 |
| GA | Very Slow | Yes | Yes | Yes | Yes | 4 |
| Adjoint | Slow | ? | Yes | No | No | 1.5 |
| Augment Lagrangian | Slow | ? | No | No | No | 1 |
| MPC | Medium | ? | No | No | Yes | 3 |

Speed and stability are the most important criteria for our choice. The instability of SA, SPSA, Adjoint and Augment Lagrangian methods was not discussed in the published literature. However, all these methods use derivatives calculated by perturbation, leading to inaccurate results and instability.

The methods based on the thresholds (fixed or flexible) and the Direct Search method show the highest score. They are both fast and reliable. Moreover, these strategies can be easily used for On/Off and discrete-positions valves. Therefore, these two strategies are the highest-ranked candidates for the further investigation.

It should be noticed, that though EnKF and GA gave a satisfactory an overall score, the run time of these methods is extremely slow. Therefore, they will not be analysed. SLP, SQP and Adjoint methods are available in Petroleum Engineering (PE) software and can be relatively easy investigated, despite them having a low score according our ranking.

The result of each optimisation method depends on the production strategy used to control the well's operation. The next section specifies the optimisation problem to be solved, its constraints, input and control parameters.

## 2.5 Problem Formulation

The reactive optimisation problem of liquid production well is to be investigated. Consider a production well with N zones completed with ICVs that is constrained at well head (Fig 2-11).

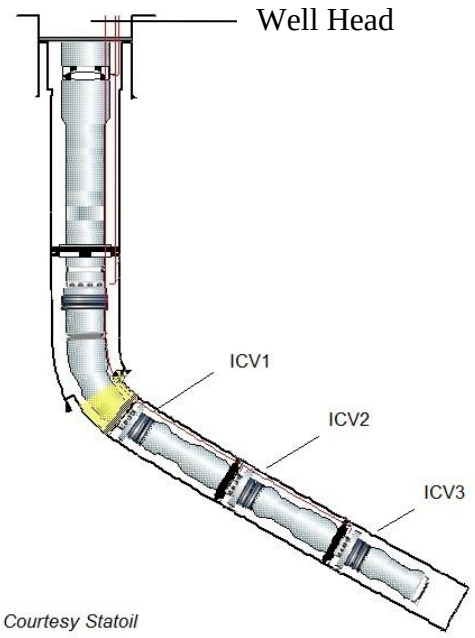


*Figure 2-11 Intelligent Well Schematic*

### *2.5.1 Constraints*

Two types of constraints can be imposed: constant liquid rate and constant well head pressure. The liquid rate constraint is observed when the field operates under a surface facility limit. This situation normally can be met at the initial stage of field development at plateau period. The reactive control can be implemented if water production is observed. The well head pressure (WHP) constraint is a more common situation. The first stage separator operates at a fixed pressure. It thus forms one end of the surface production network connecting the different wells in the field. The wellheads in an offshore platform are often close one to another, implying that WHP after the choke is similar for the various wells. The WHP of an individual well in an onshore field may depend on the pressure distribution in the surface network. However, the pressure in each element of the network can be measured and controlled with surface valves. Therefore, we can assume that WHP is fixed at each optimisation time step, though it can change in reality between control steps for optimising the network flow.

The optimisation of production networks can be efficiently performed by several commercial softwares and need not be included in this research study.

### *2.5.2 Input Data*

The flow rate of each individual zone, zonal water cuts and pressures are assumed to be known. All these parameters can be easily recovered from a dynamic model, though all this information is not available instantly in real life. The data availability should be examined in details for each individual field. Different types of sensors and gauges are normally installed in IWs, providing information about zonal inflow. The information may suffer from noise and inaccuracy of measurement and interpretation. Anyway, the devices and their interpretation methods are constantly improving, increasing the availability of the measured data and the confidence that can be placed in them. The above is discussed in detail in (Silva, Muradov et al. 2012).

### *2.5.3 Control Parameters*

The inflow of each individual zone is controlled with an ICV. The ICV's choke diameter will thus be used as the control parameter, since it restricts the liquid inflow from the corresponding zone. Application of On/Off, discrete-positioned and infinitely variable valves will be analysed.

### *2.5.4 Objective Function*

Net Present Value (NPV) will be used as an objective function:

$$NPV = \sum_{t=0}^{N} \frac{\text{Revenue}_t - OPEX_t}{(1+d)^t} - CAPEX \qquad (2\text{-}2)$$

$$\text{Revenue}_t = \text{OilPrice} \cdot Q_{oil}^t \qquad (2\text{-}3)$$

$$OPEX_t = OperationalCost \cdot Q_{liquid}^t + WaterHandlingCost \cdot Q_{water}^t \qquad (2\text{-}4)$$

Where $t$ – is a time step which normally is equal 1 month, $d$ – discount factor, $CAPEX$ – is capital cost of wells and facilities, $Q_{oil}^t$ - is an oil rate at the time step $t$.

We assume that all taxes and other possible expenditures are included in the oil price and the operational cost.

Since the optimisation is reactive, the actual cash flow (CF) is the optimisation parameter at every time step:

$$CF_t = \text{OilPrice} \cdot Q_{oil}^t - OperationalCost \cdot Q_{liquid}^t - WaterHandlingCost \cdot Q_{water}^t \qquad (2\text{-}5)$$

This value will be used for optimisation by comparing the current result with the fully open case; while NPV will be used to compare different scenarios: conventional well, On/Off or multiple-positioned ICVs, since they have a different capital cost. We also

assume that the capital cost of facilities is the same for all scenarios. Therefore the *CAPEX* is different only due to the difference in the completion cost.

Tables 2-3 and 2-4 summarise economic parameters used in this work. These parameters were only used as an example and will normally be different in each situation.

*Table 2-3 Oil Price, Water Handling Cost, Operational Cost and Discount Factor*

| Oil Price | Water Handling Cost | Operational Cost | Discount factor | Discount factor |
|---|---|---|---|---|
| **$/m$^3$** | **$/m$^3$** | **$/m$^3$** | **%/Year** | **%/month** |
| 380 | 6.5 | 15.75 | 10 | 0.80 |
| **$/stb** | **$/stb** | **$/stb** | **%/Year** | **%/month** |
| 60.42 | 1.03 | 2.50 | 10 | 0.80 |

*Table 2-4 Well Cost for different types of completion and number of ICVs*

| | | Well Cost, MM$ | | | |
|---|---|---|---|---|---|
| **Well Type** | **ICV Cost** | **Horizontal Well without ICVs** | **2 ICVs** | **3 ICVs** | **4 ICVs** |
| **Conventional** | - | 63.3 | - | - | - |
| **2 positions** | 0.4 | 63.3 | 64.1 | 64.5 | 65.3 |
| **10 positions** | 0.8 | 63.3 | 64.9 | 65.7 | 67.3 |
| **Infinite ICV** | 1.5 | 63.3 | 66.3 | 67.8 | 70.8 |

## 2.6 Criteria for Algorithms Comparison

The algorithms will be compared with respect to the following four parameters:

1. Optimal value of objective function
2. Run time
3. Dependence upon time step length
4. Smoothness of the result

The optimisation algorithm's ability to find the maximum value to the objective function is certainly the major consideration when comparing algorithms. Another important characteristic of any optimisation method used for uncertainty investigation is the run time, since the running of multiple realisations is required. Therefore, a preference will normally be given to the faster method if the difference between the optimised values of the two algorithms is small.

The run time depends on the length of the simulation time steps and the optimisation process. Normally, the model run is faster with larger time steps. However, increasing the time step may reduce the accuracy of the results. Three constant values of the time step were chosen for the sensitivity analysis: 2 weeks, 1 month and 2 months. In addition, RESOLVE has the ability to adjust the time step based on the magnitude of the change in the simulation model's calculated values of tubing head or reservoir

pressure. This adaptive time step option with a variation between 5 days and 2 months has also been investigated.

It is well known that some optimisation methods suffer from instability and oscillations; factors that affect both the result and the speed of convergence of the optimisation algorithm. A "smoothness coefficient" (SC) has been developed to rank various optimisation algorithms with respect to this parameter. Its utility is illustrated by considering the following simple example (Fig 2-12). Assume that an objective function is described by the function **1/x**. This is to be compared with a second function **1/x+RANDOM(-0.5; 0.5)** which adds a random value drawn from a uniform distribution between -0.5 and 0.5 to the original function **1/x**.

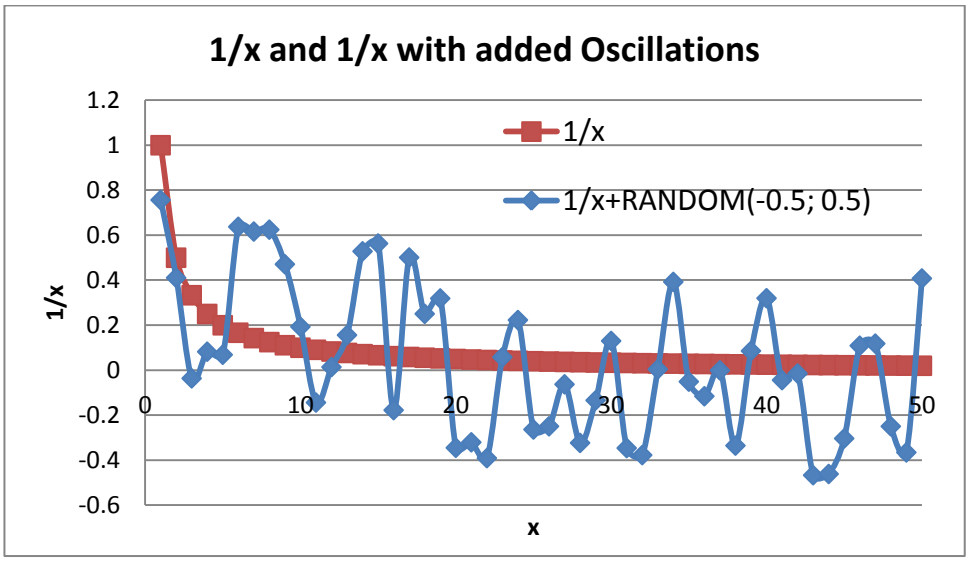


*Figure 2-12* ***1/x*** *and* ***1/x+RANDOM(-0.5; 0.5)*** *functions in interval from 1 to 50*

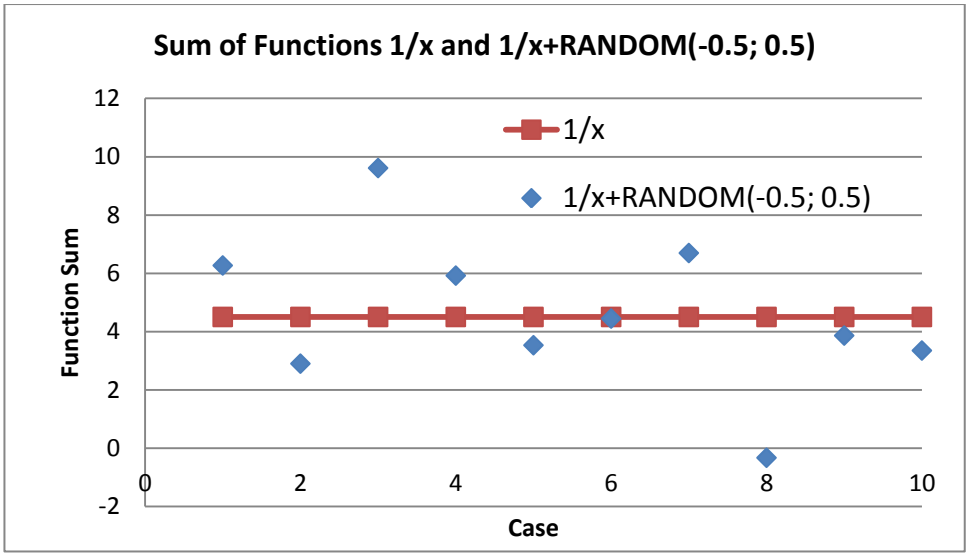


*Figure 2-13 Comparison of the Sum of Functions* ***1/x*** *and* ***1/x+RANDOM(-0.5; 0.5)*** *for 10 cases*

The cumulative sum of the values for the **1/x** function for the values of **x** between 1 and 50 is equal to 4.5. Figure 2-13 depicts the cumulative sum of the values of the function

**1/x+RANDOM(-0.5; 0.5)** for 10 trials. It can be seen that the variation of the sum for **1/x+RANDOM(-0.5; 0.5)** is significant, even though the average value for 10 cases equals 4.62 and is close to the sum of the original function **1/x**. This illustrates how oscillation near to the optimal solution of values of the oil rates or revenue can result in significant changes in the cumulative values.

A smoothness coefficient *SC*, has been defined to allow comparison of the extent of the oscillations (or smoothness) present in the results from different optimisation methods:

$$SC = \frac{\sum_{t=1}^{N-1} \left| \frac{\text{Revenue}_{t+1} + \text{Revenue}_{t-1}}{2 \cdot \text{Revenue}_t} - 1 \right|}{N} \qquad (2\text{-}6)$$

where $\text{Revenue}_t$ is a Revenue at time step $t$ calculated by formula *2-3*, $N$ is a total number of time steps.

For the above example:

*SC (1/x) = 0.0152 and*

*SC (1/x+RANDOM(-0.5; 0.5)) = 8.603*

Indicating that **1/x** is much smoother than **1/x+RANDOM(-0.5; 0.5).**

## 2.7 Summary

This chapter reviewed the optimisation strategies from literature and specified the criteria for the optimisation algorithm choice.

The uncertainty analysis requires a fast and robust optimisation method. All methods can be divided into two groups: reactive and proactive. Proactive methods can increase the recovery factor and provide a global optimum. However, they are usually more complex than reactive methods and require significantly greater computational resources. Reactive methods are the preferred workflow during the uncertainty investigation.

All algorithms were ranked based on four criteria: speed, stability, availability and capability for using them for discrete position and On/Off ICVs optimisation. *Direct Search* and control methods based on water cut threshold show the highest score in terms of the run time and stability.

The next chapter will analyse the performance of WC threshold-based algorithm for uncertainty investigation. This algorithm has not only received the highest score but also can be easily realised in reservoir simulation software.

# Chapter 3 - Impact of an Intelligent Well Completion Controlled by Threshold-Based Algorithm on the Oil Production Uncertainty

This chapter describes a workflow for the static and dynamic parameters uncertainty analysis. It compares intelligent and conventional completions for two scenarios: liquid rate and pressure constrained.

The impact of an intelligent completion on production uncertainty is investigated in this chapter. ICVs were controlled with the simple reactive strategy based on the WC from each well's segment.

Birchenko and others in their work (Birchenko, Demyanov et al. 2008) examined the impact of choking by an IW's ICVs on the geological uncertainty attributed to the statistical distribution of the formation's properties. It was found that using ICVs can reduce the production uncertainty up to 50% (Fig 3-1) for the limited liquid rate scenario.

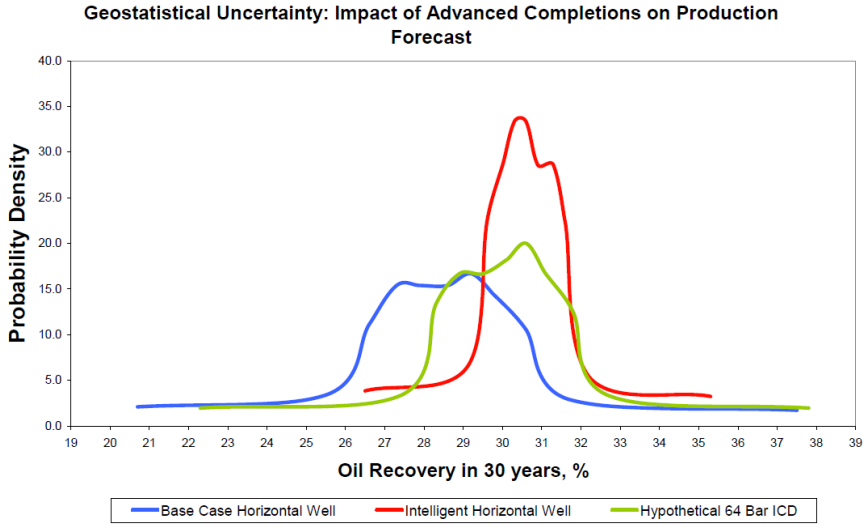


*Figure 3-1 Probabilistic Comparison of the Oil Production Forecast (after Birchenko)*

This study has been extended to the "dynamic" parameters such as fluid contacts, relative permeabilities, aquifer strength and zonal skin.

## 3.1 Intelligent Completion Model

The performance of an IW was simulated using the commercial reservoir simulator *Eclipse 100*$^{TM}$ (Schlumberger 2009). The multi-segment option was used for modelling the fluid flow from the reservoir grid to the tubing via the ICVs (Fig. 3-2). Fluid is allowed to move freely between certain annulus segments and then passes into the tubing via the ICV.

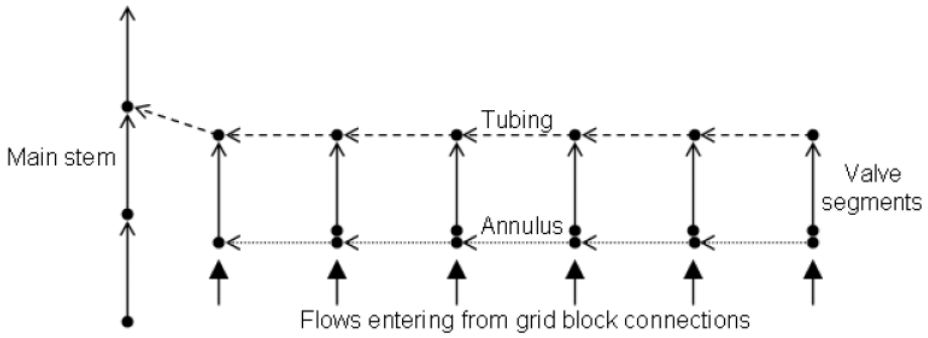


*Figure 3-2 Schematic of a multi-segmented well after (Schlumberger 2009)*

The well segment inflows are controlled at each simulation step with a productivity multiplier $a_i$:

$$J_i = a_i \cdot J_i^0 = \left( \frac{1 - WC_i}{1 - WC_{\min}} \right)^B \cdot J_i^0 \qquad (3\text{-}1)$$

where i is the interval number; $J_i$ - productivity index of zone i; $J_i^0$ – initial productivity index of zone i; $WC_i$ – zonal water cut; $WC_{min}$ – minimal zonal water cut and $B$ – a scalar coefficient.

This strategy stronger affects zones with a higher WC and keeps an inflow with the minimal WC fully open. The coefficient $B$ can be chosen to provide the maximum value in each case.

The strategy was tested in two cases: PUNQS3 and AINSA II.

### 3.2 Case 1: PUNQS3 Reservoir Model

The PUNQS3 reservoir model is a publically available synthetic model (Floris, Bush et al. 2001) based on real field data from 6 vertical wells originally built by Elf Exploration Production. It has an aquifer, an impermeable fault at the east and south side of the field and a relatively weak gas cap at the centre of the model (Fig 3-3). The 3.2 x 5 km model is quite coarse, the cell size being 180 x 180 x 5 m. Its 1761 active cells result in a fast simulation time. The model is also quite heterogeneous. These two aspects make it popular with reservoir engineers when investigating the role of uncertainty.

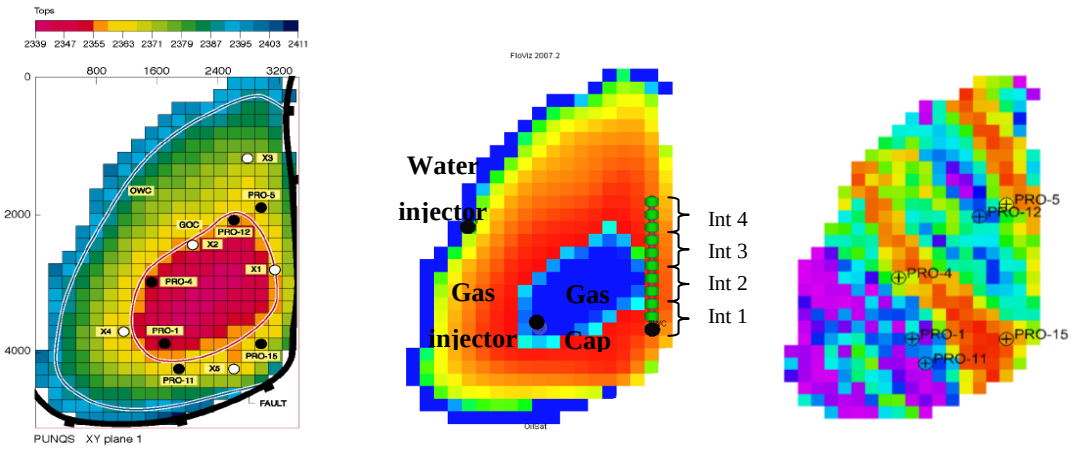


*Figure 3-3 Structure, wells location and permeability distribution of the PUNQS3 model (after Floris)*

Our development strategy for the PUNQ-S3 model called for production from a single horizontal well of 1800 m. length combined with two vertical injectors. The water injector helps to support the reservoir pressure in cases where the aquifer strength is insufficient to compensate for the volume of production while the gas injector returns any produced gas to the reservoir crest. The horizontal production well was drilled with a 8½" open hole for the base case. This was converted to an IW by installing 4 ICVs connected by a 3½" tubing installed in the 8½" open hole. The well production limits were a Liquid Rate ≤ 600 $m^3$/day and a BHP > 120 bar. This production limit equals the maximum total liquid rate of the six vertical wells in the original model. The injection wells are operated under BHP control at 300 bar.

A horizontal well was placed in the thickest oil bearing zone as far from water and gas sources as possible (Fig 3-4). This optimal well location chosen by a trial and error process delayed water and gas breakthrough and increased the recovery factor compared to all other, alternative locations tested.

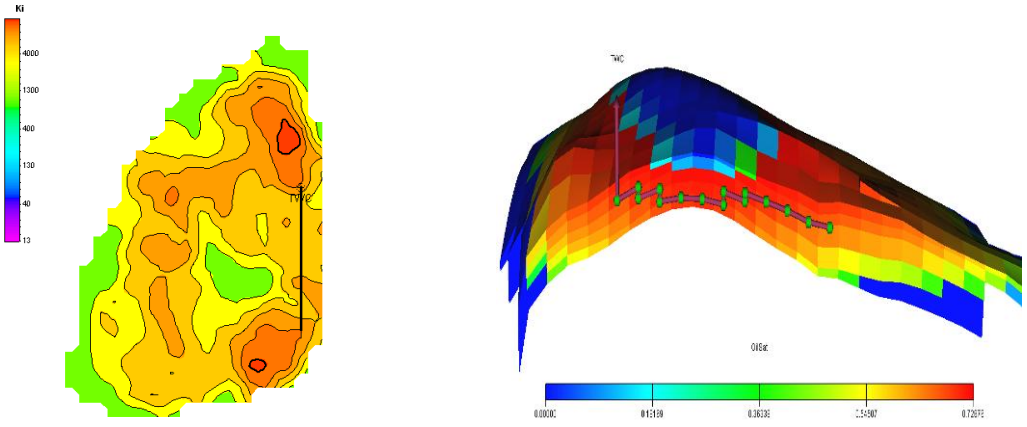


*Figure 3-4 The optimum horizontal well location*

### 3.3 Case 2: AINSA II Reservoir Model

The AINSA II model is based on the outcrop description (Stephen, Clark et al. 2002). A very detailed description of the facies location was available (Fig 3-5). The cell dimensions of the original model are 20 x 20 x 0.5 m. which were upscaled to 60 x 60 x 2 m. This level of upscaling retained a detailed description of the reservoir while limiting the model resolution to 43750 active cells.

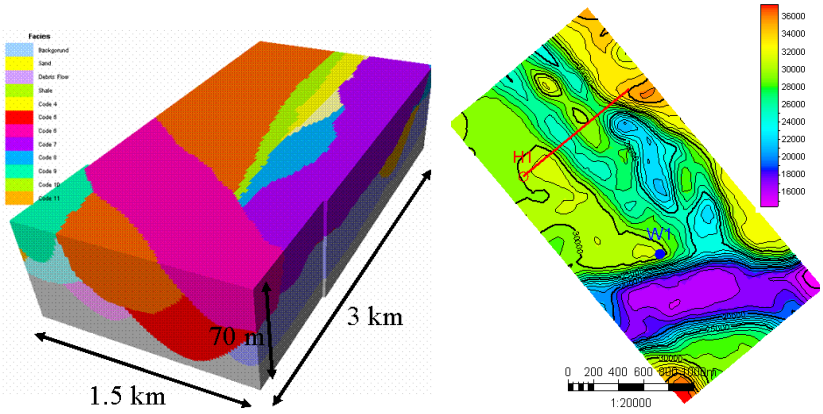


*Figure 3-5 The AINSA II model facies and the well locations*

A 1200 m. long horizontal production well and a vertical injection well complete the dynamic model. The production well was also restricted to a liquid production rate less than 1200 $m^3$/day while the injection pressure was also limited a BHP of 300 bar.

### 3.4 Geological Parameter Variation

One hundred realisations of the porosity and permeability distribution for the PUNQS3 model were made with a sequential Gaussian simulation algorithm based on data from the six original wells. The correlation length values and anisotropy in the orientation of each layer were randomly generated based on the parameters listed in Table 3-1.

The AINSA II geological model was originally built based on an outcrop description. Thirteen turbidity channels were carefully correlated and included in the initial model. A stochastic, object modelling method based on the variation of original channel parameters such as width, thickness and orientation was used to build one hundred realisations for this case.

*Table 3-1 Geological parameter variation of PUNQS3 model*

| | Range along | | Range across | | Angle | |
|---|---|---|---|---|---|---|
| **Layer** | **Lower limit** | **Upper limit** | **Lower limit** | **Upper limit** | **Lower limit** | **Upper limit** |
| 1 | 2000 | 5000 | 700 | 900 | 100 | 160 |
| 2 | 700 | 1300 | 700 | 1300 | -10 | 10 |
| 3 | 2000 | 5000 | 700 | 1300 | 100 | 160 |
| 4 | 500 | 5000 | 500 | 5000 | -10 | 10 |
| 5 | 2000 | 5000 | 700 | 900 | 100 | 160 |

## 3.5 Variation of the "Dynamic" Parameters

Variation of the "dynamic" parameters relative permeability, oil-water contact, gas-oil contact, aquifer strength and the formation damage skin for each interval are summarised in Fig 3-6 and Table 3-2:

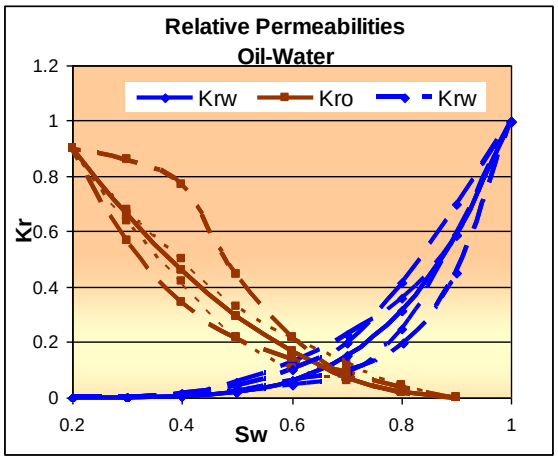


*Figure 3-6 Relative permeability functions*

*Table 3-2 Dynamic parameters variation*

| **Model** | **PUNQS3** | | | **Ainsa II** | | | **Distribution** |
|---|---|---|---|---|---|---|---|
| **Parameter** | **min** | **max** | **original** | **min** | **max** | **original** | |
| **AQUIPerm, mD** | 1 | 300 | 137.5 | 1 | 1000 | 200 | lognormal |
| **AQUIPoro, %** | 10 | 30 | 20 | 10 | 40 | 25 | normal |
| **GOC, m** | 2352.5 | 2357.5 | 2355 | - | - | - | normal |
| **OWC, m** | 2392.5 | 2497.5 | 2395 | 2425 | 2435 | 2430 | normal |
| **Skin effect Intervals 1-4** | 0 | 10 | 1 | 0 | 10 | 1 | triangular |

The shape, intersection and critical points for the oil and water relative permeabilities were changed when modelling their variation (Fig. 3-6). Aquifer porosity, OWC and GOC have a normal distribution with a mean value equal to that of the original case. The aquifer response usually has a large uncertainty associated with it, especially during the early stages of the field development. We therefore used a lognormal distribution for the aquifer permeability to allow for high aquifer strength.

A skin is often observed in wells due to drilling and completion formation damage. Its severity can be different in the various parts of the well; hence we decided to vary the skin value at the zone level in our model. It was assumed that an effective, well clean-up procedure had been employed to minimise this skin value; hence the minimum skin value was set to 0 and the maximum value was 10, with a triangular distribution between these values and the most probable value skin value of 1.

### 3.6 Experimental Design

Calculations employing many realisations with different values for the uncertain parameters are required to evaluate the production uncertainty. This approach identifies which parameters have greater influence on the production response and provides an estimate of the possible range of the results. However, this method becomes computationally expensive when the number of the parameters is high. For example, evaluation of our 5 uncertain "dynamic" parameters with 10 intermediate points for each parameter requires running $10^5$ realisations, a time consuming process for even a simple model. Manceau and other (Manceau, Mezghani et al. 2001) introduced the experimental design technique coupled with a response surface methodology (RSM) and found it to be an efficient and rigorous methodology to accurately quantify the impact of reservoir uncertainties on production forecasts. This approach was therefore used for uncertainty evaluation in this work.

Sensitivity analysis to variation of the "dynamic" parameters for both models was performed with the *Cougar*$^{TM}$ software. This software allows selection from a large number of experimental design methods (Schlumberger 2009): Full Factorial, Placket-Burman, Central Composite, D-Optimal, Space Filling and Latin Hypercube. They differ in the approach used to select specific values from all possible scenarios. Figure 3-7 illustrates 4 different approaches being used to analyse a three parameter case.

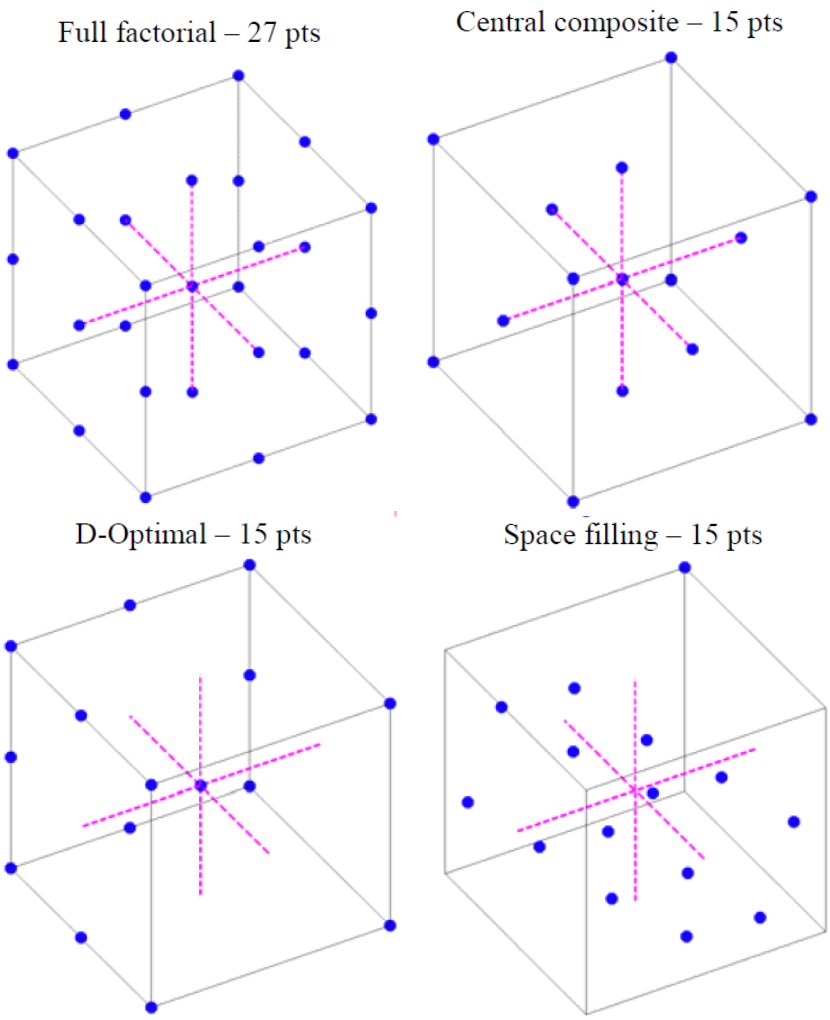


*Figure 3-7 Comparison of four methods employed to fill the parameter space for three variables (after Yeten(Yeten, Castellini et al. 2005)).*

A response surface is an approximation of the real response from the simulation model such as oil or water production, recovery factor or NPV to changes in the parameter values. The advantage of RSM is that it dramatically reduces the time-consuming model simulation work. The RSM can be built with different methodologies: kriging, splines, neural networks and least squares. The last method uses a representative function such as linear, quadratic or higher level polynomials, exponential, power functions, etc. to approximate the real result; thus allowing a confident estimation of the results for the parameter values that lie within the design space, but were not actually simulated.

Yeten and other have investigated different types of experimental design and RSMs based on three different cases (Yeten, Castellini et al. 2005). They found that central composite design showed a satisfactory performance for all the cases studied. Specifically, they found a better response and more accurate result than the D-Optimal design with similar density of calculation points. In addition, a quadratic polynomial RSM had a similar accuracy and capability to estimate the effect of changes in the

parameter's values when compared with more complex response surfaces for all three cases.

Their result corresponds with *Cougar*$^{TM}$ help file's recommendation of using "Small Face Centred Composite Design" (SFCCD) as the best quadratic experimental design method for variation of the selected parameters. Their recommendation has been confirmed for the case studied here by comparing the predictive quality of SFCCD with the "Latin Hypercube Design" (LHCD). LHCD employes many more realisations (1000), compared to the 51 realisations required by SFCCD for 9 independent parameters. The parameter values for the 1000 LHCD realisations were randomly selected according to their probability distribution; while the final distribution for SFCCD was derived using 1000 realisations based on the 51 experimental calculated results and a Monte-Carlo type selection of the input parameter's probability distribution.

Table 3-3 shows that the results for both methods are similar; SFCCD gave equally accurate results with a more than 95% reduction in the calculation time. Further, a comparison of the Response Surface built for the SFCCD results gave an almost perfect fit to the actual values.

Therefore "Small Face Centred Composite Design" (SFCCD) was used for analysing the impact of the above uncertainties on the production.

*Table 3-3 Comparison of the oil production for "Small Face Centred Composite Design" and "Latin Hypercube Design"*

| Case | Mean, $m^3$ | Standard Deviation, $m^3$ | Variation | Calculation time, hours:minutes: seconds |
|---|---|---|---|---|
| "Small Face Centred Composite Design" | 4474000 | 383200 | 8.6% | 00:27:07 |
| "Latin Hypercube Design" | 4394000 | 366700 | 8.3% | 09:28:07 |
| Difference | 1.8% | 4.5% | 0.3% | 09:01:00 or 95% |

## 3.7 Results and Discussion

The results of the oil water production distribution for PUNQS3 and AINSA II model are shown in Figs. 3-8 and 3-9 and Table 3-4.

The variation in Table 3-4 was calculated by formula 3-3:

$$Variation = \frac{P10 - P90}{P50} \qquad (3\text{-}2)$$

where P10 is an optimistic estimation representing 10% of the cases which value higher than this number, P50 is the most likely value and P90 represents the lower and the

most certain margin from deterministic approach with 90% of the cases higher than this value.

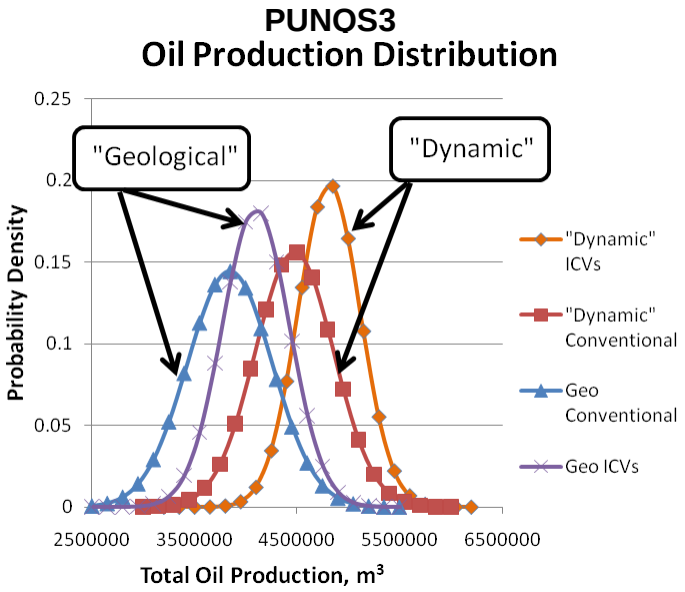


*Figure 3-8 Total oil production distribution for the conventional and IW cases, PUNQS3*

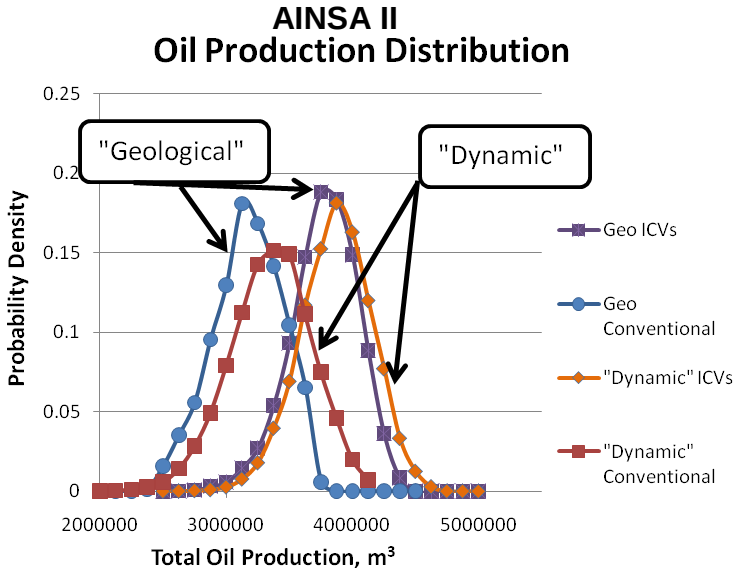


*Figure 3-9 Total oil production distribution for the conventional and IW cases, AINSA II*

*Table 3-4 Total oil and water production (MM m3) variation for conventional and IW cases*

| | Model | | PUNQS3 | | | | Ainsa II | | | |
|---|---|---|---|---|---|---|---|---|---|---|
| | Case | Uncertainty | P50 | P90 | P10 | Variation | P50 | P90 | P10 | Variation |
| Oil Production | Base Case | Geological | 3.91 | 3.31 | 4.35 | 26.6% | 3.12 | 2.73 | 3.46 | 23.4% |
| | | Dynamic | 4.55 | 3.9 | 4.92 | 22.4% | 3.14 | 2.63 | 3.59 | 30.6% |
| | ICV | Geological | 4.16 | 3.66 | 4.52 | 20.7% | 3.73 | 3.37 | 4.04 | 18.0% |
| | | Dynamic | 4.87 | 4.42 | 5.15 | 15.0% | 3.81 | 3.44 | 4.16 | 18.9% |
| Water Production | Base Case | Geological | 2.57 | 3.17 | 2.13 | 40.5% | 9.75 | 10.1 | 9.41 | 7.1% |
| | | Dynamic | 1.93 | 2.58 | 1.56 | 52.8% | 9.73 | 10.2 | 9.28 | 9.5% |
| | ICV | Geological | 2.32 | 2.82 | 1.96 | 37.1% | 9.14 | 9.5 | 8.83 | 7.3% |
| | | Dynamic | 1.61 | 2.06 | 1.33 | 45.3% | 9.06 | 9.43 | 8.71 | 7.9% |

IW achieves a reduction in both cases for the oil production variation caused by geological and dynamic uncertainty. Moreover, for this development strategy, IW increases the average oil production by approximately 6% for PUNQS3 and 20% for the AINSA II model when compared with the conventional case. Additionally, it decreases the absolute value of the average water production as well as its variation. This is also important because it reduces both the uncertainty in the required size of the surface facilities (reduced capital cost) as well as the operational cost of water recycling.

It is significant that the mean value of the total oil production is larger for the dynamic rather than the geological uncertainty cases for the PUNQS3 model. This occurs because the production well has been located in an optimum position in the original model. Therefore, any changes in the geological properties tend to reduce the oil production. This example shows the importance of employing an uncertainty investigation when analysing for the optimum well location and development strategy.

The next question to be answered was to try and understand when an IW completion is capable of reducing the impact of uncertainty on the volume of hydrocarbon produced.

### 3.8 IW Efficiency for Reducing the Impact of Uncertainty

Variation of the productivity index (PI) was analysed and compared for the PUNQS3 model for both the IW and conventional cases. Firstly, the PI multipliers were changed from 0.3 to 3 for each of the 4 intervals of the horizontal well (Fig 3-10a). In a second study, this PI variation was only implemented in the 4$^{th}$ interval. This interval has the highest water cut and is the most regulated (choked) by the IW completion.

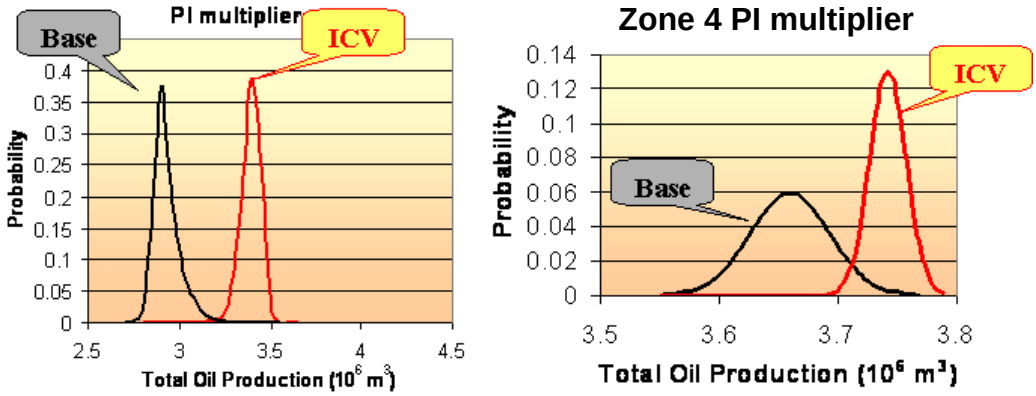


a b

*Figure 3-10 Comparison of the impact of the uncertainty in the PI multiplayer on the oil production a) for all intervals and b) for the 4$^{th}$ interval only, PUNQS3*

Fig. 3-10 shows that the intelligent well increases the production compared to the conventional well, but has little impact on the associated uncertainty when it is evenly

distributed across the well. The result changes dramatically if the uncertainty is concentrated in only one part of the well (Fig. 3-10b).

The impact of different levels of uncertainty can also be illustrated for the geological uncertainty analysis. The toe area of the horizontal well becomes more uncertain than the heel if wells PRO-5 and PRO-12 are excluded from the geological model building process (Fig. 3-11). Both the average volume of oil and the uncertainty associated with it hardly changes for an IW completed with an ICV, while the conventional well shows a reduced recovery with an increase in the impact of uncertainty of a factor 2 (Table 3-5).

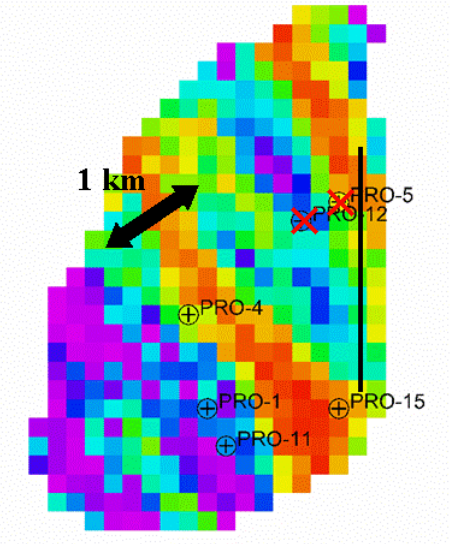


*Figure 3-11 Well data location for the geological parameters distribution. PUNQS3 model*

*Table 3-5 Cumulative oil production variation for geological parameters distribution with and without well's information from near the toe of the horizontal well*

| Cumulative Production, MM $m^3$ | | | | | | | | |
|---|---|---|---|---|---|---|---|---|
| **Case** | **With well data from near the horizontal well's toe (original model)** | | | | **Without well data from near the horizontal well's toe** | | | |
| | P50 | P90 | P10 | Variation | P50 | P90 | P10 | Variation |
| Base Case | 3.91 | 3.31 | 4.35 | 26.6% | 3.79 | 3.11 | 4.47 | 35.9% |
| ICV | 4.16 | 3.66 | 4.52 | 20.7% | 4.22 | 3.84 | 4.59 | 17.8% |

Another situation where different levels of uncertainty within the reservoir impact the production is water or gas coning. A horizontal well designed for oil production is normally drilled above the water contact, below the gas cap or within the oil rim. Water and gas inflow into such a well can be affected by several forms of heterogeneity, e.g. a varying productivity in different parts of the well caused by formation damage skin, reservoir permeability or the heel-toe effect. This latter problem may be solved by completing the well with ICDs.

A second reason for heterogeneity in the breakthrough time of unwanted fluids is a variable distribution of thin shale layers (or baffles) which are preventing / hindering vertical flow in different parts of the reservoir. This problem is often only discovered after production has commenced. A well intervention for preventing production of an unwanted fluid at this time is normally expensive (at least in terms of lost oil production).

In our example there was a shale barrier below the third interval in AINSA II model (Fig 3-12). In the original model it had zero vertical permeability, i.e. it was a barrier. However, such thin shaly layers often allow some vertical fluid flow, i.e. they behave as a baffle rather than an absolute barrier. Hence we analysed the impact of variation of the vertical permeability of this (originally shale) layer on the oil and water production.

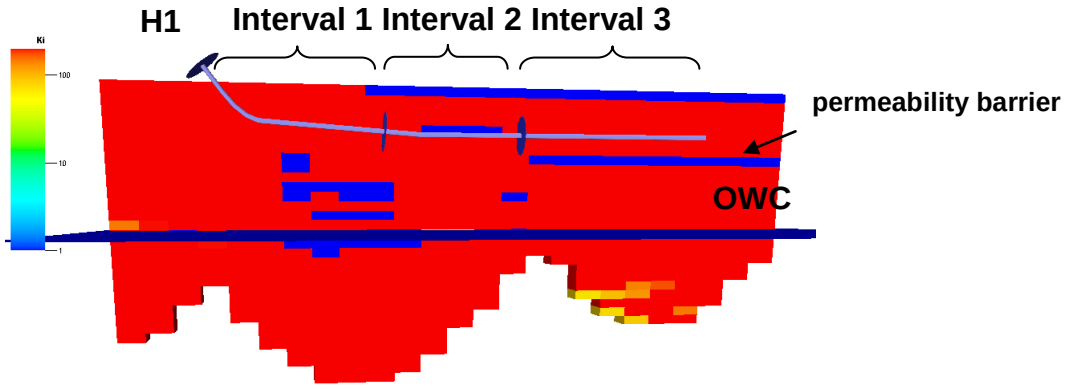


*Figure 3-12 Horizontal well location and permeability barrier below third interval. AINSA II model*

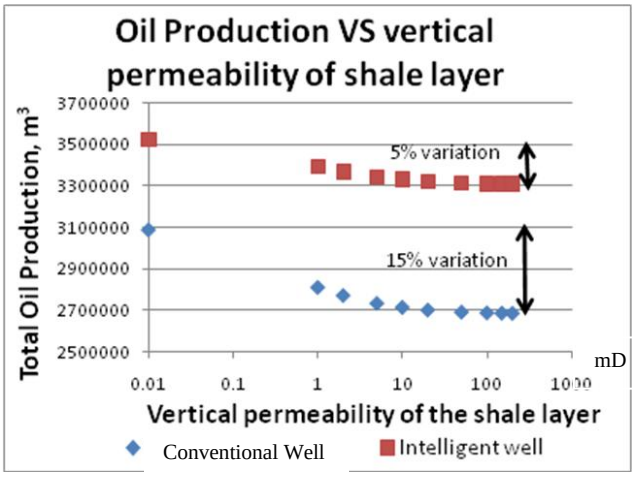


*Figure 3-13 Oil production variation depends on (shale) barrier permeability*

Fig. 3-13 shows that even a relatively limited vertical permeability across the shale layer has a dramatic impact on the produced oil volume and the time when the water breaks through into the well. For instance, a change of vertical permeability from 0.01 mD to 1

mD reduces the oil production by 9% for conventional well and by only 3 % for the IW. In addition, the accompanying uncertainty of the IW case is reduced to 33% of that shown by the conventional completion.

### 3.9 Impact of the Control Parameters and Optimisation Strategy

The development strategy chosen in a specific case will depend on the field type, location, reserves and many other parameters. The uncertainty reduction effect is dependent on the field development strategy employed.

In the previous study the liquid rate constraint was used for production control. A relatively simple control strategy can be employed in this case. Zones and/or wells with the highest WC can be closed or choked, until the maximum liquid production is reached. This strategy provides minimum water production with a constrained total liquid rate implying that the total oil rate is maximum at this time step. However, normally faster production is preferred by operators by employing a more aggressive development strategy where wells are controlled by pressure instead of liquid rate.

This strategy was applied now in PUNQS3 reservoir, where the well production is to be controlled by (BHP and THP) pressure limits without any rate constraints.

Smart completions, with their central tubing, will intrinsically impose an additional pressure drop in comparison with a conventional well constructed with a similar borehole diameter. Pressure control (BHP or THP) of a well with a smart completion will therefore produce less fluid than the equivalent conventional well. Additional value generate by an intelligent well will therefore depend, in this case, on the ability to optimise the oil production by decreasing the volumes of (unwanted) gas and/or water being produced.

A quick look nodal analysis procedure was implemented for the PUNQS3 model. The horizontal well was modelled in PROSPER while the Kuchuk & Goode model was used to calculate the Inflow Performance Relationship (IPR) curve for the conventional well and an intelligent well equipped with either 3.5 in. or 4.5 in. ICVs (Fig 3-14).

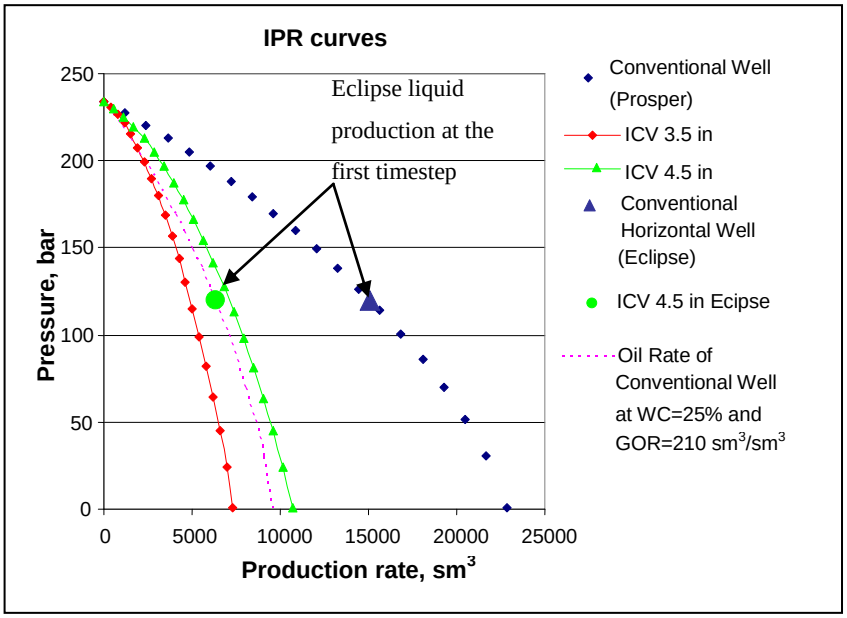


*Figure 3-14 IPR curves for the horizontal well in the PUNQS3 model*

Liquid production at the first time step from the original *Eclipse* model with 120 bar BHP control shows that the above analytical models are sufficiently accurate. The analysis also shows that the conventional horizontal well's production equals the initial liquid production for an Intelligent Well (IW) when the conventional horizontal well is producing with a Water Cut (WC) of 25% and a Gas Oil Ratio (GOR) of 210 $sm^3/sm^3$ (these are the average values for the conventional well development during the 10 years of field production period).

Production of an equivalent volume of oil to the conventional well requires that the IW prevents all this water and gas flowing into the well. However, the choking action required to achieve this will create an additional pressure drop on some of the producing intervals; an action which will lead to an additional decrease in the oil.

For the dynamic model THP = 10 bar was used as a constraint. Artificial (gas) lift was provided to increase the oil production and prevent well shutdown at high water cut. The fixed injected gas volume of $100*10^3$ $Sm^3$/day was used for the gas lift. Figure 3-15 shows that this value is reasonably optimal for different values of WC.

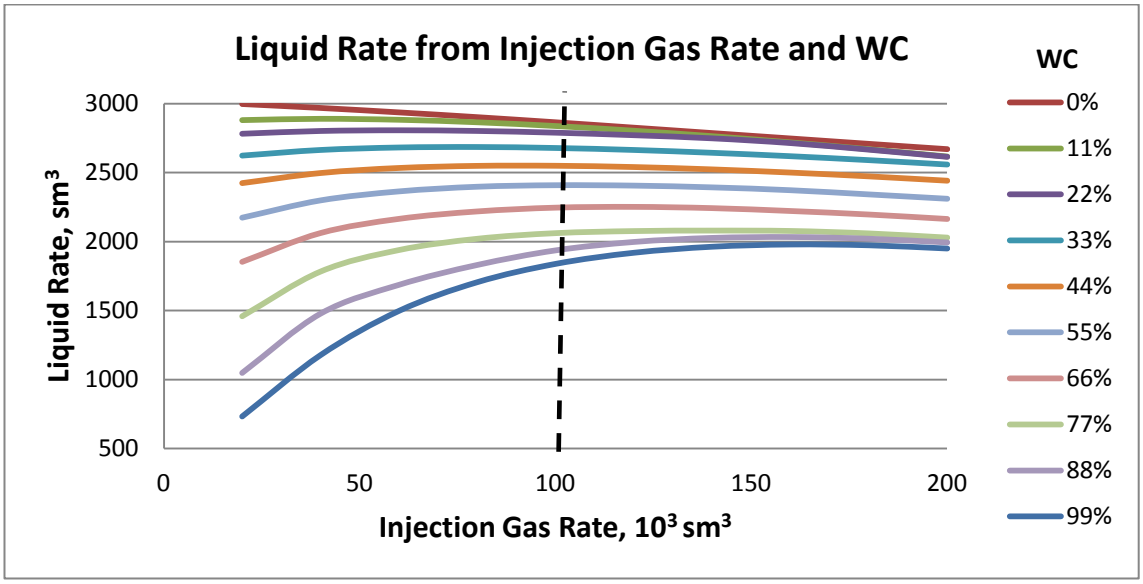


*Figure 3-15 Operating rate depending on GL injection rate and WC*

The total oil production over a 30 year period with a pressure constrained strategy increased by more than 50% (Fig 3-16). The difference in oil and water rates and cumulative production for conventional and intelligent completions is shown in Fig.3-17, 3-18 and Table 3-6.

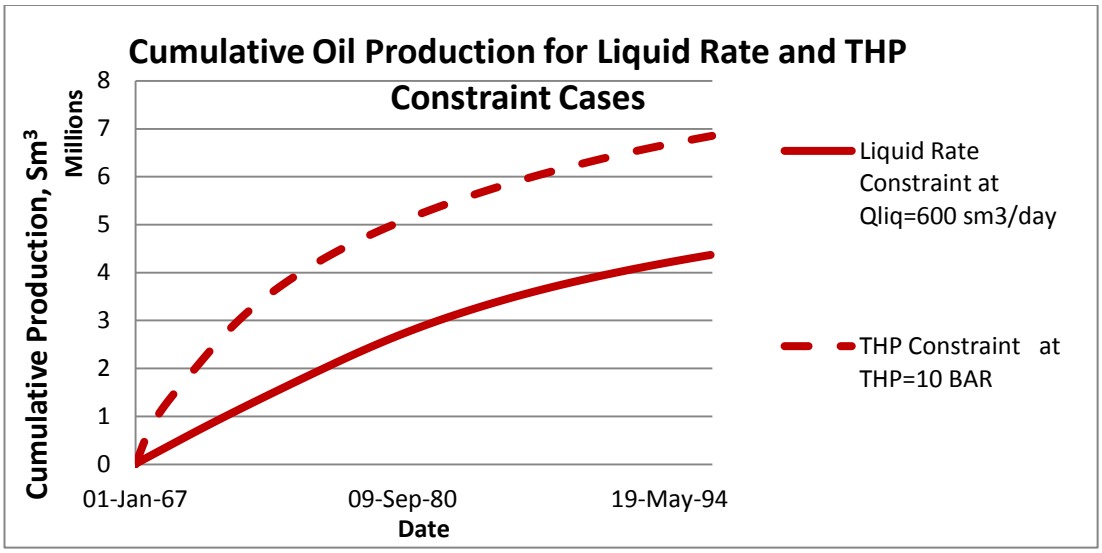


*Figure 3-16 Cumulative Oil Production for Liquid Rate and THP Constraint Cases*

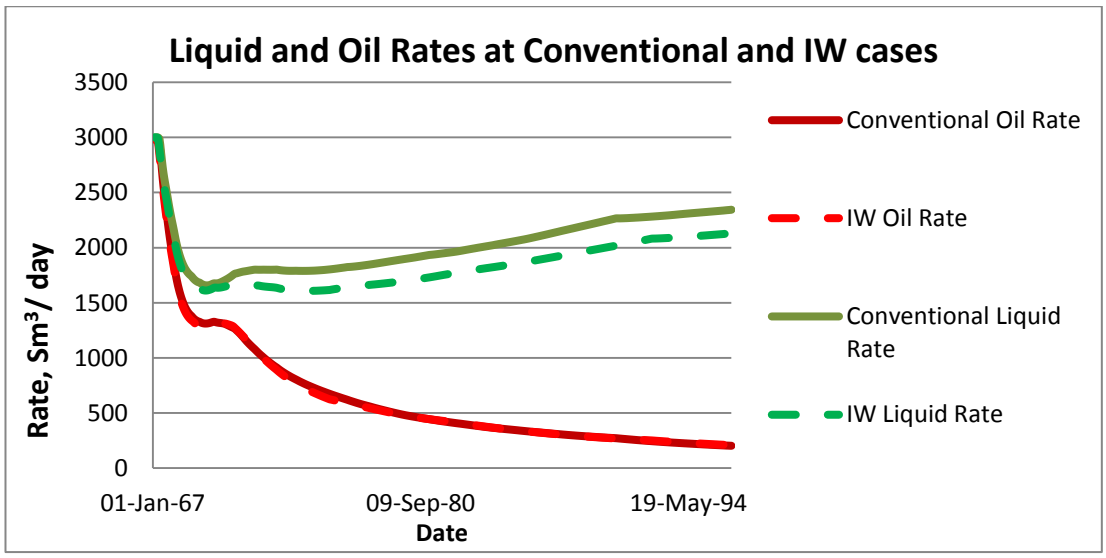


*Figure 3-17 Liquid and Oil Rates at Conventional and IW cases*

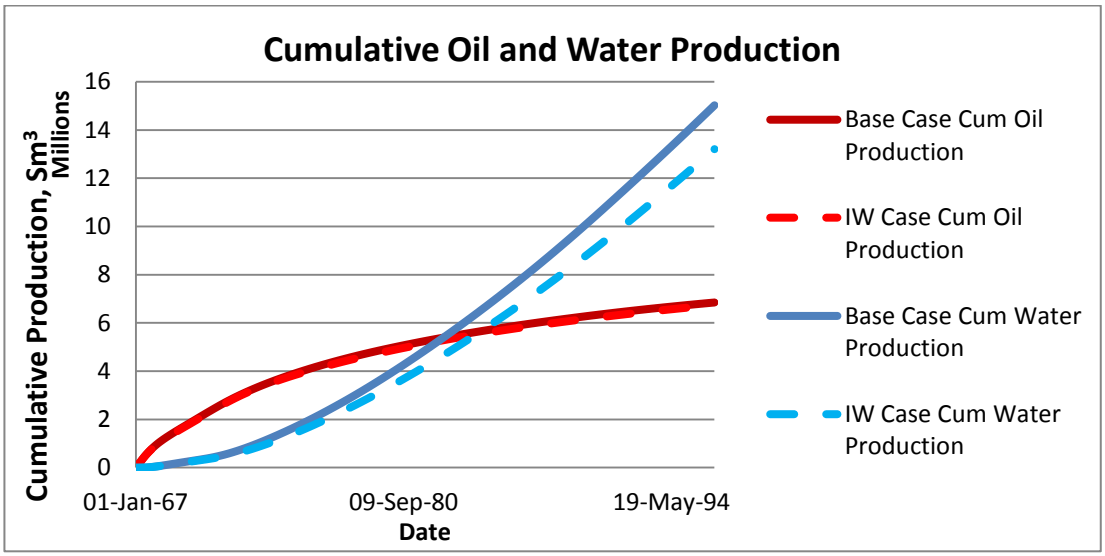


*Figure 3-18 Cumulative Oil and Water Production at Conventional and IW cases*

*Table 3-6 Cumulative NPV, Oil and Water Production at Conventional and IW cases*

| Case | Conventional | IW | Difference |
|---|---|---|---|
| **Cumulative Oil Production, Million sm$^3$** | 6.99 | 6.87 | -1.7% |
| **Cumulative Water Production, Million sm$^3$** | 16.17 | 14.21 | -12.1% |
| **NPV, Million $** | 1139 | 1117 | -1.9% |

Use of intelligent completion with the previous control strategy reduced the total water production by 12%. The cumulative oil production and NPV were also reduced by 1.7% and 1.9% correspondingly. Reduced NPV and oil production makes it difficult to justify using an intelligent completion for the pressure constraint scenario. In fact, almost all published reporting an increased oil production from intelligent wells used liquid rate as the production constraint.

### *3.9.1 Sensitivity to a Grid Resolution*

The result of a model simulation depends on the grid resolution. Fig. 3-19 demonstrates that a model with a smaller grid size has sharp water front and faster water propagation in a high permeable layer than the less detailed realization.

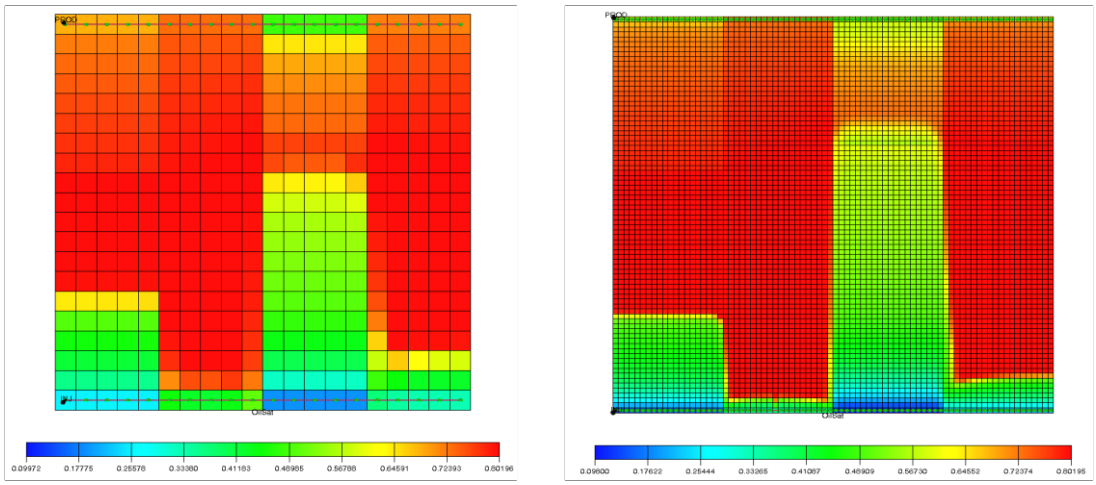

*a* *b*

*Figure 3-19 Water Front Propagation in (a) Coarse and (b) Refined Models*

In the PUNQS3 case, the initial model has a quite coarse grid size equal 180 x 180 x 5 m. which may affect on the water front propagation and reduce the value of IW. The grid size has been refined by 4 times in both X and Y directions and 5 times in a vertical direction. Thus, the new refined model has a 45 x 45 x 1 m cell size, which is similar to a usual geological model resolution. The number of active cells in this model is equal 140880 which is still appropriate for a dynamic simulation run.

Table 3-7 demonstrates the difference between cumulative values in the original and refined cases. The water propagates faster in the refined case which results in higher cumulative water injection and production. However, it should be noticed that the relative permeabilities have not been rescaled in this case, which could help to avoid this effect.

*Table 3-7 Cumulative NPV, Oil and Water Production at Conventional and IW cases in Refined model*

| Parameter | Original | Refined | Difference |
|---|---|---|---|
| Cum. Oil Production, Million $sm^3$ | 6.99 | 7.27 | 3.96% |
| Cum. Water Production, Million $sm^3$ | 16.17 | 19.26 | 19.10% |
| Cum. Water Injection, Million $sm^3$ | 21.38 | 23.35 | 9.23% |
| Run Time, sec | 13 | 1782 | 137 times |

More important for our study is that the IW demonstrates the same result comparing to the conventional completion than in the original case (Table 3-8). Therefore, the original grid size will be used for the further uncertainty analysis, considering that it

runs significantly faster. However, in general, the possible impact of the model upscaling on the results of the uncertainty analysis should not be ignored.

*Table 3-8 Cumulative NPV, Oil and Water Production at Conventional and IW cases in Refined model*

| Case | Conventional | IW | Difference |
|---|---|---|---|
| **Cumulative Oil Production, Million $sm^3$** | 7.27 | 7.14 | -1.79% |
| **Cumulative Water Production, Million $sm^3$** | 19.26 | 16.81 | -12.72% |
| **NPV, Million $** | 1173 | 1144 | -2.48% |

### *3.9.2 Statistical Analysis*

Statistical analysis was made for 100 realisations representing geological uncertainty of PUNQS3 model. The results are summarised in Fig.3-20, Table 3-7 and Table 3-8. The mean value of NPV and production for IW scenario is 4.5% less than for conventional well. Moreover, the intelligent completion reduces water production by 26%. This may make intelligent well attractive depending on the economic and production scenarios. The variation of oil production has not changed for IW case. The variation of water production has increased, because the mean value of cumulative water production has decreased, while the difference between P10 and P90 is approximately the same as in base case.

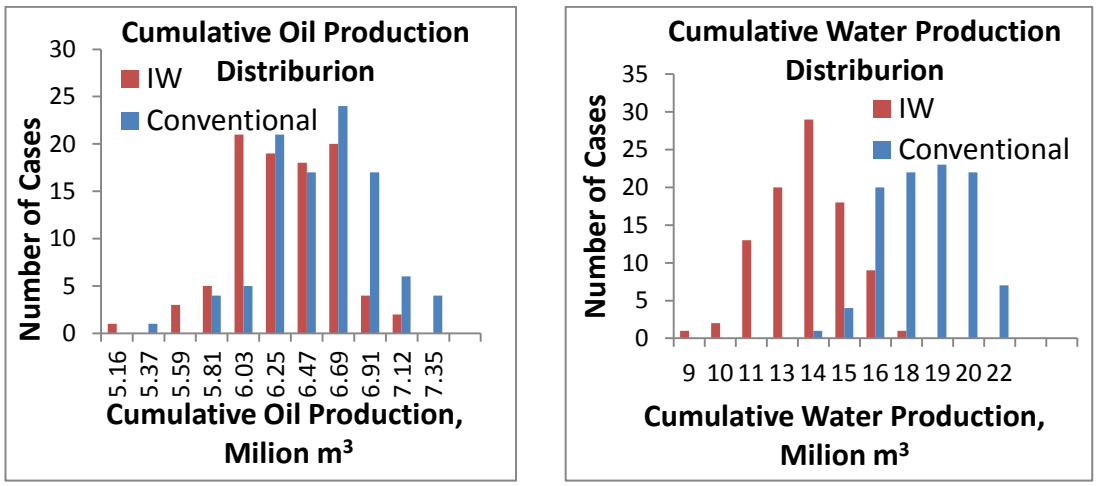


*a* *b*

*Figure 3-20 Distribution of Cumulative (a) Oil and (b) Water Production due to Geological Uncertainty in the PUNQS3 case with Conventional and I-Wells*

*Table 3-9 Total oil and water production (MM $m^3$) variation for conventional and IW cases*

| Parameter | Case | P50 | P90 | P10 | Variation |
|---|---|---|---|---|---|
| **Cumulative Oil Production, Million $m^3$** | **Conventional** | 6.51 | 6.06 | 6.88 | 13% |
| | **IW** | 6.22 | 5.83 | 6.66 | 13% |
| **Cumulative Water Production, Million $m^3$** | **Base Case** | 17.92 | 15.74 | 19.94 | 23% |
| | **ICV** | 13.19 | 10.83 | 15.29 | 34% |

*Table 3-10 P50 of Cumulative NPV, Oil and Water Production at Conventional and IW cases*

| Case | Conventional | IW | Difference |
|---|---|---|---|
| **Cumulative Oil Production, Million $sm^3$** | 6.51 | 6.22 | -4.5% |
| **Cumulative Water Production, Million $sm^3$** | 17.92 | 13.19 | -26.4% |
| **NPV, Million $** | 982 | 939 | -4.4% |

## 3.10 Conclusion

The workflow to investigate the ability of an intelligent well with active interval control valves to manage uncertainty in the geological and "dynamic" parameters uncertainty was demonstrated in this chapter.

Uncertainty in the "dynamic" parameters gives a comparable (or even larger) variation in the total oil production than the uncertainty associated with the "static" reservoir properties distribution. Both sources of uncertainty cannot be ignored and should be analysed at the same time in order to evaluate the total impact of uncertainty on the expected production.

Applying the *liquid production limit* strategy to IWs gave an increased volume of oil produced coupled with a decrease in its variation. In addition, the total volume of water production and its variation was also decreased.

The IW's ability to reduce the oil and water production variation increases if different levels of uncertainty are shown within the various completion zones. The impact of local variations in parameters such as (barrier) shale transmissibility, fault transmissibility, inflated OWC or GOC can be mitigated by the installation of completions employing IW technology.

The IW's success at increasing production and reducing the uncertainty was shown to be strongly dependant on the production strategy employed to control the well's operation.

An IW completion normally creates an extra pressure drop in the tubing installed across the length of the completion as well as across the downhole valves. An IW's production performance will thus be reduced when compared with that of a conventional well when the well's production rates are *constrained by pressure*. An example employing simple control strategy confirmed that less oil was produced by an IW in this situation. A more efficient control strategy thus should be used for this scenario.

In the next chapter we will analyse the SLP, SQP and Adjoint optimisation methods which are already available in commercial software.

# Chapter 4 - Available Optimisation Methods

This chapter describes the results of a pressure constrained IW optimisation by methods available in commercial software. The SLP and SQP algorithms have been implemented in PETEX Integrated Production Modelling (IPM) software. SLP is used in the RESOLVE module which connects all other modules together; allowing the optimisation to be applied to the whole system. By contrast, the SQP algorithm is implemented in a GAP module for optimisation of the production system. An Adjoint optimisation is performed in ECLIPSE 300.

## 4.1 Test Models

Two reservoir models were used for testing and comparing different optimisation methods. One of them is a simple "Box-shaped" model (Fig 3-11). The model size is 2000 x 2000 x 20 m (20 x 20 x 20 cells) and the total number of cells is 8000. It has 4 homogeneous blocks with different porosity and permeability (Table 3-5). It is assumed that there is no horizontal anisotropy, with the vertical permeability equalling 10% from horizontal value.

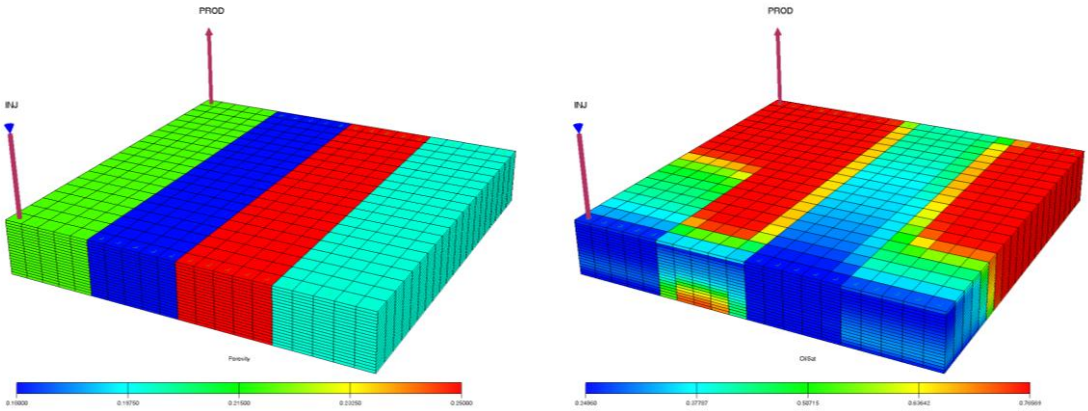


a b

*Figure 4-1 Porosity(a) and oil saturation at breakthrough time (b) of the boxed-shaped model*

*Table 4-1 Porosity and permeability of different zones*

| Parameter | Zone1 | Zone2 | Zone3 | Zone4 |
|---|---|---|---|---|
| Porosity, fraction | 0.22 | 0.18 | 0.25 | 0.2 |
| Permeability, mD | 200 | 20 | 1000 | 100 |

The reservoir conditions and fluid properties are summarised in Table 3-6. The relative permeabilities and capillary pressures are taken from PUNQS3 model.

*Table 4-2 Reservoir and fluid properties*

| Parameter | Value |
|---|---|
| Reservoir Depth | 2400 m |
| Reservoir Pressure | 245 Bar |
| Oil Gravity | 860 kg/m$^3$ |
| Gas Gravity | 0.83 sp. gravity |
| GOR | 74 Sm$^3$/Sm$^3$ |
| Water Salinity | 200000 ppm |
| Pb, Rs, Bo Correlation | Standing |
| Oil Viscosity Correlation | Beal et al |
| Reservoir Temperature | 93 deg C |

The model has one horizontal producer and one injector. Both of them are 2000 m long and located at the opposite edges of the model. The injector is controlled by bottom hole pressure BHP=270 bar. The producer is completed with ESP for avoiding well shutdown due to a high water cut and increasing liquid production. The well is constrained with WHP = 20 bar. It is vertical from the surface to the reservoir top and completed with 5.5 inches tubing.

The conventional completion is modelled with 7 inches open hole horizontal well. The intelligent completion has 5.5 inches tubing in the horizontal section which is divided by packers into 4 sections corresponding to the 4 blocks in the model. Each section is completed with an ICV with choke diameter adjustable from 0 to 0.1 m. The well is modelled in PETEX's GAP software. The well schematic is shown in Fig. 3-12.

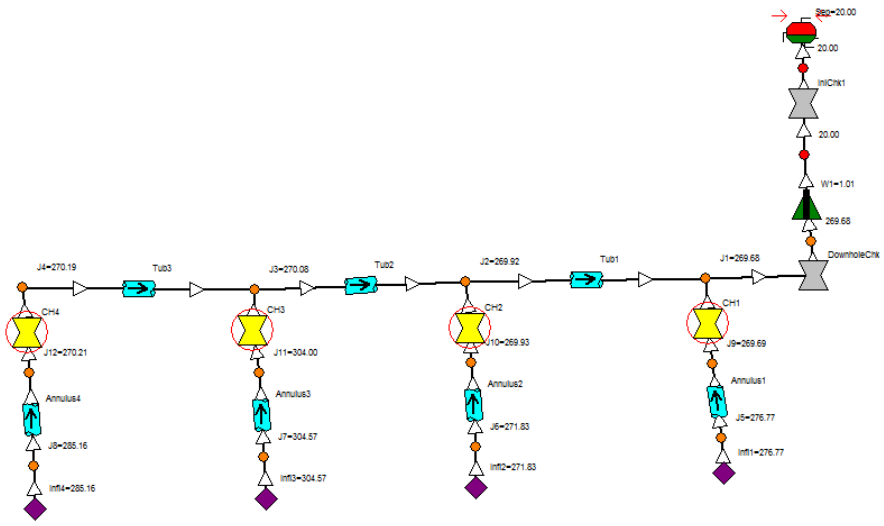


*Figure 4-2 Schematic of the horizontal intelligent well with 4 ICVs*

The advantages of the model are that it is simple and the run time is fast. The contrast in reservoir properties gives different breakthrough time which is easy to observe and

predict. Therefore, the optimal solution is easy to find and compare with result of the algorithm, which can be useful for the algorithm debugging.

The algorithms will be also tested in the PUNQS3 model, which is a more complex case and represents the heterogeneity of a real field.

## 4.2 Control and Optimisation Procedure

The cases described below employ an ECLIPSE reservoir simulator model coupled to GAP modelling of the well out-flow (Fig. 4-3).

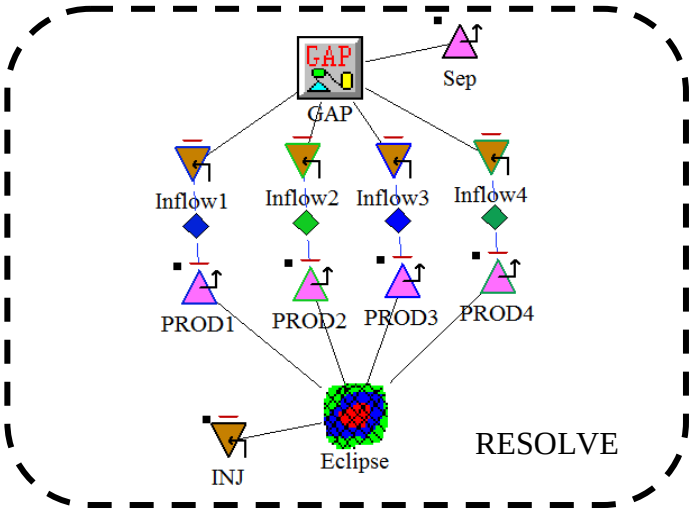


*Figure 4-3 Connection of reservoir dynamic model (Eclipse) and well production model (GAP)*

Two types of time steps can be distinguished when referring to a RESOLVE model (Fig. 4-4):

- The RESOLVE time steps are the times at which dynamic coupling between the applications take place: at this point in time data is passed from one application to another and results are written in RESOLVE
- The internal application time steps required by certain applications (i.e. the reservoir simulators) for convergence purposes. These time steps are respected during a model running in RESOLVE; however, a synchronisation will be performed at each RESOLVE time step. For example, if a one month time step is specified in RESOLVE, the numerical simulator will take as many time steps as needed during this one month period, but will be forced to provide information exactly after one month period for synchronisation the with production system in GAP and the optimiser.

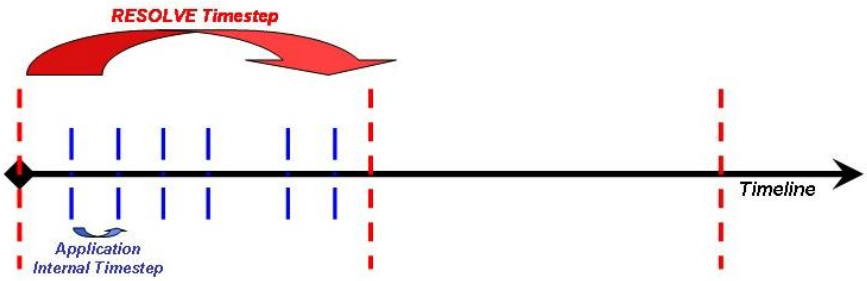


*Courtesy of Petroleum Experts*

*Figure 4-4 Relation between RESOLVE and applications internal timesteps*

During the synchronisation phase GAP solves the production system, GAP or RESOLVE (depending on the chosen algorithm) optimises production and finally RESOLVE defines the down hole control parameters, which are zonal liquid rates in our case, for ECLIPSE.

More details about GAP, RESOLVE and their interaction with the other modules can be found in Petroleum Experts User Guides (PETEX 2012).

The result of the simulation depends on the chosen time step. The larger time steps reduce the model run time; however, the result can be inaccurate. Three fixed time steps of 2 weeks, 1 month and 2 months has been analysed. An adaptive time step has also been chosen for comparing the different methods. This approach reduces the time step when the changes in the model are high and increases it once the changes are less significant; with the aim of providing a balance between the accuracy and the run time.

The objective function of the optimisation is an NPV and control variables are 4 ICV diameters for the 20 year production period.

## 4.3 Results of "Box-shaped" model

Figure 4-5 shows liquid, oil and water rates for the base case which employed a conventional well. The well and the zonal water cuts are illustrated in Fig. 4-6. Zone 3 has the highest permeability, 1000 mD, leading to early water breakthrough in this zone. This is followed a few months later by water production being observed in the neighbouring zones (2 and 4) which had been invaded by water from zone 3. Finally, after 12 years production, water arrives in zone 1 (permeability 200 mD).

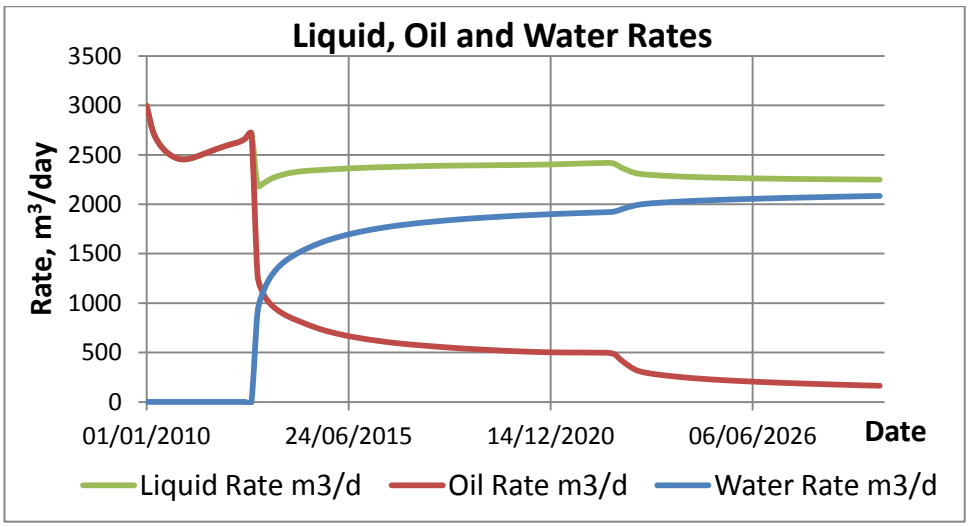


*Figure 4-5 Liquid, Oil and Water Rates of the Base Case*

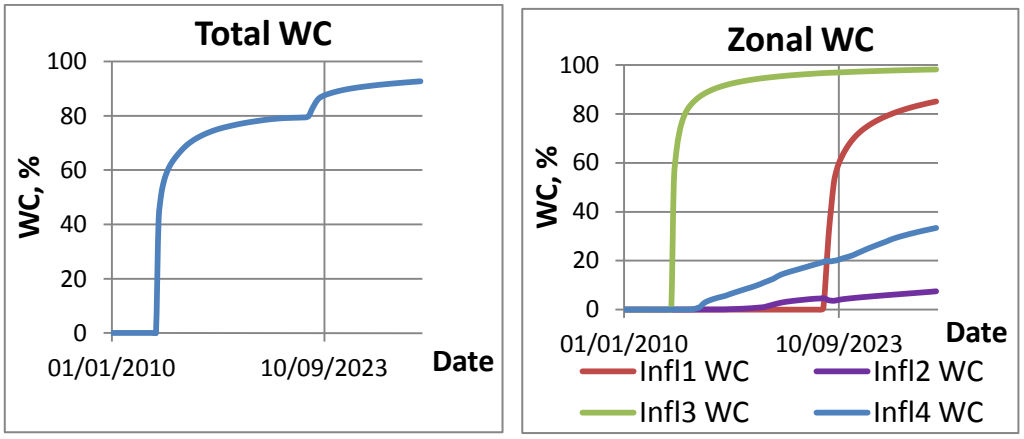


a b

*Figure 4-6 Total (a) and Zonal (b) Water Cuts of the Base Case*

Oil and water production rates for the IW case without optimisation (all ICVs fully open) are summarised in Fig. 4-7. The extra pressure drop caused by the tubing installed across the horizontal section of the well slightly reduces the total liquid rate compared to the base case. In particular, the oil rate is reduced at the beginning of the production period (Fig.4-7). This extra pressure drop, being caused by friction of the flowing fluid, increases as the flow rate increases. It will thus have a stronger effect on the zones with the higher permeability, a factor that will tend to equalize the invading water front. This results in the first breakthrough is observed slightly later in the IW case (see Figures 4-7 and 4-8).

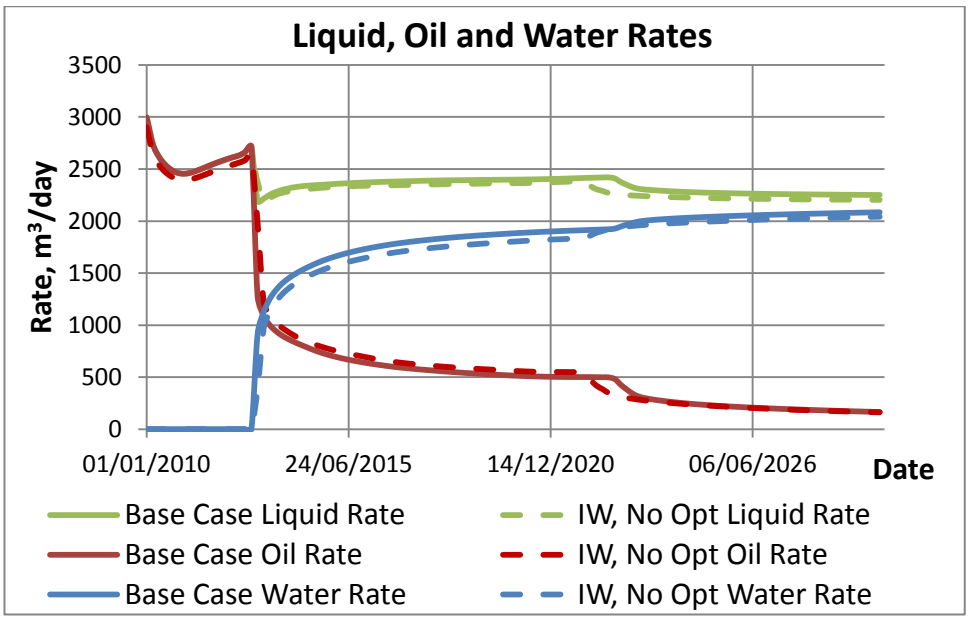


*Figure 4-7 Comparison of Liquid, Oil and Water Rates of the Base Case and IW Case without optimisation*

Figures 4-9 shows the difference in oil saturation in the middle of the reservoir for (a) the Base case and (b) the IW Case after 5 years of production. The slower movement of the water from zone 3 into zones 2 and 4 is clearly observed for IW case; while the water remains more localised to zone 3 for the base case. The restriction of production from zone 3 by the IW completion lead to an increase in the oil production from the other zones, the faster movement of the water front in zone 1 being particularly noteworthy.

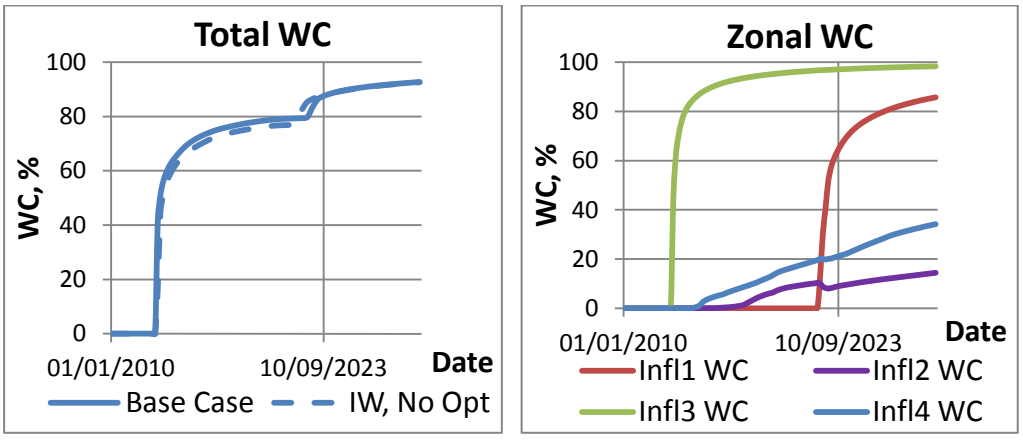


a b

*Figure 4-8 Total (a) and Zonal (b) Water Cuts of the IW Case without optimisation*

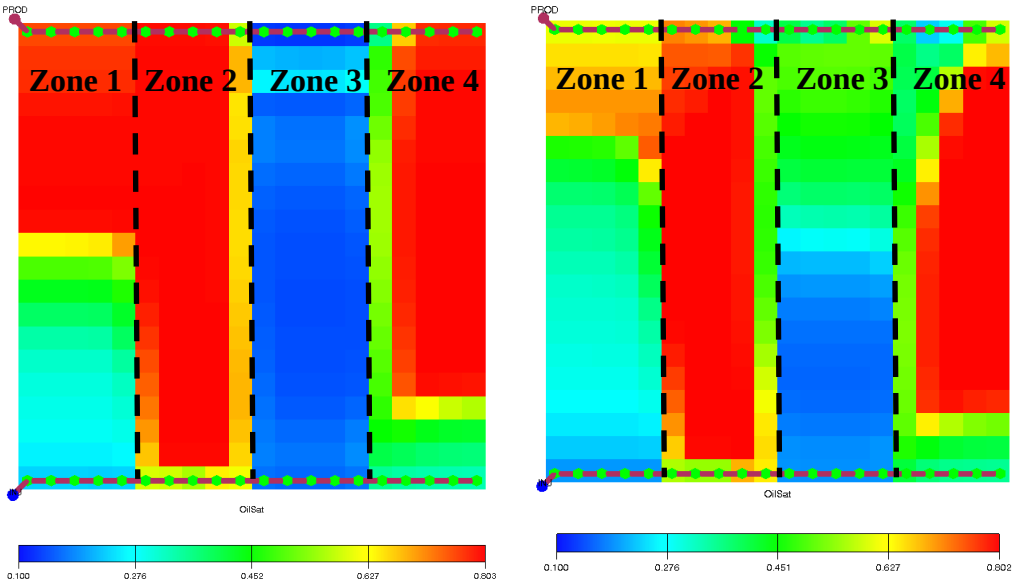


a b

*Figure 4-9 Oil Saturation profiles in the middle of the reservoir (layer 10) in the Base Case (a) and IW Case (b)after 5years of production*

### *4.3.1 Results of SLP and SQP Optimisation*

The oil and water production rates calculated by the SLP and SQP algorithms using the adaptive time step approach are shown in Fig. 4-10 and 4-11. Both methods show oscillations, which are more intensive in the SQP case. It is clear that the solution is not optimal at some points. If the optimisation process does not converge, it will deliver an intermediate result which is non-optimal. RESOLVE provides a report, when it cannot converge. A significant problem with convergence in the "Box-Shaped" model is observed for a period from 01/06/2015 to 01/01/2018 (Fig. 4-10 and 4-11).

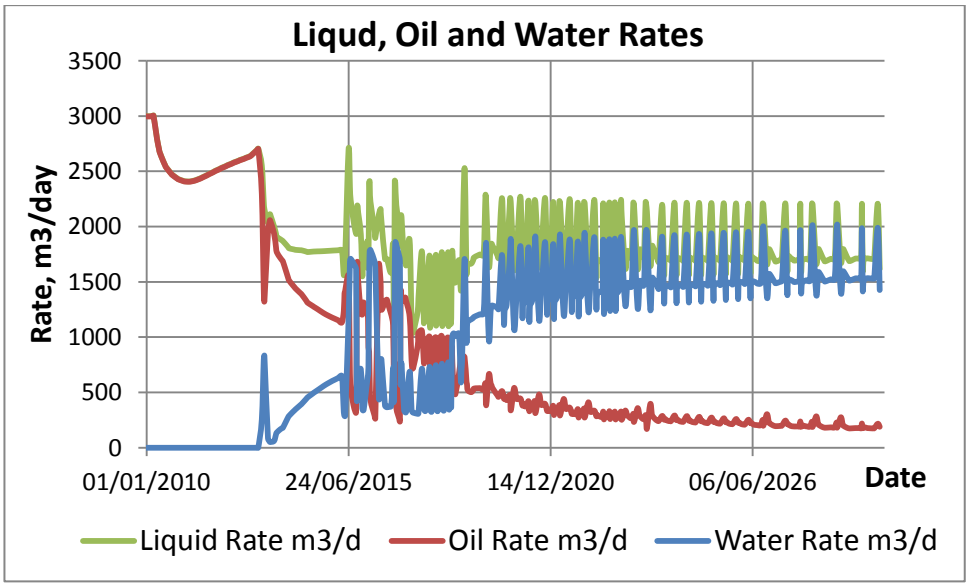


*Figure 4-10 Liquid, Oil and Water Rates of the IW Case optimised by SLP algorithm*

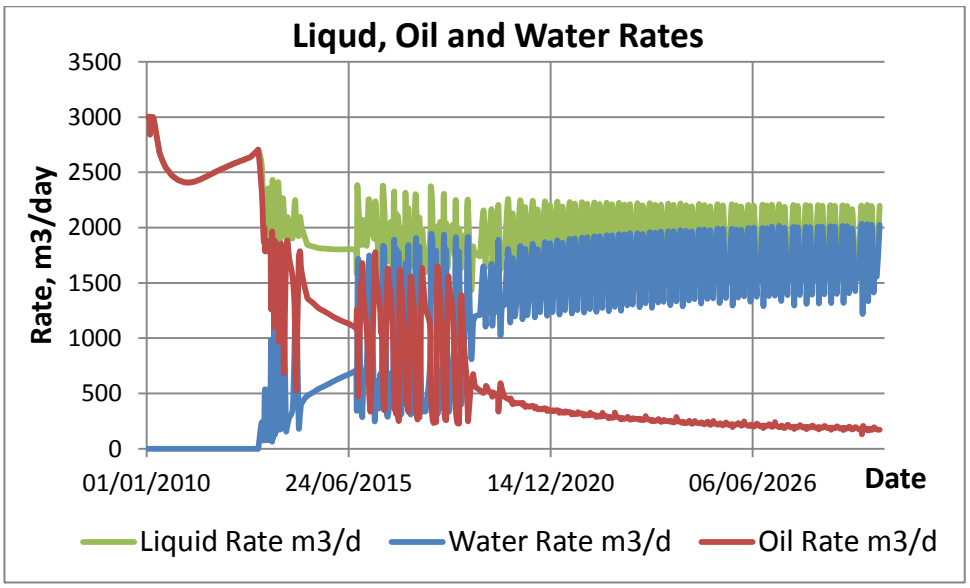


*Figure 4-11 Liquid, Oil and Water Rates of the IW Case optimised by SQP algorithm*

The Run time, Cumulative Oil, Cumulative Water and Smoothness coefficients of No Optimised, SLP and SQP algorithms employing four time step scenarios (three fixed and one adaptive) are summarised in Table 4-3.

*Table 4-3 Run time, Cumulative Oil, Cumulative Water and Smoothness coefficients of No Optimised, SLP and SQP algorithms at different time step scenarios*

| Method | Time Step | Run Time | | Cum Oil | Cum Water | SC of Revenue |
|---|---|---|---|---|---|---|
| | | Sec | hh:mm:ss | Million $m^3$ | Million $m^3$ | |
| No Control | Adaptive | 332 | 00:05:32 | 5.798 | 11.279 | 0.0051 |
| | 2 Weeks | 363 | 00:06:03 | 5.793 | 11.290 | 0.0039 |
| | 1 Month | 196 | 00:03:16 | 5.817 | 11.254 | 0.0076 |
| | 2 Months | 126 | 00:02:06 | 5.843 | 11.222 | 0.0142 |
| SLP | Adaptive | 1019 | 00:16:59 | 6.407 | 7.304 | 0.1096 |
| | 2 Weeks | 1327 | 00:22:07 | 6.476 | 7.376 | 0.0674 |
| | 1 Month | 758 | 00:12:38 | 6.592 | 7.452 | 0.0893 |
| | 2 Months | 419 | 00:06:59 | 6.428 | 7.443 | 0.0880 |
| SQP | Adaptive | 723 | 00:12:03 | 6.443 | 8.038 | 0.1256 |
| | 2 Weeks | 714 | 00:11:54 | 6.418 | 7.930 | 0.1123 |
| | 1 Month | 382 | 00:06:22 | 6.515 | 8.006 | 0.1761 |
| | 2 Months | 238 | 00:03:58 | 7.015 | 8.236 | 0.3781 |

Cumulative oil production is similar for both SLP and SQP methods and is higher than the fully open case by approximately 10%. Fig. 4-12 shows how the cumulative oil production depends on the time step interval. The cumulative oil tends to increase slightly with increasing of time step interval in the “No Control” case, though the change is not significant at less than 1%. The difference of cumulative oil between 2 weeks and 2 month time steps in SQP algorithm is much higher, at almost 10%. Such difference can be explained by the impact of oscillation. Indeed, the revenue calculated

by SQP for the 2 month time step has the highest smoothness coefficient, being 27 times larger than the SC for the "No Control" case. The reason for that is the high oscillation of the revenue in SQP case especially in a period from 01/11/2014 to 01/11/2018 (Fig. 4-13). The 2 month time step is therefore too long.

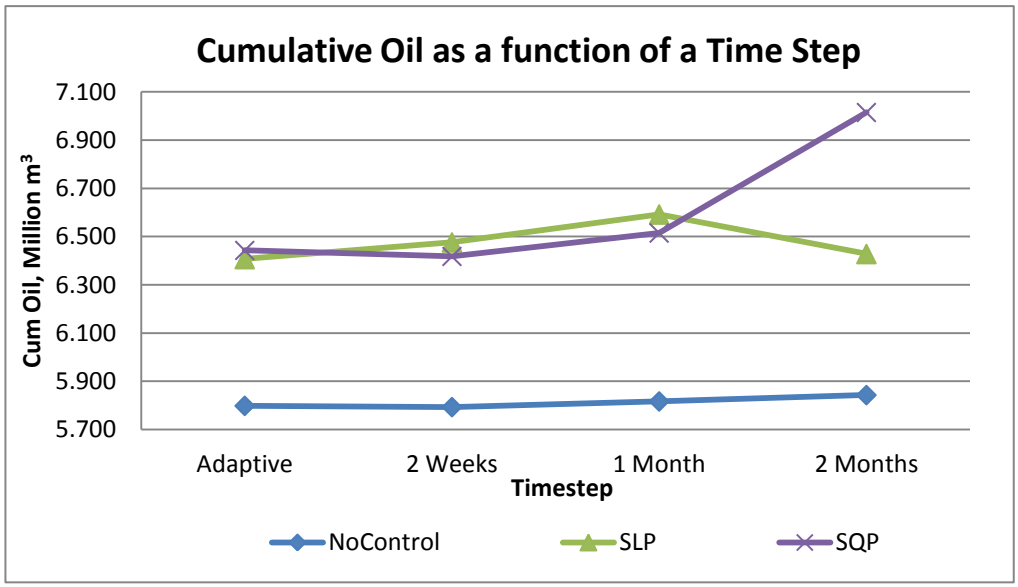


*Figure 4-12 Cumulative Oil as a function of a Time Step*

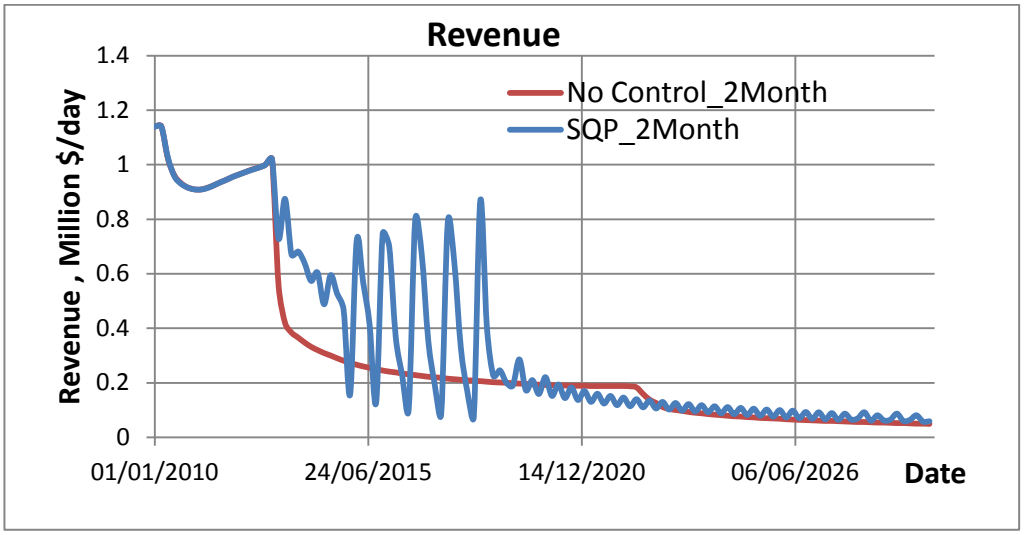


*Figure 4-13 Revenue of the "No Control" and IW Case optimised by SLP algorithm simulated with a 2 month time step*

The run time with adaptive time steps is 2 times longer with SQP optimisation and 3 times longer in SLP when compared with the No Control case (Table 4-4). These are appropriate values for an uncertainty investigation.

*Table 4-4 Run time of No Control, SLP and SQP cases at adaptive time step*

| Method | hours:minutes:seconds | Times to a case without optimisation |
|---|---|---|
| No Control | 00:05:32 | - |
| SLP | 00:16:59 | 3.07 |
| SQP | 00:12:03 | 2.18 |

The cumulative oil, water production and NPV of the base case, IW with fully open valves, SLP and SQP methods are summarised in Fig.4-14, 4-15, 4-16 and Table 4-5.

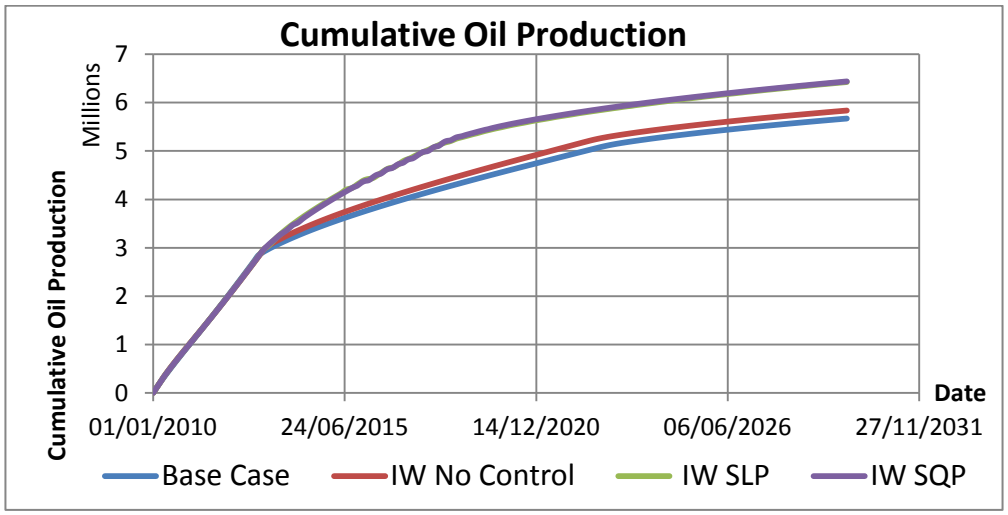


*Figure 4-14 Cumulative oil production of the Base case, IW without optimisation, SLP and SQP methods*

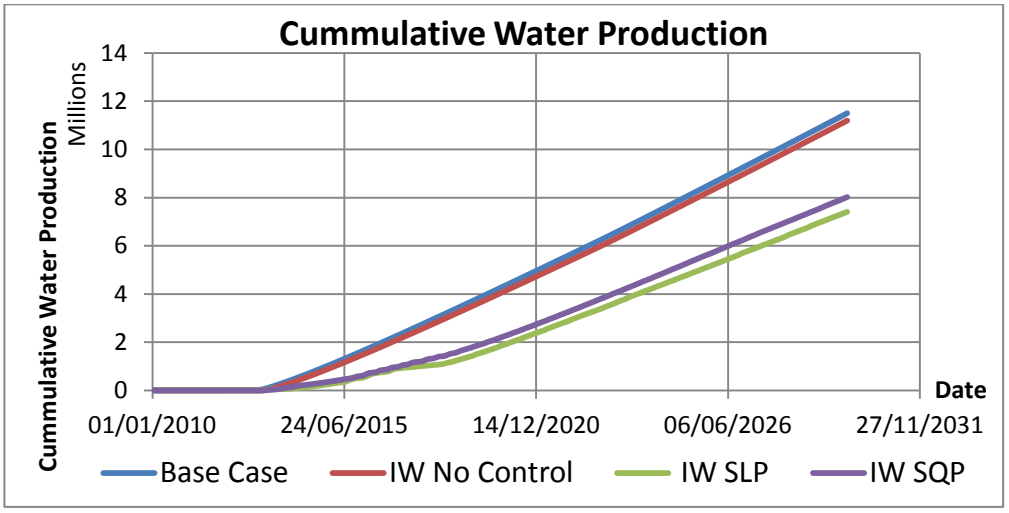


*Figure 4-15 Cumulative water production of the Base case, IW without optimisation, SLP and SQP methods*

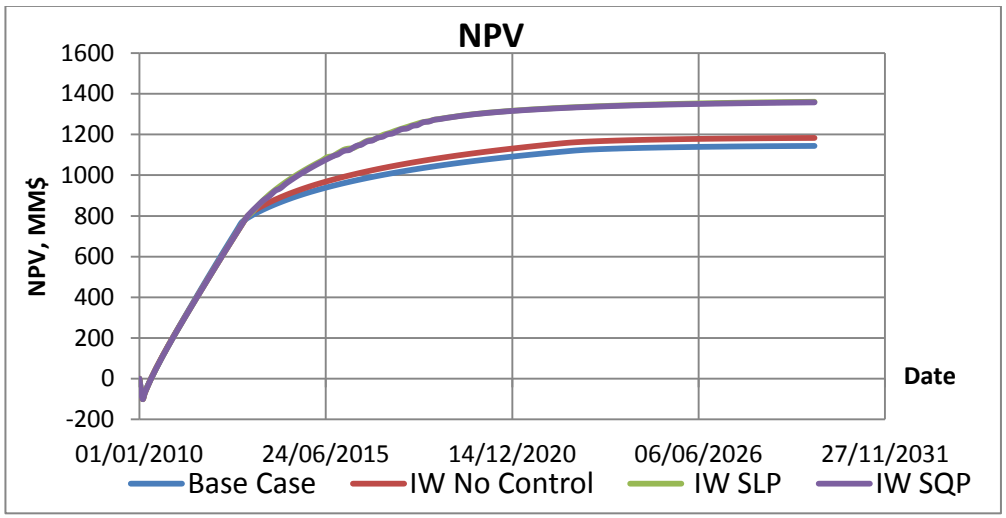


*Figure 4-16 NPV of the Base case, IW without optimisation, SLP and SQP methods*

*Table 4-5 Cumulative oil, water production and NPV of the Base case, IW without optimisation, SLP and SQP methods*

| Case | Cumulative NPV | | | Cumulative Oil Production | | | Cumulative Water Production | | |
|---|---|---|---|---|---|---|---|---|---|
| | NPV | Difference from Base Case | | Cum Oil | Difference from Base Case | | Cum Water | Difference from Base Case | |
| | Million $ | Million $ | % | Million $m^3$ | Million $m^3$ | % | Million $m^3$ | Million $m^3$ | % |
| **Base Case** | 1144 | - | - | 5.77 | - | - | 11.75 | - | - |
| **IW No Control** | 1182 | 38 | +3.4% | 5.80 | 0.03 | +0.4% | 11.28 | -0.47 | -4.0% |
| **IW SLP** | 1361 | 217 | +19.0% | 6.41 | 0.63 | +11.0% | 7.30 | -4.45 | -37.8% |
| **IW SQP** | 1357 | 175 | +14.8% | 6.44 | 0.64 | +11.1% | 8.04 | -3.24 | -28.7% |

The IW case with fully open valves demonstrates a slightly higher cumulative oil production and a reduction in cumulative water. As result, the NPV for this scenario is higher than in the base case, even though the equipment is more expensive. The optimised scenarios resulted in a further increasing in oil production and a reduction in water production of up to 38%.

The cumulative oil production is almost the same for the SLP and the SQP methods, with a minor advantage to the SQP. However, SLP demonstrated a higher efficiency in water reduction, resulting in a higher NPV.

In theory, SQP should show better results than the SLP method, because it uses a more accurate approximation. However, the errors in second derivatives required by SQP will normally be greater than the equivalent error in the first derivative (used by SLP). This probably accounts for the greater instability of the SQP scenario. However, both methods suffer from instability which may affect the final result.

### *4.3.2 Adjoint Algorithm Optimisation Results*

An adjoint optimisation was performed in Eclipse 300 with 2 month time step with choke areas being used as the control parameter and cumulative NPV being used as an objective function for the optimisation.

The first run (case 1 of Table 4-6) with all valves fully open at the beginning of simulation ended with a similar result to the "No Control" case. The optimiser converged in 1 iteration, considering that the valve positions are already optimal and no change is required (Table 4-6). The initial values of the choke areas have been greately reduced in case 2 to force the optimiser to change them in order to increase the objective function. The optimiser started searching for the optimal solution, but had not

converged after the specified limit of 600 iterations. An increased value of the initial open area in case 3 allowed the optimiser to converge successfully. The optimisation increased the run time significantly: from 3 minutes for the "No Control" case to more than 12 hours. The choke area of zones 1, 2 and 4 was reduced in case 4, since we know from the previous results that zone 3 has the major effect. The run time was more than halved when compared with case 3, with the cumulative oil being the same, while the water production increased. A further attempt (case 5) to restrict ICV's 3 area resulted in non-convergence of the optimisation.

*Table 4-6 Results of Adjoint optimisation depending on the initial values of the control parameters*

| Case | Initial Choke Area | Range of Choke Area | Run Time | | Result | |
|---|---|---|---|---|---|---|
| | $10^{-3}$ m$^2$ | $10^{-3}$ m$^2$ | sec | hh:mm:ss | Last Cum Oil, Million m$^3$ | Comment |
| 1 | 10 | 0.001-10 | 201 | 0:03:21 | 5.85 | Converged in 1 iteration. Optimiser realised that the chosen value is optimal |
| 2 | 0. 1 | 0.001-10 | 97410 | 27:03:30 | 5.27 | Did not converge after 600 simulations |
| 3 | 1 | 0.001-10 | 45447 | 12:37:27 | 6.35 | Converged after 220 simulations |
| 4 | 1 | ICVs 1,2, 4: 0.1-10 ICV 3: 0.001-10 | 19537 | 5:25:37 | 6.35 | Converged after 76 simulations |
| 5 | 1 | ICVs 1,2, 4: 0. 1-10 ICV 3: 0.01-2.5 | 99365 | 27:36:05 | 5.28 | Did not converge after 600 simulations |

It may be concluded that the results and convergence of the Adjoint algorithm depend on the initial point, with case 3 providing the best result. Fig. 4-17 shows liquid, oil and water rates of the "No Control" and Adjoint strategy for this version. Note that the liquid rate decreased prior to the water arriving at the well in the Adjoint case. It implies that the optimiser reduced the ICV size before water breakthrough, hence it was acting proactively. As a result, the breakthrough time was delayed in comparison to the non-optimised case. Proactive optimisation is discussed in greater details in chapter 5.

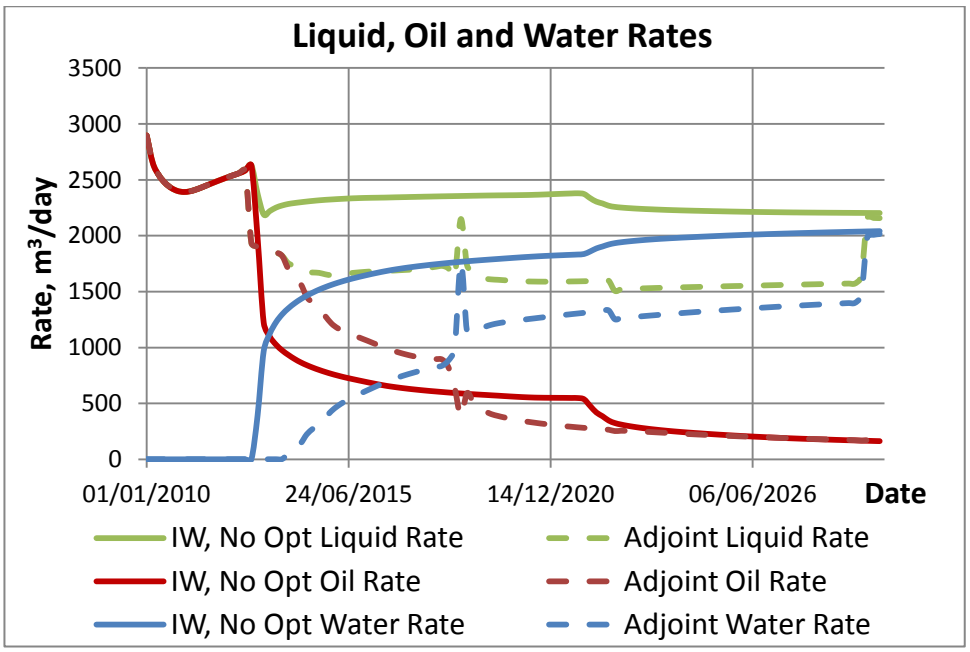


*Figure 4-17 Comparison of Liquid, Oil and Water Rates of the No Control and Adjoint Strategy*

The cumulative oil, water production and NPV of Adjoint methods are summarised in Fig.4-18, 4-19, 4-20 and Table 4-7.

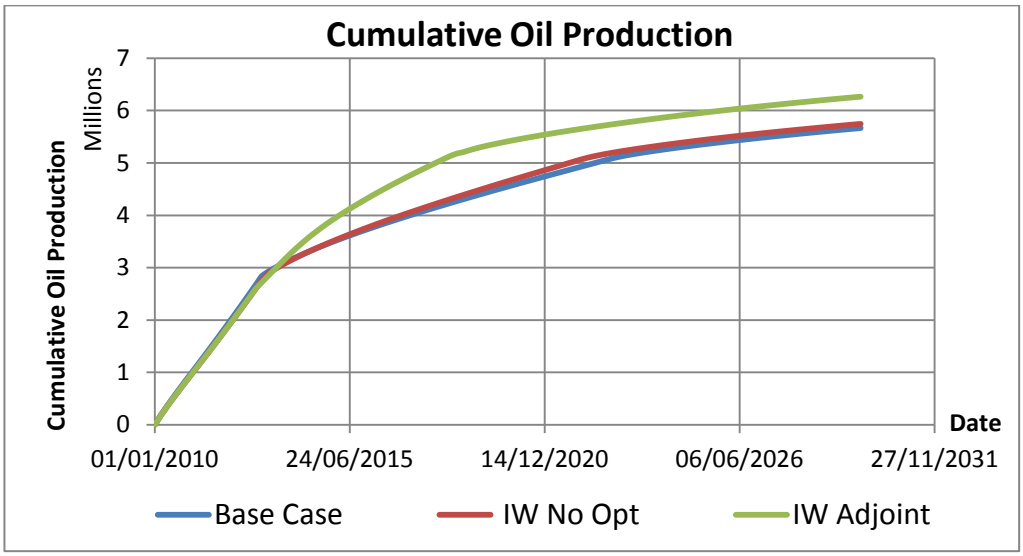


*Figure 4-18 Cumulative oil production the Base, IW without optimisation and Adjoint Cases*

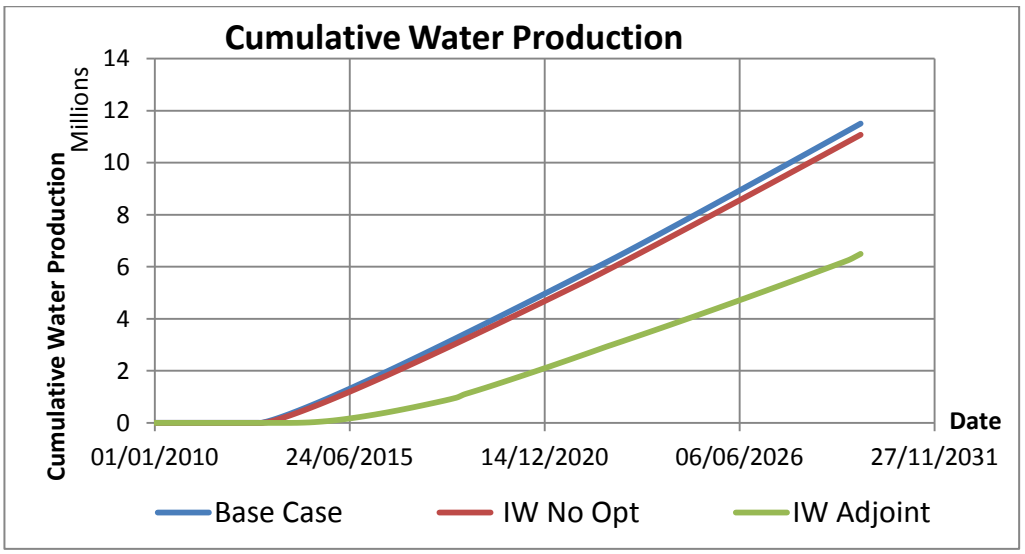


*Figure 4-19 Cumulative water production the Base, IW without optimisation and Adjoint Cases*

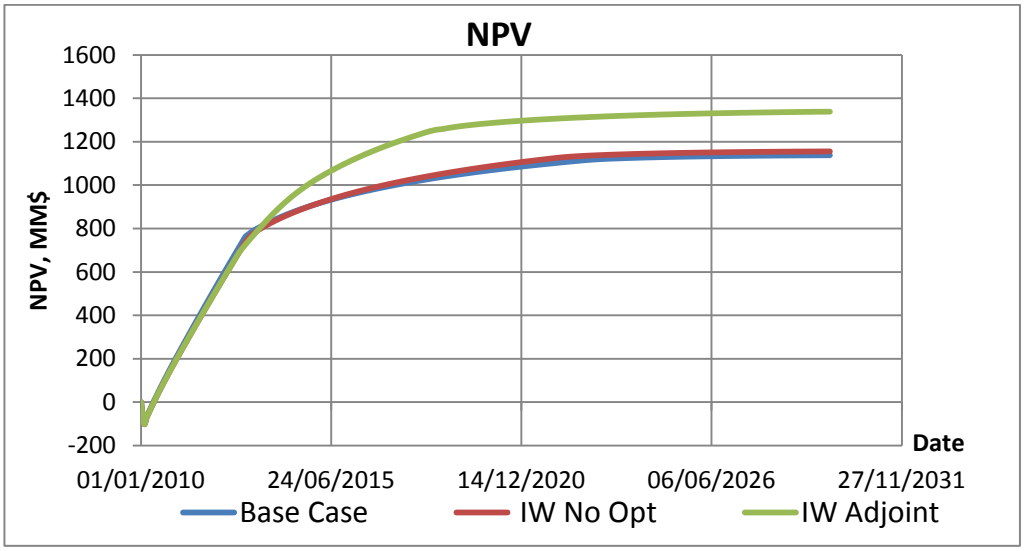


*Figure 4-20 NPV of the Base, IW without optimisation and Adjoint Cases*

*Table 4-7 Cumulative oil, water production and NPV of the Base, IW without optimisation and Adjoint Cases*

| Case | Cumulative NPV | | | Cumulative Oil Production | | | Cumulative Water Production | | |
|---|---|---|---|---|---|---|---|---|---|
| | NPV | Difference from Base Case | | Cum Oil | Difference from Base Case | | Cum Water | Difference from Base Case | |
| | Million $ | Million $ | % | Million $m^3$ | Million $m^3$ | % | Million $m^3$ | Million $m^3$ | % |
| Base Case | 1138 | - | - | 5.77 | - | - | 11.75 | - | - |
| IW No Control | 1155 | 17 | +1.5% | 5.85 | 0.08 | +1.3% | 11.18 | -0.57 | -4.8% |
| IW Adjoint | 1338 | 200 | +17.6% | 6.35 | 0.57 | +9.9% | 6.63 | -5.12 | -43.6% |

Comparison of tables 4-5 and 4-7 lead to similar, but slightly different results for the Base and "No control" cases. This is due to the different software used to control the wells production: GAP and Eclipse 300 respectively.

The Adjoint method thus showed similar results with SLP and SQP approaches, but run time was much longer.

### 4.4 PUNQS3 model

The same methodology will now be used for PUNQS-3 simulation model as employed in Section 4.3 for the "Box-Shaped" model. Figure 4-21 shows that the liquid, oil and water rates for the Base case and the IW "No Control" case are very similar. The total and zonal WCs are shown in Fig. 4-22.

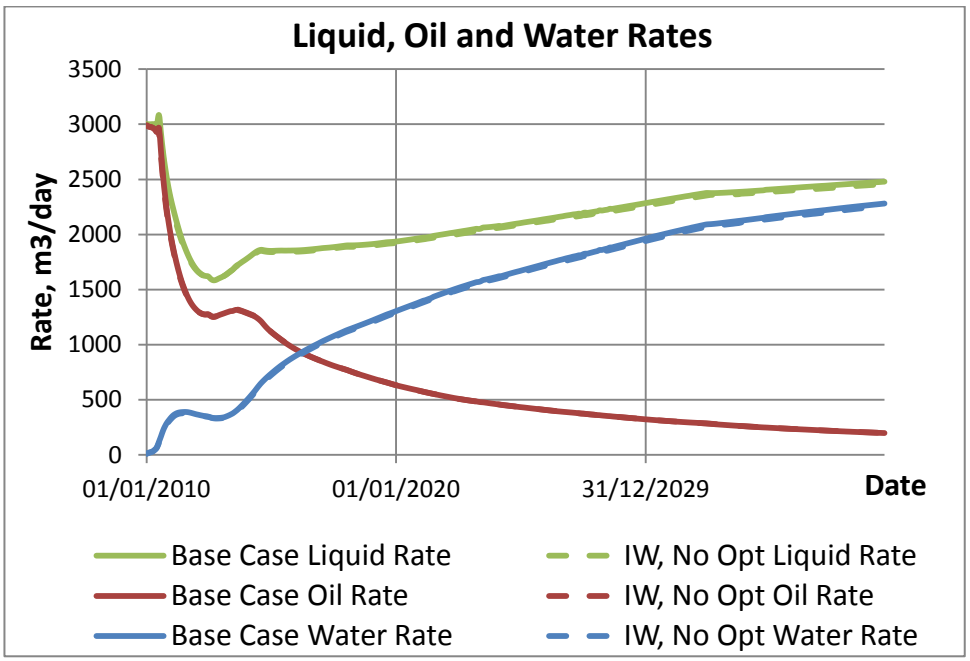


*Figure 4-21 Comparison of Liquid, Oil and Water Rates of the Base Case and IW Case without optimisation. PUNQS-3*

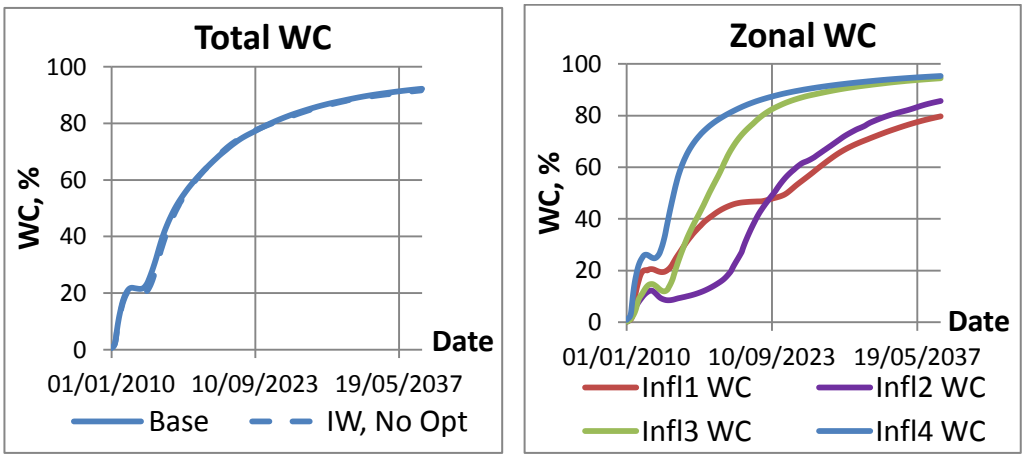


a b

*Figure 4-22 Total (a) and Zonal (b) Water Cuts of the IW Case without optimisation. PUNQS-3*

### *4.4.1 Results of SLP and SQP optimisation*

The liquid, oil and water rates of SLP and SQP algorithms for the adaptive time step are shown in Fig. 4-23 and 4-24. Instability is again present for both these optimisation methods. Unrealistic values were recorded by the SQP case at two time steps which were excluded from further analysis.

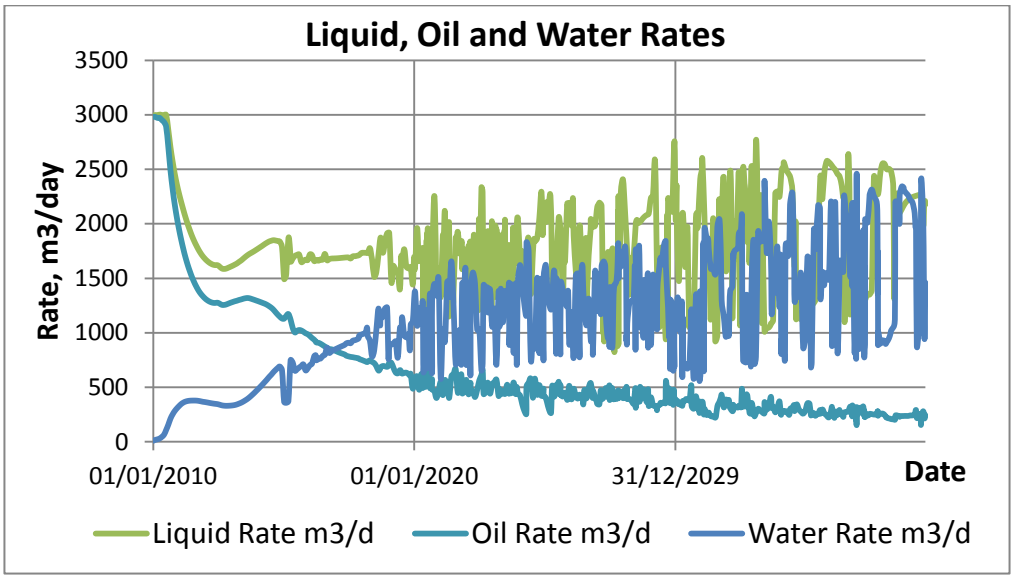


*Figure 4-23 Liquid, Oil and Water Rates of the IW Case optimised by SLP algorithm. PUNQS-3*

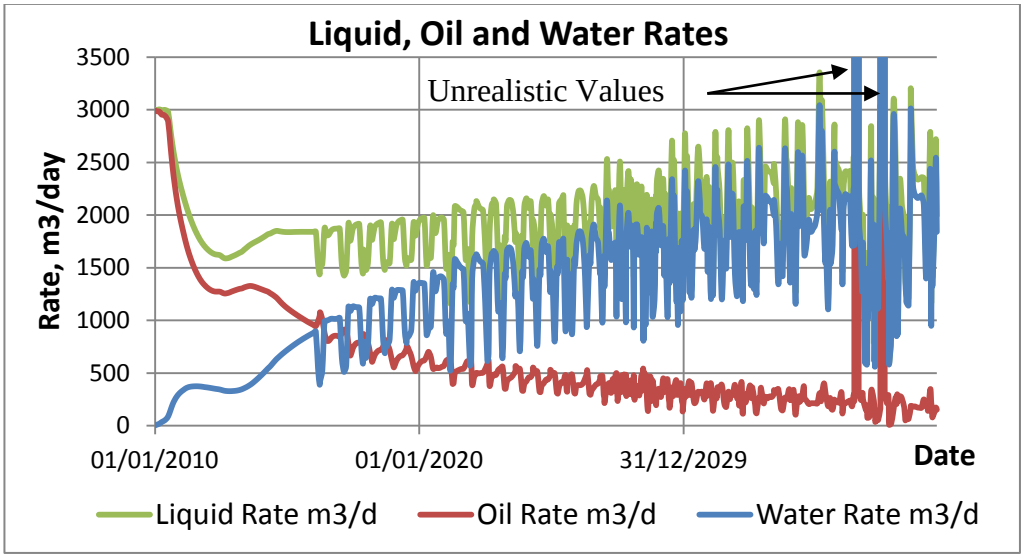


*Figure 4-24 Liquid, Oil and Water Rates of the IW Case optimised by SQP algorithm. PUNQS-3*

The Run time, Cumulative Oil, Cumulative Water and Smoothness Coefficients of "No Control", SLP and SQP algorithms for the different time step scenarios are summarised in Table 4-8. PUNQS-3, being a more complex model than the "Box-Shaped" case, has an increased run time. The run time of the optimised cases is greater than the No Control case (Table 4-9); although the ratio of less than 6 times is still appropriate for uncertainty investigations. Moreover, both optimisation methods provided a lower cumulative oil production than in the No Control case, i.e. reactive optimisation can

reduce the cumulative value even if the value at each time step is optimal. The main reason for this is that reactive strategies do not consider the changes in the reservoir performance caused by production alterations due to the optimisation process.

*Table 4-8 Run time, Cumulative Oil, Cumulative Water and Smoothness coefficients for the No Control, SLP and SQP algorithms at different time step scenarios. PUNQS3*

| Method | Time Step | Run Time | | Cum Oil | Cum Water | SC (Revenue) |
|---|---|---|---|---|---|---|
| | | Sec | hh:mm:ss | Million $m^3$ | Million $m^3$ | |
| No Control | Adaptive | 541 | 00:09:01 | 6.99 | 15.99 | 0.0039 |
| | 2 Weeks | 1530 | 00:25:30 | 6.97 | 16.02 | 0.0026 |
| | 1 Month | 536 | 00:08:56 | 6.99 | 15.99 | 0.0039 |
| | 2 Months | 200 | 00:03:20 | 7.01 | 15.93 | 0.0057 |
| SLP | Adaptive | 3008 | 00:50:08 | 6.82 | 12.84 | 0.0896 |
| | 2 Weeks | 3833 | 01:03:53 | 6.77 | 12.67 | 0.0682 |
| | 1 Month | 1529 | 00:25:29 | 6.84 | 13.08 | 0.0867 |
| | 2 Months | 766 | 00:12:46 | 6.92 | 13.44 | 0.1093 |
| SQP | Adaptive | 1719 | 00:28:39 | 6.89 | 14.13 | 0.1928 |
| | 2 Weeks | 2480 | 00:41:20 | 6.92 | 14.52 | 0.1393 |
| | 1 Month | 916 | 00:15:16 | 6.94 | 14.64 | 0.1029 |
| | 2 Months | 428 | 00:07:08 | 7.00 | 14.54 | 0.1358 |

*Table 4-9 Run time of No Control, SLP and SQP cases at adaptive time step. PUNQS-3*

| Method | hours:minutes:seconds | Times to a case without optimisation |
|---|---|---|
| No Control | 00:09:01 | - |
| SLP | 00:50:08 | 5.56 |
| SQP | 00:28:39 | 3.18 |

Dependence of the cumulative oil production as a function of the time step period is demonstrated in Fig. 4-25. The SQP algorithm shows, once more, greater oscillations than the SLP approach (Table 4-8), although the SQP value of the cumulative oil production is less sensitive to the time step.

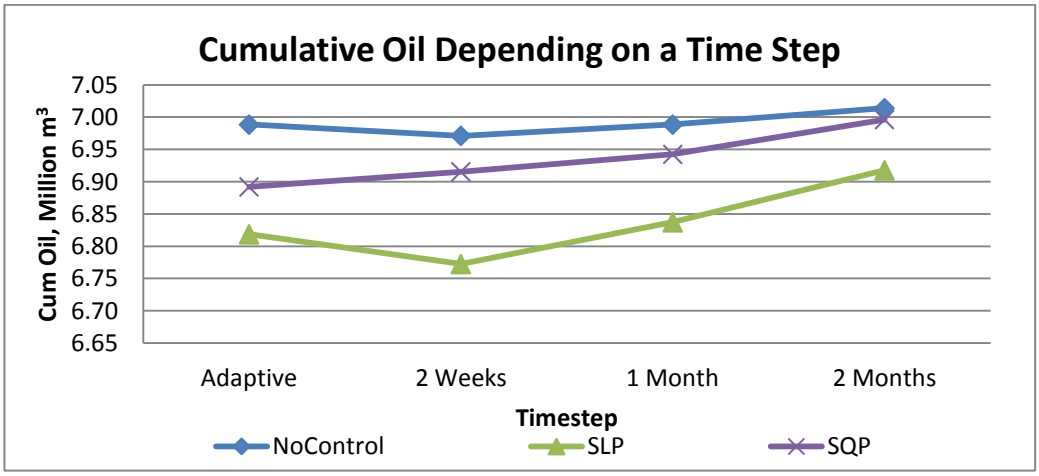


*Figure 4-25 Cumulative Oil Depending on the Time Step. PUNQS-3*

### *4.4.2 Adjoint Algorithm Results*

Application of the adjoint algorithm to the PUNQS3 case showed once again that the result depended on the initial point (Table 4-10). The initial point with fully open valve positions converged in 1 iteration, this solution itself being considered as being as optimal. Reduction in the initial valve cross section areas resulted in the optimiser failing to converge. Examination of the optimiser log indicated that the algorithm had extrapolated the PVT properties to very high pressure values that were much greater than the injection pressure constraint of 300 Bar. This failure occurred with the ICVs being set to a very low open area. It was therefore decided to increase this minimum ICV area (cases 4-7). Initial increases in this flow area were unsuccessful (cases 5 and 6), but a further increase (case 7) allowed successful optimiser convergence after 33 iterations. However, the resulting inflow restriction was very limited. Table 4-11 shows that the chosen choke area of $0.5*10^{-3}$ $m^2$ reduces the liquid rate by only 10% from the fully open ICV value. The rate profiles of the adjoint algorithm optimised case and the fully open scenario are thus very similar (Fig. 4-26).

*Table 4-10 Results of the Adjoint Optimisation depending on the initial values of the control parameters. PUNQS-3*

| Case | Initial Choke Area | Range of Choke Area | Run Time | | Result | |
|---|---|---|---|---|---|---|
| | $10^{-3}$ $m^2$ | $10^{-3}$ $m^2$ | sec | hh:mm:ss | Last Cum Oil, Million $m^3$ | Comment |
| 1 | 10 | 0.001-10 | 83 | 0:01:23 | 6.99 | Converged in 1 iteration. Optimiser realised that the chosen value is optimal |
| 2 | 0.1 | 0.001-10 | 452 | 0:07:32 | 6.87 | Failed at 4th iteration. Incorrect PVT properties at P=608 Bar |
| 3 | 1 | 0.001-10 | 345 | 0:05:45 | 5.58 | Failed at the 2nd iteration. ncorrect PVT properties at P=854 Bar |
| 4 | 1 | ICVs 1, 2: 0.1-10 ICV 3, 4: 0.001-10 | 487 | 0:08:07 | 5.83 | Failed at 3rd iteration. Incorrect PVT properties at P=798 Bar |
| 5 | 1 | 0.01-10 | 477 | 0:07:57 | 5.63 | Failed at 3rd iteration. Incorrect PVT properties at P=719 Bar |
| 6 | 1 | 0.1-10 | 131 | 0:02:11 | 6.98 | Converged in 1 iteration. Optimiser realised that the value is optimal |
| 7 | 1 | 0.5-10 | 4343 | 1:12:23 | 6.99 | Converged in 33 iterations |

*Table 4-11 Reduction of inflow rate depending on the choke area*

| Choke Area | Liquid Rate | % from fully open |
|---|---|---|
| $10^{-3}$ $m^2$ | $m^3$/day | % |
| 10 | 889 | 100% |
| 1 | 863 | 97% |
| 0.5 | 799 | 90% |
| 0.1 | 368 | 41% |
| 0.01 | 46 | 5% |
| 0.001 | 5 | 1% |

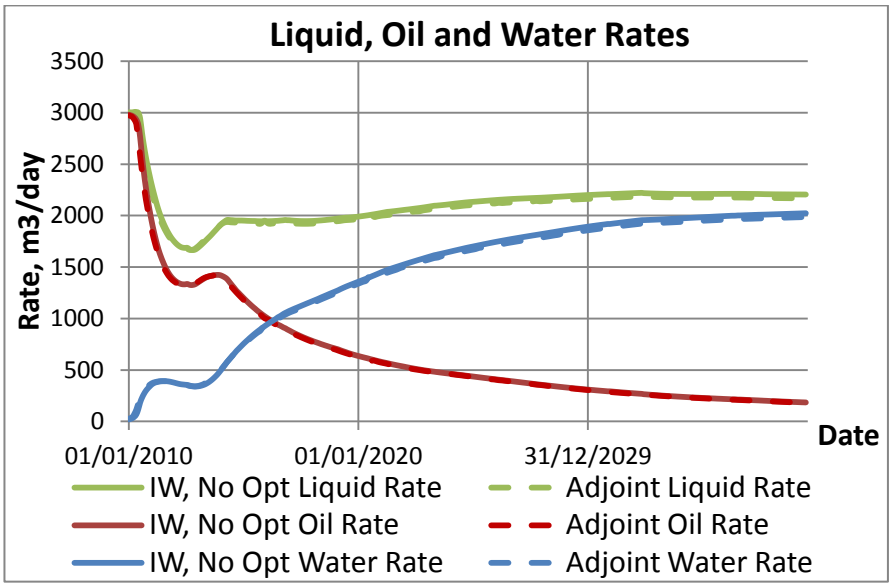


*Figure 4-26 Comparison of Liquid, Oil and Water Rates of the No Control and Adjoint Strategy. PUNQS3*

### *4.4.3 PUNQS3 Optimisation Results*

The cumulative oil, water production and NPV of the base case, IW with fully open valves, SLP, SQP and Adjoint methods are summarised in Fig.4-27, 4-28, 4-29 and Table 4-12. The NPV and cumulative oil production are similar for different optimisation methods and slightly less than in "No Control" case. Reactive control has thus reduced the cumulative oil production and the NPV for the PUNQS3 model, even if the value is optimal at every time step.

Table 4-13 shows how NPV changes with oil price in each scenario. The SLP method is the most effective in preventing water production. Contribution of water handling in NPV increases with the oil price drop. As a result, an IW optimised by the SLP method becomes more valuable than a conventional well at the oil price of about 170\$/$m^3$ (Fig. 4-30). The value of the No Control case conversely reduces with the oil price drop, because NPV reduces and the difference in the completion costs becomes more significant.

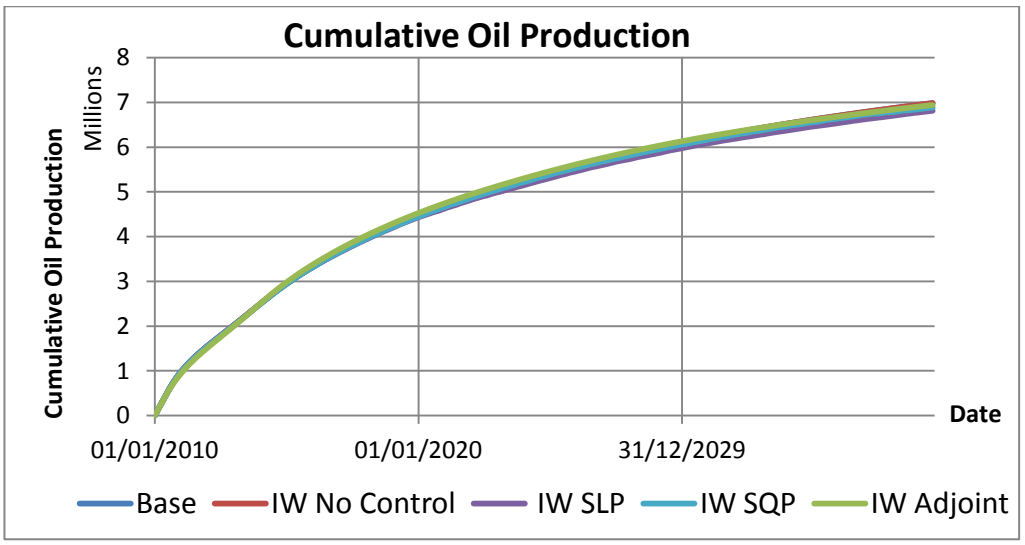


*Figure 4-27 Cumulative oil production of the Base case, IW without optimisation, SLP, SQP and Adjoint methods*

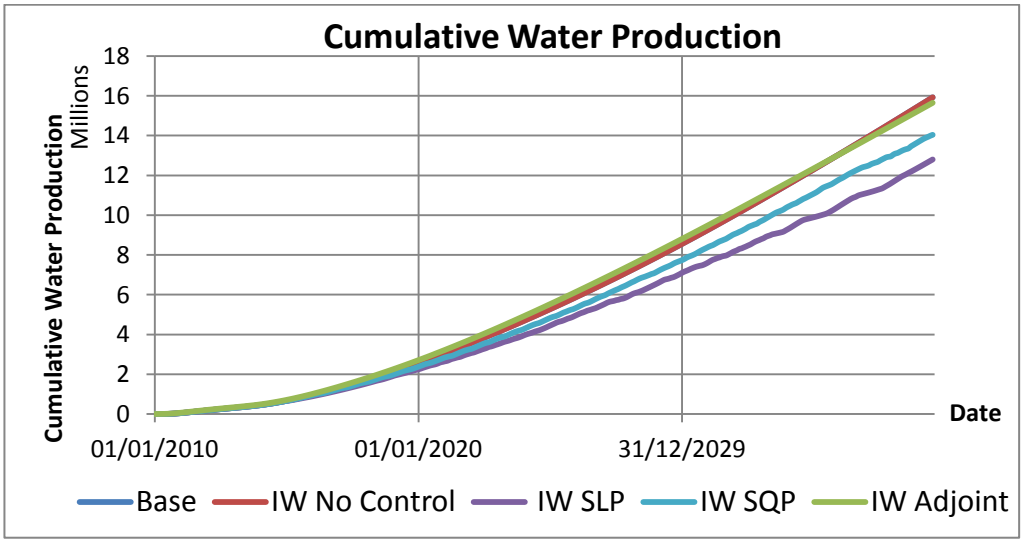


*Figure 4-28 Cumulative water production of the Base case, IW without optimisation, SLP, SQP and Adjoint methods*

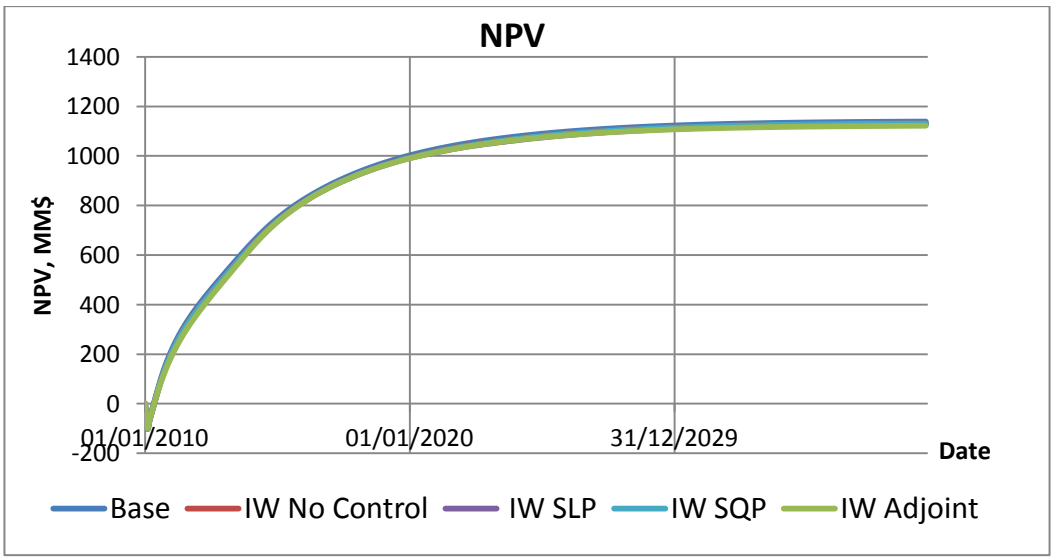


*Figure 4-29 NPV of the Base case, IW without optimisation, SLP, SQP and Adjoint methods*

*Table 4-12 Cumulative oil, water production and NPV of the Base case, IW without optimisation, SLP, SQP and Adjoint method. PUNQS3*

| Case | Cumulative NPV | | | Cumulative Oil Production | | | Cumulative Water Production | | |
|---|---|---|---|---|---|---|---|---|---|
| | NPV | Difference from Base Case | | Cum Oil | Difference from Base Case | | Cum Water | Difference from Base Case | |
| | Million $ | Million $ | % | Million $m^3$ | Million $m^3$ | % | Million $m^3$ | Million $m^3$ | % |
| Base Case | 1139 | - | - | 6.99 | - | - | 16.17 | - | - |
| IW No Control | 1132 | -8 | -0.7% | 6.99 | 0.00 | -0.1% | 15.99 | -0.18 | -1.1% |
| IW SLP | 1128 | -11 | -1.0% | 6.82 | -0.17 | -2.5% | 12.84 | -3.33 | -20.6% |
| IW SQP | 1131 | -8 | -0.7% | 6.89 | -0.10 | -1.4% | 14.13 | -2.04 | -12.6% |
| IW Adjoint | 1122 | -17 | -1.5% | 6.99 | -0.01 | -0.1% | 15.68 | -0.49 | -3.0% |

*Table 4-13 NPV depending on the Oil Price*

| Oil Price, $/m^3$ | NPV, Million $ | | | | |
|---|---|---|---|---|---|
| | Base | IW No Control | IW SLP | IW SQP | IW Adjoint |
| 380 | 1139 | 1132 | 1128 | 1131 | 1122 |
| 340 | 992 | 984 | 982 | 985 | 976 |
| 300 | 844 | 837 | 837 | 838 | 831 |
| 260 | 696 | 689 | 691 | 692 | 685 |
| 220 | 549 | 542 | 546 | 545 | 539 |
| 180 | 401 | 395 | 400 | 398 | 393 |
| 140 | 253 | 247 | 255 | 252 | 247 |

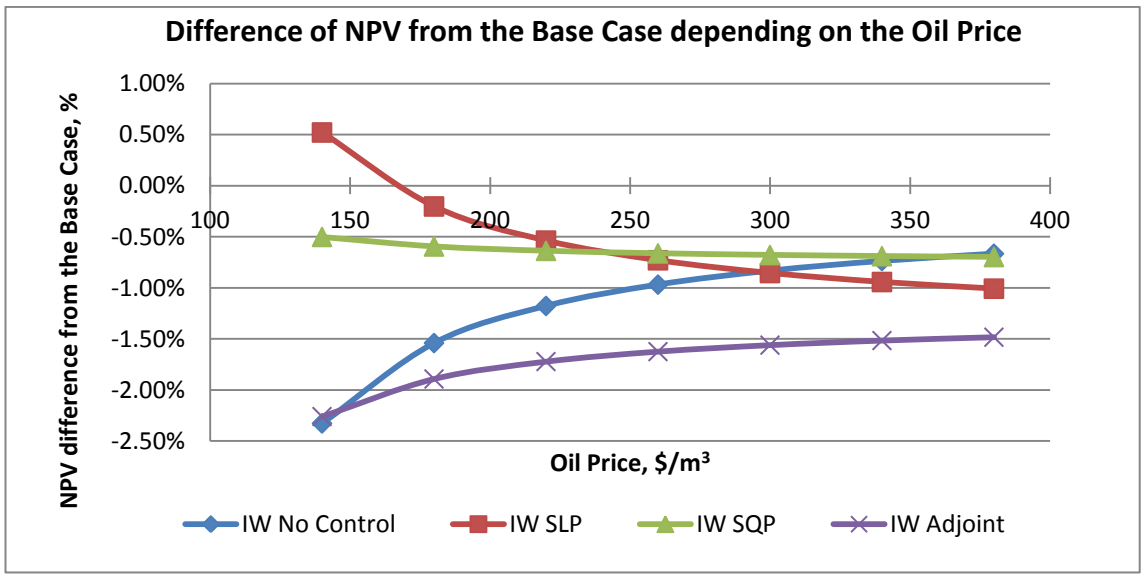


*Figure 4-30* Difference of NPV from the Base Case depending on the Oil Price

## 4.5 Summary

The SLP, SQP and Adjoint optimisation algorithms have been employed for the IW optimisation in two example cases operated with wellhead pressure limit. All algorithms showed a similar optimal value of NPV, with SLP providing a slightly better result and lower water production.

The run time of the SQP algorithm is slightly less than for the SLP method. However, the increase over a "No Control" case is less than 6 times, hence both methods can potentially be used for running multiple realisations. By contrast, the Adjoint method demonstrated a significant increase in a run time with the result being strongly dependent on the initial point and the search area chosen for the optimisation variables. The optimisation often stopped due to problems during the optimisation process; also convergence sometimes was very slow. Hence, the Adjoint method is not recommended for uncertainty investigation.

Both SLP and SQP algorithms suffer from oscillations and instability. The smoothness coefficient (SC) of the SQP algorithm was higher than that for the SLP method, i.e. the SQP method calculated more variable rate and revenue profiles. As a result, the variation of NPV with a time step length is higher for this method. The instability can impact on the cumulative value and the error can be significant. For example, the variation in cumulative oil for the SQP algorithm depends on the time step length and is greater than 9%; while in No Control case it is less than 1%. Such differences may be sufficiently large to alter conclusions of a study based on the predicted value of an IW.

All in all, the two available methods: SLP and SQP can be used for optimising IWs completed with infinitely variable ICVs, though the instability and/or the errors for some cases can be inacceptable.

The next chapter describes novel optimisation methods. A direct search method has been proposed for optimisation of discrete position and On/Off ICVs. The proactive optimisation strategy has been developed for production optimisation during a plateau period.

# Chapter 5 - Novel Optimisation Methods

The novel optimisation algorithms for reactive and proactive ICV control are described in this chapter.

The reactive control employs *Direct Search (DS)* method which is a simple method for the optimisation of discrete position valves. In contrast to the continuous gradient optimisation methods it does not require derivative calculation and avoids the errors and stability problems associated with this later procedure. A detailed description of the method can be found in Kolda et al (Kolda, Lewis et al. 2003). This chapter describes the methodology employed to apply the method to IW production optimisation. The results will be compared with those from the SLP and SQP approaches.

A proactive optimisation algorithm is proposed for production optimisation during a plateau period. The algorithm aims to equalise the inflow breakthrough time and, as a result, delay water production and improve sweep efficiency. The method will be demonstrated in three simple examples including PUNQS3 model.

## 5.1 Discrete Position ICVs Optimisation: the Direct Search Method

### *5.1.1 ICVs Design*

The choke positions of a discrete ICV must be specified prior to starting any optimisation process. An example of a discrete, 8 position ICV is shown in Fig.5-1. The number of positions and available choke sizes are case specific. They depend on the type of fluid being produced (gas and liquid require significantly different settings), the expected well out-flow and reservoir inflow performance. The standard approach for liquid inflow is to design the valve with an approximately equal size ratio between adjacent valve positions (Fig. 5-1a); unlike the ICV illustrated in Fig. 5-1 b which is designed for gas production.

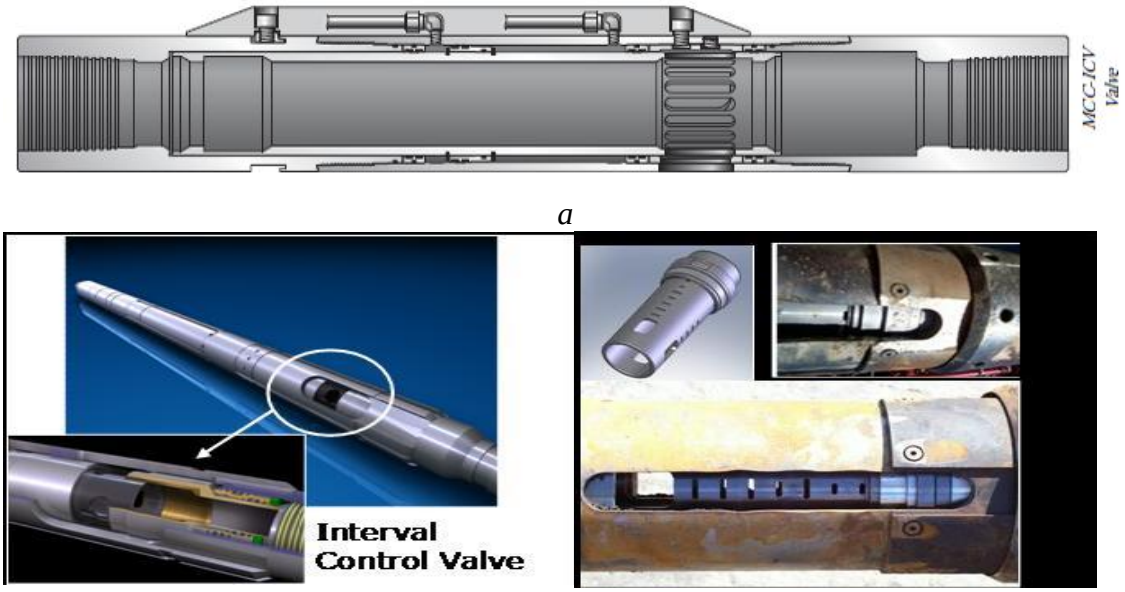


*Figure 5-1 A Discrete ICV with 8 positions. Courtesy Halliburton*

The pressure drop across a circular choke for a single phase, incompressible liquid can be represented by equation 5-1:

$$Q_{Liq} = C_1 C_d d^2 \sqrt{\frac{\Delta P}{\rho_{Liq}}} \qquad (5\text{-}1)$$

where $Q_{Liq}$ – liquid rate through the valve;

$C_1$- unit dependant constant;

$C_d$- discharge coefficient of the choke;

d – choke diameter;

ΔP – pressure drop across the choke;

$\rho_{Liq}$ – liquid density.

The practical situation is more complex: a multiphase, possibly non-newtonian, fluid is flowing through a non-circular choke etc. The actual design of the flow control element (the choke) will not only depend on the well's production conditions, but also on the equipment manufacturer. Different valve designs can be compared via the value of the valve coefficient $C_v$, where:

$$Q_{Liq} = C_v \sqrt{\frac{\Delta P}{\rho_{Liq}}} \qquad (5\text{-}2)$$

This work will assume that the valves are circular; allowing formula 5-1 may be used to describe the flow through the valve. Moreover, the equations will be further simplified by assuming that there is no free gas present in either the reservoir or the completion.

The inflow into each zone can therefore be described by use of a constant productivity index:

$$Q_{Liq,n} = dP_n \cdot J_n \qquad (5\text{-}3)$$

where, $Q_{Liq,\,n}$ – liquid rate from zone n,

$dP_n$ – is a drawdown of zone n and

$J_n$ - is a productivity index of zone n.

Note that the same workflow can be used for both gas and multiphase flow.

Equation 5-1 for a fully open ICV installed in zone n can be re-written as Equation 5-4:

$$Q_{Liq,n}^{Open} = C_1 C_d d_{Open}^2 \sqrt{\frac{\Delta P_{Open}}{\rho_{Liq}}} = (dP_n - \Delta P_{Open}) \cdot J_n \approx dP_n \cdot J_n \qquad (5\text{-}4)$$

The fully open position of an ICV is usually specified to have a flow area that is the same or even greater than that of tubing. Hence, the pressure drop through a fully open choke, $\Delta P_{Open}$, is much smaller than the drawdown and may therefore be removed from the right side of the equation. The new liquid rate, after reducing the ICV's flow area, (choking) can be described with Equation 5-5:

$$Q_{Liq,n}^{Choked} = C_1 C_d d_{Choked}^2 \sqrt{\frac{\Delta P_{Choked}}{\rho_{Liq}}} = (dP_n - \Delta P_{Choked} + \Delta P_{BHP}) \cdot J_n \qquad (5\text{-}5)$$

This new flow restriction changes the well's operating conditions, reducing the bottom hole pressure $P_{BHP}$ (Fig. 5-2).

Konopczynski and Ajayi (Konopczynski and Ajayi 2004) suggested using a surface wellhead choke to control the bottom hole pressure by maintaining it at a constant value. Our approach, by contrast, is to keep the THP constant and regulate the inflow by use of only the downhole valves. This change in BHP must therefore be kept in the subsequent calculations. The choke pressure drop, $\Delta P_{Choked}$, can be expressed from the difference in zonal liquid flow rates by subtracting 5-5 from 5-4:

$$\Delta Q_{Liq,n} = Q_{Liq,n}^{Open} - Q_{Liq,n}^{Choked} = (\Delta P_{Choked} - \Delta P_{BHP}) \cdot J_n \qquad (5\text{-}6)$$

$$\Delta P_{Choked} = \frac{\Delta Q_{Liq,n}}{J_n} + \Delta P_{BHP} \qquad (5\text{-}7)$$

Finally, the choke diameter for the required difference of the zonal liquid rate can be found by placing $\Delta P_{Choked}$ from equation 5-7 into equation 5-5:

$$d^2_{Choked} = \frac{Q^{Choked}_{Liq,n}}{C_1 C_d} \cdot \sqrt{\rho_{Liq} \Big/ \left(\frac{\Delta Q_{Liq,n}}{J_n} + \Delta P_{BHP}\right)} \qquad (5\text{-}8)$$

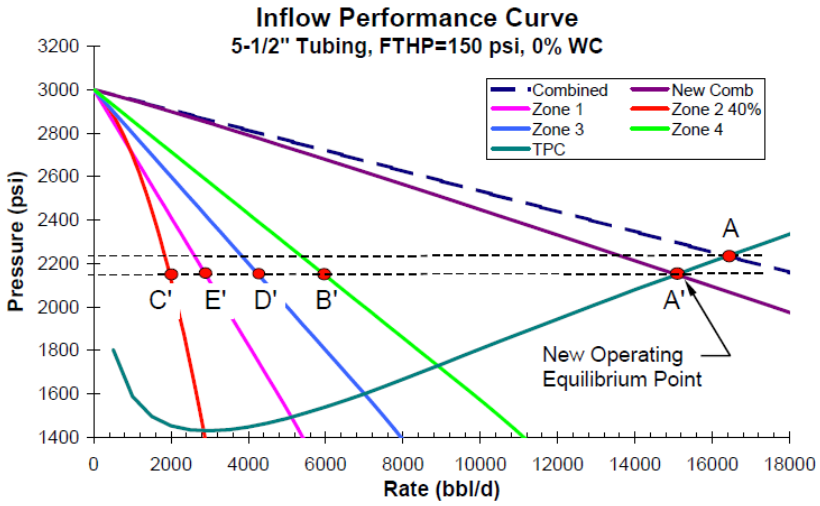


*Figure 5-2 Initial and changed operating point after choking one of the ICVs (after Konopczynski(Konopczynski and Ajayi 2004))*

$\Delta P_{BHP}$ in equation 5-8 is a function of the choke's position, hence, an iterative process is required to find the appropriate choke diameter. This process will now be demonstrated with the "Box-Shaped" reservoir model.

### *5.1.2 ICV Design for the "Box-Shaped" Case*

The zonal completion performance data with fully open chokes is summarised in Table 5-1. Note that this table confirms our assumption that the pressure drop across a fully open choke, $\Delta P_{Open}$, has a low value for all zones. It has been decided to design a 10 position ICV with an equal increase in zonal liquid rate, $\Delta Q_{Liq,n}$, as the choke position number increases. The required zonal choke diameters for each position were calculated using formula 5-8. In the first iteration $\Delta P_{BHP} = 0$. The liquid rates and the difference from the equal step are summarised in Table 5-2 and Fig 5-3.

*Table 5-1 Choke and zonal parameters for the fully open case*

| Zoness | Choke Diameter m | $\Delta P_{Open}$ Bar | $Q_{liq}$ $m^3$/day | J $m^3$/day/bar | WC % | $P_{res}$ Bar |
|---|---|---|---|---|---|---|
| Inflow1 | 0.1 | 0.0223 | 894 | 26 | 0 | 227 |
| Inflow2 | 0.1 | 0.0003 | 106 | 3 | 0 | 234 |
| Inflow3 | 0.1 | 0.1026 | 1909 | 65 | 0 | 225 |
| Inflow4 | 0.1 | 0.0030 | 325 | 14 | 0 | 221 |

*Table 5-2 Simulated zonal $Q_{liq}$ and difference from equal $\Delta Q$ after the first iteration*

| | Calculated Zonal $Q_{liq}$, $m^3$/day | | | | Difference from Equal ΔQ step, % | | | |
|---|---|---|---|---|---|---|---|---|
| Choke Position | Inflow1 | Inflow2 | Inflow3 | Inflow4 | Inflow1 | Inflow2 | Inflow3 | Inflow4 |
| 1 | 0 | 0 | 0 | 0 | 0% | 0% | 0% | 0% |
| 2 | 110 | 12 | 277 | 38 | 10.76% | -0.13% | 30.51% | 4.79% |
| 3 | 218 | 24 | 543 | 76 | 9.75% | 0.05% | 28.03% | 4.46% |
| 4 | 324 | 35 | 796 | 113 | 8.77% | 0.08% | 25.15% | 4.08% |
| 5 | 428 | 47 | 1031 | 150 | 7.62% | 0.08% | 21.53% | 3.63% |
| 6 | 528 | 59 | 1249 | 186 | 6.35% | 0.08% | 17.82% | 3.12% |
| 7 | 627 | 71 | 1448 | 222 | 5.21% | 0.07% | 13.75% | 2.52% |
| 8 | 721 | 83 | 1622 | 258 | 3.72% | 0.05% | 9.26% | 1.82% |
| 9 | 811 | 94 | 1779 | 292 | 2.01% | 0.03% | 4.86% | 1.00% |
| 10 | 894 | 106 | 1909 | 325 | 0.00% | 0.00% | 0.00% | 0.00% |

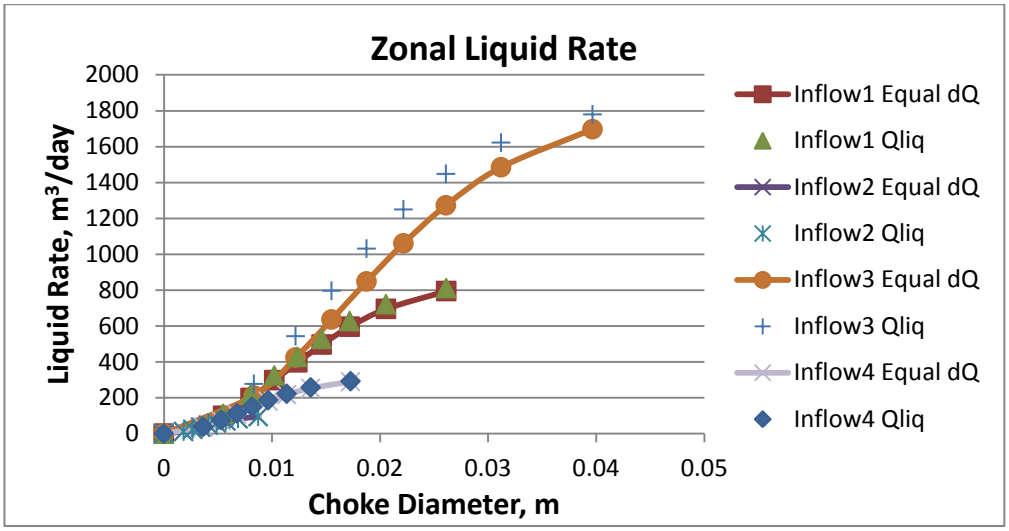


*Figure 5-3 Simulated zonal $Q_{liq}$ and equal $\Delta Q$ after the first iteration*

Zone 3 has the highest mismatch with the equal step profile, up to 30%. $\Delta P_{BHP}$ can be found now from the production model (Table 5-3) and used for correction of the choke diameters.

*Table 5-3 $\Delta P_{BHP}$ after the first iteration*

| $\Delta P_{BHP}$, Bar | | | |
|---|---|---|---|
| Inflow1 | Inflow2 | Inflow3 | Inflow4 |
| 8.1 | 0.6 | 20.8 | 1.8 |
| 7.0 | 0.5 | 17.7 | 1.6 |
| 5.9 | 0.5 | 14.7 | 1.4 |
| 5.0 | 0.4 | 11.9 | 1.2 |
| 4.0 | 0.3 | 9.3 | 1.0 |
| 3.1 | 0.3 | 6.8 | 0.8 |
| 2.3 | 0.2 | 4.6 | 0.6 |
| 1.5 | 0.1 | 2.8 | 0.4 |
| 0.7 | 0.1 | 1.3 | 0.2 |
| 0.0 | 0.0 | 0.0 | 0.0 |

After next iteration the mismatch has reduced significantly and became less than 7% (Table 5-4). Ten iterations were required to find the choke diameters with inflow performance within 2.5% of the desired value (Table 5-5 and Fig. 5-4).

*Table 5-4 Simulated Zonal $Q_{liq}$ and Difference from Equal $\Delta Q$ after the second iteration*

| Choke Position | Calculated Zonal $Q_{liq}$, $m^3$/day | | | | Difference from Equal ΔQ step, % | | | |
|---|---|---|---|---|---|---|---|---|
| | Inflow1 | Inflow2 | Inflow3 | Inflow4 | Inflow1 | Inflow2 | Inflow3 | Inflow4 |
| 1 | 0 | 0 | 0 | 0 | 0% | 0% | 0% | 0% |
| 2 | 100 | 12 | 222 | 37 | 0.52% | -0.75% | 4.86% | 1.17% |
| 3 | 200 | 23 | 449 | 73 | 0.58% | -0.64% | 5.75% | 1.13% |
| 4 | 300 | 35 | 677 | 110 | 0.66% | -0.56% | 6.47% | 1.08% |
| 5 | 400 | 47 | 908 | 146 | 0.72% | -0.49% | 7.08% | 0.99% |
| 6 | 500 | 59 | 1133 | 182 | 0.72% | -0.41% | 6.81% | 0.88% |
| 7 | 600 | 71 | 1353 | 218 | 0.70% | -0.33% | 6.35% | 0.74% |
| 8 | 700 | 82 | 1555 | 254 | 0.61% | -0.24% | 4.72% | 0.56% |
| 9 | 798 | 94 | 1746 | 290 | 0.42% | -0.13% | 2.90% | 0.33% |
| 10 | 894 | 106 | 1909 | 325 | 0.00% | 0.00% | 0.00% | 0.00% |

*Table 5-5 Simulated Zonal $Q_{liq}$ and Difference from Equal $\Delta Q$ after ten iterations*

| Choke Position | Calculated Zonal $Q_{liq}$, $m^3$/day | | | | Difference from Equal ΔQ step, % | | | |
|---|---|---|---|---|---|---|---|---|
| | Inflow1 | Inflow2 | Inflow3 | Inflow4 | Inflow1 | Inflow2 | Inflow3 | Inflow4 |
| 1 | 0 | 0 | 0 | 0 | 0% | 0% | 0% | 0% |
| 2 | 100 | 12 | 216 | 37 | 0.40% | -0.75% | 1.87% | 1.16% |
| 3 | 199 | 23 | 433 | 73 | 0.35% | -0.64% | 2.07% | 1.10% |
| 4 | 299 | 35 | 650 | 110 | 0.31% | -0.56% | 2.13% | 1.03% |
| 5 | 399 | 47 | 869 | 146 | 0.29% | -0.49% | 2.44% | 0.93% |
| 6 | 498 | 59 | 1083 | 182 | 0.27% | -0.42% | 2.14% | 0.82% |
| 7 | 597 | 71 | 1299 | 218 | 0.24% | -0.33% | 2.10% | 0.68% |
| 8 | 697 | 82 | 1508 | 254 | 0.20% | -0.24% | 1.60% | 0.50% |
| 9 | 796 | 94 | 1716 | 290 | 0.15% | -0.13% | 1.12% | 0.29% |
| 10 | 894 | 106 | 1909 | 325 | 0.00% | 0.00% | 0.00% | 0.00% |

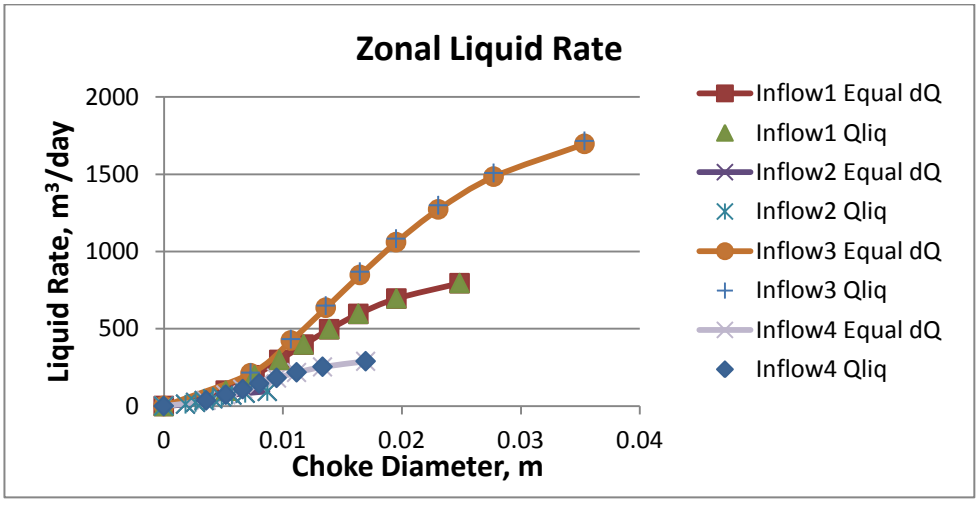


*Figure 5-4 Simulated zonal $Q_{liq}$ and equal $\Delta Q$ after ten iterations*

The valve positions can thus be designed very accurately at the initial stage of a field life. However, these conditions will alter during the production life of a reservoir;

changing the choke's pressure drop and causing a mismatch with the initial performance with a corresponding reduction in the ICV's control resolution.

For example, the choke control sensitivity for a 10 position ICV is equal to 11% of the zonal liquid production at the fully open position within an accuracy of 2.5% for the "Box-Shaped" model. Zonal liquid rates for each ICV position were calculated after 5, 10, 15 and 20 years of production with the highest mismatch from the desired values being summarised in Table 5-6 and Fig 5-5.

*Table 5-6 The worst sensitivity at different time steps*

| Years | Inflow1 | Inflow2 | Inflow3 | Inflow4 |
|---|---|---|---|---|
| 0 | 100% | 101% | 103% | 101% |
| 5 | 136% | 165% | 131% | 135% |
| 10 | 130% | 181% | 122% | 159% |
| 15 | 175% | 170% | 125% | 173% |
| 20 | 157% | 188% | 121% | 181% |

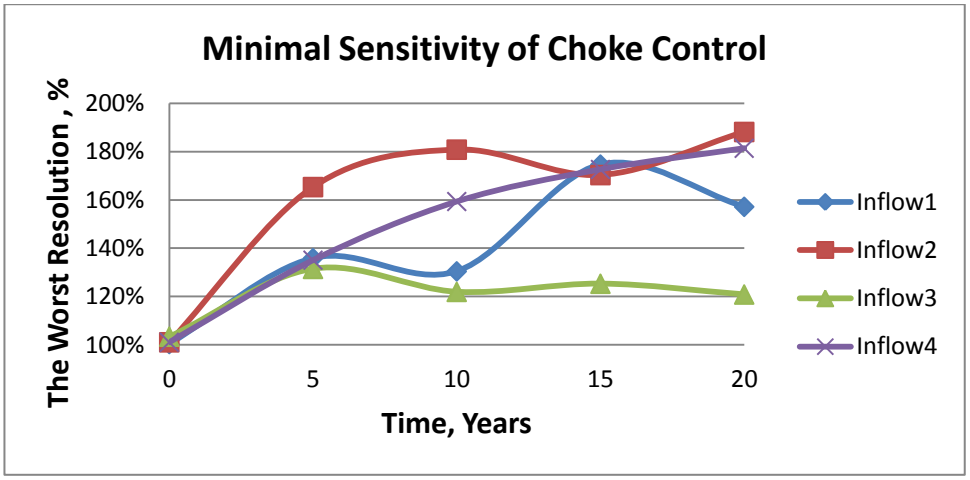


*Figure 5-5 The worst sensitivity at different time steps*

The poorest choke control sensitivity for the "Box-Shaped" model is up to 190% after 20 years of production (remember that the ideal value is 100%). That means that the liquid rate between some choke positions can be adjusted to only 20% value of the fully open flow rate instead of 11% per step.

The expected changes in the inflow conditions should therefore also be considered at the valve design stage.

### *5.1.3 Direct Search Algorithm*

The optimisation process can be started once the valves have been designed. The first important question is *"how to choose the initial point?"* We assume that the reservoir conditions do not change dramatically from one time step to another. Therefore, the

status of the ICV positions at the previous time step is most likely to be close to the optimum and provide fast convergence.

The second question is *"in which order ICVs should be optimised?"* Water production has a negative effect on our objective function (both in terms of oil rate and NPV), by increasing the required flowing bottom hole pressure, leading to decrease in the liquid production rate. Also, the water handling cost further reduces the NPV. Therefore, it should be reasonable to choke the zone with the highest WC first.

The optimisation scheme for the ***Direct Search*** method is shown in Fig. 5-6. The algorithm starts with the choke positions from a previous time step (or with all valves are fully open if this is the first time step). Then there are two loops: *Opening Search* and *Closing Search*. In the "Opening Search" loop the algorithm checks if the objective function (OF) increases with valve opening. The verification process starts by choosing the valve with a lowest WC. The algorithm opens the valve by one position and evaluates if the OF is increased. The algorithm moves to the next valve with the lowest WC if the OF does not increase or the valve is already fully open. This continues until all valves are checked. In the next stage, the ICVs are reviewed for closing following a similar procedure to the above; the only difference being that the search starts with the zone having the highest WC. The algorithm stops when all zones have been checked for valve opening and closing.

Choking a zone with a lower WC will not normally increase the objective function in most cases if previously closing a zone with a higher WC had not delivered an improvement. This can only be incorrect if the higher water cut zone had a lower oil density or a higher GOR . However, zones with significantly different PVT properties are unlikely to be produced together. Therefore, in most cases the algorithm can be simplified (Fig. 5-7) by reducing a number of iterations by not checking if lower WC zones need to be choked when a zone with higher WC is not fully closed.

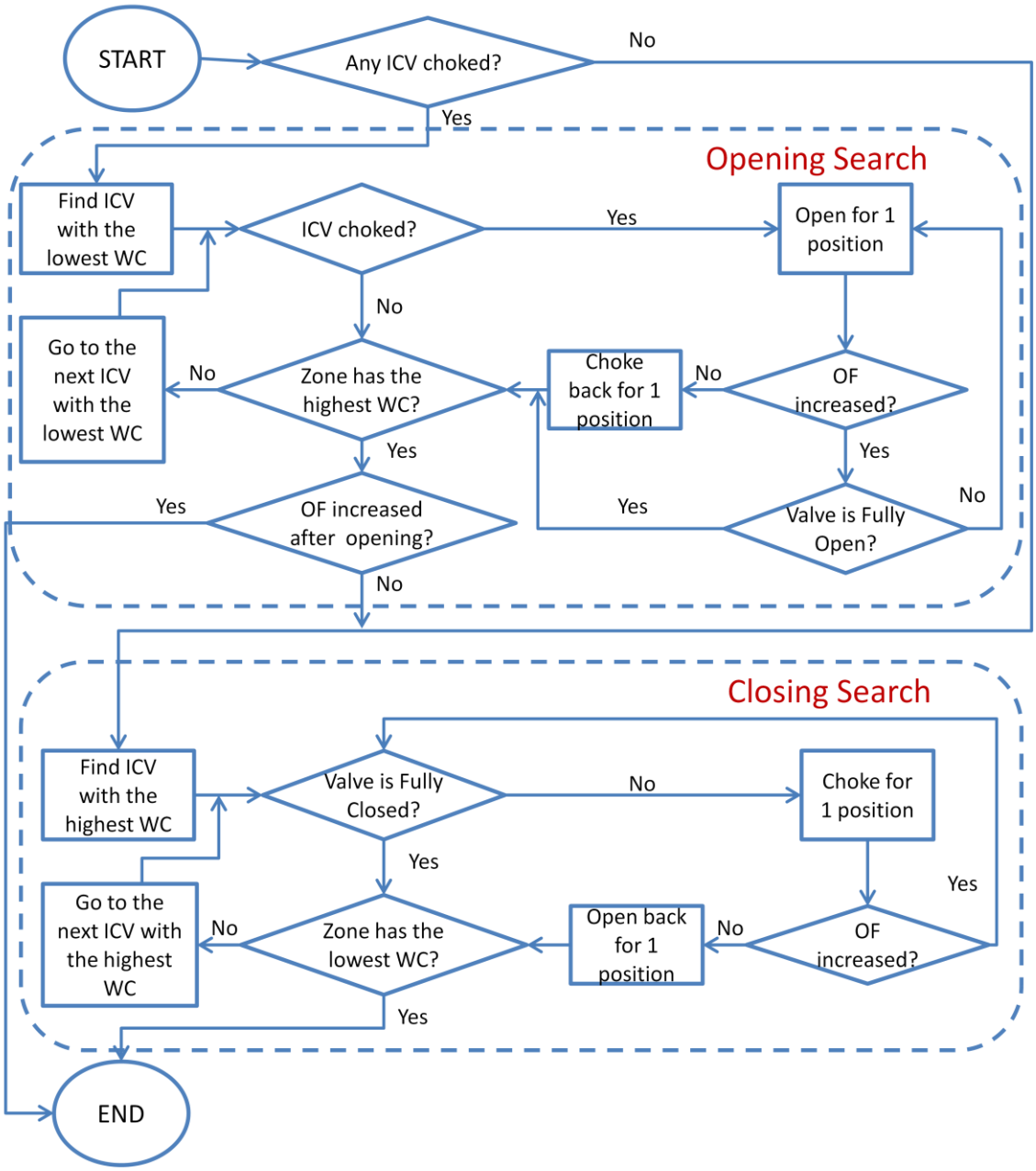


*Figure 5-6 Optimisation Schematic of a Direct Search Method*

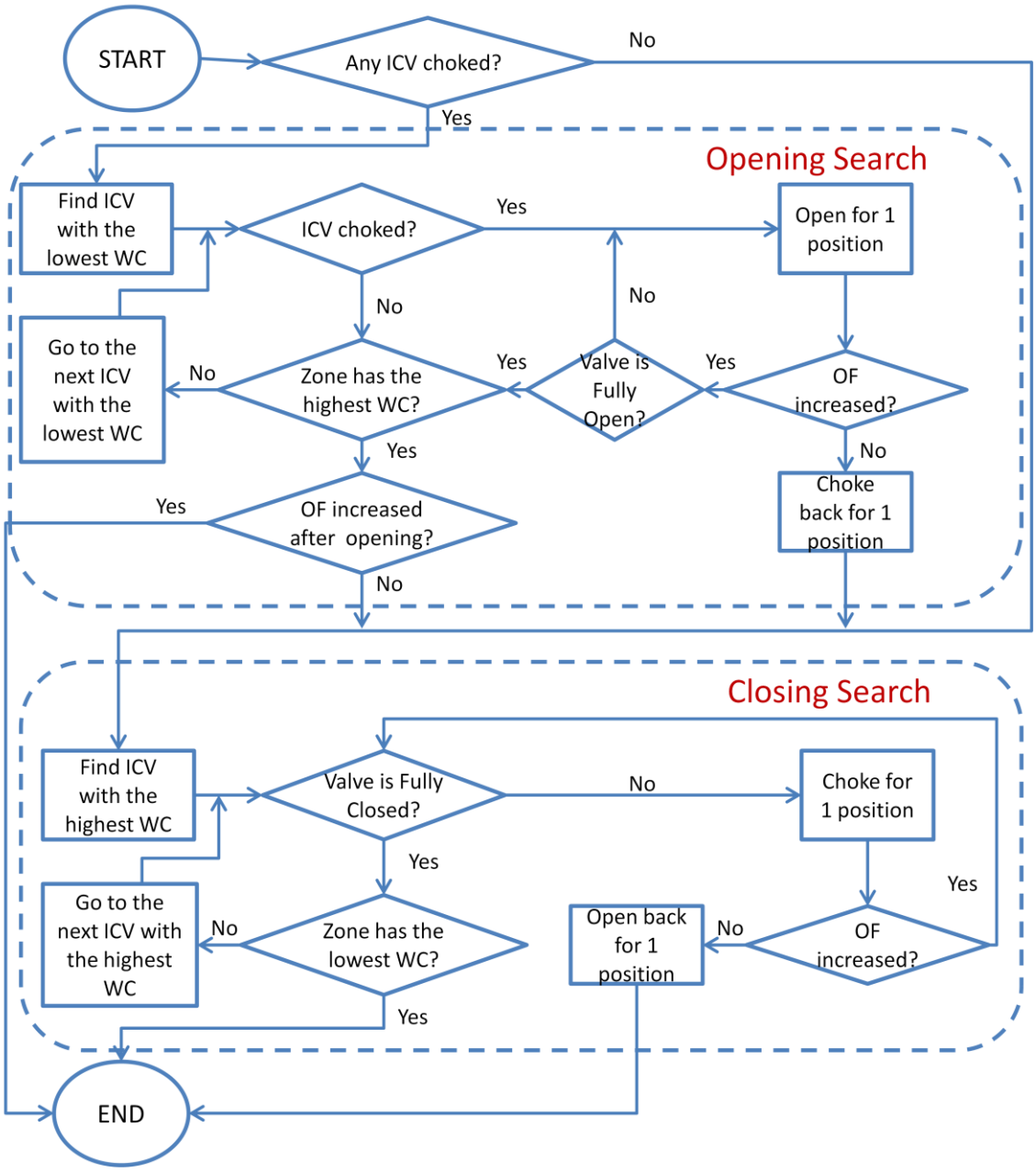


*Figure 5-7 Modified Optimisation Schematic of a Direct Search Method assuming zones produce oil with similar PVT properties*

The algorithm was implemented in Visual Basic for Applications (VBA) in Excel using RESOLVE's Open Server option which includes the capability for a user developing their own optimiser. Both 10 position and On/Off valves were analysed. The choke positions for 10 position ICV were designed to provide an equal change in a zonal liquid rate for each valve at the initial production conditions, as described earlier.

### *5.1.4 The "Box-shaped" model Results*

The liquid, oil and water rates for the Direct Search (DS) Algorithm for the 10 position and On/Off completions for adaptive time steps are shown in Fig. 5-8 and 5-9.

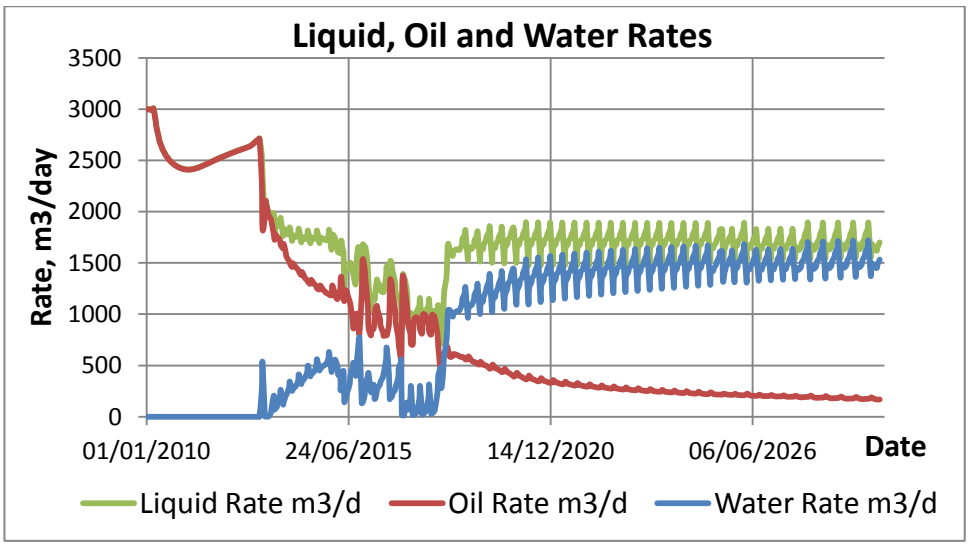


*Figure 5-8 Liquid, Oil and Water Rates for an IW optimised by the DS algorithm with a 10 position choke*

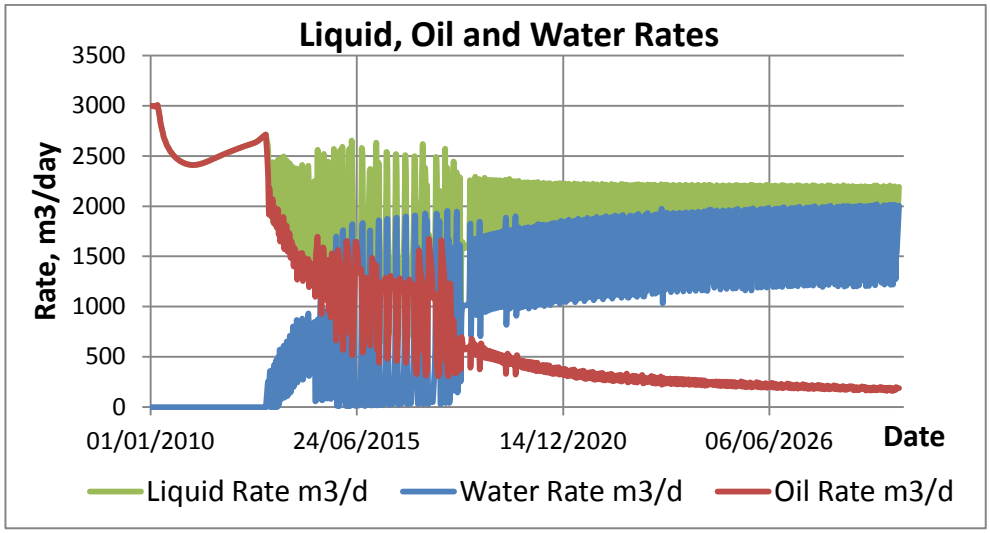


*Figure 5-9 Liquid, Oil and Water Rates for an IW optimised by the DS algorithm with an On/Off choke*

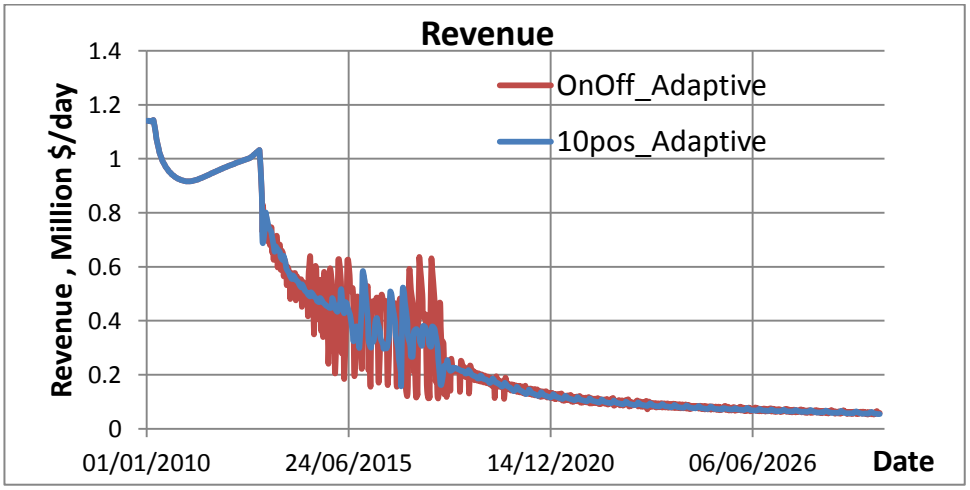


*Figure 5-10 Revenue of an IW optimised by the DS algorithm with a 10 position and an On/Off choke*

The 10 position scenario shows a smoother profile for the revenue than the On/Off case, which naturally, has considerably larger oscillations caused by the significant change in the flow rate as a valve is opened and closed. The smoothness coefficient for the above

calculation for the revenue of the On/Off case is similar to that calculated with the SLP and SQP algorithms (see Table 4-1 and Table 5-7). The corresponding SC for the discrete position scenario with the 10 position valves is lower.

The Run time, Cumulative Oil, Cumulative Water and Smoothness coefficients of No Control and DS algorithm with 10 positions and On/Off chokes at different time step scenarios are summarised in Table 5-7.

*Table 5-7 Run time, Cumulative Oil, Cumulative Water and Smoothness coefficients of the No Control and the DS algorithm optimisation for the 10 position and the On/Off chokes for the different time step scenarios*

| Method | Time Step | Run Time | | Cum Oil | Cum Water | SC of Revenue |
|---|---|---|---|---|---|---|
| | | Sec | hh:mm:ss | Million $m^3$ | Million $m^3$ | |
| No Control | Adaptive | 332 | 00:05:32 | 5.798 | 11.279 | 0.0051 |
| | 2 Weeks | 363 | 00:06:03 | 5.793 | 11.290 | 0.0039 |
| | 1 Month | 196 | 00:03:16 | 5.817 | 11.254 | 0.0076 |
| | 2 Months | 126 | 00:02:06 | 5.843 | 11.222 | 0.0142 |
| 10 Position | Adaptive | 3793 | 01:03:13 | 6.359 | 6.701 | 0.0218 |
| | 2 Weeks | 3857 | 01:04:17 | 6.344 | 6.685 | 0.0152 |
| | 1 Month | 2079 | 00:34:39 | 6.382 | 6.752 | 0.0192 |
| | 2 Months | 912 | 00:15:12 | 6.422 | 6.806 | 0.0320 |
| On/Off | Adaptive | 6076 | 01:41:16 | 6.435 | 7.052 | 0.1001 |
| | 2 Weeks | 3739 | 01:02:19 | 6.565 | 7.042 | 0.0627 |
| | 1 Month | 1899 | 00:31:39 | 6.786 | 7.279 | 0.0890 |
| | 2 Months | 1052 | 00:17:32 | 7.113 | 7.504 | 0.1098 |

In general, the cumulative oil and water production of the discrete ICVs scenarios is similar to the SLP and SQP results. However, a difference can be noticed in the dependence of the cumulative oil as a function of the time step (Fig 5-11). Thus, the 10 position ICV case has the same trend as No Control scenario, with a maximum range of cumulative oil of only 1.2%. Application of the DS method with a 10 position ICV is more stable with the results being more independent of the time step than the other methods, making it more attractive for use during uncertainty investigation.

Table 5-7 shows that the run time for this algorithm is significantly higher than that of the SLP and SQP cases. This increased run time is not caused by the algorithm itself, but by the way it was implemented. The DS code is written with VBA code in Excel (Fig. 5-12), requiring RESOLVE to launch an Excel file and transfer data between the production module in GAP and the optimiser at each time step. This operation is time consuming and would not be required if the algorithm is included within the code.

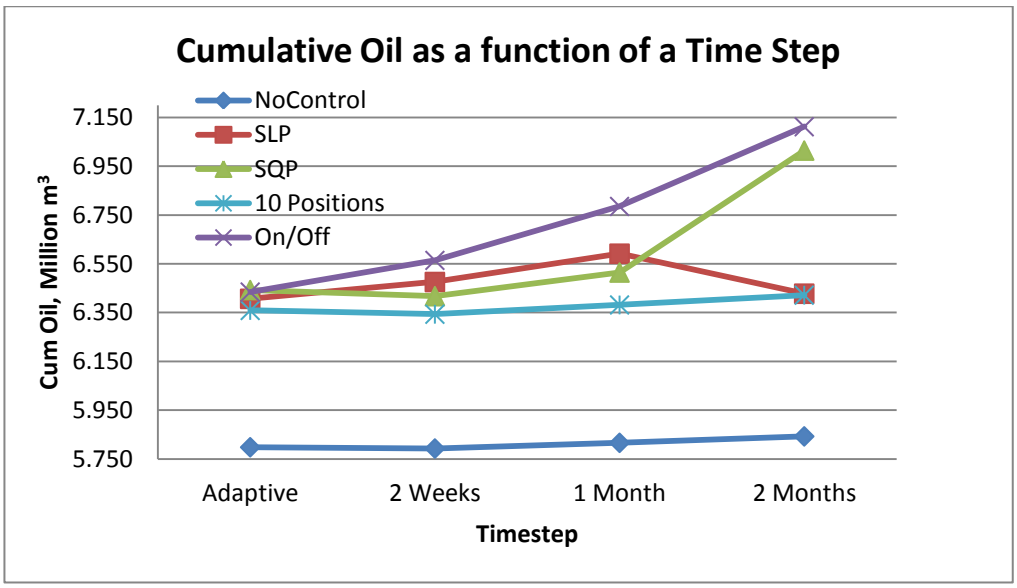


*Figure 5-11 Cumulative Oil as a function of a Time Step*

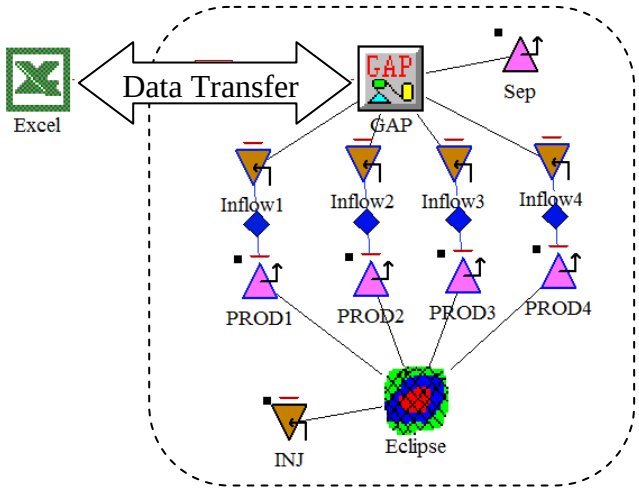


*Figure 5-12 Data transfer between the DS code and the production model in GAP*

Solving the production system model in GAP for the "Box-Shaped" model takes approximately 0.15 sec (Table 5-8).

*Table 5-8 Run Time of GAP with optimisation by SQP and without optimisation*

| Case | Total Run Time of GAP | Number of Iterations | Run Time for each Iteration |
|---|---|---|---|
| | Sec | | Sec |
| **SQP** | 1.76 | 12 | 0.15 |
| **No Optimisation** | 0.14 | 1 | 0.14 |

Table 5-9 summarises the number of DS iterations required at the different time step, giving an estimated time required for each optimisation of 0.15 sec. Fig. 5-13 compares the optimisation time of the SLP and SQP methods with the estimated value for the DS method. According to this estimation, DS with 10 position valves would take slightly longer time than SQP if it was realised in GAP. The DS with On/Off valves takes the same time as SQP for the fixed time step scenarios. However, the run time of this

method increased significantly when the adaptive time step option was chosen, due to the sharp changes in the production system caused by an increase in the number of time steps due to the valves opening and closing. The SLP method shows a longer run time for all scenarios. Most likely, this is because the SLP algorithm is realised within RESOLVE and also needs extra time for the RESOLVE to GAP data transfer.

*Table 5-9 Number of time steps and iterations for the DS method*

| Method | Time Step | Number of Time Steps | Number of Iterations | Iterations / Time Step | Extra time Sec |
|---|---|---|---|---|---|
| 10 Position | Adaptive | 508 | 3389 | 6.67 | 432 |
| | 2 Weeks | 480 | 3245 | 6.76 | 415 |
| | 1 Month | 240 | 1783 | 7.43 | 231 |
| | 2 Months | 120 | 775 | 6.46 | 98 |
| On/Off | Adaptive | 809 | 5017 | 6.20 | 631 |
| | 2 Weeks | 480 | 2953 | 6.15 | 371 |
| | 1 Month | 240 | 1495 | 6.23 | 188 |
| | 2 Months | 120 | 765 | 6.38 | 97 |

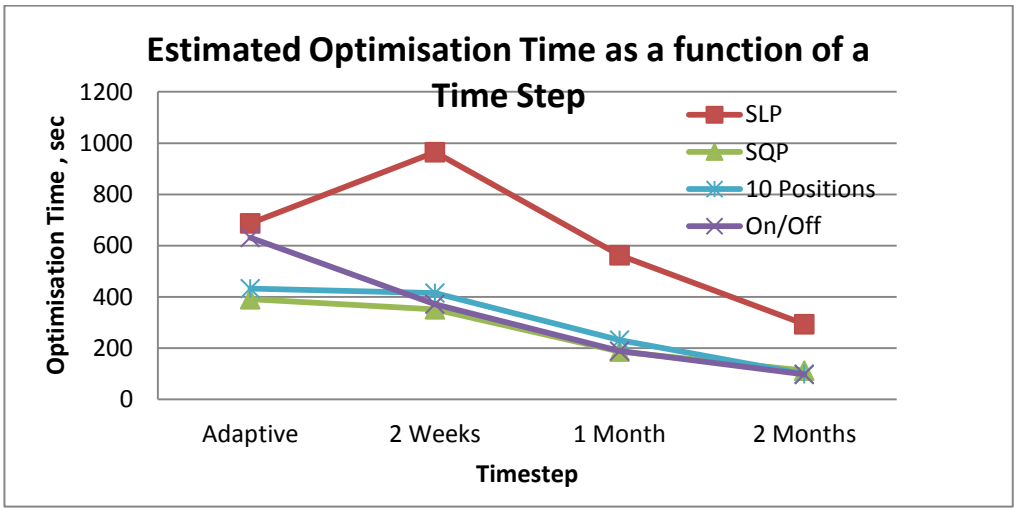


*Figure 5-13 Estimated Optimisation Time for the SLP, SQP and DS methods for 10 position and On/Off ICVs for multiple Time Steps*

The cumulative oil, water production and NPV of the base case, IW with fully open valves, SLP, SQP and DS algorithm with 10 position and On/Off ICVs are summarised in Table 5-10.

*Table 5-10 Cumulative oil, water production and NPV for all methods*

| Case | Cumulative NPV | | | Cumulative Oil Production | | | Cumulative Water Production | | |
|---|---|---|---|---|---|---|---|---|---|
| | NPV | Difference from Base Case | | Cum Oil | Difference from Base Case | | Cum Water | Difference from Base Case | |
| | Million $ | Million $ | % | Million $m^3$ | Million $m^3$ | % | Million $m^3$ | Million $m^3$ | % |
| **Base Case** | 1144 | - | - | 5.77 | - | - | 11.75 | - | - |
| **IW No Control** | 1182 | 38 | +3.4% | 5.80 | 0.03 | +0.4% | 11.28 | -0.47 | -4.0% |
| **IW SLP** | 1361 | 217 | +19.0% | 6.41 | 0.63 | +11.0% | 7.30 | -4.45 | -37.8% |
| **IW SQP** | 1357 | 175 | +14.8% | 6.44 | 0.64 | +11.1% | 8.04 | -3.24 | -28.7% |
| **IW DS 10 Pos** | 1363 | 219 | +19.1% | 6.36 | 0.59 | +10.1% | 6.70 | -5.05 | -43.0% |
| **IW DS On/Off** | 1369 | 225 | +19.7% | 6.43 | 0.66 | +11.5% | 7.05 | -4.70 | -40.0% |

### *5.1.5 Results of PUNQS3 model*

The results of Direct Search (DS) Algorithm for 10 positions and On/Off completions for PUNQS-3 model are summarised in Fig. 5-14, 5-15, 5-16, Table 5-11 and Table 5-13. The conclusions from this study are similar to the "Box-Shaped" model:

- DS with 10 position valves provides a smoother production profile and smaller smoothness coefficient
- The cumulative oil, water and liquid production volumes and NPV are similar to the SLP and SQP methods
- The change between the cumulative oil of DS with 10 position valves from one time step to the next is similar to that for the No Control case (Fig 5-16) and is much less than for the other methods.

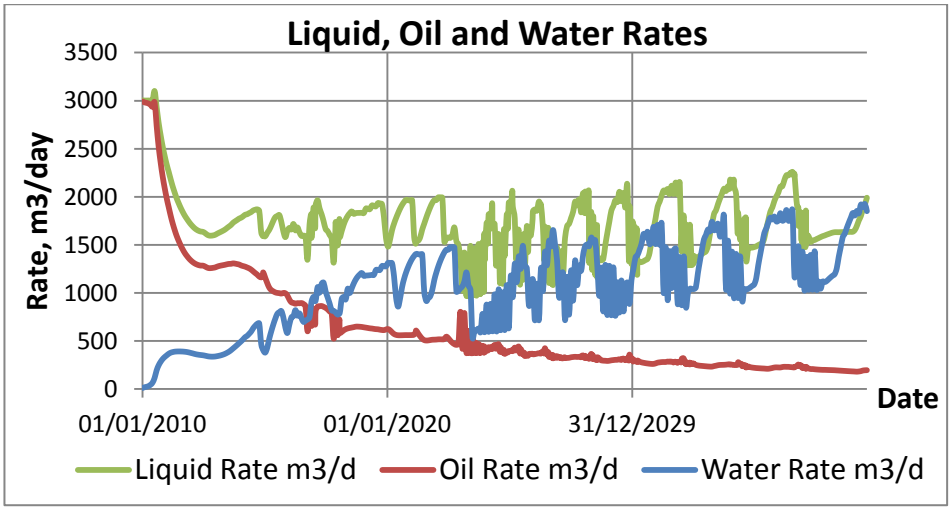


*Figure 5-14 Liquid, Oil and Water Rates for the PUNQS3 IW Case optimised by the DS algorithm with 10 position chokes*

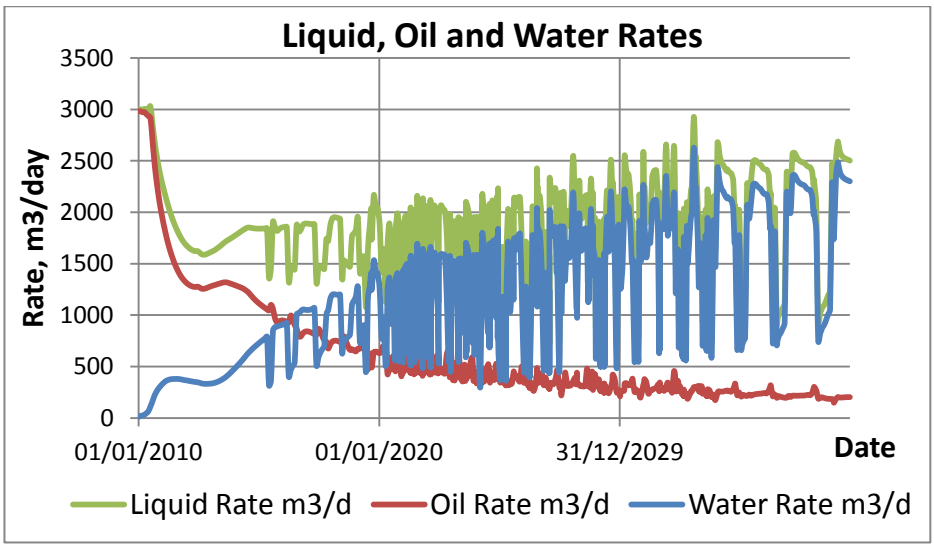


*Figure 5-15 Liquid, Oil and Water Rates for the PUNQS3 IW Case optimised by the DS algorithm with On/Off chokes*

*Table 5-11 Run time, Cumulative Oil, Cumulative Water and Smoothness coefficients for the No Control and optimised with the DS algorithm with 10 position and On/Off chokes at different time step scenarios*

| Method | Time Step | Run Time | | Cum Oil | Cum Water | SC for the Revenue |
|---|---|---|---|---|---|---|
| | | Sec | hh:mm:ss | Million $m^3$ | Million $m^3$ | |
| No Control | Adaptive | 541 | 00:09:01 | 6.99 | 15.99 | 0.0039 |
| | 2 Weeks | 1530 | 00:25:30 | 6.97 | 16.02 | 0.0026 |
| | 1 Month | 536 | 00:08:56 | 6.99 | 15.99 | 0.0039 |
| | 2 Months | 200 | 00:03:20 | 7.01 | 15.93 | 0.0057 |
| 10 Position | Adaptive | 3331 | 00:55:31 | 6.90 | 13.83 | 0.0225 |
| | 2 Weeks | 6812 | 01:53:32 | 6.88 | 13.80 | 0.0470 |
| | 1 Month | 3197 | 00:53:17 | 6.90 | 13.89 | 0.0442 |
| | 2 Months | 1541 | 00:25:41 | 6.92 | 13.91 | 0.0403 |
| On/Off | Adaptive | 5517 | 01:31:57 | 6.80 | 13.18 | 0.1047 |
| | 2 Weeks | 6436 | 01:47:16 | 6.74 | 12.99 | 0.0795 |
| | 1 Month | 2945 | 00:49:05 | 6.76 | 13.03 | 0.0814 |
| | 2 Months | 1546 | 00:25:46 | 6.86 | 13.26 | 0.1015 |

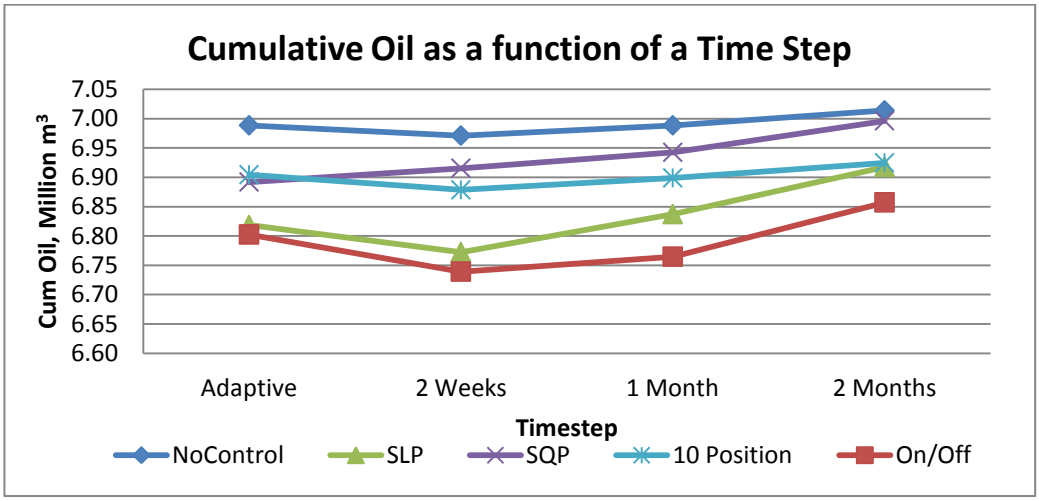


*Figure 5-16 Cumulative Oil as a function of a Time Step*

A significant increase in run time is observed in the PUNQS3 case (Table 5-11). However, if the optimisation time is based on the number of iterations it is estimated to be only 30% of that of the SQP algorithm for the adaptive time step scenario. Both the SLP and SQP algorithms show an increased run time than in the "Box-Shaped" model, presumably due to the greater complexity of the PUNQS3 model.

*Table 5-12 Number of time steps and iterations of the DS method for the PUNQS3 model*

| Method | Time Step | Number of Time Steps | Number of Iterations | Iterations / Time Step | Extra time Sec |
|---|---|---|---|---|---|
| 10 Position | Adaptive | 379 | 2401 | 6.34 | 303 |
| | 2 Weeks | 724 | 4547 | 6.28 | 573 |
| | 1 Month | 362 | 2329 | 6.43 | 295 |
| | 2 Months | 181 | 1193 | 6.59 | 152 |
| On/Off | Adaptive | 625 | 3591 | 5.75 | 445 |
| | 2 Weeks | 724 | 3925 | 5.42 | 480 |
| | 1 Month | 362 | 2011 | 5.56 | 247 |
| | 2 Months | 181 | 1047 | 5.78 | 130 |

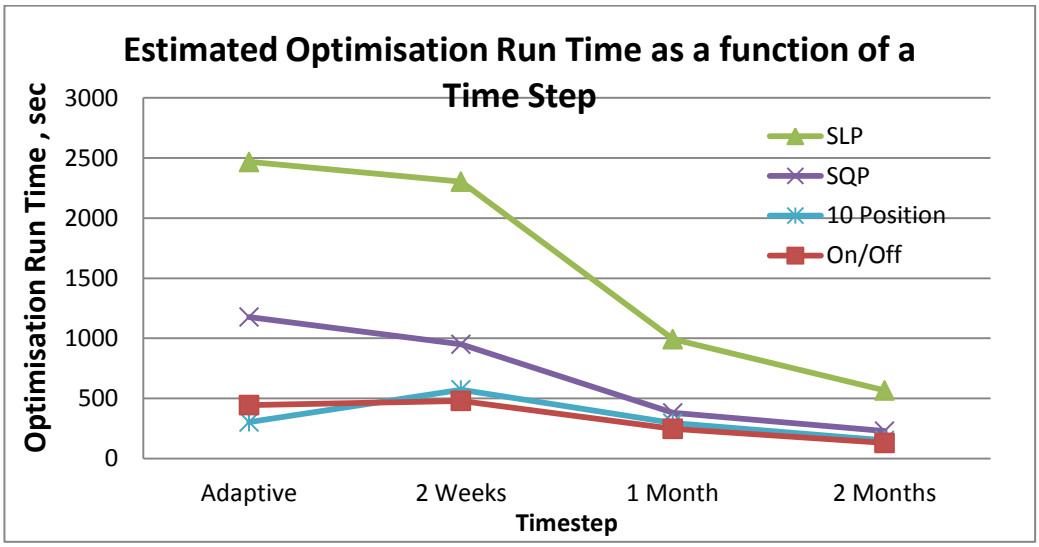


*Figure 5-17 Estimated Optimisation Time of SLP, SQP, DS for 10 positions and On/Off ICVs as a function of a Time Step*

Table 5-13 summarises cumulative oil**,** water production and NPV for all methods. In general, DS shows similar results with SLP and SQP methods. This time On/Off shows a slightly lower cumulative oil and NPV.

Water production was reduced using reactive control in the PUNQS-3 in average by 15% compared to the different optimisation methods. However, the oil production and NPV is also reduced, the Base Case (conventional well) gives the best result.

*Table 5-13 Cumulative oil, water production and NPV for all methods for the PUNQS3 model for 30 years period*

| Case | Cumulative NPV | | | Cumulative Oil Production | | | Cumulative Water Production | | |
|---|---|---|---|---|---|---|---|---|---|
| | NPV | Difference from Base Case | | Cum Oil | Difference from Base Case | | Cum Water | Difference from Base Case | |
| | Million$ | Million$ | % | Million $m^3$ | Million $m^3$ | % | Million $m^3$ | Million $m^3$ | % |
| **Base Case** | 1139 | - | - | 6.99 | - | - | 16.17 | - | - |
| **IW No Control** | 1132 | -8 | -0.7% | 6.99 | 0.00 | -0.1% | 15.99 | -0.18 | -1.1% |
| **IW SLP** | 1128 | -11 | -1.0% | 6.82 | -0.17 | -2.5% | 12.84 | -3.33 | -20.6% |
| **IW SQP** | 1131 | -8 | -0.7% | 6.89 | -0.10 | -1.4% | 14.13 | -2.04 | -12.6% |
| **IW DS 10 Pos** | 1131 | -8 | -0.7% | 6.90 | -0.09 | -1.3% | 13.83 | -2.34 | -14.5% |
| **IW DS On/Off** | 1125 | -14 | -1.2% | 6.80 | -0.19 | -2.7% | 13.18 | -2.99 | -18.5% |

### *5.1.6 Summary of the Direct Search Method*

This section described the application of the Direct Search algorithm for production optimisation of an oil well producing with a fixed tubing head pressure constraint. The proposed workflow consists of two stages: ICVs design and algorithm implementation for production optimisation.

The algorithm for On/Off and 10 position ICVs was tested for two cases: a ”Box-Shaped” and a PUNQS-3 model. The cumulative oil, water and NPV for both On/Off and 10 position scenarios are similar to the SLP and SQP results. However, the DS method for a 10 position valves shows a more stable production profile that is independent of the length of the time step. Also the estimated optimisation time of DS algorithm is potentially less than in SQP and SLP for complex models.

## 5.2 Proactive Optimisation

### *5.2.1 Problem Formulation*

The reactive strategy cannot be applied during the plateau period because the oil rate is restricted and cannot be increased. The proactive strategy can be employed in this case for equalising the water front to improve sweep efficiency and increase the future oil production. The objective function for this form of proactive optimisation is to minimise the difference between breakthrough times (equation 5-9):

$$T = \frac{1}{N}\sqrt{\sum_{i=1}^{N}(t_i - \bar{t})^2} \rightarrow \min \qquad (5\text{-}9)$$

where N - number of inflows (ICVs or wells), $t_i$ – breakthrough time in each inflow, $\bar{t}$ - average breakthrough time of all inflows.

The control variables for this task are choke diameters $d_i$ of ICVs for intelligent and wellhead chokes for conventional wells. The constraint is the total oil production $Q_{Total}^{Oil}$.

Finally, the problem is formulated as follows:

Find $d^*$ such as

$$\begin{cases} d^* = \arg\min_{d \in R^{N \times K}} T(d) \\ 0 \le d_{i,k} \le D_i, \mathrm{i} \in \{0,...,\mathrm{N}\} \\ Q_{Total}^{Oil}(\{d_1,...,d_N\}^k) = Q^0 \text{ - constant for every } \mathrm{k} \in \{0,...,\mathrm{K}\} \end{cases} \quad (5\text{-}10)$$

where K – is a number of optimisation time steps, T is defined by equation 5-9 and $D_i$ – the maximum choke diameter.

This optimisation task brings two main problems. The first problem is the high number of control variables (the number of inflows multiplied by the number of optimisation time steps). This number can be large if the number of wells is high and they need to be optimised frequently. The second problem is that the calculation of the objective function is a time consuming procedure because it requires running the model simulation until at least the last breakthrough has occurred. These two issues dramatically increase the optimisation time, requiring that the task be simplified.

### *5.2.2 Reducing the Number of Variables*

The breakthrough time depends on the well's production rate and is hence often highly correlated with the cumulative liquid production.

The example below demonstrates this correlation between the cumulative production and the breakthrough moment. This example is a PUNQS3 model with original 6 vertical production wells (see section 5.2.4 for details). In the initial case all wells are controlled by THP=10 bar. Fig 5-18 shows water cut of one of the wells for the initial case.

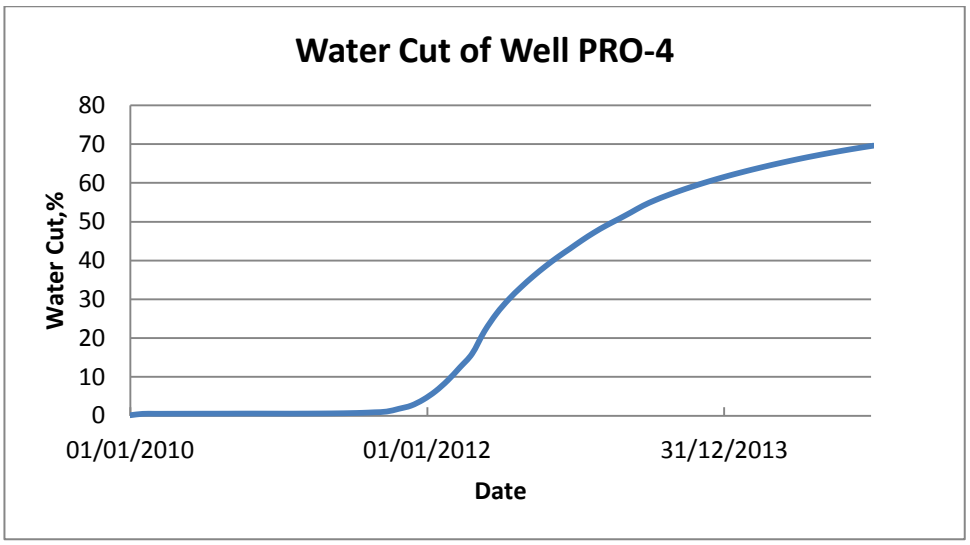


*Figure 5-18 Water Cut of Well PRO-4*

The well PRO-4 has been choked by fixed wellhead pressure varying from 10 to 100 bars for three periods of time: from 01/01/2010-01/01/2011, 01/06/2010-01/06/2011 and 01/01/2011-01/01/2012 (Fig. 5-19).

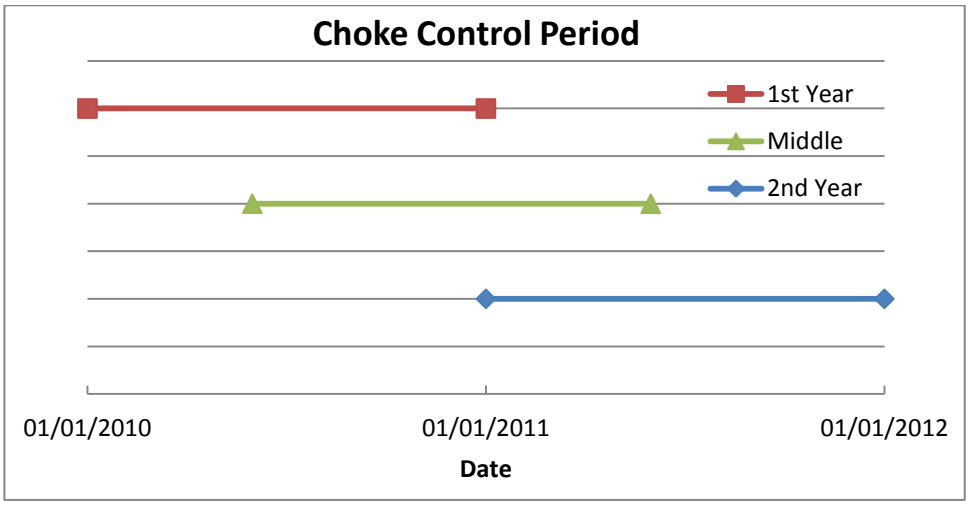


*Figure 5-19 Wellhead Choke Control Time*

Figure 5-20 shows that water breakthrough moment has a good linear relationship with the cumulative production and does not depend on the period in which the well has been controlled. Therefore, the control variables can be set up for the whole optimisation period and the number of the control parameters can be significantly reduced.

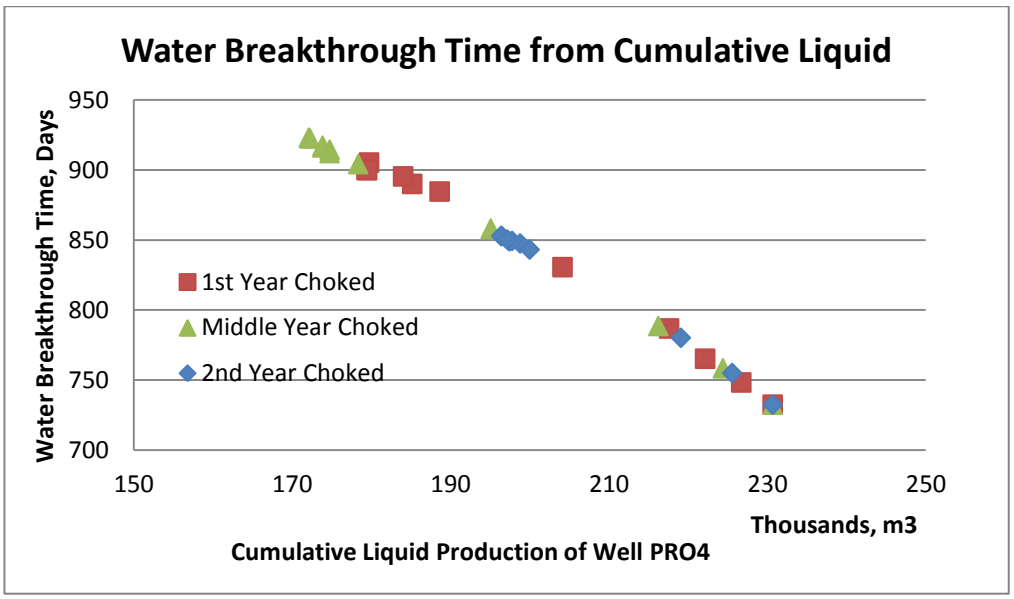


*Figure 5-20 Water Breakthrough Time from Cumulative Liquid for 3control scenarios*

The reservoir pressure changes during production period. Therefore fixed choke diameters are not able to satisfy total oil constraint. The inflow's oil rates can be used as a variable instead of the choke diameters with the choke diameter values calculated at each time step. The problem 5-2 can thus be reformulated as 5-3:

$$\begin{cases} x^* = \arg\min_{Q \in R^N} T(d(Q)) \\ d_{i,k} = \arg\{ x_i(d_{i,k}) = x_i^* \} \\ 0 \le x_i^* \le x_i(D_{i,k}), \text{for every k} \in \{0,...,\text{K}\} \text{ and i} \in \{0,...,\text{N}\} \quad \text{(c1)} \\ Q_{Total}^{Oil}(\{d_1,...,d_N\}^k) = \sum_{i=1}^{N} x_i^* = Q^0 \text{ - constant for every k} \in \{0,...,\text{K}\} \quad \text{(c2)} \end{cases} \tag{5-11}$$

where $x_i^*$ is the optimal oil rate of each inflow, c1 and c2 – two constraint sets, representing total and each individual well production limit.

### *5.2.3 Methodology*

The problem 5-11 can be solved by a 1st order optimisation method with a gradient projection (Kuznetsov 1992). A schematic diagram of the algorithm workflow is shown in Fig. 5-21.

The initialisation stage includes searching for the upper boundaries and the initial points. Sequential running of the model with only one ICV open at each time step and the total oil production constrained by $Q^0$ provides the upper boundaries:

$$x_i^{\max} = Cum\, Q_{oil}^i / T_{plateau} \tag{5-12}$$

where $T_{plateau}$ is a plateau period.

The initial point can be also calculated from equation 5-12 for the model run with all valves open and controlled by an upper wellhead choke to meet the total oil constraint (Fig. 5-22).

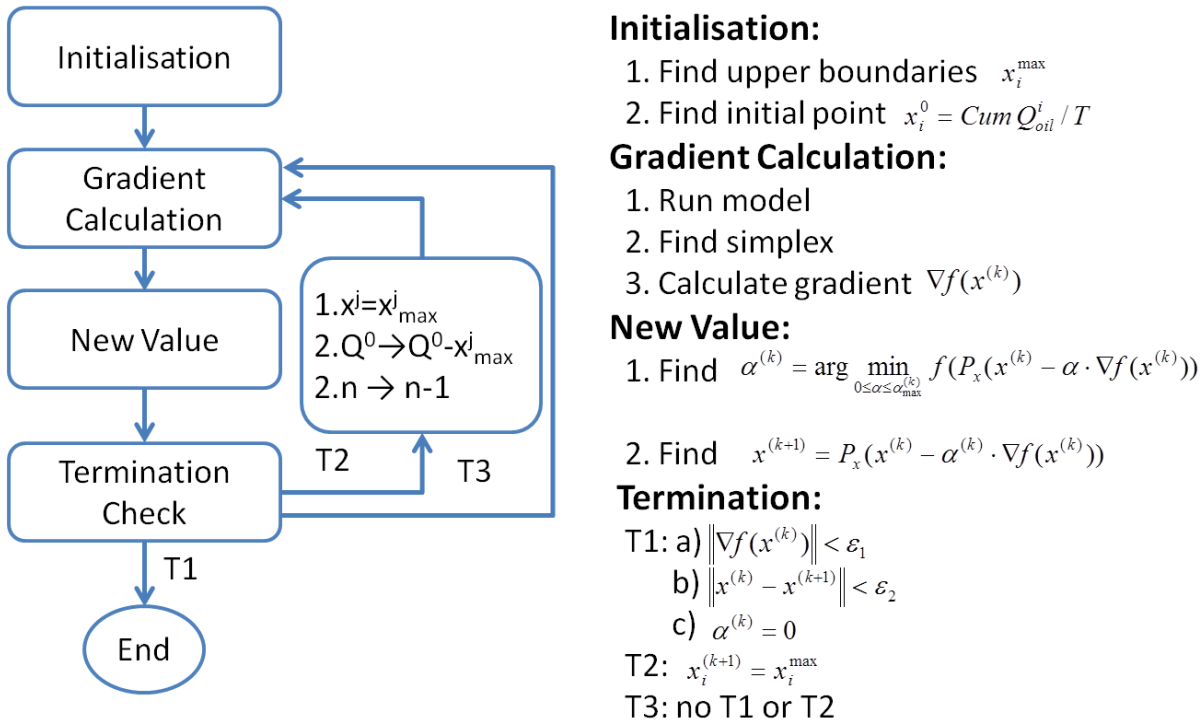


*Figure 5-21 Proactive algorithm schematic workflow*

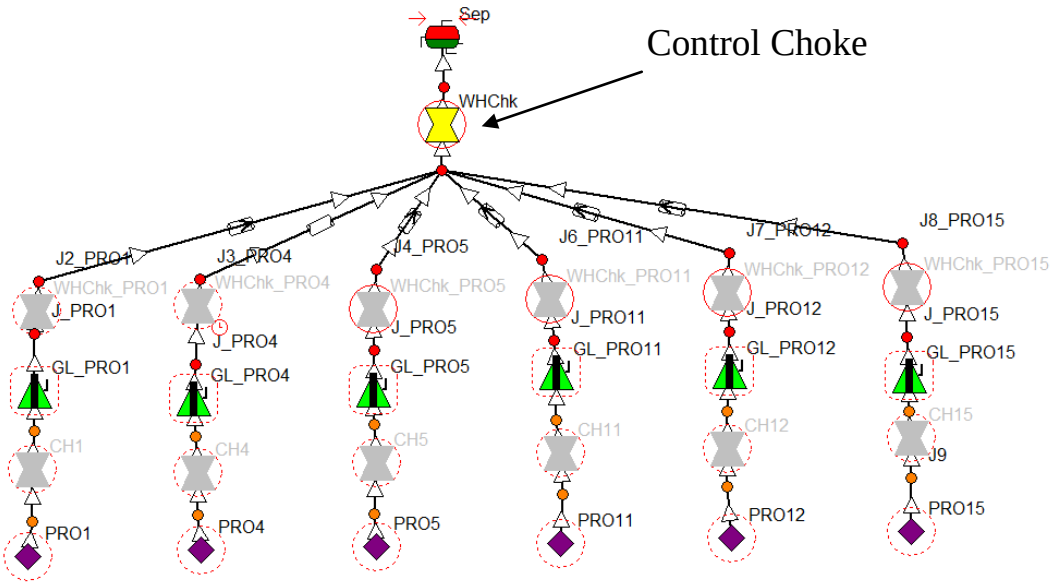


*Figure 5-22 System control with upper wellhead choke*

The gradient in each optimisation iteration is calculated with a simplex method (see Appendix A). It provides the search direction for the value of the new control variables. The classic steepest descent method uses antigradient direction and step size providing the minimum for the objective function in this direction:

$$\begin{cases} x^{(k+1)} = x^{(k)} - \alpha^{(k)} \cdot \nabla f(x^{(k)}) \\ \alpha^{(k)} = \arg\min_{\alpha \geq 0} f((x^{(k)} - \alpha \cdot \nabla f(x^{(k)})) \end{cases} \quad (5\text{-}13)$$

In the constrained case the solution should be projected to the hyper plane defined by constraint ***c2***. The projection method is described in Appendix A. Moreover, the solution should lie in a feasible region defined by constraint ***c1***, which restricts the maximum step size $\alpha^{(k)}$. Equation 5-14 describes the iteration step for the constrained case:

$$\begin{cases} x^{(k+1)} = P_x(x^{(k)} - \alpha^{(k)} \cdot \nabla f(x^{(k)})) \\ \alpha^{(k)} = \arg\min_{0 \leq \alpha \leq \alpha_{\max}^{(k)}} f(P_x(x^{(k)} - \alpha \cdot \nabla f(x^{(k)})) \end{cases} \quad (5\text{-}14)$$

where $P_x$ is a projection of solution to the constraint ***c2*** and $\alpha_{\max}^{(k)}$ is a maximum step size in a feasible region ***c1***.

There are three possible scenarios: 1) $\alpha^{(k)} = 0$; 2) $\alpha^{(k)} = \alpha_{\max}^{(k)}$ and 3) $0 < \alpha^{(k)} < \alpha_{\max}^{(k)}$.

In the first scenario a new solution equal to the solution of the previous iteration, which means that this is the local optimum and the algorithm has converged (T1c in Fig. 5-21).

If $\alpha^{(k)} = \alpha_{\max}^{(k)}$ then one of the control variables reached the maximum boundary. This control variable can be excluded from the next iteration (T2 in Fig. 5-21).

In the third case the solution lies in a feasible region and satisfies all constraints. The algorithm can be moved to the next iteration step.

The algorithm converges when the tolerance criterion is reached for the gradient or the objective function change:

$$\left\| \nabla f(x^{(k)}) \right\| < \varepsilon_1 \quad (5\text{-}15)$$

$$\left\| f(x^{(k)}) - f(x^{(k+1)}) \right\| < \varepsilon_2 \quad (5\text{-}16)$$

where $\varepsilon_1$ and $\varepsilon_2$ small positive values.

### *5.2.4 Results and Discussion*

The method has been tested in 3 cases: two analytical models and one numerical simulation model performed in *Eclipse*.

***Case 1. Analytical Model without boundaries***

The first model has 5 wells with initial parameters summarised in table 5-14.

We assume that drawdown **dP** does not change during production period. $Q^0$=1000 $m^3$/day is a maximum total oil production for this case. This constraint can be achieved

with control of the wellhead choke which provides a common extra pressure drop of 15.3 Bar for all wells.

The breakthrough times for all five wells are calculated by the equation 5-17:

$$t^i = \frac{60000}{Q_{oil}^i} + 12 \quad \text{(month)} \qquad (5\text{-}17)$$

*Table 5-14 Initial well's parameters of Case 1*

| Well | PI | DP (unconstrained) | $Q_{max}$ | DP (constrained) | Q | $T_{break}$ |
|---|---|---|---|---|---|---|
| | $m^3$/day/bar | bar | $m^3$ | bar | $m^3$/day | month |
| 1 | 75 | 32 | 2400 | 17 | 1252 | 37 |
| 2 | 70 | 30 | 2100 | 15 | 1029 | 41 |
| 3 | 80 | 35 | 2800 | 20 | 1576 | 33 |
| 4 | 100 | 50 | 5000 | 35 | 3470 | 24 |
| 5 | 90 | 45 | 4050 | 30 | 2673 | 27 |

The solution for this example can be found analytically. It is easy to check that $T = \frac{1}{N}\sqrt{\sum_{i=1}^{N}(t_i - \bar{t})^2} = 0$ is the minimum of the objective function at $Q_i^{oil} = 2000\,\mathrm{m}^3$ for all $i \in \{1,..,5\}$.

The task was solved with the proactive optimisation algorithm described before. Table 5-15 and Fig. 5-23 shows the results of the method at each iteration.

*Table 5-15 Results of the proactive optimisation algorithm*

| Iteration | 0 | 1 | 2 | 3 | 4 | 5 |
|---|---|---|---|---|---|---|
| T, month | 6.85 | 4.42 | 2.23 | 1.24 | 0.20 | 0.00 |
| Bounded well | No | No | No | No | No | No |
| N free | 5 | 5 | 5 | 5 | 5 | 5 |
| alpha | 1149 | 1102 | 688 | 438 | 65 | 0 |
| alpha max | 1500 | 980 | 1489 | 2070 | 194 | 900 |
| $\|\|f'\|\|$ | 0.00763 | 0.0047 | 0.0032 | 0.0028 | 0.0030 | 0.0011 |
| $\|\|\Delta f\|\|$ | 6.85 | 2.43 | 2.19 | 0.99 | 1.04 | 0.19 |
| t1, month | 60 | 56 | 44 | 44 | 42 | 42 |
| t2, month | 70 | 44 | 50 | 40 | 43 | 42 |
| t3, month | 50 | 57 | 43 | 45 | 42 | 42 |
| t4, month | 29 | 31 | 34 | 38 | 41 | 42 |
| t5, month | 34 | 38 | 43 | 44 | 42 | 42 |
| q1, m3/day | 1252 | 1375 | 1854 | 1860 | 1997 | 2001 |
| q2, m3/day | 1029 | 1850 | 1596 | 2117 | 1949 | 2000 |
| q3, m3/day | 1576 | 1343 | 1929 | 1844 | 2008 | 2000 |
| q4, m3/day | 3470 | 3124 | 2713 | 2333 | 2040 | 2000 |
| q5, m3/day | 2673 | 2308 | 1909 | 1846 | 2006 | 1999 |

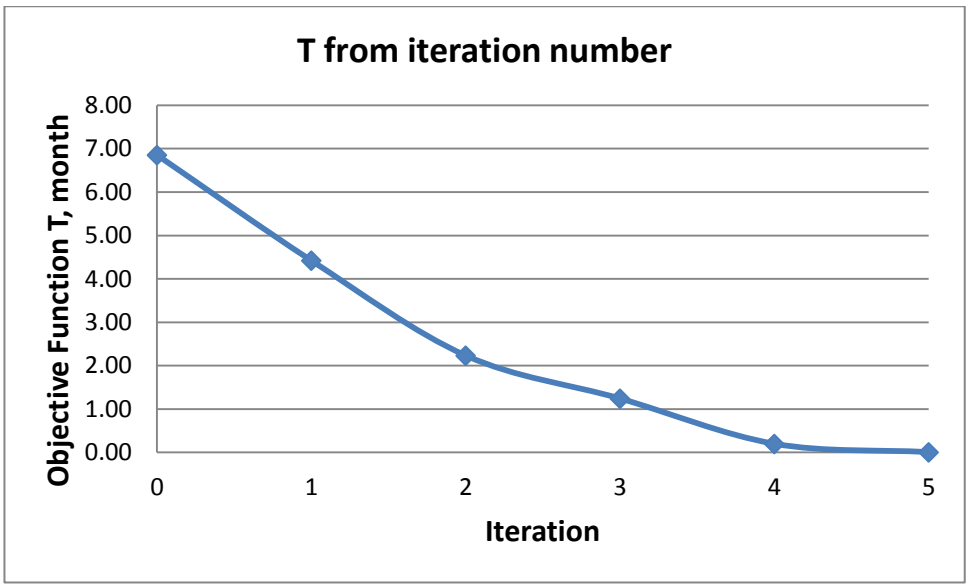


*Figure 5-23 Objective Function T at each iteration*

The method converged to the optimal solution in 5 iterations when the termination criterion (T1c) is satisfied.

***Case 2. Analytical Model with boundaries***

In the previous example the algorithm did not meet the boundaries. The input data was modified (Table 5-16) in such a way that wells 2 and 5 would have maximum oil rates at the optimal solution.

*Table 5-16 Initial well's parameters of Case 2*

| Well | PI | DP (unconstrained) | $Q_{max}$ | DP (constrained) | Q | $T_{break}$ |
|---|---|---|---|---|---|---|
| | $m^3$/day/bar | bar | $m^3$ | bar | $m^3$/day | month |
| 1 | 75 | 32 | 2400 | 21 | 1541 | 51 |
| 2 | 20 | 30 | 600 | 19 | 371 | 174 |
| 3 | 90 | 35 | 3150 | 24 | 2120 | 40 |
| 4 | 120 | 50 | 6000 | 39 | 4626 | 25 |
| 5 | 40 | 45 | 1800 | 34 | 1342 | 57 |

Table 5-17 shows the results for this case. The minimum value of the objective function after the first iteration has been achieved at Well 2 maximum oil production (T2 termination criterion). The well's 2 rate has been set up to the maximum value of 600 $m^3$ and was excluded from the further iterations. The number of free variables ***Nfree*** reduced from 5 to 4. In the next two iterations wells 5 and 1 also reached the maximum values. Finally, the method has converged after 4 iterations.

*Table 5-17 Results of the proactive optimisation algorithm*

| Iteration | 0 | 1 | 2 | 3 | 4 |
|---|---|---|---|---|---|
| T, month | 23.84 | 13.14 | 5.98 | 5.10 | 0.00 |
| Bounded well | 2 | 5 | 1 | No | No |
| N free | 5 | 4 | 3 | 2 | 2 |
| alfa | 283 | 980 | 1489 | 1192 | 0 |
| alfa max | 283 | 980 | 1489 | 2070 | 1320 |
| ‖f'‖ | 0.07737 | 0.0041 | 0.0045 | 0.0065 | 0.0018 |
| ‖Δf‖ | 23.84 | 10.70 | 7.16 | 0.88 | 5.10 |
| t1, month | 51 | 52 | 49 | 37 | 37 |
| t2, month | 174 | 112 | 112 | 112 | 112 |
| t3, month | 40 | 41 | 45 | 44 | 35 |
| t4, month | 25 | 25 | 26 | 30 | 35 |
| t5, month | 57 | 59 | 45 | 45 | 45 |
| q1, m3/day | 1541 | 1485 | 1608 | 2400 | 2400 |
| q2, m3/day | 371 | 600 | 600 | 600 | 600 |
| q3, m3/day | 2120 | 2061 | 1797 | 1854 | 2600 |
| q4, m3/day | 4626 | 4570 | 4195 | 3346 | 2600 |
| q5, m3/day | 1342 | 1284 | 1800 | 1800 | 1800 |

***Case 3. PUNQS3 Model with 6 vertical wells***

PUNQS3 model with original 6 vertical wells (Fig. 5-24) has been used for testing this algorithm.

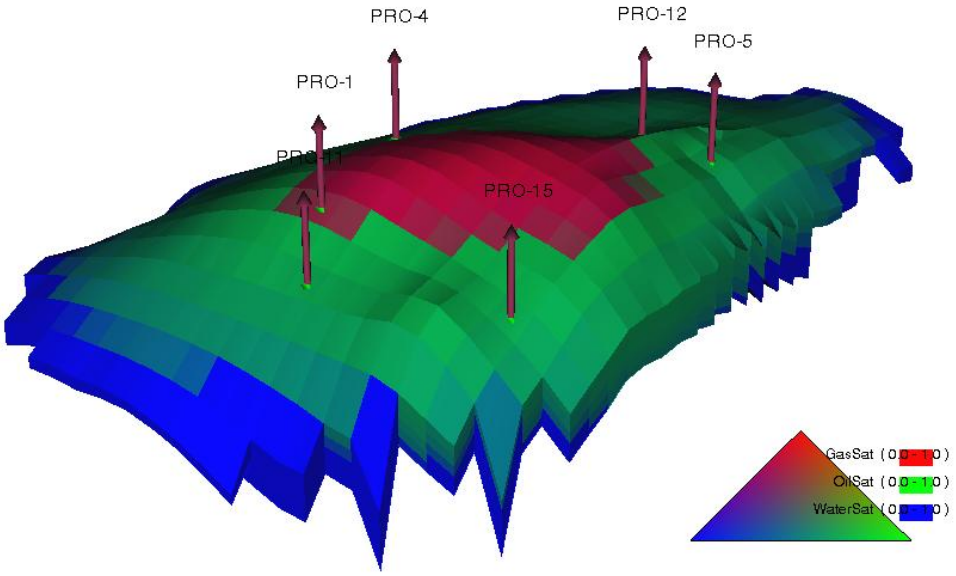


*Figure 5-24 PUNQS3 Model with 6 vertical wells*

The gas lift was used in all wells with constant gas injection rate equal $50*10^3$ $m^3$/day. The initial oil and water production with a total oil constraint of $Q^0=1000m^3$/day and wellhead THP=10 bar is shown in Fig. 5-25.

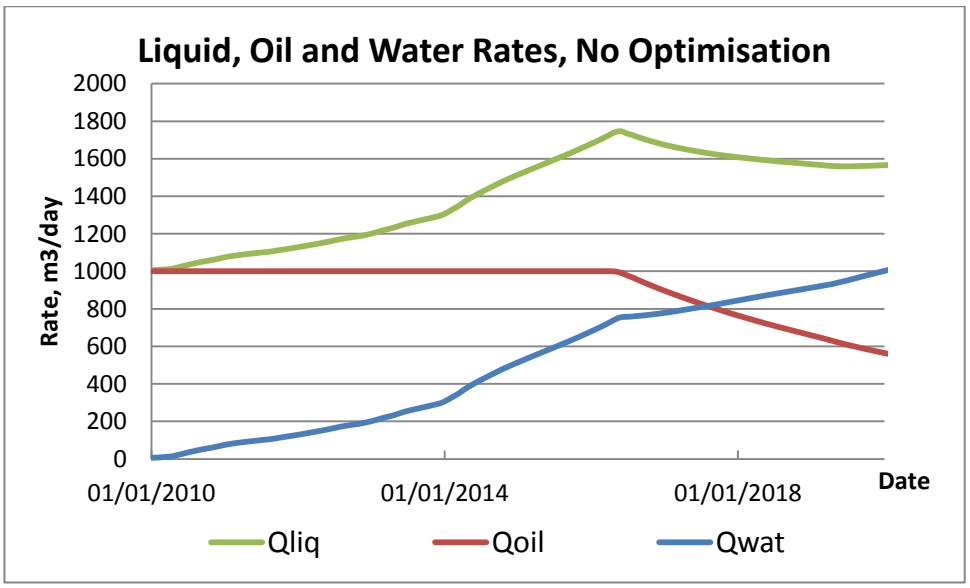


*Figure 5-25 Initial Total Liquid, Oil and Water Rates of PUNQS3 model*

The initialisation stage included calculation of the maximum oil constraint for each well and specifying the initial point (Table 5-18). The model has been run 6 times with one of the wells well constrained by THP only and maximum oil rate was calculated by formula 5-12 for that well. The initial point for all wells $Q_{oil}$ initial=180 $m^3$/day except of the well PRO-12 which has lower maximum boundary.

*Table 5-18 Maximum oil boundary and initial point for each well*

| Well | $Q_{oil}$ max | $Q_{oil}$ initial |
|---|---|---|
| | $m^3$/day | $m^3$/day |
| PRO-1 | 255 | 180 |
| PRO-11 | 190 | 180 |
| PRO-12 | 139 | 100 |
| PRO-15 | 432 | 180 |
| PRO-4 | 231 | 180 |
| PRO-5 | 546 | 180 |

The algorithm was realised in Excel VBA and connected with Eclipse via Resolve. The control parameter at each simulation time step is oil rate while THP=10 bar is constant. Table 5-19 shows the results of the algorithm at each iteration. The method has converged in 7 iterations. The difference between breakthrough moments reduced from 14.5 to 12.2.

*Table 5-19 Results of the proactive optimisation algorithm of PUNQS3 model controlled by Qoil*

| Iteration | 0 | 1 | 2 | 3 | 4 | 5 | 6 | 7 |
|---|---|---|---|---|---|---|---|---|
| **T, month** | 14.48 | 13.10 | 12.54 | 12.31 | 12.30 | 12.27 | 12.18 | 12.16 |
| **Bounded** | No | No | No | No | No | No | No | No |
| **N free** | 6 | 6 | 6 | 6 | 6 | 6 | 6 | 6 |
| **alfa** | 84 | 100 | 18 | 5 | 8 | 40 | 1 | 0 |
| **alfa max** | 419 | 250 | 480 | 265 | 136 | 170 | 550 | 135 |
| **‖f'‖** | 0.0262 | 0.0292 | 0.0627 | 0.0159 | 0.0186 | 0.1151 | 0.0174 | 0.1402 |
| **‖Δf‖** | 14.479 | 1.381 | 0.558 | 0.227 | 0.017 | 0.029 | 0.084 | 0.018 |
| **t1, month** | 124 | 115 | 109 | 110 | 110 | 110 | 108 | 108 |
| **t2, month** | 11 | 12 | 14 | 15 | 15 | 15 | 16 | 16 |
| **t3, month** | 54 | 57 | 56 | 56 | 55 | 55 | 56 | 56 |
| **t4, month** | 41 | 33 | 26 | 27 | 27 | 27 | 24 | 24 |
| **t5, month** | 46 | 45 | 43 | 43 | 44 | 44 | 45 | 45 |
| **t6, month** | 29 | 38 | 66 | 55 | 56 | 52 | 60 | 59 |
| **q1, m3/day** | 180 | 194 | 197 | 195 | 198 | 196 | 192 | 192 |
| **q2, m3/day** | 180 | 162 | 135 | 130 | 128 | 126 | 122 | 122 |
| **q3, m3/day** | 100 | 98 | 107 | 106 | 108 | 110 | 105 | 105 |
| **q4, m3/day** | 180 | 230 | 288 | 286 | 287 | 285 | 320 | 319 |
| **q5, m3/day** | 180 | 183 | 193 | 190 | 188 | 186 | 174 | 174 |
| **q6, m3/day** | 180 | 133 | 80 | 93 | 91 | 97 | 87 | 88 |

Provided that the main purpose of the optimisation is not the breakthrough time mismatch, but the potential improvement in the production. Figure 5-26 shows the oil rates of the original case (controlled with a single wellhead choke), initial step and optimised cases.

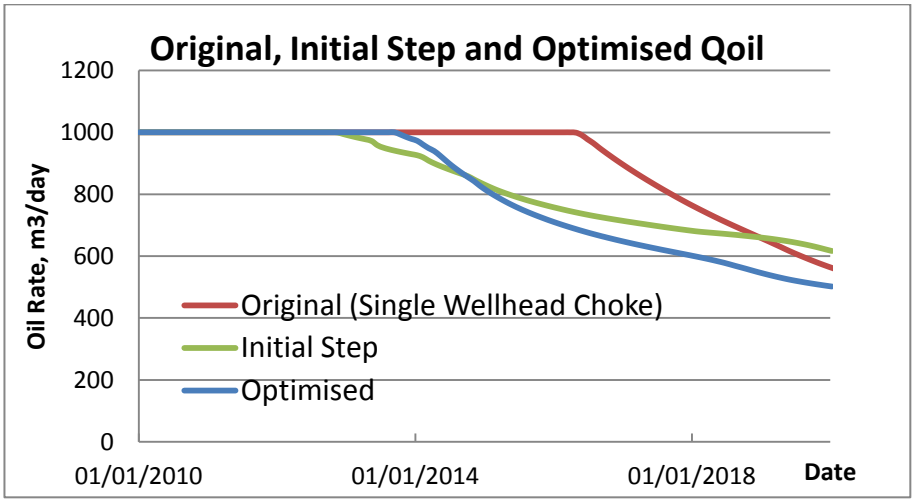


*Figure 5-26 Original, Intial Step and Optimised Oil Rate*

The optimal case has extended the plateau period in compare to the initial step of optimisation, but the overall result is worse than in the original case. This is due to the production capacity of some of the wells being less than the maximum value which had

originally been found resulting in an early decline in production. The other wells are producing at restricted rates and cannot compensate for this production loss.

The control was therefore returned to a single wellhead choke control once the production decline process had started. Figure 5-27 shows the difference between the original and optimised cases. The optimisation did not extend the plateau period and the total oil production was not increased. The benefit of the optimisation was a slightly decreased water rate for a limited period.

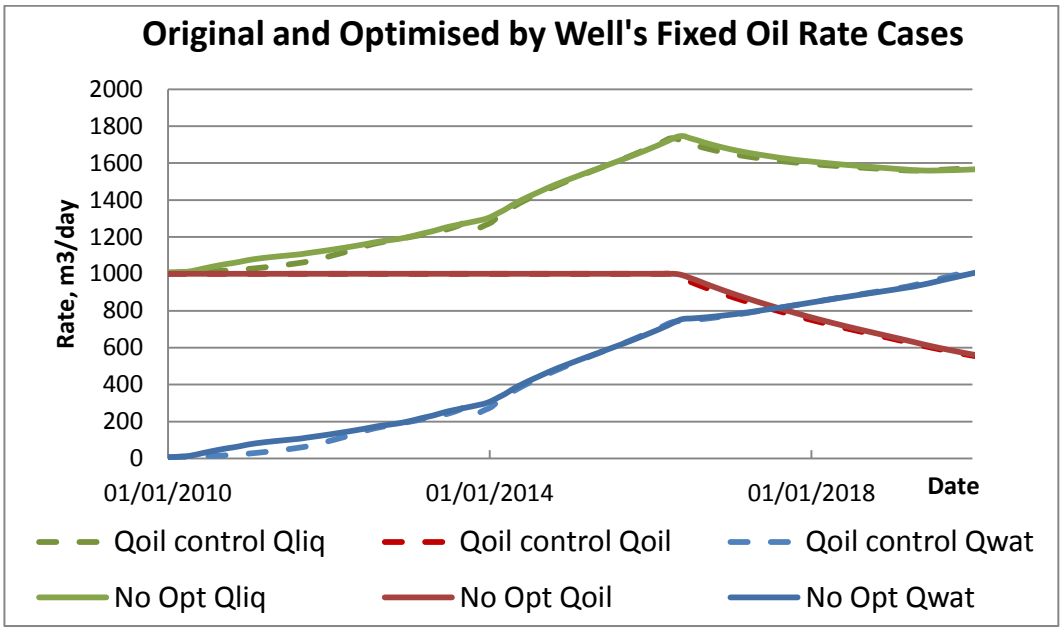


*Figure 5-27 Original and Optimised by Well's Fixed Oil Rate Cases*

### *5.2.5 New Control Variables: Reduction Coefficients*

The previous example demonstrated that fixing the well's rates is not always efficient since the reservoir conditions change and the control strategy needs to compensate for these changes. One of the solutions to this problem is to use several optimisation steps with updating of the input information at each step. However, this approach increases the number of control variables and results in a time consuming optimisation process.

Another approach is to use a control variable that considers the changes in reservoir conditions, but remains constant for the whole optimisation period. Reduction coefficients (RC) can be employed for this purpose (Fig. 5-28). The maximum potential oil rate at each time step can be found and any surplus greater than the constraint can be distributed among all inflows and the RCs used to reduce their current rates. The inflow is then closed if its current rate is lower than the volume by which it should be reduced (e.g. inflow 2 in Fig. 5-29b) and the rest of extra potential oil (if any) is redistributed among the other inflows.

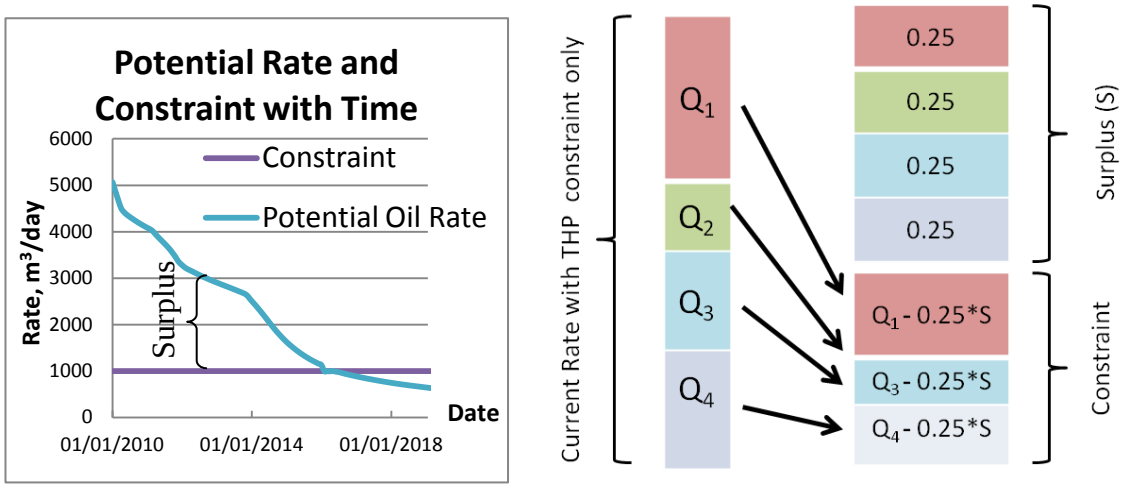


*a* *b*

*Figure 5-28 Rate control with fixed Reduction Coefficients: a) Change of Surplus over the time; b) Conversion of well's rates with Reduction Coefficients*

The mathematical formulation of this conversion is described by equations 5-18 - 5-23:

$$\eta : \{Q_{oil}^{i}\}^{t} \rightarrow \{q_{oil}^{i}\}^{t} \tag{5-18}$$

$$\sum_{i=1}^{N} \{Q_{oil}^{i}\}^{t} = \{Q_{oil}^{Total}\}^{t} \quad - \text{current total oil rate} \tag{5-19}$$

$$\sum_{i=1}^{N} \{q_{oil}^{i}\}^{t} = Q^{0} \quad - \text{total oil rate constrain} \tag{5-20}$$

$$SP^{t} = \{Q_{oil}^{Total}\}^{t} - Q^{0} \quad - \text{surplus} \tag{5-21}$$

where t –time step, $\{Q_{oil}^{i}\}^{t}$ - is inflow oil rate with THP control, $\{q_{oil}^{i}\}^{t}$ - is converted inflow rate at each time step, $RC_i$ - reduction coefficients.

$$\begin{cases} 0 \le RC_i \le 1 \\ \sum_{i=1}^{N} RC_i = 1 \end{cases} \tag{5-22}$$

Then

$$\eta(\{Q_{oil}^{i}\}^{t}) = \begin{cases} 0, i \in CLOSED^{t} \\ RC_i \cdot \{Q_{oil}^{i}\}^{t}, i \notin CLOSED^{t} \end{cases} \tag{5-23}$$

where $CLOSED^{t}$ is a set of closed inflows which can be found from the iterative process:

**Step 1.**

$$\{\sigma^{(0)}\}^{t} = SP^{t} \tag{5-24}$$

$$\{CLOSED^{(0)}\}^{t} = \{i \in \{0,...,N\} \mid \{Q_{oil}^{i}\}^{t} < RC_i \cdot SP^{t}\} \tag{5-25}$$

Set k=1

**Step 2.**

$$\{\sigma^{(k)}\}^t = \{\sigma^{(k-1)}\}^t - \sum_{i\in\{CLOSED^{(k-1)}\}^t} \{Q_{oil}^i\}^t \qquad (5\text{-}26)$$

$$\{X^{(k)}\}^t = \{i \notin \{CLOSED^{(k-1)}\}^t \mid \{Q_{oil}^i\}^t < RC_i \cdot \{\sigma^{(k-1)}\}^t\} \qquad (5\text{-}27)$$

If $\{X^{(k)}\}^t$ is empty then $CLOSED^t = \{CLOSED^{(k-1)}\}^t$ and stop.

If $\{X^{(k)}\}^t$ is not empty then:

$$\{CLOSED^{(k)}\}^t = \{CLOSED^{(k-1)}\}^t \cup \{X^{(k)}\}^t \qquad (5\text{-}28)$$

Set k=k+1 and go to **Step 2.**

### *5.2.6 Application of the Algorithm in the PUNQS3 Model*

The algorithm was tested in the PUNQS3 model. The results are summarised in table 5-20 and Fig. 5-30 and 5-31.

*Table 5-20 Results of the proactive optimisation algorithm of PUNQS3 model controlled by Reduction Coefficients*

| Iteration | 0 | 1 | 2 | 3 | 4 | 5 | 6 | 7 |
|---|---|---|---|---|---|---|---|---|
| **T, month*** | 15.07 | 7.54 | 5.84 | 4.57 | 4.43 | 3.94 | 3.14 | 1.73 |
| **Bounded** | PRO-1 | PRO-12 | No | No | PRO-4 | No | No | No |
| **N free** | 6 | 5 | 4 | 4 | 4 | 3 | 3 | 3 |
| **alfa** | 0.25 | 0.32 | 0.276 | 0.0003 | 0.005 | 0.0172 | 0.0132 | 0 |
| **alfa max** | 0.5 | 0.32 | 0.46 | 0.011 | 0.005 | 0.043 | 0.044 | 0.006 |
| **‖f'‖** | 19.350 | 19.369 | 7.027 | 13.181 | 14.677 | 16.496 | 10.927 | 27.73 |
| **‖Δf‖** | 15.1 | 7.5 | 1.7 | 1.3 | 0.1 | 0.5 | 0.8 | 1.4 |
| **t1, month** | 123 | 118 | 117 | 119 | 119 | 119 | 119 | 119 |
| **t2, month** | 15 | 20 | 55 | 37 | 39 | 34 | 54 | 39 |
| **t3, month** | 73 | 74 | 49 | 50 | 50 | 50 | 48 | 44 |
| **t4, month** | 30 | 21 | 19 | 23 | 23 | 28 | 37 | 43 |
| **t5, month** | 55 | 49 | 53 | 42 | 42 | 37 | 36 | 33 |
| **t6, month** | 23 | 33 | 45 | 51 | 50 | 50 | 39 | 40 |
| **RC1, m3/day** | 0.167 | 0 | 0 | 0 | 0 | 0 | 0 | 0 |
| **RC2, m3/day** | 0.167 | 0.208 | 0.379 | 0.284 | 0.290 | 0.263 | 0.394 | 0.276 |
| **RC3, m3/day** | 0.167 | 0.239 | 0 | 0 | 0 | 0 | 0 | 0 |
| **RC4, m3/day** | 0.167 | 0.117 | 0.046 | 0.119 | 0.116 | 0.185 | 0.275 | 0.342 |
| **RC5, m3/day** | 0.167 | 0.139 | 0.165 | 0.070 | 0.072 | 0 | 0 | 0 |
| **RC6, m3/day** | 0.167 | 0.297 | 0.406 | 0.528 | 0.522 | 0.543 | 0.332 | 0.382 |

* For iterations 1-7 only wells 3-6 were used for T calculation

The algorithm converged in 7 iterations. The reduction coefficients of three wells reached their boundaries during the optimisation process. The production rate of those wells was not reduced by the optimiser.

Figure 5-29 shows that the breakthrough moment in the wells became closer after optimisation. Well PRO-1 shows the latest breakthrough moment which is about 3 times

longer than for the other wells even if the well is fully open all the time. This well has been kept open and excluded from the objective function calculation for faster convergence and better solution of the other wells.

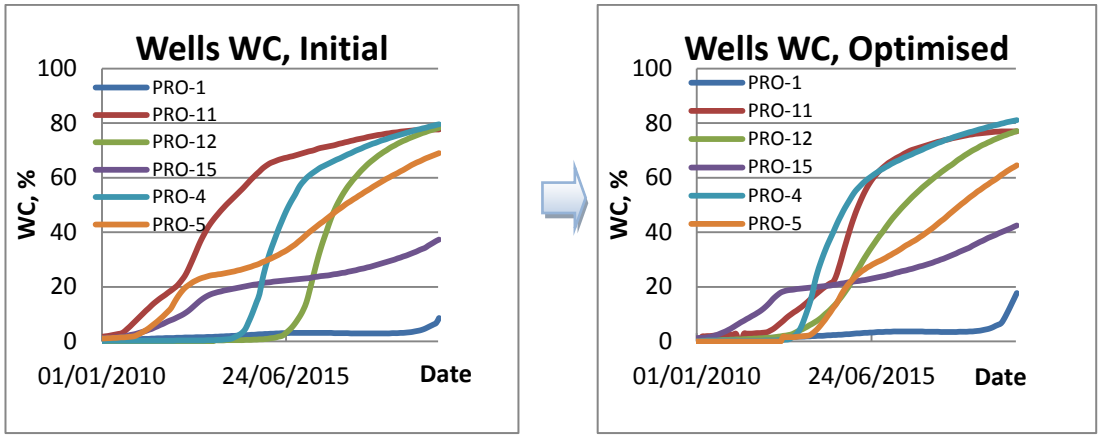


*a* *b*

*Figure 5-29 Well water cuts for the initial(a) and optimised(b) cases*

Figure 5-30 shows that the plateau has been extended for 4 months in the optimised case and the water production delayed. The total oil production has been increased by 0.5% and total water production reduced by 9%.

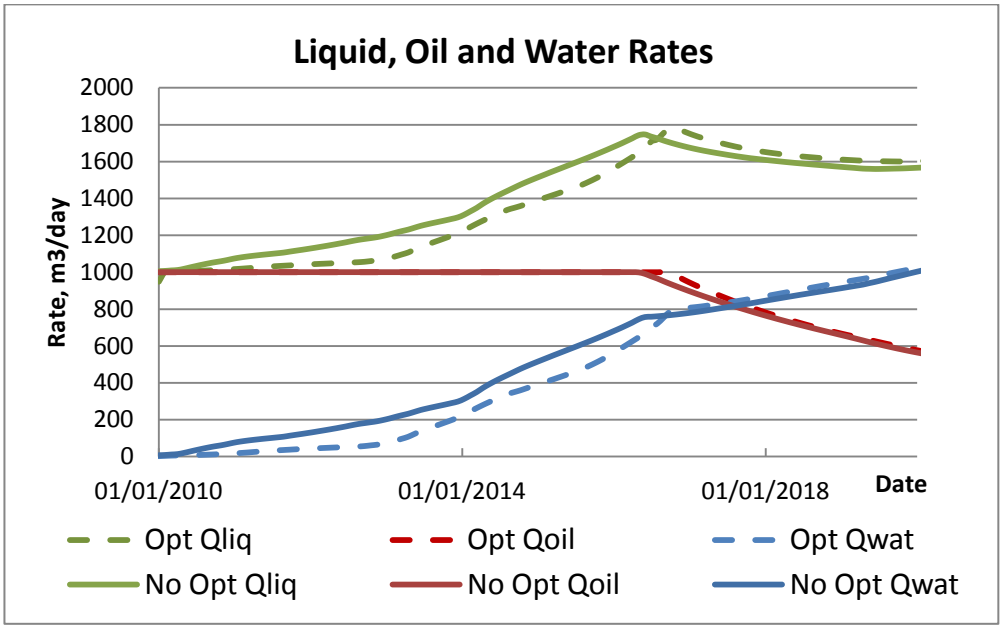


*Figure 5-30 Liquid, Oil and Water Rates before and after optimisation*

### *5.2.7 Summary of Proactive Optimisation*

A simple proactive optimisation algorithm has been developed for production optimisation during a plateau period. The algorithm aims to equalise the inflow breakthrough time and, as a result, delay water production and improve sweep efficiency.

The algorithm was tested in an analytical model and a reservoir simulation PUNQS3 model with 6 production wells. This model is small, yet has enough level of a complexity to confirm that the algorithm can be applied for a complex real field case. Two types of control parameters have been employed: wells oil rates and reduction coefficients (RC).

Fixed oil rate control gave an optimal solution with fast convergence in an analytical model. However, only small improvements were achieved in the dynamic model, because the boundary conditions for each well were inconsistent with the changing reservoir conditions.

RC control demonstrated the ability to partially equalise the breakthrough time at the different wells, extend the plateau period and decrease the total water production.

The algorithm converged after only 7 iterations. However, general application of this approach will require a full theoretical analysis of all aspects of the convergence process in all possible situations. The algorithm is promising and can be a powerful instrument for the proactive optimisation at the plateau period while implemented in the commercial software.

### 5.3 Summary

Novel algorithms of proactive optimisation and reactive control of discrete position and On/Off ICVs were described in this chapter. They allow operators to increase the value of IWs in the areas were methods available in today's commercial software are not applicable or provide poor results (such as Eclipse's Adjoint algorithm). In addition, the reactive direct search optimisation method generates a more stable production profile and potentially less time required for optimisation than for the SLP and SQP algorithms.

This chapter compared the different algorithms based on their ability to optimise. The difference in completion cost was not considered in NPV calculation, with the cost of infinitely variable completion being used for all IW cases. Not only will the cost of On/Off, discrete position and infinitely variable ICV completions be different, but they will also have a different reliability. Hence, the next chapter will compare the value of optimising the production with different types of ICVs in terms of their cost and reliability.

# Chapter 6 – Comparison of Infinitely Variable, Discrete Valve Position and On/Off strategy. Reliability Analysis

This chapter compares Infinitely Variable, Discrete Valve Position and On/Off ICVs based on their reliability and cost. The different types of the intelligent completion provide different levels of flow flexibility and hence can potentially deliver different levels of added value. Infinitely variable valves thus provide a greater level of flexibility when controlling and optimizing the flow in the well than On/Off valves. However, the increased complexity of the more flexible devices increases the number of ways they can fail and therefore reduces their reliability and their potential to add value throughout the well's life.

The reliability of intelligent wells was an important topic during the early stage of the introduction of IWs to the field. Thus, the Intelligent Well Reliability Group, formed in 2001, provided a forum for major operators and vendors to develop a fundamental analysis of the IW failure issue and identify options to improve their reliability (Hother 2003). The reliability of IWs has increased significantly since that time; however this factor can still be an important consideration when choosing the equipment to be installed for particular application.

There are two different measures of reliability: mission and system reliability. *Mission reliability* is the probability that zonal completion equipment will work as specified initially to meet an optimisation target. This includes intelligent completion such as ICVs and ICDs, gravel pack system, packers or reservoir zone failure, such as scale build up. *System reliability* is the probability of the whole system such as an intelligent well will work as specified originally. System failure includes all the above failure modes, but also includes failure modes due to electronics, cables, connectors, control lines, control and monitoring devices, etc.

Ajayi et al. (Ajayi, Mathieson et al. 2005) investigated the impact of system failure on the IW's Added Value. They looked at the probable changes in the oil recovery if the IW failed at different time. Almeida et al (Almeida, Tupac et al. 2007) included mission reliability directly into the optimisation GA algorithm which they used for IW optimisation. Aggrey and Davies (Davies and Aggrey 2007) used stochastic approach for reliability analysis. This approach provides a comprehensive analysis of the reliability impact on the IWs potential added value and delivers a distribution of all possible values for each scenario.

A similar approach to that employed by Aggrey and Davies will be used in this chapter, with the addition of a more sophisticated technique for NPV estimation after valve failure.

## 6.1 Methodology

The stochastic approach requires performing a large number of simulations with the Monte Carlo method to provide a NPV probability distribution for all possible scenarios. Mission reliability analysis considers the probability of failure of each downhole valve during the production period. This failure may affect the cumulative oil and water production and the NPV.

The Weibull equation (Bryan 2006) is a common method for describing equipment failure:

$$R(t) = e^{-(\frac{t}{\eta})^{\beta}} \qquad (6\text{-}1)$$

Where R is reliability,

t is time,

β is the shape factor and

η is the equipment's characteristic life.

The most realistic values of the above equation parameters can be determined from real field data on the number and timing of valves failure, for example (WellDynamics and Halliburton 2009). The reliability curves and Weibull's equation parameters of On/Off, 10 position and infinitely variable cases are shown in Fig. 6-1.

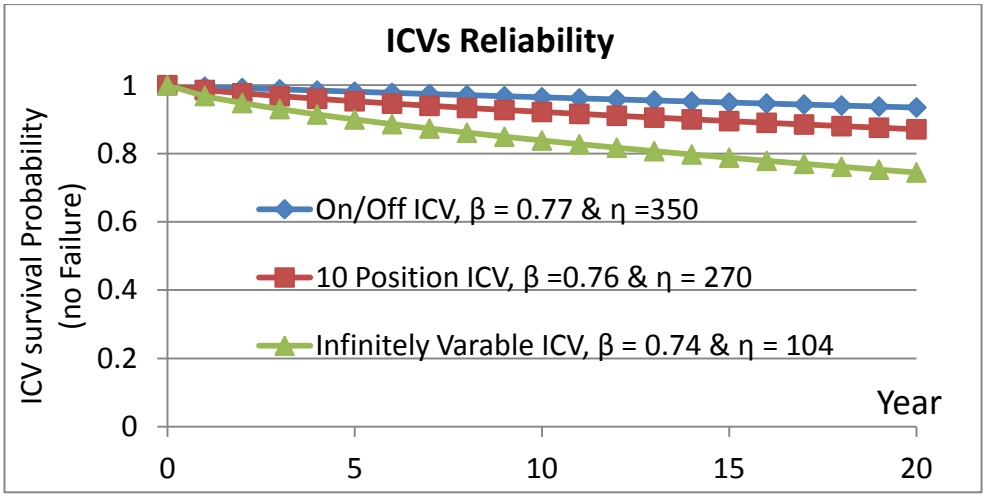


*Figure 6-1 Reliability curves of On/Off, 10 position and Infinitely Variable cases*

The impact of the failure on the production or economic result can be calculated, once the probability of the valve operating without failure for the specified number of years

for each scenario is estimated. We assume that the valve is placed is in the fully open mode after failure. However, the failure mode of most valves is "fail-as-is", i.e. the valve maintains its position at failure. The fully open failure assumption is realistic since a shifting tool can be used to move the valve into the desired position.

Figure 6-2 illustrates the impact of ICV failure on the well's water production rate. Failure of valve 4 occurred almost at the start of the production in this example; therefore the impact on the result is not noticeable in this case. ICV2 failed after 5 years and 9 months. The water inflow is still reduced by ICV3, however more water is produced after that date than in the optimised case with all operational valves. ICV3's failure 5 years later significantly increased water production. As a result, the total NPV in the case with ICVs failure was reduced by 2% (Fig. 6-3).

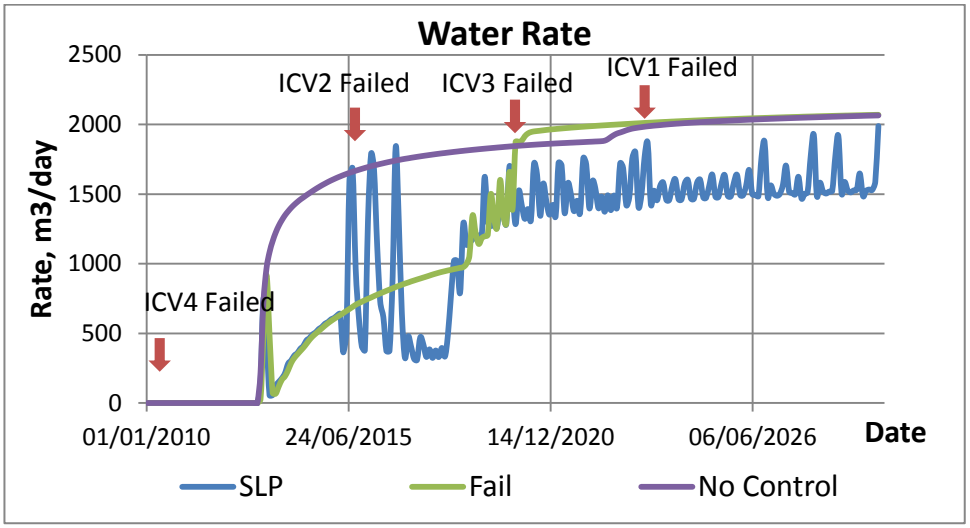


*Figure 6-2 Impact of ICVs failure on the well's water production rate*

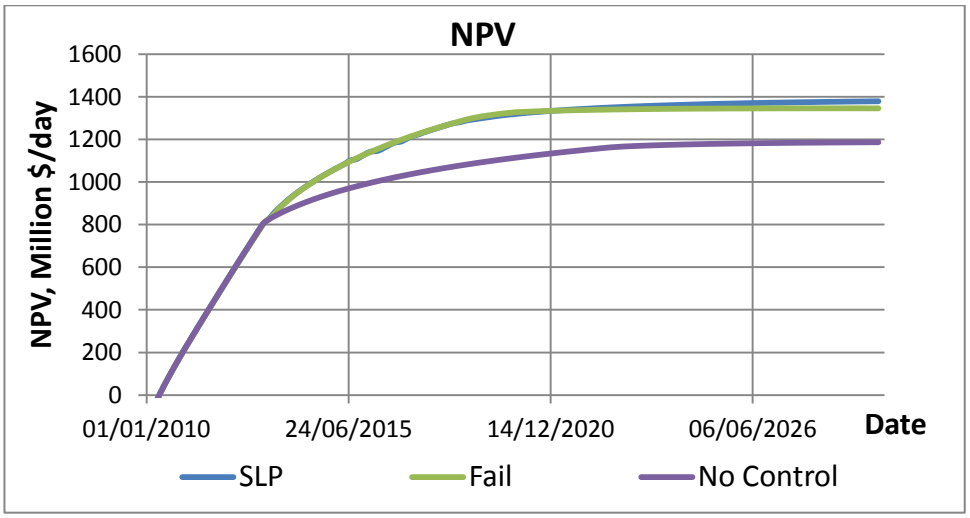


*Figure 6-3 Impact of ICVs failure on the well's NPV*

Calculating the NPV for each possible scenario generated by a Monte Carlo analysis, where each ICV can fail with a certain probability based on the valve's reliability can be

very time consuming process requiring a large number of simulations. A faster procedure is to use a response surface method (RSM) based on the experimental design instead of the direct calculation of NPV from the simulation models.

A modified workflow for this reliability analysis is shown in Fig. 6-4 followed by its application to a "Box-Shaped" model in the next section of this chapter.

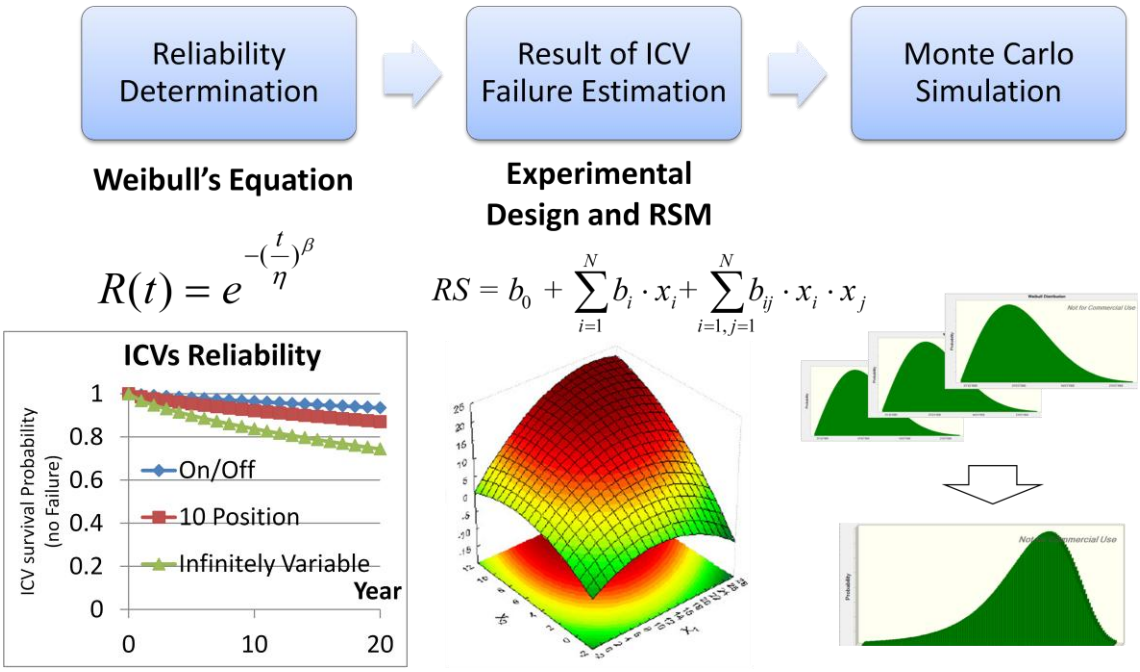


*Figure 6-4 Reliability Analysis Workflow*

## 6.2 Reliability Analysis of "Box-Shaped" model

### *6.2.1 Experimental Design Selection*

The "Box-Shaped" model has one horizontal producer with four ICVs. A mission failure of each of the valves is considered in this analysis with reliability parameters described in Fig. 6-1, which was based on the field performance of the equipment from one major manufacturer (WellDynamics and Halliburton 2009).

The central composite design (CCD) was chosen as the procedure for building the response surface (see Fig. 3-7 in Chapter 3) with the normalised time for the ICV's failure as the design parameter:

$$\begin{cases} FT(t) = \dfrac{t}{T_{Start} - T_{End}}, if\ t \le T_{End} \\ FT(t) = 1, if\ t > T_{End} \end{cases} \quad (6\text{-}2)$$

Where *FT* is normalised failure time,

t – time of the ICV's failure,

$T_{Start}$ is the start of production (01/01/2010),

$T_{End}$ is the end of production period (01/01/2030).

If any valve fails during the production period the normalised failure time will be a number between 0 and 1. FT equal to 1 represents ICV failure at or after the end of production, i.e. it does not affect the result. The FT will thus be equal 1 in this case.

The parameters and results for the CCD are summarised in a Table 1 of Appendix B. The CCD requires 25 simulations for 4 ICVs. The difference between the case with all ICVs working during the whole production period and uncontrolled case in which all valves are assumed to fail at the start of the production is 16%. This is the optimisation capacity (OC) of the infinitely variable ICVs for this case.

A quadratic response surface (RS) was built based on the results of these 25 simulations using STATISTICA$^{TM}$ software. The RS is described by the following equation:

$$RS = b_0 + \sum_{i=1}^{N} b_i \cdot x_i + \sum_{i=1,\, j=1}^{N} b_{ij} \cdot x_i \cdot x_j \qquad (6\text{-}3)$$

where $b_i$, $b_{ij}$ – numerical coefficients;

$x_i$ , $x_j$ – variables, failure time (FT) in our case;

N - number of the variables.

The numerical and regression coefficients between RS and the "true" values from the model are summarised in table 6-1. The regression coefficient is close to 1; the CCD therefore shows a very good correlation with the results of the simulation. In fact, the maximum NPV mismatch is less than 0.1% with an average mismatch of 0%.

*Table 6-1 Numerical and regression coefficients between RS and "true" values*

| Case/ Coeff. | CCD | CCD Corrected | CCD Corrected + ICV3 2 points | CCD Corrected + ICV3 7 points | ICV3 10 points |
|---|---|---|---|---|---|
| ***b0*** | 1195.0 | 1193.9 | 1191.9 | 1191.0 | 1201.6 |
| ***b1*** | -1.0 | -2.0 | -2.4 | -0.2 | 0.0 |
| ***b11*** | -2.3 | 0.4 | 2.2 | 1.1 | 0.0 |
| ***b2*** | -5.9 | -5.2 | -5.6 | -3.4 | 0.0 |
| ***b22*** | 5.9 | 3.6 | 5.5 | 4.4 | 0.0 |
| ***b3*** | 422.7 | 464.8 | 475.3 | 472.9 | 460.8 |
| ***b33*** | -232.7 | -273.9 | -278.5 | -275.3 | -285.8 |
| ***b4*** | 0.6 | 2.7 | -0.7 | 3.4 | 0.0 |
| ***b44*** | -1.2 | -4.9 | 0.1 | -2.9 | 0.0 |
| ***b12*** | 0.4 | 0.1 | 2.8 | 1.6 | 0.0 |
| ***b13*** | 3.2 | 0.9 | -5.0 | -5.9 | 0.0 |
| ***b23*** | -0.6 | 1.1 | -4.8 | -5.6 | 0.0 |
| ***b14*** | 1.8 | 0.5 | 3.0 | 1.8 | 0.0 |
| ***b24*** | 0.4 | 1.0 | 3.5 | 2.4 | 0.0 |
| ***b34*** | 0.7 | 4.4 | -1.7 | -2.5 | 0.0 |
| $R^2$ | 0.999966 | 0.999959 | 0.997305 | 0.995944 | 0.982720 |

The next step, to check if the correlation also applies to a random scenario, was modelled by 20 scenarios with random failure time for each ICV (Table 3 of Appendix B). Figure 6-5 shows that most of the estimated values have a good match with the simulated NPV; however there is a high mismatch at the lower NPVs, corresponding to scenarios when the ICVs failed in the early stages of the production period.

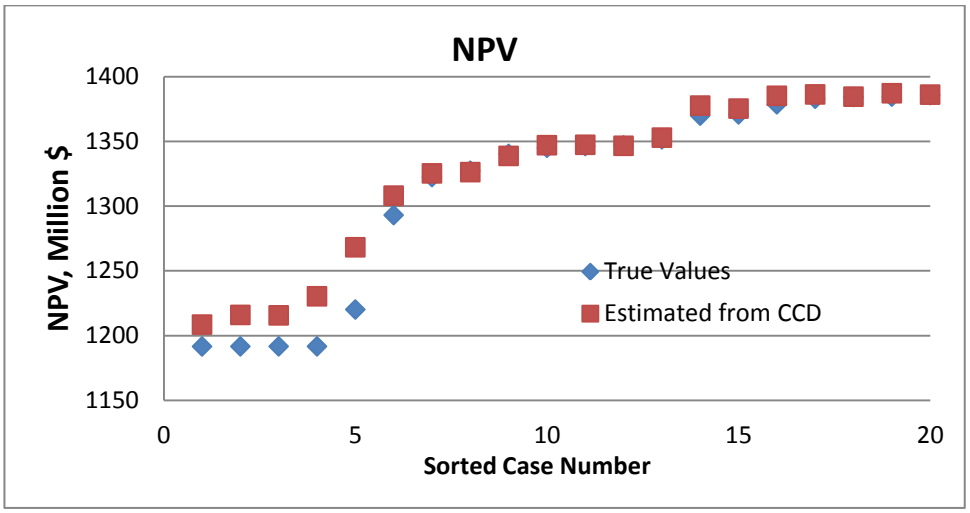


*Figure 6-5 NPVs Simulated and Estimated by a CCD based Response Surface*

The ICVs were not operated prior to 01/01/2013 since no water production was observed in the "Box-Shaped" model (Fig. 6-2). Therefore, the effect on the NPV of any early time ICV failure between 01/01/2010 and 01/01/2013 will be the same as if it failed on 01/01/2010. It should be realised that the CCD considers only the end and the central points; intermediate values being estimated by interpolation. Hence, the estimated value of the NPV suggested by the CCD in the period 01/01/2010-01/01/2013 is too high for an early FT, resulting in the mismatch observed in Fig. 6-5.

This effect can be eliminated by shifting the start point of the FT parameterisation to 01/01/2013. The estimated NPV values are now very close to the true values once this correction has been implemented (Fig. 6-6).

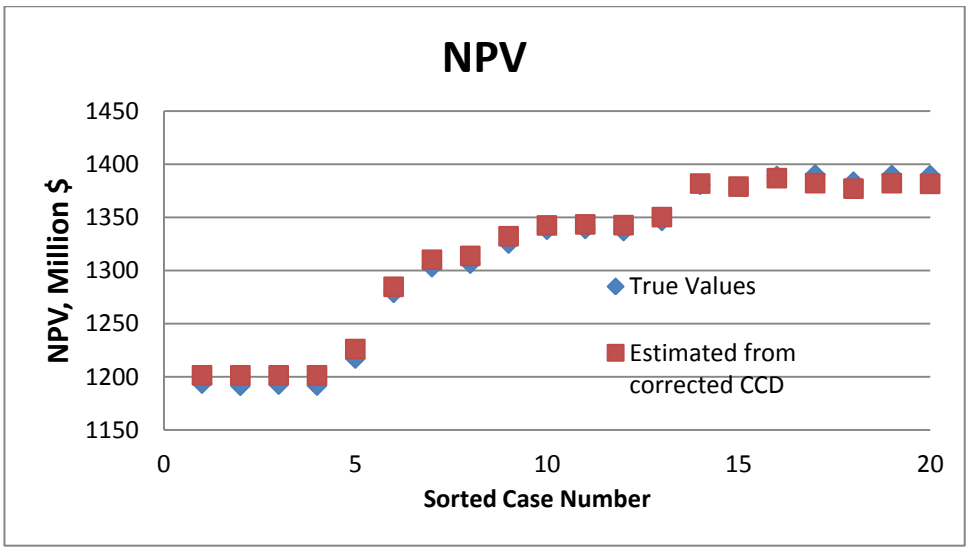


*Figure 6-6 NPVs Simulated and Estimated by Response Surface based on Corrected CCD*

ICV 3 failure time has the largest impact on the response surface (Fig. 6-7). This is to be expected for the "Box-Shaped" model since zone 3 has the highest permeability and water production.

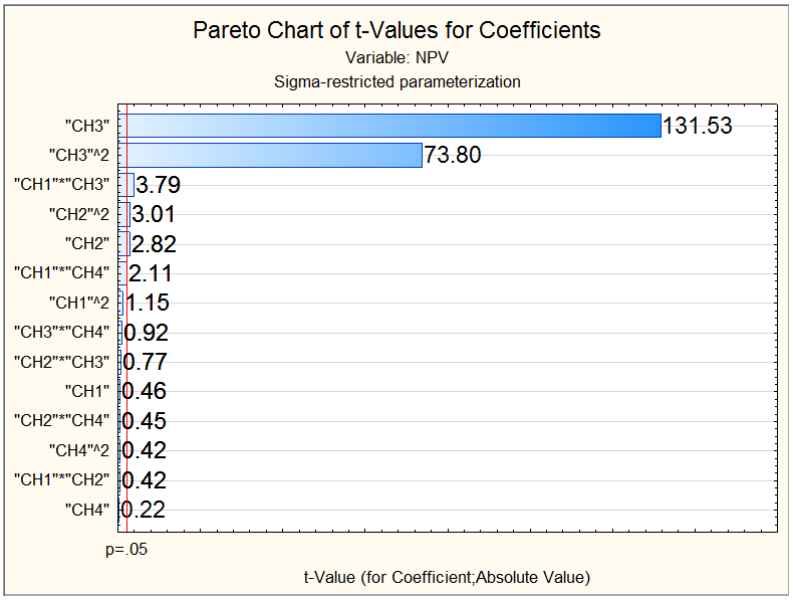


*Figure 6-7 Pareto Chart of the RS coefficients*

Two and seven intermediate FT points for ICV3 were added to the CCD to check whether it improved the estimated results and reduced the error (Table 4 of Appendix B). Further, a productivity model based on the intermediate FT of ICV3 only was constructed. The RS coefficients (Table 6-1) and the results summary (Table 6-2) are presented in greater details in Table 4 of Appendix B. The NPV mismatch (or Error) was calculated by equation 6-4 and the "added" value mismatch by equation 6-5:

$$Mismatch\,(NPV)=\frac{NPV_{True}-NPV_{Estimated}}{NPV_{True}}\cdot 100\% \qquad (6\text{-}4)$$

$$Mismatch\,(AddedValue) = \frac{AddedValue_{True} - AddedValue_{Estimated}}{AddedValue_{True}} \cdot 100\% \qquad (6\text{-}5)$$

where *Added Value* is the difference between the current and the "fully open no-control case":

$$AddedValue = NPV - NPV_{FullyOpen} \qquad (6\text{-}6)$$

Adding the intermediate ICV3 points to the CCD did not improve the prediction for 20 random cases. The prediction model based on only the ICV3 failure time demonstrated a lower average mismatch than the CCD based response surface. However, this case shows a higher mismatch at the start and end points: 01/01/2013 and 01/01/2030. The ICVs failure at the end point has the highest probability and strongest influence on the Monte Carlo simulation results. Therefore, the estimated value at this point should be close to the true NPV. The corrected CCD demonstrates better results from this point of view than the case based on ICV3 failure only. The end point value for this design is essentially the same as the true NPV and the average mismatch is only 1%. The above *Corrected CCD* response surface can thus be chosen to estimate the NPV.

*Table 6-2 NPV and "Added" Value Mismatch statistic for 20 Random Cases*

| Experimental Design | NPV Mismatch of 20 Random Cases | | | | "Added" Value Mismatch of 20 Random Cases | | | |
|---|---|---|---|---|---|---|---|---|
| | Average | Max. | Start Point | End Point | Average | Max. | Start Point | End Point |
| **CCD** | +0.80% | +3.9% | 0.0% | 0.0% | +5.00% | +24.63% | +0.08% | +0.09% |
| **CCD_Corrected** | -0.19% | -1.6% | -0.1% | 0.0% | -1.19% | -9.69% | -0.53% | +0.25% |
| **CCD_Corrected + ICV3 2 points** | -0.21% | -1.5% | -0.3% | -0.1% | -1.31% | -9.19% | -1.57% | -0.56% |
| **CCD_Corrected + ICV3 7 points** | -0.19% | -1.5% | -0.3% | -0.3% | -1.19% | -9.19% | -2.03% | -1.78% |
| **ICV3** | -0.06% | -1.0% | 0.6% | -0.7% | -0.38% | -6.31% | 3.51% | -4.66% |

### *6.2.2 On/Off and Discrete Position NPV Estimation*

Installation of On/Off and 10 position cases in the "Box-Shaped" model which were optimised by DS method delivered a slightly higher NPV compared to the use of infinitely variable ICV cases optimised by SLP and SQP (see Table 4-10 of Chapter 4). An On/Off completion is thus preferred especially once its greater reliability and lower cost is included in the calculation. However, in an ideal situation the infinitely variable ICV has a greater flexibility and delivers the greatest value (Fig. 6-8). Here the optimisation capacity (OC) of a discrete position and On/Off completion can be calculated with an infinitely variable ICV's is set to 100% and fully open valves (no control) to 0%.

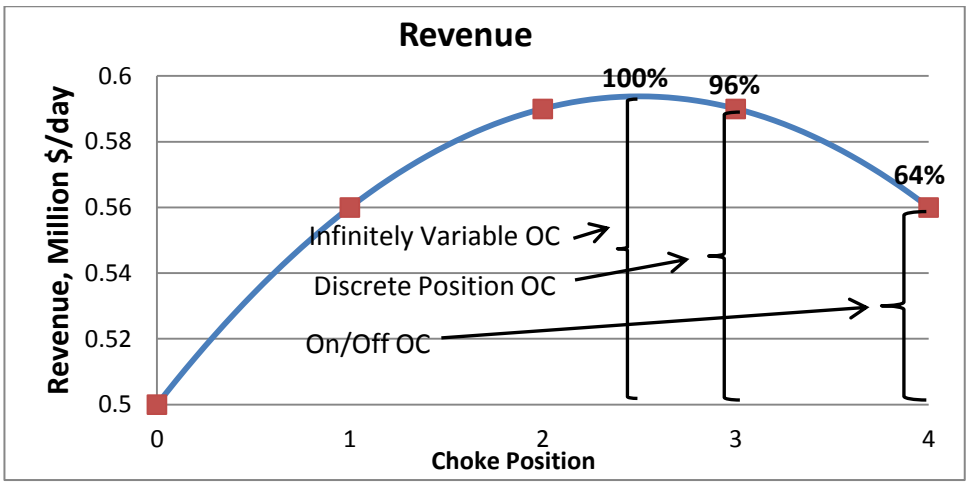


*Figure 6-8 Comparison of the Optimisation Capacity for an Infinitely Variable, a Discrete Position and an On/Off ICV*

The optimisation capacity for the whole production period can be defined by equation 6-7:

$$Cumulative\,OC^{Discrete} = \frac{NPV^{Discrete} - NPV_{NoControl}}{NPV^{Infinit} - NPV_{NoControl}} \qquad (6\text{-}7)$$

In the next section the lower threshold of discrete position and On/Off ICVs OC will be found at which they have the same economical value as infinitely variable valves.

### *6.2.3 Monte Carlo Simulation*

Monte Carlo simulation was performed in *CrystalBall*$^{TM}$. Ten thousand realisations for the On/Off, 10 position and infinitely variable ICV scenarios were run based on their reliability as defined by Weibul's equation (Fig. 6-1) with the NPV (Table 6-3) calculated from the Corrected CCD response surface (Table 6-1).

*Table 6-3 Summary statistics of Monte Carlo Simulation*

| Statistics | NPV Infinite | NPV 10 Position | NPV On/Off |
|---|---|---|---|
| Trials | 10000 | 10000 | 10000 |
| Base Case | 1387 | 1387 | 1387 |
| Mean | 1368 | 1378 | 1383 |
| Median | 1387 | 1387 | 1387 |
| Mode | 1387 | 1387 | 1387 |
| Standard Deviation | 50.86 | 36.89 | 23.97 |
| Variance | 2587 | 1361 | 575 |
| Skewness | -2.75 | -4.28 | -6.96 |
| Kurtosis | 9.24 | 20.50 | 52.47 |
| Coeff. of Variability | 0.04 | 0.03 | 0.02 |
| Minimum | 1195 | 1195 | 1195 |
| Maximum | 1393 | 1393 | 1393 |
| Range Width | 198 | 198 | 198 |
| Mean Std. Error | 0.51 | 0.37 | 0.24 |

The most probable value is described by the *Mode*. The most probable NPV equals the value of fully optimised case, 1387 Million $, for all scenarios, since the situation that all valves are still operational at the end of production period has the highest probability. By contrast, the *Mean*, or average NPV value, takes the failure cases into account. Figure 6-9 shows that 23% of the cases have an NPV of less than 1385 Million $ for the infinitely variable ICVs case. The corresponding figure for the 10 position valves is 11% and only 4% for the On/Off completion.

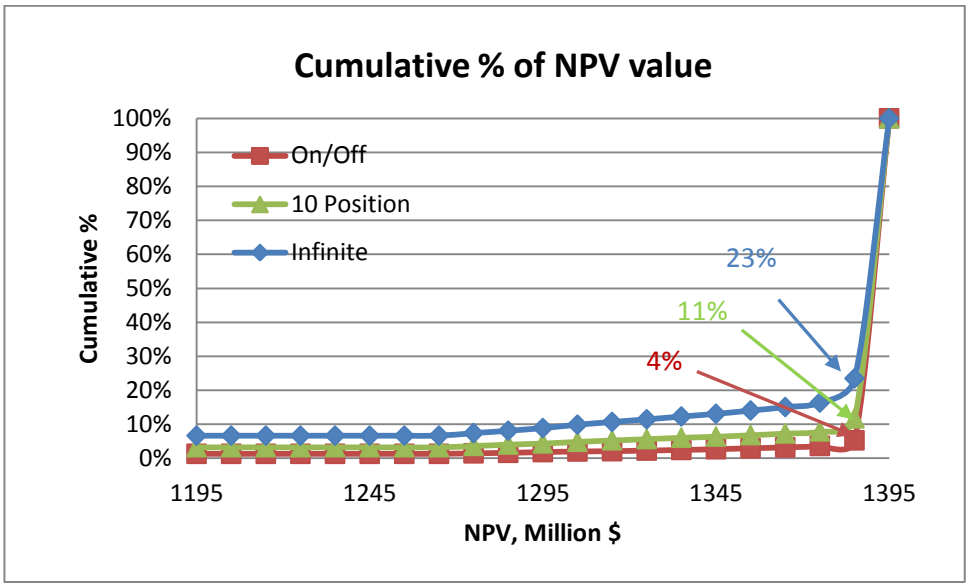


*Figure 6-9 Cumulative % of NPV valuefor On/Off, 10 position and Infinitely variable cases*

Infinite variable case lost 10% of the "added" value because of the possible valve failure (Table 6-4). The loss of 10 position and On/Off cases is less: 5% and 2% correspondingly. Therefore, they require less cumulative optimisation capacity for providing the same NPV as the infinitely variable case. The completion cost difference (see Table 3-4 of Chapter 3) adds a further reduction to the required OC. As a result, for "Box-shaped" model the cumulative OC of On/Off and 10 position cases should be 90% and 93% correspondingly to provide the same "added" value as the infinitely variable completion. The discrete position valves should be used if the OC is higher than this threshold; otherwise an infinitely variable ICV completion is more beneficial.

Thus, the methodology proposed here, allows quantifying the possible loss due to the valve failure and compares the various completion hardware types of different reliability.

*Table 6-4 "Added" Value loss and Optimisation Capacity*

| Case | NPV, Million $ | | "Added" Value loss | Cost is the same | Cost is different | |
|---|---|---|---|---|---|---|
| | Median | Mean | | Cum OC, % | Cost Difference for 4 ICVs, MM$ | Cum OC, % |
| **On/Off** | 1387 | 1383 | 2% | 92% | 4.4 | 90% |
| **10 Position** | 1387 | 1378 | 5% | 95% | 2.8 | 93% |
| **Infinite** | 1387 | 1368 | 10% | 100% | 0 | 100% |

## 6.3 Summary

The influence of the IWs reliability on the "added" value has been analysed in this chapter. The methodology for reliability analysis was proposed. It includes:

- Use of the Weibul's equation for reliability calculation;
- Building the experimental design and response surface for NPV estimation;
- Employing Monte Carlo simulation for estimation of the reliability impact on the "added" value of various completion options.

The proposed workflow was tested on a "Box-shaped" model. The "added" value loss reached up to 10% in the infinitely variable ICV case.

The analysis shows that the On/Off case is more beneficial if its optimisation capacity is higher than 90% of the infinitely variable case. In fact, optimisation employing the Direct Search method provided 100% OC (see Table 4-10) for this scenario. This result is consistent with Zandvliet's (Zandvliet, Bosgra et al. 2007; Zandvliet 2008) conclusions that On/Off ICVs are sufficient for the optimal performance in almost all situations. It also confirms the industry's preference for hydraulically operated ICVs (Tirado 2009).

In the next chapter the theoretical aspects of production control will be analysed to identify situations where an On/Off completion delivers optimum value.

# Chapter 7 - Theoretical Aspects of On/Off strategy

This chapter investigates the reactive optimisation problem for a production well. It demonstrates that On/Off ICV control provides an optimal solution if some assumptions are satisfied.

## 7.1 Problem Formulation

Consider a production well with N zones completed with ICVs that are constrained by a constant well head pressure (WHP) (Fig. 7-1). A gas cup (or free gas) is absent from the reservoir.

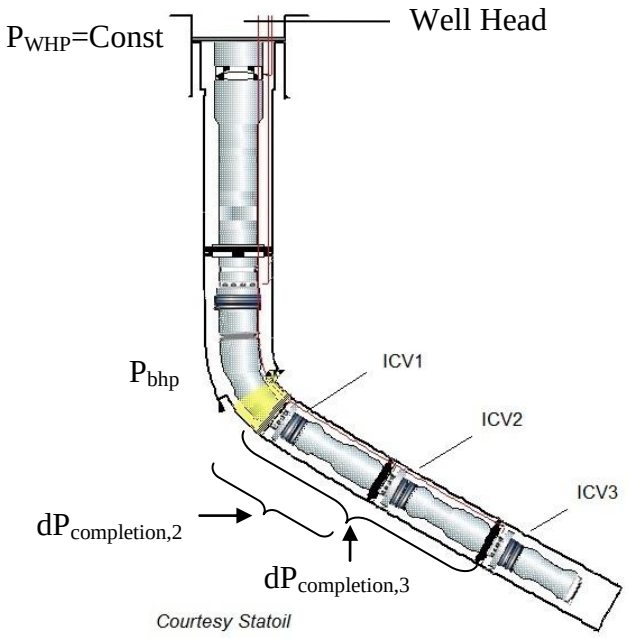


*Figure 7-1 Intelligent Well Schematic*

The new liquid production rate (or operating point) after choking one or more of the ICVs can be expressed by equation 7-1:

$$Q_{new}^{Liquid} = Q_{Open}^{Liquid} - \Delta Q_{choked}^{Liquid} + \Delta Q_{BHP}^{Liquid} + \Delta Q_{friction,completion}^{Liquid} + \Delta Q_{gravity,completion}^{Liquid} \quad (7\text{-}1)$$

where $Q_{Open}^{Liquid}$ – is the liquid rate when all chokes are fully open.

$$\Delta Q_{choked}^{Liquid} = \sum_{i=1}^{N} a_i Q_i^{Liquid} \quad (7\text{-}2)$$

where $\Delta Q_{choked}^{Liquid}$ is the change in the liquid rate of zone ***i*** due to the additional pressure drop across the ICV and $a_i$ is a coefficient varying from 0 (when the ICV is fully open) to 1 (the ICV is fully closed). *N* is the number of zones, each of which is separately controlled by an ICV.

$\Delta Q_{BHP}^{Liquid} = \sum_{i=1}^{N} J_i \cdot \Delta P_{bhp}$ - is the change in the liquid production in the fully open zones due to a change in the bottom hole pressure when the density of the fluid components changes; where $\Delta P_{bhp}$ is the change in the bottom hole pressure and $J_i$ is the productivity index of zone ***i***.

$\Delta Q_{friction,completion}^{Liquid} = \sum_{i=1}^{N} J_i \cdot \Delta P_{friction,i}$ - is a change caused by friction pressure changes in downhole completion area (at production interval);

$\Delta Q_{gravity,completion}^{Liquid} = \sum_{i=1}^{N} J_i \cdot \Delta P_{gravity,i}$ - is a change due to density changes in downhole area.

$\boldsymbol{i} \in \{\mathbf{1}..\boldsymbol{N}\} -$ number of the production zone/ICV

The objective function to be maximised during the particular time step is the well's current oil production rate. The objective function will be recalculated at the multiple time steps employed by the reservoir simulator.

In this chapter we will try to define the situations where On/Off valves are sufficient for optimal performance or, in other words, the maximum oil rate can be achieved at a choke's end points: either fully open or fully closed.

## 7.2 Model Simplification

Solving a model of a well's production system is, in general, a complex, non-linear task. There is no universal system of equations accurately describing the fluid flow in the wellbore. A number of different correlations such as Hagedorn & Brown (Hagedorn and Brown 1965), Duns & Ros (Duns and Ros 1963), Fancher & Brown, G.G.(Fancher. and Brown 1963), Beggs & Brill (Beggs and Brill 1973) and others have been developed for calculating pressure drop along the tubing. Most of them are empirical correlations based on the different flow regimes which may change along the well length and depend on the number of input parameters (Figure 7-2).

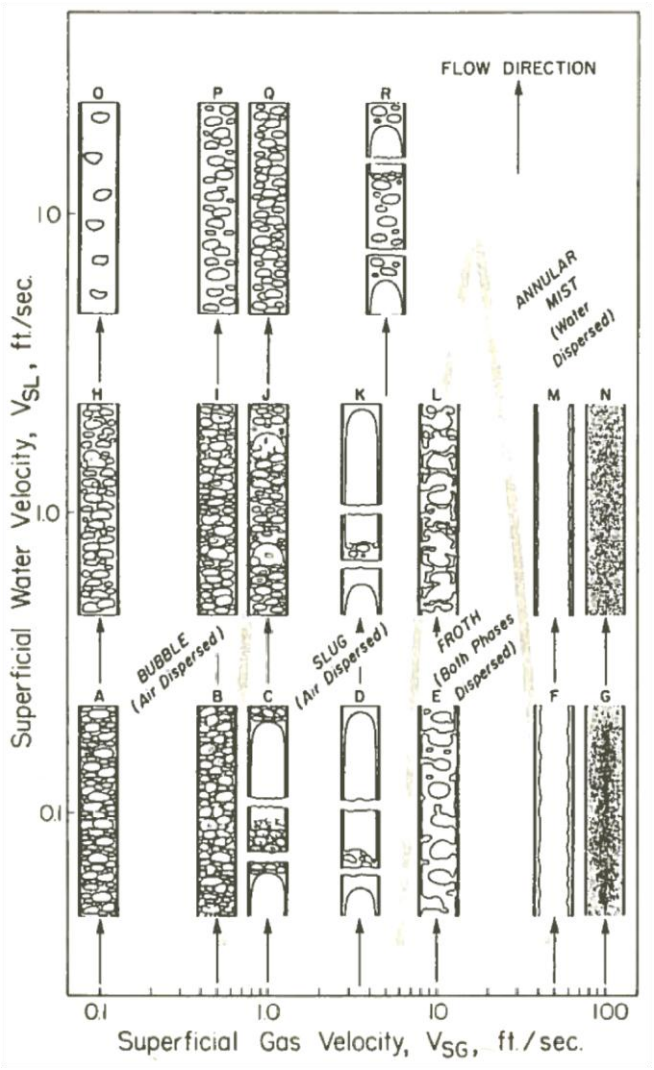


*Figure 7-2 Two-phase vertical flow patterns (afterBeggs (Beggs 1991))*

Several assumptions were made to simplify the equation 7-1 and allocate conditions where maximum oil rate is produced at open or closed ICVs positions.

First of all two last terms in equation 7-1 can be eliminated.

**Assumption 1 (A1)**

*The change in the hydrostatic pressure across the completion interval due to a change in the fluid density across the completion* $\Delta Q^{Liquid}_{gravity,completion}$ *is small compared to the total hydrostatic pressure across the length of the well and the term can be ignored.*

**Assumption 2 (A2)**

*Changes in the friction pressure due to fluid flow across the production interval* $\Delta Q^{Liquid}_{friction,completion}$ *are small and can be ignored.*

The 5th term of the equation 7-1 is proportional to the change in the true vertical depth across production interval while the 4th term is proportional to the length of the

completion zone. Hence, the changes in friction and gravity forces will be also small in comparison to the friction and gravity changes in the hydrostatic head in the whole well, if both of them are small compared with the well's true vertical depth and length.

For example, the change in friction and hydrostatic forces along completion is about 1% compared with the bottom hole pressure for a vertical well with a 100 ft thick production interval at a vertical depth of 10,000 ft below the surface:

$$\Delta P_{friction,completion} + \Delta P_{gravity,completion} \approx 1\% \ (\Delta P_{BHP}) \qquad (7\text{-}3)$$

These assumptions are normally satisfied in wells that are either vertical or deviated at a low angle and the production interval is not extremely thick.

**Assumption 3 (A3)**

*Changes in the acceleration pressure are small and can be ignored.*

This assumption is also used in order to simplify the mathematical proof. Nevertheless, it is true in most oil fields and applies to virtually all wells apart from low pressure gas wells.

The equation 7-1 after A1-A3 can be rewritten as:

$$\begin{aligned} Q_{new}^{Liquid} &= Q_{Open}^{Liquid} - \Delta Q_{choked}^{Liquid} + \Delta Q_{BHP}^{Liquid} = \\ &= \sum_{i \in Ch} a_i \cdot Q_i^{Liquid} + \sum_{i \notin Ch} Q_j^{Liquid} + (\Delta P_{BHP}^{gravity} + \Delta P_{BHP}^{friction}) \sum_{j \notin Ch} J_j \end{aligned} \qquad (7\text{-}4)$$

where *Ch* – is the set of zones where the ICVs have been choked.

The reservoir pressure may change if there is a communication between zones. This change will be included in the productivity indexes $J_j$. To simplify the equation we assume that zones are not connected and therefore the productivity indexes are constant.

**Assumption 4 (A4)**

*Production zones are not hydrodynamicly connected.*

## 7.3 Sequence of Optimisation Variables

The order in which the variables should be controlled is an important consideration in all optimisation problems since the result and the speed of convergence may depend on this order. We will now show, that for some specific situations, the order can be defined by input parameters.

**Assumption 5 (A5)**

*Choking (or closing) of an ICV decreases the well's liquid production rate.*

This assumption implies that well's tubing is large enough to be able to produce at the maximum possible liquid production rate. Friction across the length of the tubing usually has a lower value than the hydrostatic head in liquid producing wells. I.e. the friction has a smaller influence on the well's outflow performance than the hydrostatic pressure. This situation applies in oil fields which are producing a crude oil with either a reasonably low viscosity or a high water cut. This is a reasonable assumption since the tubing diameter is normally optimised to achieve the maximum production rate from the well. The tubing is normally designed for friction pressure not exceeding 25% of hydrostatic pressure(PETEX 2012).

One situation where ICV closure can increase the liquid production is when there is a large difference in oil density between the various layers. Here, reducing production from a layer containing dense oil might reduce the hydrostatic pressure sufficiently to cause an increase in the production rate. This would be an unusual case since reservoirs with very different fluid properties are not normally considered to be candidates for commingled development. ICV choking will not increase the liquid production if the difference in oil density for various production zones is less than $100g/m^3$. Assumption 5 is thus satisfied.

Another case, where this assumption may not be satisfied, is that of a high water cut in operating zone, significantly increasing hydrostatic pressure. The liquid density difference between the operating zone and the other layers is now significant and will normally be higher than the changes in friction pressure when the choke is closed. The liquid rate will normally increase monotonically in such situations and the oil rate will increase due to less water being produced from the other zones. Therefore, the ICV of such a zone should be fully closed to provide the highest well production rate and the zone can be excluded from further analysis.

The two zones case is the first simple situation where we can select uniquely which zone should be operated.

**Statement 7.1**

*In a vertical well with 2 zones if assumptions 1-5 are satisfied zone with the highest water cut should be closed first.*

The mathematical proof of this statement as well as the other statements of this chapter can be found in Appendix C.

The next situation is a field with similar fluid properties for different layers.

**Statement 7.2**

*If liquid properties such as water and oil density and GOR in different layers are the same, then the zone with the highest water cut should be closed first.*

This statement requires assumption:

**Assumption 6 (A6)**

*The well's tubing pressure is a monotonically increasing function of density and liquid rate.*

This assumption is satisfied in the region of stable flow where the flowing hydrostatic head increases with an increase in the water cut. For example, the tubing intake pressure increases with increasing production rates for all water cuts and liquid rates higher than 5000 Stb/day in Figure 7-3.

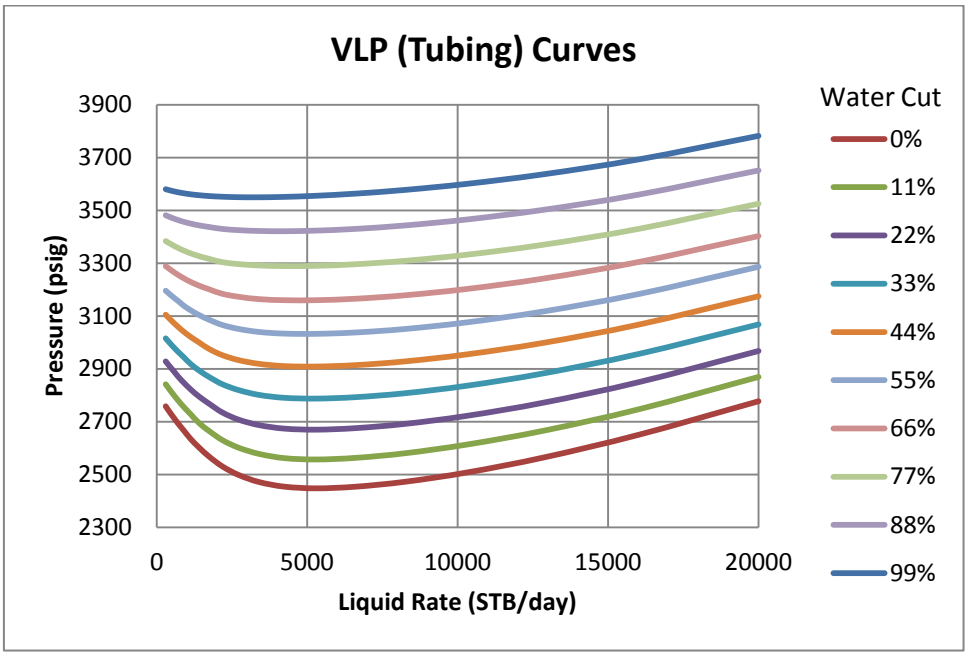


*Figure 7-3 Outflow curves depending on current WC*

Choking zone with WC higher than the well's average may increase the oil production if the bottom hole pressure reduces and more oil can be produced from other zones. The bottom hole pressure in case of fixed well head pressure is controlled by the pressure drop in the tubing. This pressure drop depends on two forces: gravity and friction, since from *Assumption 3* allows the acceleration pressure to be neglected.

$$dP = dP_{gravity} + dP_{friction} = \rho g H + \rho \frac{C_f}{D^5} L \cdot f \cdot Q^2 \qquad (7\text{-}5)$$

where $\rho$ is a density, $g$ is a gravity constant, $H$ is a true vertical depth of the bottom hole, $C_f$ is a unit dependant constant, $D$ is a tubing inner diameter, $L$ is a well's measure depth (length), $f$ is the Fanning friction factor, $Q$ is a liquid rate.

The hydrostatic head does not depend on the liquid rate in a stable region, while friction pressure increases proportional to $Q^2$ .

Also, both terms are dependent on the liquid density; their value becomes smaller, when the density decreases.

With a new density $\rho^* = \rho + \Delta\rho$ the pressure drop becomes

$$dP^* = \rho^* g H + \rho^* \frac{C_f}{D^5} L \cdot f^* \cdot Q^{*2} \qquad (7\text{-}6)$$

If the friction pressure drop increased, then $dP^* > dP$ and assumption is satisfied.

If the friction pressure drop decreased, then

$$dP^* - dP > \Delta\rho g H - \Delta\rho \frac{C_f}{D^5} L \cdot f^* \cdot Q^{*2} = \Delta\rho (g H - \frac{C_f}{D^5} L \cdot f^* \cdot Q^{*2}) \qquad (7\text{-}7)$$

If $dP_{gravity} > dP_{friction}$ at any possible scenarios then $dP^* - dP > 0$ that means that the tubing pressure increased.

Therefore, Assumption 6 can in the most cases be replaced by

**Assumption 6a (A6a)**

*Friction pressure drop is less than hydrostatic pressure in the well.*

Having the same value as Assumption 6, this modification is easier to check in practice.

The consequence of these two statements is that choking of a zone with a lower water cut will not be beneficial if the highest water cut zone has not been fully closed. Therefore, each time when we investigate a new ICV for the optimal choke position, all other zones are fully open or closed.

In a general case some zones may be partially choked. To simplify the Equation 1-4 we assume temporarily that:

**Assumption 7 (A7)**

*Only one zone is operated at a time and the other zones are fully open or closed.*

We will return to the situation with partially choked zones at the end of this chapter.

## 7.4 Conditions for On/Off ICVs

Three main types of ICVs are used to control the production of IWs:

- On/Off valves;
- Valves with discrete positions;
- Infinitely variable valves.

Let us propose that the ICV is operated in zone **n**, the zone with the highest water cut. This zone will now be called "the operating zone". The ICVs controlling the well's inflows from all other zones remain fully open. Assumption 5 implies that the liquid rate:

$$Q_{new}^{Liquid}(a) = \sum_{i \neq n}^{N} Q_i^{Liquid} + a \cdot Q_n^{Liquid} + \sum_{i \neq n}^{N} J_i \cdot \Delta P_{BHP}(a) \qquad (7\text{-}8)$$

is a monotonously increasing function (Figure 7.4) where $0 \leq a < 1$. $a = 0$ for a completely closed ICV while a = 1 if it is fully open.

We intend to identify conditions at which On/Off valve is sufficient the optimal control, e.g. maximal oil rate is produced when $a = 0$ or $a = 1$.

The extra oil can be produced from other zones if $\Delta P_{BHP}(a)$ is positive. According assumption **A6a;** $\Delta P_{BHP}(a) > 0$ if the fluid density after choking the valve is less than the initial value. The necessary and sufficient condition for this is that the density of operating zone is higher than the density of extra fluid from the other zones:

$$\rho_n > \sum_{j \neq n}^{N} \rho_j J_j \Big/ \sum_{j \neq n}^{N} J_j \qquad (7\text{-}9)$$

Therefore the flowing bottom hole pressure also increases and $\Delta P_{BHP}(\alpha)$ reduces as the ICV is opened (Figure 7-5).

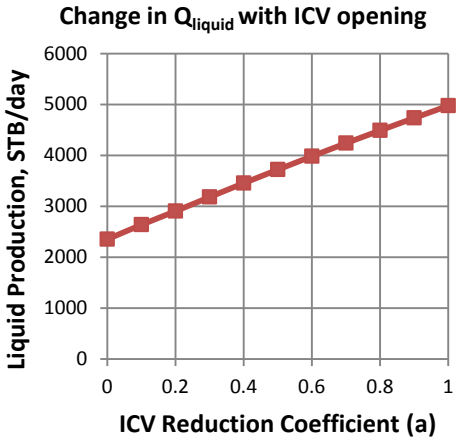


*Figure 7-4 Liquid production as a function of the ICV (or choke) position*

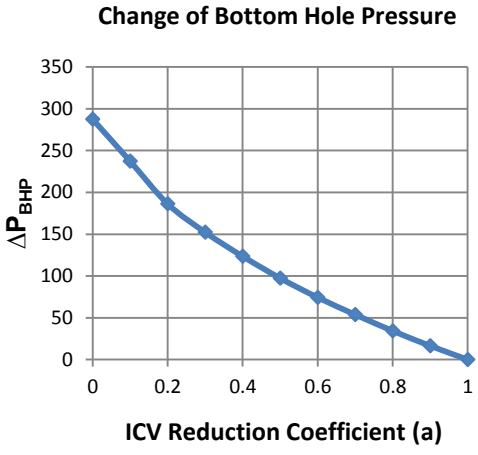


*Figure 7-5 The change of the bottom hole pressure as a function of the ICV (or choke) position*

Our further analysis of equation 7-8 will express it in discrete terms:

$$Q^i = i \cdot \Delta Q + \sum_{j \neq n}^{N} Q_j^{Liquid} + \Delta P_{BHP}^i \cdot \sum_{j \neq n}^{N} J_j \qquad (7\text{-}10)$$

$Q^i$ is the liquid production after choking the valve to the position ***i***.

Here $i \in \{0,..,K\}$ is the number of a valve position and $\Delta Q \cdot K = Q_n^{Liquid}$.

Nevertheless, this expression does not restrict our application area only to the discrete valve case. It is also applicable for infinitely variable valves since the ΔQ can be made as small as necessary.

First of all we are going to show that $\Delta P_{BHP}$ is a convex function. In other words the change of bottom hole pressure progressively reduces with the valve opening.

The following statements allow to prove that the density and the gravity component of the pressure drop are convex.

**Statement 7.3**

*The well's fluid density increases while opening the valve of operating zone.*

**Statement 7.4**

*The change in Δρ decreases as the ICV is opened for the operating zone.*

Unfortunately, the same statement is not always satisfied for friction pressure. However, if the gravity component is dominated and the friction pressure drop change is not significant with the valve opening; then the change in $\Delta P_{BHP}$ decreases. Currently we will keep this statement as assumption:

**Assumption 8**

*The change in $\Delta P_{BHP}$ decreases as the ICV is opened for the operating zone.*

Based on this assumption the following statement can be proved (Appendix C):

**Statement 7.5**

*If the oil production increases when the ICV is opened, then it will continue to increase if the choke is opened further.*

This statement excludes the situation where oil production starts to reduce at large ICV openings having initially increased when the ICV was first opened (Figure 7-6 a and b).

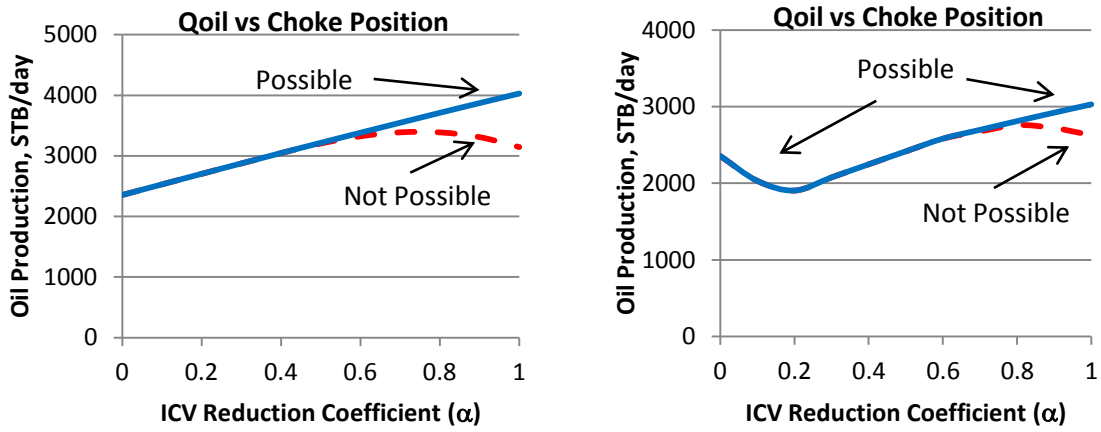


*Figure 7-6 a, b Oil production continuously increases at larger ICV openings once it begins to increase on opening the ICV*

The consequence of this last statement is that the maximum oil production can be achieved only at the end points; i.e. the fully open or fully closed ICV positions.

## 7.5 Partially Choked Valves

If some of the non-operating valves are choked, then equation 7-4 can be written as

$$Q_{new}^{Liquid} = a \cdot Q^{Liquid} + \sum_{i \neq n}^{N} Q_i^{Liquid} + \sum_{i \neq n}^{N} J_i \cdot \Delta P_{BHP,i}^{ex} \qquad (7\text{-}11)$$

Thus, $\Delta P_{BHP}$ replaced by a $\Delta P_{BHP,i}^{ex}$. This is the extra pressure drop which depends on the choke diameter and zonal liquid rate.

The liquid production through the choked valve can be expressed by the equation(Konopczynski and Ajayi 2004):

$$Q = C_V \sqrt{\frac{\Delta P}{\rho}} \qquad (7\text{-}12)$$

Where ***Q*** is a liquid flow rate through the valve;

$\boldsymbol{C_V}$ is a valve coefficient;

$\boldsymbol{\Delta P}$ is a pressure drop through the valve and

$\boldsymbol{\rho}$ is a relative density of the liquid.

The coefficient $C_v$ is a valve characteristic, which depends on the type of the valve and the valve position. All valves that are used to control the inflow in the well are assumed to have the same characteristic. Therefore, the valve coefficients for different ICVs are the same at the same valve positions.

On the other side zonal liquid production can be expressed as:

$$Q = dP \cdot J \qquad (7\text{-}13)$$

Where ***dP*** is a drawdown and J is a productivity index.

In this situation the drawdown is reduced in comparison with the fully open valve case to the value of ***ΔP***:

$$dP = dP_{open} - \Delta P \tag{7-14}$$

From these two equations can be found that

$$Q = C_V \sqrt{\frac{\Delta P}{\rho}} = (dP_{open} - \Delta P) \cdot J \tag{7-15}$$

The pressure drop through the valve ***ΔP*** can be calculated from this quadratic equation:

$$\Delta P = dP_{open} - \frac{\frac{C_V}{J\sqrt{\rho}} \sqrt{\frac{C_V{}^2}{J^2\rho} + 4dP_{open}} - \frac{C_V{}^2}{J^2\rho}}{2} \tag{7-16}$$

The new liquid rate through the valve after a change of the bottom hole pressure can be expressed as:

$$Q = C_V \sqrt{\frac{\Delta P^*}{\rho}} = (dP_{open} + \Delta P_{BHP} - \Delta P^*) \cdot J \tag{7-17}$$

The changed pressure drop through the valve is

$$\Delta P^* = dP_{open} + \Delta P_{BHP} - \frac{\frac{C_V}{J\sqrt{\rho}} \sqrt{\frac{C_V{}^2}{J^2\rho} + 4(dP_{open} + \Delta P_{BHP})} - \frac{C_V{}^2}{J^2\rho}}{2} \tag{7-18}$$

and the extra pressure drop can be found:

$$\Delta P_{BHP}^{ex} = \Delta P_{BHP} - (\Delta P^* - \Delta P) = \frac{C_V}{2J\sqrt{\rho}} \left( \sqrt{\frac{C_V{}^2}{J^2\rho} + 4(dP_{open} + \Delta P_{BHP})} - \sqrt{\frac{C_V{}^2}{J^2\rho} + 4dP_{open}} \right) \tag{7-19}$$

**Statement 1.6**

*$\Delta P_{BHP}^{ex}$ is a convex function if $\Delta P_{BHP}$ is convex.*

***Proof***

Assigning $f = \frac{C_V{}^2}{J^2\rho} + 4(dP_{open} + \Delta P_{BHP})$ gives

$$\Delta P_{BHP}^{ex} = \frac{C_V}{2J\sqrt{\rho}} \left( \sqrt{f} - \sqrt{\frac{C_V{}^2}{J^2\rho} + 4dP_{open}} \right) \tag{7-20}$$

In this equation only ***f*** depends on the reducing coefficient ***a***.

The second derivative of $\sqrt{f}$ by ***a*** is

$$(\sqrt{f})_a'' = -\frac{1}{4} f^{-3/4} \cdot f_a' + \frac{1}{2} f^{-1/2} \cdot f_a'' \qquad (7\text{-}21)$$

where $f_a' = 4(\Delta P_{BHP})_a'$ and $f_a'' = 4(\Delta P_{BHP})_a''$.

$(\Delta P_{BHP})_a' < 0$ since $\Delta P_{BHP}$ monotonically decreases with the choke opening.

$(\Delta P_{BHP})_a'' \geq 0$ because $\Delta P_{BHP}$ is a convex function.

$(\Delta P_{BHP}^{ex})_a'' = \frac{C_V}{2J\sqrt{\rho}} (\sqrt{f})_a'' > 0$ and therefore $\Delta P_{BHP}^{ex}$ is also convex.

■

This last statement shows that for partially choked situation the change in bottom hole pressure is most likely to reduce if it was convex in fully open case. Therefore, the On/Off valve is also sufficient.

## 7.6 The Critical Water Cut Criterion

We will now examine in more detail the conditions required when we need to shut the zone producing water to increase the well's oil production by closing the zone with the highest water production.

The production rate from a well producing from N zones is:

$$Q_{initial}^{Liquid} = \sum_{i=1}^{N} Q_i^{Liquid} \qquad (7\text{-}22)$$

$$Q_{initial}^{Oil} = \sum_{i=1}^{N} Q_i^{Liquid}(1-WC_i) = \sum_{i \neq n}^{N} Q_i^{Liquid}(1-WC_i) + Q_n(1-WC_n) \qquad (7\text{-}23)$$

with the highest water cut being observed in zone ***n.*** The new production rate on closing this zone is:

$$Q_{New}^{Liquid} = \sum_{i \neq n}^{N} Q_i^{Liquid} + \Delta P_{BHP} \sum_{i \neq n}^{N} J_i \qquad (7\text{-}24)$$

$$Q_{New}^{Oil} = \sum_{i \neq n}^{N} Q_i^{Liquid}(1-WC_i) + \Delta P_{BHP} \sum_{i \neq n}^{N} J_i(1-WC_i) \qquad (7\text{-}25)$$

$$Q_{New}^{Oil} \geq Q_{initial}^{Oil} \;\Leftrightarrow\; \Delta P_{BHP} \sum_{i \neq n}^{N} J_i(1-WC_i) \geq Q_n(1-WC_n) \;\Leftrightarrow$$

$$WC_n \geq 1 - \frac{\Delta P_{BHP} \sum_{i \neq n}^{N} J_i(1-WC_i)}{J_n \cdot dP_n} \qquad (7\text{-}26)$$

where $dP_n$ is a drawdown of zone ***n.***

The value of the term $1-\frac{\Delta P_{BHP}\sum_{i\neq n}^{N} J_i(1-WC_i)}{J_n \cdot dP_n}$ provides the objective function criterion for the optimisation algorithm.

We will call this value the *Critical Water Cut* (CWC) for zone n: $WC_n^{Critical}$. The ICV should be closed if the current WC exceeds this value, otherwise it should remain open.

### 7.7 Summary

The On/Off valves provide the maximum oil rate for the reactive control if assumptions A1-A8 are satisfied.

These assumptions indicate that our method is applicable:

1. For reactive control for vertical or slightly deviated wells constrained by wellhead pressure.
2. To oil fields at pressures greater than the bubble point (free gas is absent from the reservoir).
3. If the hydrostatic pressure is the dominant cause of the pressure loss across the well's production well tubing.
4. When friction and acceleration forces are small compared to the hydrostatic head. This allows changes in the bottom hole pressure due to operation of the ICVs to be correlated with changes in the density of the inflowing liquid.

Assumptions 1, 2, 3 and 6 can be checked for a particular case by using nodal analysis for all possible scenarios during production life of the well: water cut, zonal pressures, wellhead pressure, changes in artificial lift control, etc. The others are not easy to check. In the most cases the evaluation of all intermediate choke positions is required which needs the same time that was required for solving the initial optimisation problem. Moreover, even though these assumptions are required for an accurate mathematical proof, they may be not necessary for the On/Off strategy to provide the optimal solution.

Using On/Off valves and CWC criteria can significantly simplify the optimisation problem and reduce the run time. Also the convergence problem can now be avoided.

We will now use the results achieved here to define the application area of On/Off control strategy in the next chapter.

# Chapter 8 - On/Off Zonal Control Strategy Application Area

This chapter will analyse the application area of the On/Off control strategy.

It was mathematically proved in the previous chapter that an On/Off control is sufficient in situations, providing all the assumptions discussed there are met. These assumptions restrict the application area, but at the same time do not specify precisely the fluid, reservoir and operational conditions at which they are satisfied. A direct check of all these assumptions will often take significantly longer time than solving the optimisation problem for discrete position and/or infinitely variable valves. These assumptions were shown to be necessary for an accurate mathematical proof; however, the optimal position may still be at the fully open or fully closed positions even when these conditions are not satisfied. For example, Figure 8-1 shows a case when the liquid rate decreased while operating ICV choke was partially opened; i.e. Assumption 1 is not satisfied. Despite this, the maximum oil production at fully closed position with On/Off valve still gives the optimal solution for this case.

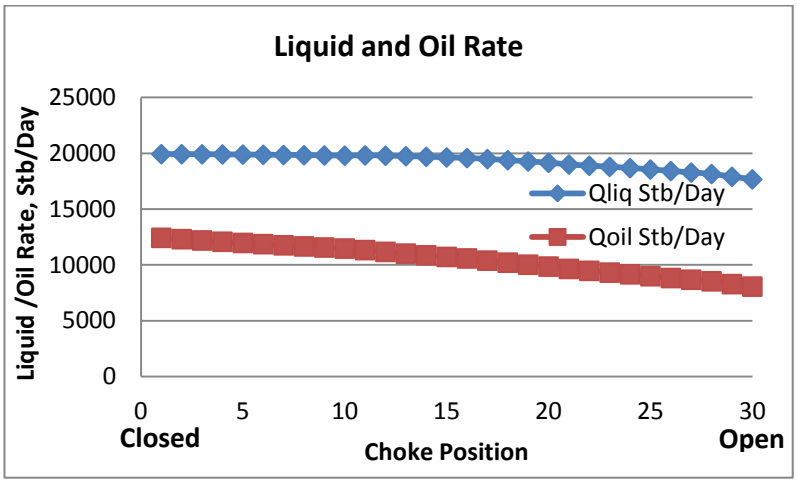


*Figure 8-1 Reducing of Liquid Rate with Choke Opening*

In this chapter we aim to answer the following questions:

- At which conditions do On/Off valves provide maximum oil production?
- What is the range of the cases where On/Off valves are sufficient for the optimal control?
- How great is the deviation from the optimum if On/Off valves do not give the maximum production?
- How to identify if On/Off valves are sufficient for a particular case?

## 8.1 Methodology

### *8.1.1 Input Data*

The following parameters were used for the analysis:

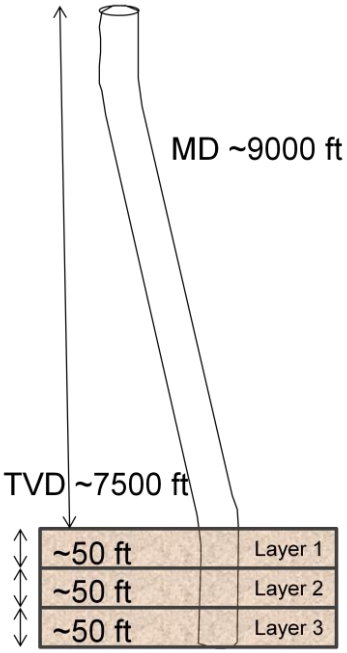


*Figure 8-2 Well Model*

**Well:**

- Deviated well; MD=9000 ft, TVD=7500 ft (Figure 8-2)
- 5.5 inches tubing;

PVT Properties:

Oil Gravity = 36 API

Gas Gravity =0.9 sp. gravity

**PVT Correlations:**

- Standing (FVF, Pb)
- Beggs et al (viscosity)

**Reservoir Parameters:**

Productivity Index: 1-100 stb/day/psi

WC: 0-100%

Reservoir Pressure: 2200-3600 psi

GOR: 50-3300 scf/stb

Both natural flow and gas lift well production scenarios were investigated.

PROSPER software was used to model VLP tables for various water cuts and GOR, while the well's production system was solved in GAP. The modelling workflow is summarised in Figure 8-3.

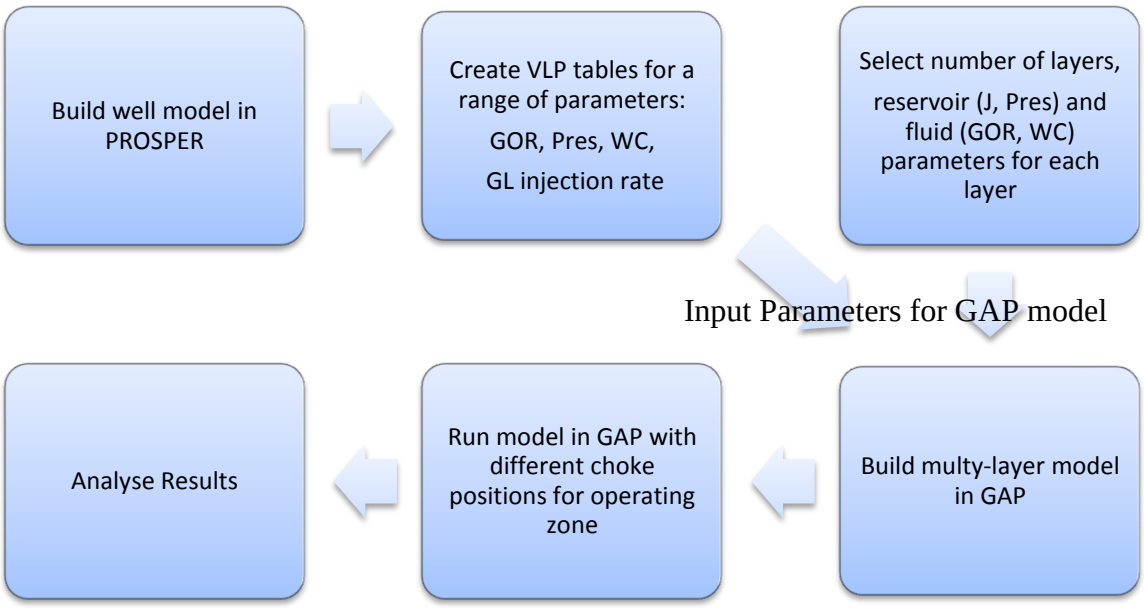


*Figure 8-3 Process to investigate application area for On/Off valves*

### *8.1.2 Number of Realisations*

A variation of the choke position of the operating zone was simulated by reducing the zone's productivity index (PI). For example, if the production zone has PI=10 bbl/psi/day, the values of PI between 1 to 10 bbl/day/psi corresponds to the intermediate positions of the ICV. 31 values of the PI varied between 1 to 100 bbl/day/psi has been selected, see Table 8-1 for details.

*Table 8-1 Productivity indexes for operating zone*

| | | | | | | | | | | | | | | | | | | | | | | | | | | | | |
|---|---|---|---|---|---|---|---|---|---|---|---|---|---|---|---|---|---|---|---|---|---|---|---|---|---|---|---|---|
| 1 | 2 | 3 | 4 | 5 | 6 | 7 | 8 | 9 | 10 | 12 | 14 | 16 | 18 | 20 | 22 | 25 | 28 | 31 | 34 | 38 | 42 | 46 | 50 | 55 | 60 | 65 | 70 | 80 | 90 | 100 |

This distribution provides a sufficient number of intermediate points, even if the initial productivity index is low (e.g. 10 bbl/day/psi), while providing a reduced total number of possible variants.

Assume that the non-operating zones are fully open. The non-operating zones must have a WC smaller than that of the operating zone, since zone with the highest WC will be choked. All other parameters may take any value throughout the chosen intervals. The total number of realisations can be calculated from the formula:

$$31 \cdot n^{3N} \sum_{i=1}^{n-1} i^{N-1} \qquad (8\text{-}1)$$

Where n – number of values for each parameter; N – number of zones.

$31 \cdot n^{3N-1}$ term describes productivity indexes, reservoir pressure and GOR variations, and $n\sum_{i=1}^{n-1} i^{N-1}$ is a number of WC variations.

The number of variants is extremely large even for 2 zones and increases exponentially as the number of zones increases. For example, if 10 values for each of the parameters is considered (e.g. n=10) the total number of variants is almost 140 million (Fig. 8-4).

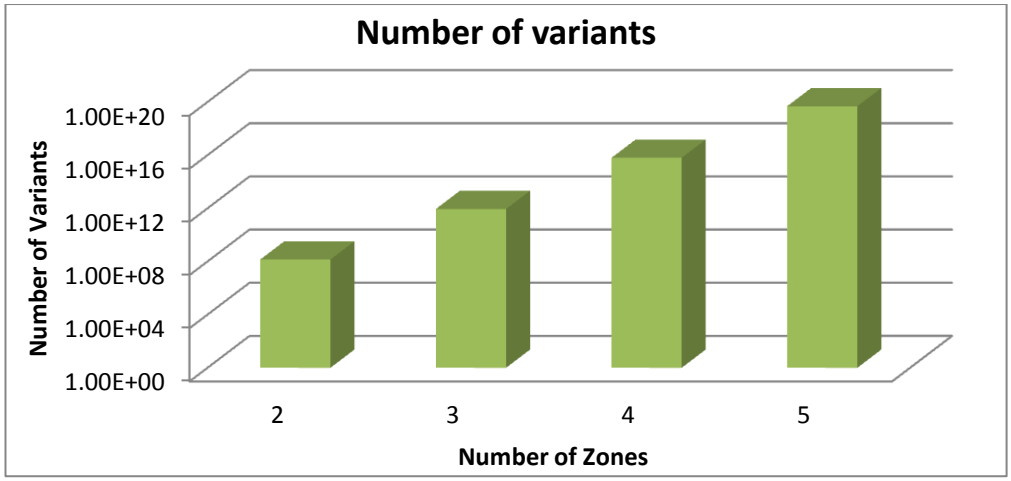


*Figure 8-4 Number of variants depending of the number of zones*

The time required for running this number of variants is also extremely high. For example, solution of the production system in GAP for one variant takes approximately 0.1 sec in a modern PC. The total time to solve all the variants (Fig. 8-5) shows that it is not possible to run all variants for even a 3 zone completion. A method to reduce the running time is thus required.

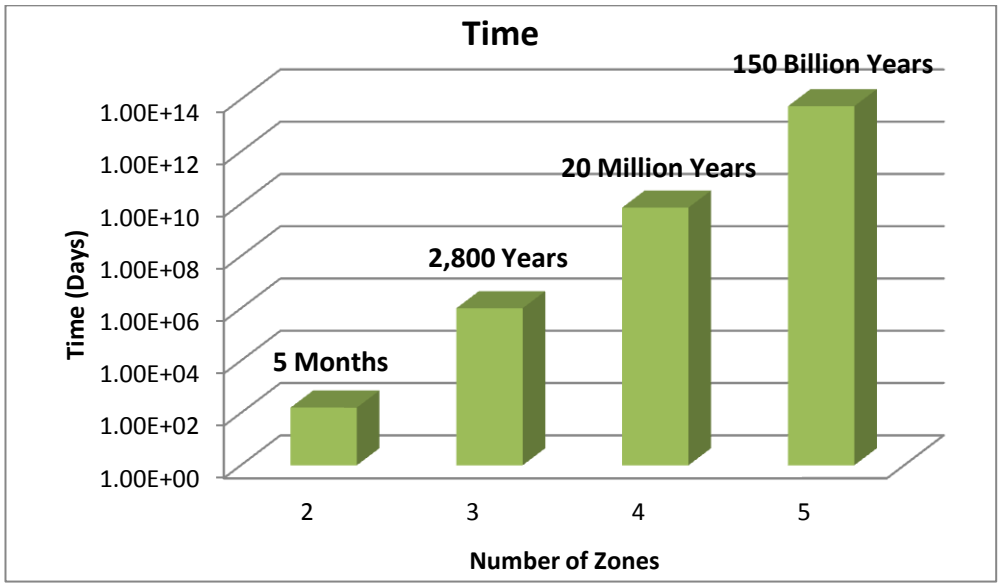


*Figure 8-5 Time required to solve for all the variants*

### *8.1.3 Partially Choked Zones*

The number of realisation becomes infinite if valve positions of non-operating zones may have any intermediate value. We are going to show, that such situation may be replaced with the case where all non-operating valves are fully open.

**Statement 8.1**

*If the maximum oil rate is achieved at partially choked positions for several valves, there is a corresponding case, were all valves are fully open except one valve which should be partially choked.*

The proof of this statement can be found in Appendix D.

Based on this statement we need only investigate cases with one operating valve; the other valves being fully open. There is a fully open analogue with the maximum oil rate at an intermediate choke position of the operating valve if an On/Off valve does not provide the optimum for the case with some ICVs being partially choked.

### *8.1.4 Converting from any Number of Zones into Three Zones*

In the previous chapter was found that the well's liquid production after an ICV choking can be expressed with the equation 8-8:

$$Q_{new}^{Liquid} = a\ Q_1^{Liquid} + \sum_{i=2}^{N} dP_i \cdot J_i + \sum_{i=2}^{N} J_i \cdot \Delta P_{BHP} \qquad (8\text{-}8)$$

The water cut and GOR of the second and third terms of this equation do not depend on the choke position. They are constant at any choke position providing there is no cross flow in other zones. Therefore, these terms can be expressed using only 2 zones. Appendix D provides a detailed explanation of how to do this. The algorithm shown in Fig. 8-6 can be used to convert any number of zones into 3 zones.

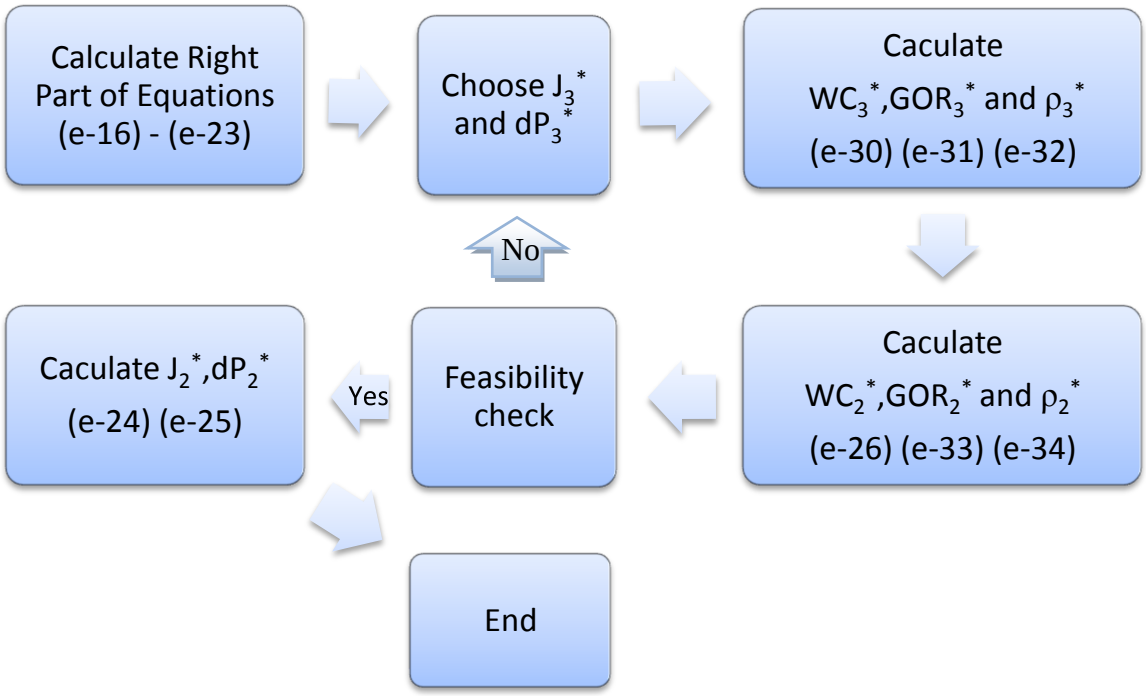


*Figure 8-6 Algorithm to convert any number of zones into 3 zones*

#### *8.1.4.1 Example*

The application of the algorithm will now be demonstrated with a case study where an example well with 5 zones will be converted into 3 zones. The reservoir and fluid parameters are summarised in a Table 8-2. Productivity indexes, reservoir pressures, water cuts and gas-oil ratios are different in this case; while the oil density is assumed the same for all zones. This assumption is caused by technical limitation of the commercial production software used for the following analysis, where it is currently not possible to specify different PVT properties for different layers. However, this is not viewed as a limitation since commingled production of reservoirs with significantly different PVT properties is normally viewed as a bad practice.

*Table 8-2 Reservoir and fluid parameters for 5 layers*

| Zones/Units | J | BHP | Pres | dP | WC | GOR |
|---|---|---|---|---|---|---|
| | Stb/psi/day | psi | psi | psi | fraction | Scf/Stb |
| Zone1 | 45 | 2534 | 2800 | 430.71 | 0.7 | 550 |
| Zone2 | 4 | 2534 | 2700 | 330.71 | 0.1 | 450 |
| Zone3 | 7 | 2534 | 2750 | 380.71 | 0.15 | 600 |
| Zone4 | 20 | 2534 | 3000 | 630.71 | 0.2 | 500 |
| Zone5 | 1 | 2534 | 2900 | 530.71 | 0 | 550 |

The algorithm was implemented in an Excel spreadsheet for calculation of the parameters required when describing any number of zones with 3 zones only. Zone 1 is the operating zone with the highest water cut; hence its parameters do not change. All other zones were amalgamated into the 2 zone equivalent. The result is summarised in Table 8-3.

*Table 8-3 Reservoir and fluid parameters for 3 layers from the converting algorithm*

| New Design | J | BHP | Pres | dP | WC | GOR |
|---|---|---|---|---|---|---|
| | Stb/psi/day | psi | psi | psi | fraction | Scf/Stb |
| Zone1 | 45 | 2534 | 2800 | 157 | 0.700 | 550 |
| Zone2 | 6.4 | 2534 | 3134 | 492 | 0.252 | 477 |
| Zone3 | 25.6 | 2534 | 2847 | 205 | 0.149 | 527 |

Wellflo software was used to model both scenarios. The choke position of zone 1 is simulated using different productivity indexes for this zone from 0.01 (fully closed) to 45 (fully open). The difference of liquid rates, oil rates and GOR for naturally flowing well for both scenarios as a function of the choke position is shown in the Figure 8-7.

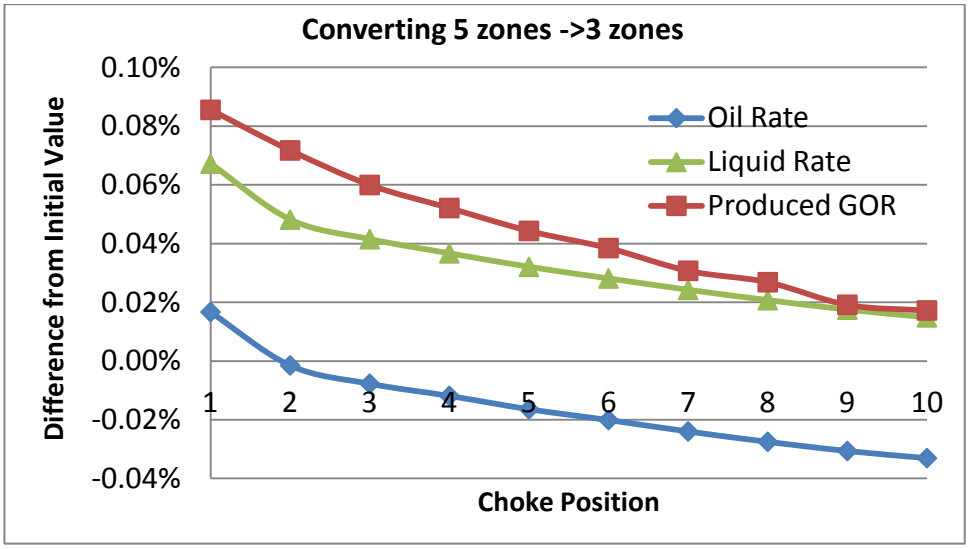


*Figure 8-7 Difference of liquid rates, oil rates and GOR as a function of the choke position*

The difference is very small, it less than 0.1% for all parameters. Therefore, the 3 layers case accurately describes original 5 layers model. The same analysis was done for production employing both Gas Lift and ESP. A gas injection rate of 2.5 MMScf/day for the gas-lift case was chosen, since this value provided the technical maximum oil production at a fully open valve position for the original case (Figure 8-8).

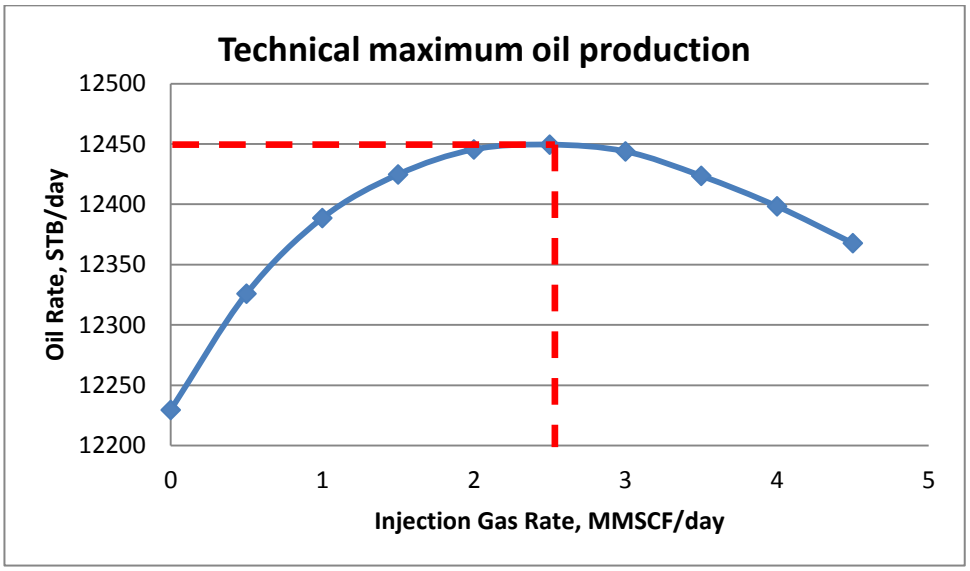


*Figure 8-8 Technical Maximum Oil Production as a function of the Injected Gas Rate*

In ESP case pump was chosen and optimised to cover the whole production interval depending on the choke position (Figure 8-9).

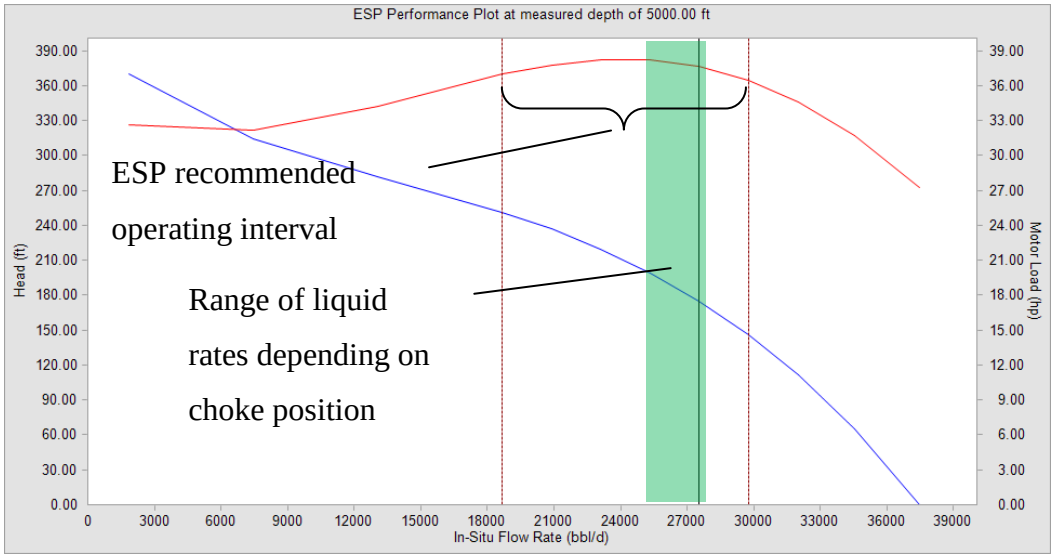


*Figure 8-9 ESP performance and liquid rate interval as a function of the choke position*

The maximum difference from the original case for all scenarios is summarised in Table 8-4 and Figure 8-10. For all cases the absolute difference from the original value is less than 0.1%; implying that the 3 zone well very accurately described the original 5 zone case (note that this small mismatch can be caused by numerical errors, rounding the

input values of water cut and GOR for the 3 zones and the small difference in pressures that inevitably occurred along the length of the completion).

*Table 8-4 Maximum difference between 5 zones case and 3 zones*

| Parameter/Case | Natural Flow | Gas Lift | ESP |
|---|---|---|---|
| **Liquid Rate** | 0.07% | 0.05% | 0.06% |
| **Oil Rate** | -0.03% | -0.10% | -0.10% |
| **Produced GOR** | 0.09% | 0.09% | 0.10% |

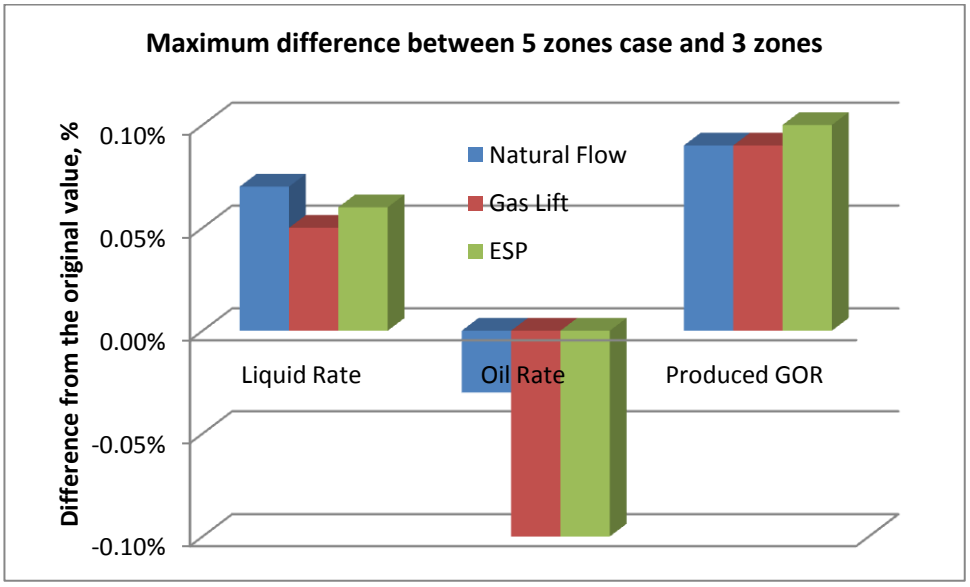


*Figure 8-10 Maximum difference between 5 zones case and 3 zones*

It is thus reasonable to assume that any number of zones can be modelled with sufficient accuracy by a 3 zone well only. However, the time required to run all 3 zone cases is still extremely high (Figure 8-5), hence we will use a statistical approach to solve this problem.

### *8.1.5 Statistical Approach*

For the statistical approach for parameters were equally distributed for 2 and 3 zones:

- Productivity Index: from 1 to 100 Stb/day/psi
- WC: from 0 to 100%
- Reservoir Pressure: from 2200 to 3600 psi
- GOR: from 50 to 3300 Scf/Stb

An example of input parameters for 3 zones case is shown in a Table 1-5.

*Table 8-5 Example of input parameters for 3 zone case*

| **Parameters** | **$J_2$** | **$J_3$** | **$P_{res1}$** | **$P_{res2}$** | **$P_{res3}$** | **$WC_1$** | **$WC_2$** | **$WC_3$** | **$GOR_1$** | **$GOR_2$** | **$GOR_3$** |
|---|---|---|---|---|---|---|---|---|---|---|---|
| **Case** | stb/psi/day | | psi | | | % | | | Scf/Stb | | |
| 1 | 71 | 5 | 2605 | 2622 | 3284 | 70 | 37 | 40 | 95 | 2522 | 2697 |

The results were analysed under the following headings:

- **[No A1]** - percentage of cases were *Assumption 1* is not satisfied
- **[No On/Off]** - percentage of cases were *On/Off* does not give maximum oil production
- **[Diff]** – average difference from the optimum for the cases where *On/Off* does not give maximum oil production (Fig. 8-11)

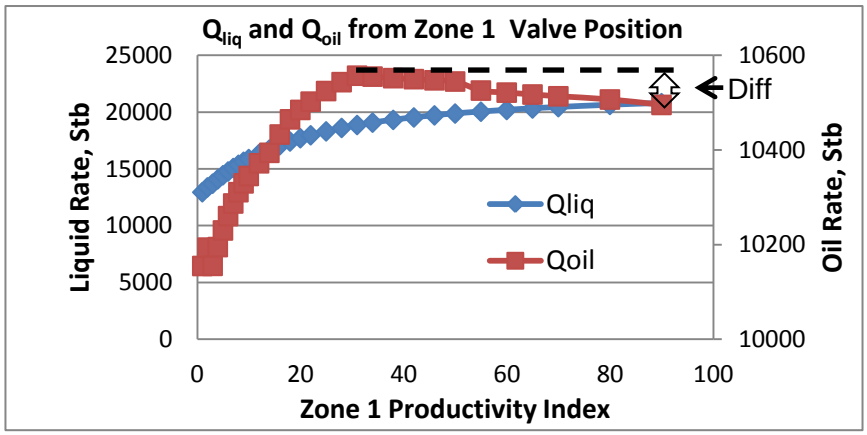


*Figure 8-11 Difference between the maximum oil production for infinitely variable valve and an On/Off valve*

The use of a statistical approach implies that the result will more accurately represent the total assembly of all cases as the number of analysed cases increases. Figure 8-12 shows how **[No On/Off]** value depends on the number of calculated cases. The variation is high when the number of cases is small, but it reduces rapidly with an increasing the number of scenarios.

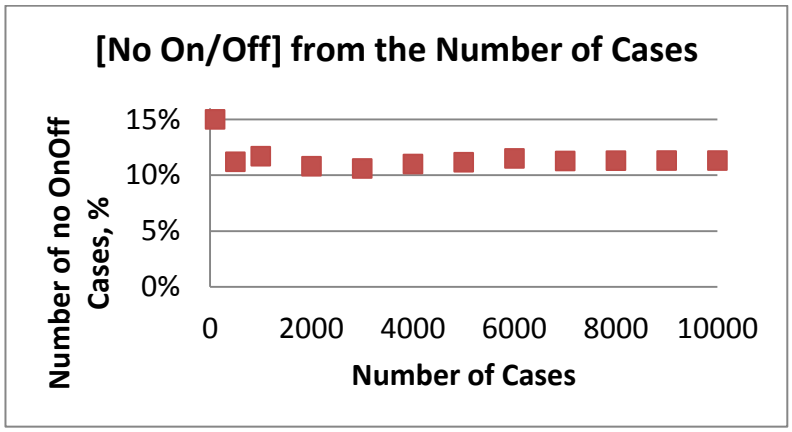


*Figure 8-12 **[No On/Off]** values depending on the number of cases*

This behaviour is explained by *Central Limit Theorem* theory (Cramer 1946). Suggest that for each case:

$$\begin{cases} V_{NoOnOff} = 1/N, & \text{if maximum oil production at the intermediate choke position} \\ V_{NoOnOff} = 0, & \text{if the maximum oil production at fully open or closed valve position} \end{cases}$$

***N*** is a number of cases.

Therefore, **[No On/Off]** value equals

$$[\text{No On/Off}] = \sum_{i=1}^{N} (V_{\text{NoOnOff}})_i \cdot 100\% \qquad (8\text{-}2)$$

All cases are assumed to be independent and equally distributed. If we define $\mathbf{[NoOn/Off]_{Total}}$ as a percentage of cases where On/Off strategy does not provide maximum oil production for ***all*** possible scenarios, then $V_{\text{NoOnOff}}$ value has a Bernoulli distribution with probability:

$$\begin{cases} p = P\{V_{NoOnOff}=1/N\} = [NoOn/Off]_{Total}/100\% \\ q = P\{V_{NoOnOff}=0\} = 1\text{-}p \end{cases} \qquad (8\text{-}3)$$

The *Moivre-Laplace Theorem* indicates that the sum of these values is asymptotically normally distributed, e.g. has a normal distribution at $N \to \infty$ .

The following formula estimates the number of required cases for the normal distribution:

$$N = \frac{t^2 s^2}{\Delta_{\bar{x}}^{\,2}} \qquad (8\text{-}4)$$

Where, t – Student's number (t=2 for 95% certainty);

s – sample coefficient of variance;

$\Delta_{\bar{x}}$ – maximum error between entire assembly and our population.

Figure 8-13 shows how statistical error reduces with the number of cases. For 10000 cases the maximum error for **[No On/Off]** is 5% and for **[Diff]** is about 10%, which means that if we have 10% of the cases where the optimal value at intermediate position for 10,000 realisations, the number of cases for all possible scenarios is 10%±0.5% with 95% certainty.

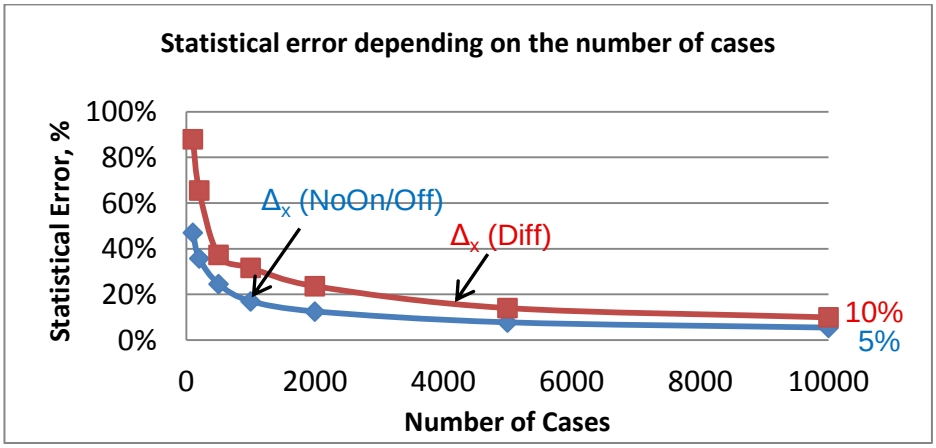


*Figure 8-13 Statistical error for **[No On/Off]** and **[Diff]** values depending on the number of cases*

Table 8-6 shows that statistical error for 10,000 realisations is small for all four scenarios, therefore this number of cases is sufficient to describe all possible scenarios for chosen intervals.

*Table 8-6 Statistical error between 10,000 realisation and all possible scenarios*

| Number of Zones | Lift Type | $\Delta_x$ (NoOn/Off) | $\Delta_x$ (Diff) |
|---|---|---|---|
| 2 Zones | Natural Flow | 5% | 10% |
| 2 Zones | Gas Lift | 7% | 14% |
| 3 Zones | Natural Flow | 5% | 12% |
| 3 Zones | Gas Lift | 6% | 11% |

## 8.2 Results

Assumption 5 is satisfied for the 2 zone natural flow scenario in about 60% of cases (Figure 8-14 a). At the same time On/Off strategy provides maximum oil production in almost 90% cases (Figure 8-14 b).

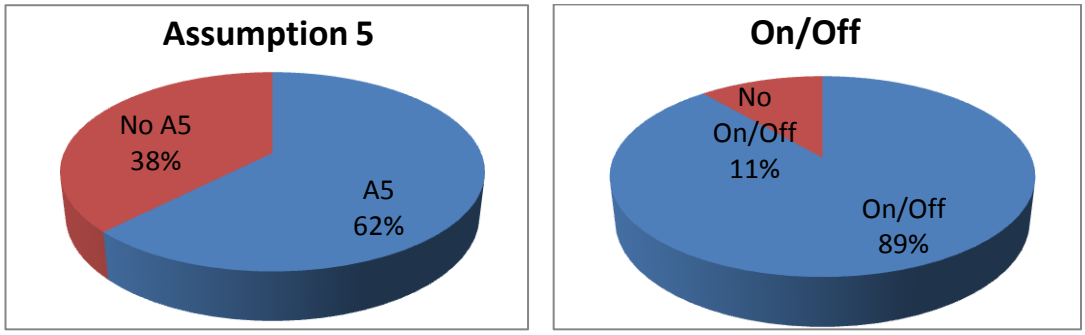


*Figure 8-14 a, b Percentage of cases where Assumption 5 and On/Off are satisfied. 2 zones, Natural Flow scenario*

Figure 8-15 shows that even if the value provided by On/Off strategy is not optimal, in the most cases the difference from the maximum oil production is less than 1%.

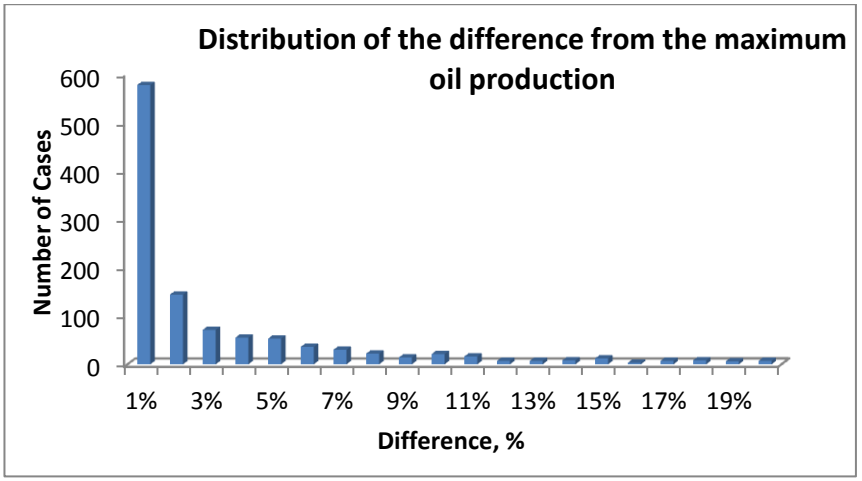


*Figure 8-15 Distribution of the difference from the maximum oil production for a 2 zone, Natural Flow well*

The result for all scenarios is summarised in Table 8-7.

*Table 8-7 Percentage of cases where Assumption 5 and On/Off are satisfied and the median of the error if On/Off is not satisfied*

| Number of Zones | Lift Type | A5 | On/Off | Median of the Error |
|---|---|---|---|---|
| 2 Zones | Natural Flow | 62% | 89% | 0.98% |
| 2 Zones | Gas Lift | 62% | 92% | 0.33% |
| 3 Zones | Natural Flow | 42% | 87% | 0.79% |
| 3 Zones | Gas Lift | 40% | 92% | 0.24% |

The number of cases where the Assumption 5 is not satisfied increased with the number of zones. This occurs because the total productivity of the well is higher in this situation, which increases friction pressure. The friction pressure may become dominant at fully open position, which reduces the liquid production. At the same time, this effect does not affect the number of cases, where On/Off strategy provides maximum oil production, and the percentage of these cases is still about 90%.

Moreover, the results show that using of gas lift increases this number, but significantly reduces the difference from the optimal solution. In fact, this difference is less than 1% in almost 99% of cases with gas lift. Therefore, in practice using On/Off valves may be still feasible, even they do not provide absolute optimal value.

The next important question is how to identify for a particular case, if On/Off ICV would be sufficient or we need to use more complex completions such as discrete position valves or infinitely variable valves. To answer this question we will try to identify which parameters have the highest impact on the mismatch from the optimal value.

## 8.3 Correlation of the Difference from Optimal Value with Input Parameters

The correlations of the difference from optimal value for 2 zones scenario with the following parameters were investigated:

J2 – productivity index

Pres1 – layer 1 reservoir pressure

Pres2 - layer 2 reservoir pressure

WC1 – zone 1 water cut

WC2 – zone2 water cut

GOR1 – zone 1 gas-oil ratio

GOR2 – zone 2 gas-oil ratio

Qliq – well’s liquid rate

Qoil – well’s oil rate

WC – well's water cut

GOR – well's gas-oil ratio

Pbhp – bottom hole pressure

Qliq1 – zone 1 liquid rate

Qliq2 – zone 2 liquid rate

GOR1-GOR2 – difference in gas-oil ratio between zone 1 and zone 2

|dGOR| - absolute difference in gas-oil ratio between zone 1 and zone 2

GOR1/GOR2 – zone1 to zone 2 gas-oil ratio

Pres1-Pres2 - difference in reservoir pressure between zone 1 and zone 2

|dPres|- absolute difference in reservoir pressure between zone 1 and zone 2

Pres1/Pres2 – ratio of reservoir pressures

WC1-WC2 - difference in water cut between zone 1 and zone 2

WC2/WC1- ratio of water cuts

OilDens – oil density

LiqDens - liquid density

Pgrav – well's tubing gravity pressure

Pfric - well's tubing friction pressure

Pfric/Pgrav– ratio of friction pressure to gravity pressure

The result is summarised in Figure 8-16.

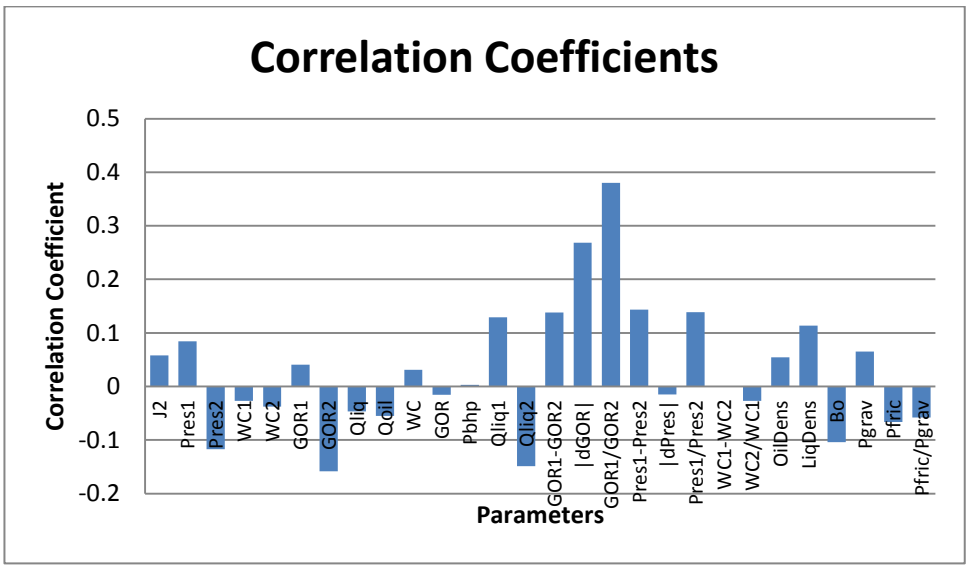


*Figure 8-16 Correlation of the Difference from Optimal Value with Input Parameters and their combinations*

The highest correlation is observed with gas-oil ratio difference (Figure 8-17).

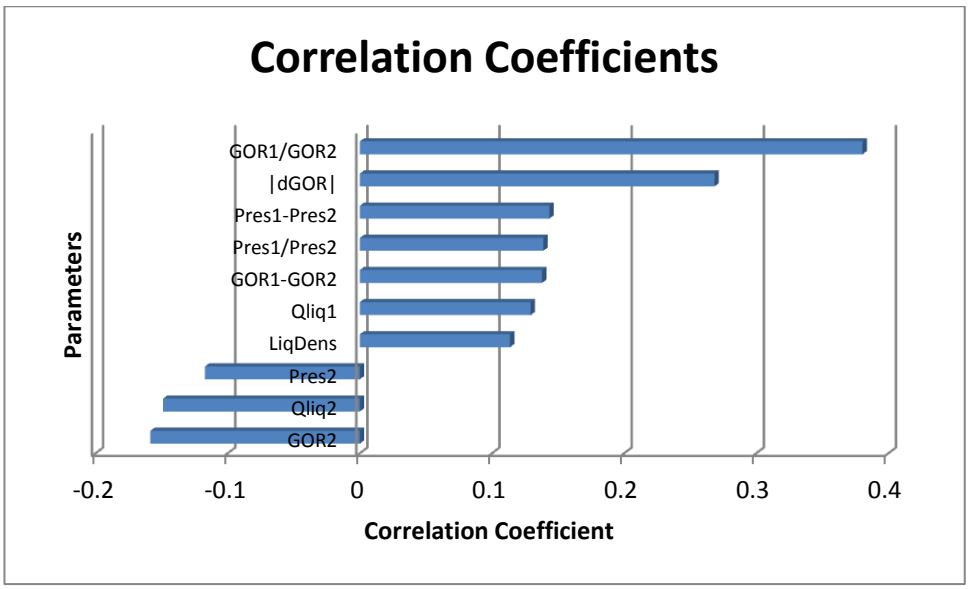


*Figure 8-17 Ten parameters with the highest correlation coefficients*

Figure 8-18 also shows that the difference is higher than 1% for the cases with significant difference in GOR, such as |ΔGOR| >350scf/Stb.

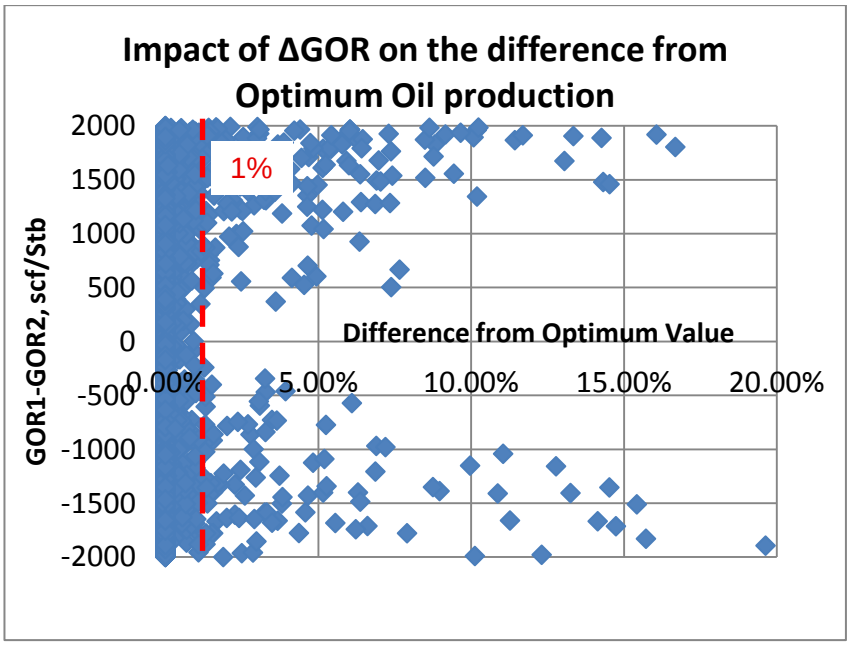


*Figure 8-18 Difference from Optimum Oil Production depending on ΔGOR*

Another parameter which has high correlation with oil rate mismatch is difference of reservoir pressure (Figure 8-17). Therefore, there is a higher risk to have optimal position at the intermediate choke position and higher difference in oil rate, if the difference of GOR and reservoir pressures is significant.

## 8.4 Risk Analysis

The probability to have a mismatch with the optimal value at certain conditions was investigated. Since the |*ΔGOR*| and (*Pres1-Pres2)* shows a good correlation with the difference from the optimal value (Figure 8-17) they were selected as input parameters for this investigation. First and last 25% of cases for each parameter were analysed. That cover the following values of |*ΔGOR*| and (*Pres1-Pres2)* (Table 8-8, Figures 8-19 and 8-20):

*Table 8-8* |ΔGOR| *and (*Pres1-Pres2) boundaries for first and last 25% cases

| Number of cases | \|ΔGOR\| | Pres1-Pres2 |
|---|---|---|
| First 25% of cases (2500) | less than 400 Scf/Stb | less than -400 psi |
| Last 25% of cases (2500) | more than 1700 Scf/Stb | more than 400 psi |

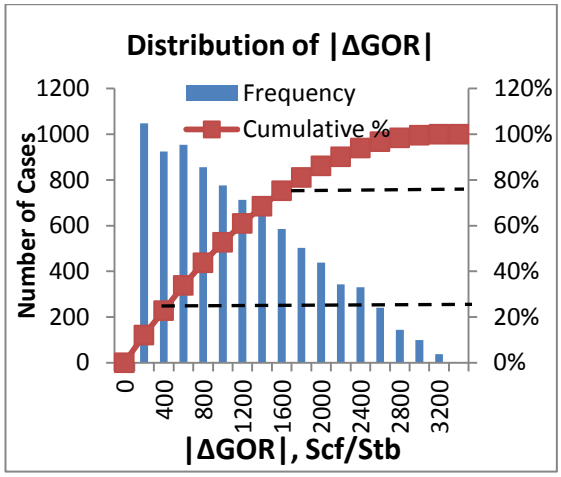


*Figure 8-19 |ΔGOR| Distribution*

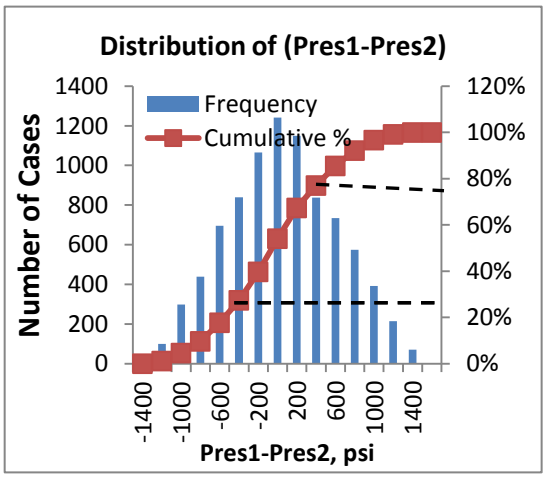


*Figure 8-20 (Pres1-Pres2) Distribution*

The number of cases providing a certain mismatch value for each situation is summarised in a Table 8-9.

*Table 8-9 Number of cases with certain mismatch from maximum oil rate*

| Difference from Maximum Oil Rate, % | Total Number of Cases | \|ΔGOR\| | | | | Pres1-Pres2 | | | |
|---|---|---|---|---|---|---|---|---|---|
| | | <400 Scf/Stb | | >1700 Scf/Stb | | <-400 psi | | >400 psi | |
| | | Number of Cases | % from total | Number of Cases | % from total | Number of Cases | % from total | Number of Cases | % from total |
| >0.50% | 691 | 17 | 2.5% | 424 | 61% | 13 | 1.9% | 240 | 35% |
| >1% | 554 | 4 | 0.7% | 377 | 68% | 5 | 0.9% | 204 | 37% |
| >2% | 410 | 2 | 0.5% | 291 | 71% | 1 | 0.2% | 168 | 41% |
| >5% | 231 | 0 | 0% | 183 | 79% | 0 | 0% | 119 | 52% |
| >10% | 108 | 0 | 0% | 94 | 87% | 0 | 0% | 63 | 58% |

This table shows that among 554 cases with mismatch higher than 1% only 4 cases has |*ΔGOR*|<400 Scf/Stb, while in almost 70% cases the difference in GOR is greater than 1700 Scf/Stb. Also the percentage of cases with significant difference in GOR

constantly increases with increasing the difference from maximum oil rate. A similar situation is observed for difference in the reservoir pressure.

This statistical analysis shows that if the difference between GOR is less than 400 Scf/Stb, then with almost 100% certainty the On/Off ICVs provides maximum oil rate or mismatch is less than 1%.

The higher GOR difference increases the probability of higher mismatch. Anyway, for example for $|\Delta GOR|$>1700 Scf/Stb, in 72% cases On/Off strategy still shows optimal result and in 80% of cases the mismatch is less than 1% (Figure 8-18).

From a practical point of view it is important to know what is the difference from the optimum value for our particular case with certain layers GORs and how this mismatch depends on the reservoirs pressure and water cut changes.

## 8.5 Particular Case Analysis

### *8.5.1 Case Description*

Simple 2 layer example was used to analyse how the mismatch changes with reservoir variation of reservoir pressure and water cut (Figure 8-21). Oil and liquid rate profiles for this case are shown in the Figure 8-11. The difference from the optimal oil rate is 0.67% at these conditions.

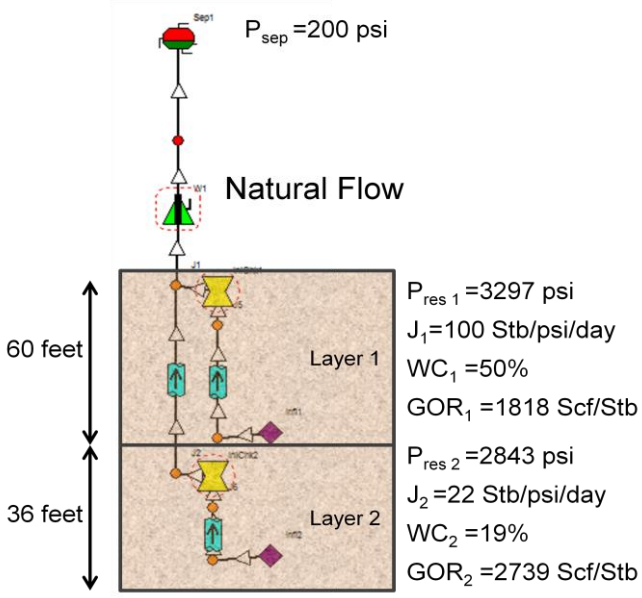


*Figure 8-21Model schematic*

### *8.5.2 Sensitivity to a Reservoir Pressure of the Operating Zone*

The well's oil rate dependence on the $ICV_1$ choke position can be expressed with the formula:

$$Q_{new}^{Oil} = a_1 Q_1^{Liquid}(1 - WC_1) + \sum_{i=2}^{N} J_i(1 - WC_i) \cdot \Delta P_{BHP} \qquad (8\text{-}5)$$

The relationship of the well's oil rate from liquid rate of zone 1 is shown in the Figure 8-22.

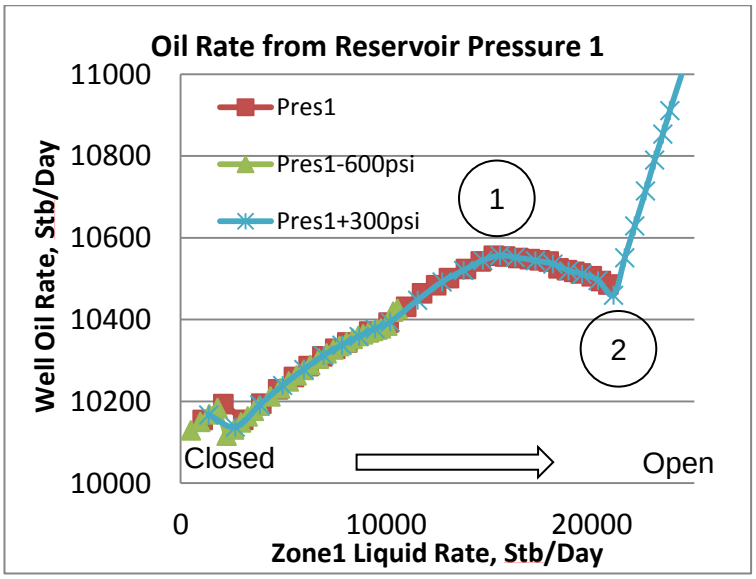


*Figure 8-22 Well's oil rate depending on zone 1 liquid rate and reservoir pressure*

The tubing pressure (VLP) does not depend on the reservoir pressure**.** It depends on the zone1 liquid rate only. Therefore, the relationship is the same for different pressures. The only difference is that the higher reservoir pressure provides the higher range of zonal liquid rates and extended profile can be observed (Figure 8-22).

Choke opening increases the liquid production from layer 1 and reduces liquid rate from second zone. Before ***Point*** 1 extra oil from operating zone is higher than the reduced oil from the other zone:

$$\Delta Q_1^{Liquid}(1 - WC_1) > \sum_{i=2}^{N} J_i(1 - WC_i) \cdot \Delta P_{BHP} \qquad (8\text{-}6)$$

$\Delta P_{BHP}$ constantly increases with the choke opening. The previous chapter showed that a change in gravity reduced with choke opening. Therefore, $\Delta P_{BHP}$ increases due to increasing of $\Delta P_{friction}$ .

After ***Point 1*** extra oil from the operating zone becomes less than the reduced oil from the other zone; hence the well's total oil rate reduces.

Cross flow into the second zone has started at ***Point 2***. We are not loosing oil from this zone anymore, and oil production increases again. Therefore, the maximum difference from the highest oil rate can be observed in this point.

### *8.5.3 Sensitivity to a Water Cut of the Operating Zone*

Water cut is another parameter which changes during the production period. Figure 8-23 shows that a change in water cut significantly impacts the well's oil rate.

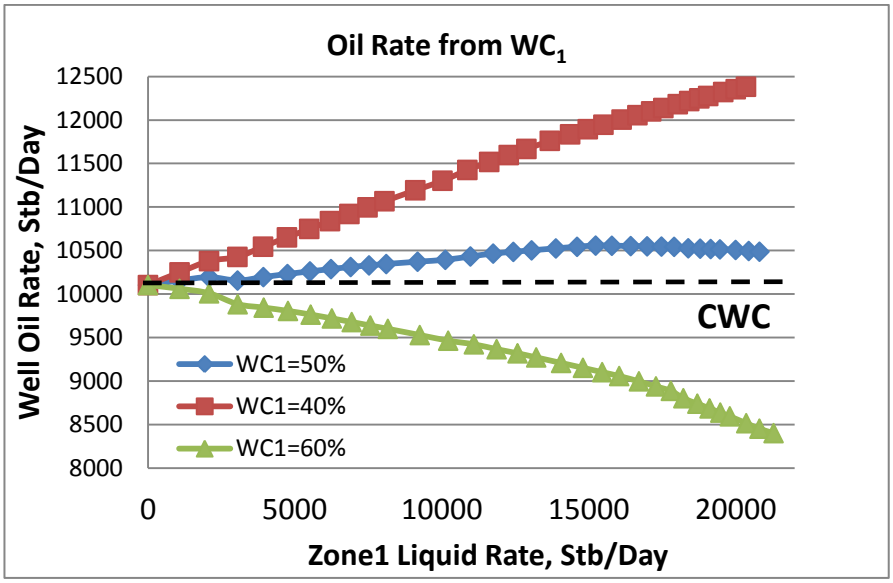


*Figure 8-23 Well's oil rate depending on zone 1 liquid rate and water cut*

The highest difference from optimum is observed at *Critical Water Cut* (CWC). The optimal position is fully open if the zonal water cut is less than this value. The fully closed position is optimum if it is higher.

### *8.5.4 Workflow to find the maximum difference from the optimum*

We found two conditions for operating zone at which the maximum difference from the optimal oil rate for On/Off strategy can be found:

- pressure at cross flow point;
- water cut equals CWC.

The workflow is summarised in Figure 8-24. First of all the reservoir pressure and water cuts of non-operating zones should be set up. Depending on these parameters the cross-flow point can be found. This value provides the maximum difference and should be chosen, if it is less than the possible maximum reservoir pressure of operating zone. After that the CWC value at these conditions can be found. Finally, we can evaluate all intermediate choke positions to find the maximum oil rate and its difference from fully closed or open position.

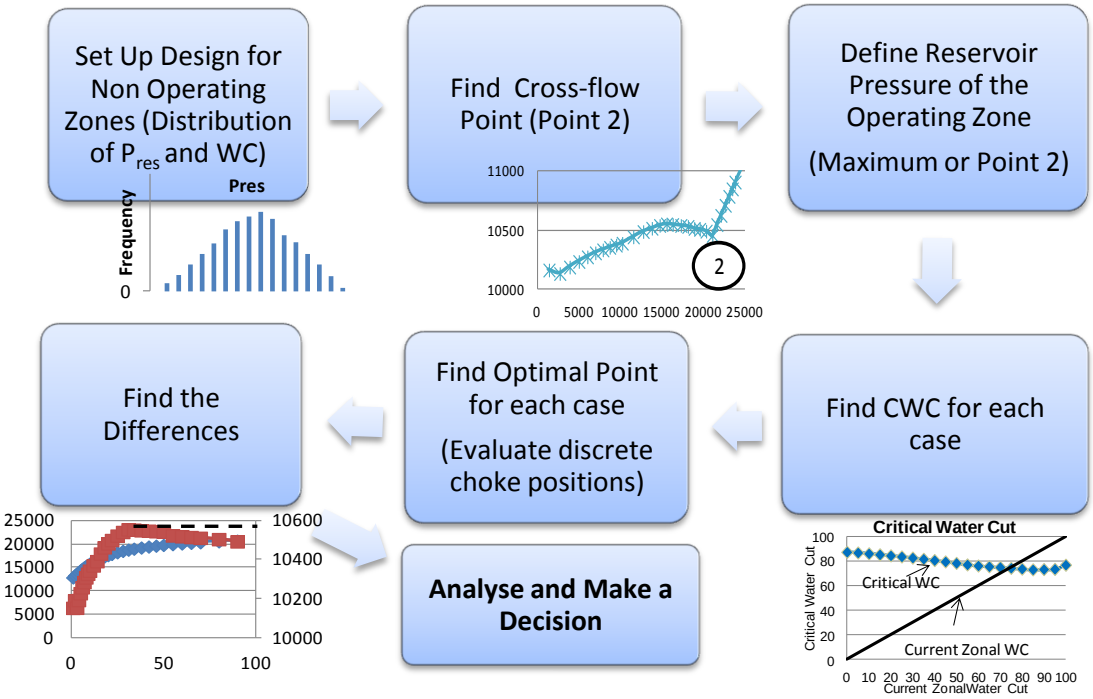


*Figure 8-24 An algorithm to find the maximum difference from the optimum*

This algorithm has been applied for our example. The pressure for zone 2 was distributed equally from 2200 to 3600 psi with 8 points and water cut from 0% to 100% with 20 points. The distribution of the difference from the maximum oil rate is shown in Figure 8-25.

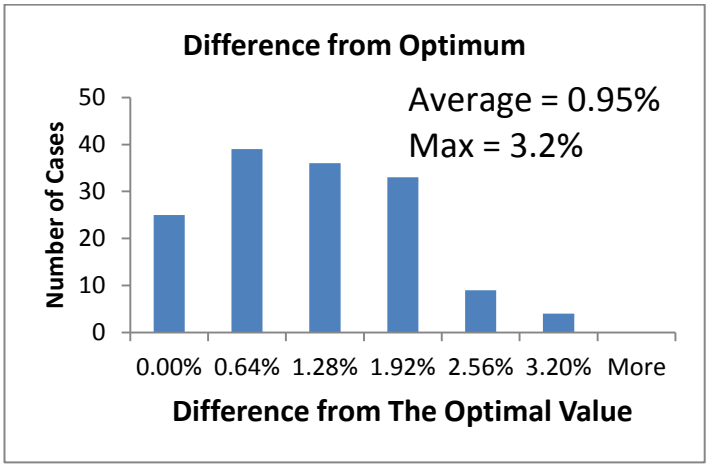


*Figure 8-25 The distribution of the difference from the maximum oil rate*

The average difference for this range of parameters is less than 1%. The maximum difference is 3.2%.

Figures 8-26 and 8-27 show how the difference depends on the zone 2 reservoir pressure and water cut. It is clear that the difference reduces with the increasing zone 2 pressure; while the water cut does not follow any trend.

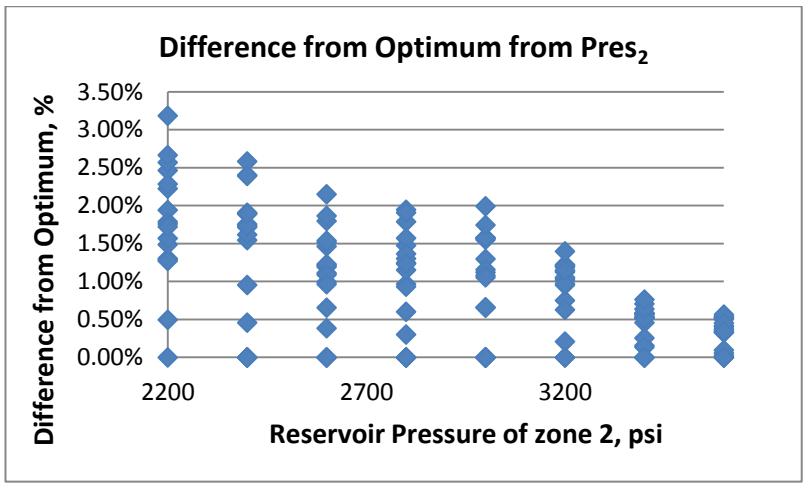


*Figure 8-26 Difference from the maximum oil rate as a function of zone 2 reservoir pressure*

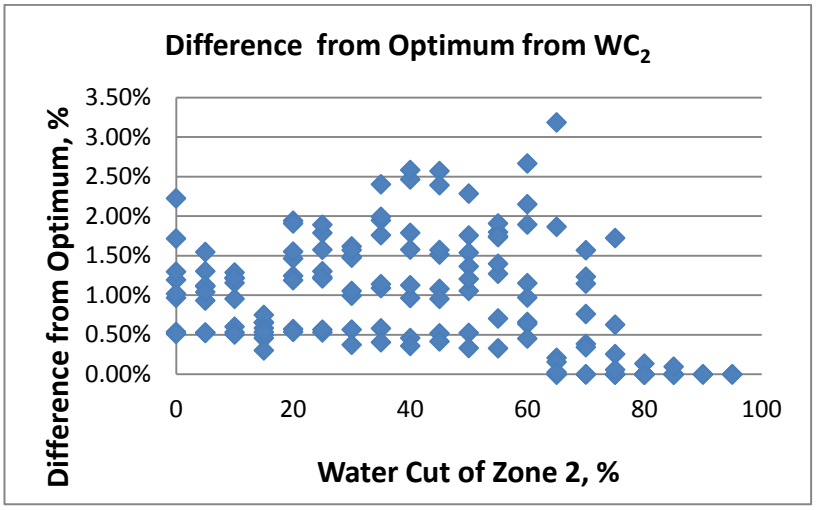


*Figure 8-27 Difference from the maximum oil rate as a function of zone 2 water cut*

### *8.5.5 Workflow to find the difference from the optimum at the most likely reservoir conditions*

Using the previous algorithm we found the distribution of the maximum mismatch from the optimal value, but in real field these conditions may be met not often or even may be not met at all. It is more useful to know what is a potential oil loss at the most likely reservoir pressure.

In practice, many field development plans try to maintain the reservoir pressure at a constant value. Therefore, assume that the reservoir pressure for both reservoirs in our example is kept constant most of the time with some deviation during the production period, which is described in Table 8-10.

*Table 8-10. P10, P50 and P90 zonal reservoir pressure*

| Zone /Case | P10 | P50 | P90 |
|---|---|---|---|
| **Zone 1** | 3000 psi | 2800 psi | 2600 psi |
| **Zone 2** | 2800 psi | 2600 psi | 2400 psi |

Figure 8-28 shows the workflow for this case. We only need to evaluate P10, P50 and P90 cases instead of searching the reservoir pressure providing maximum mismatch.

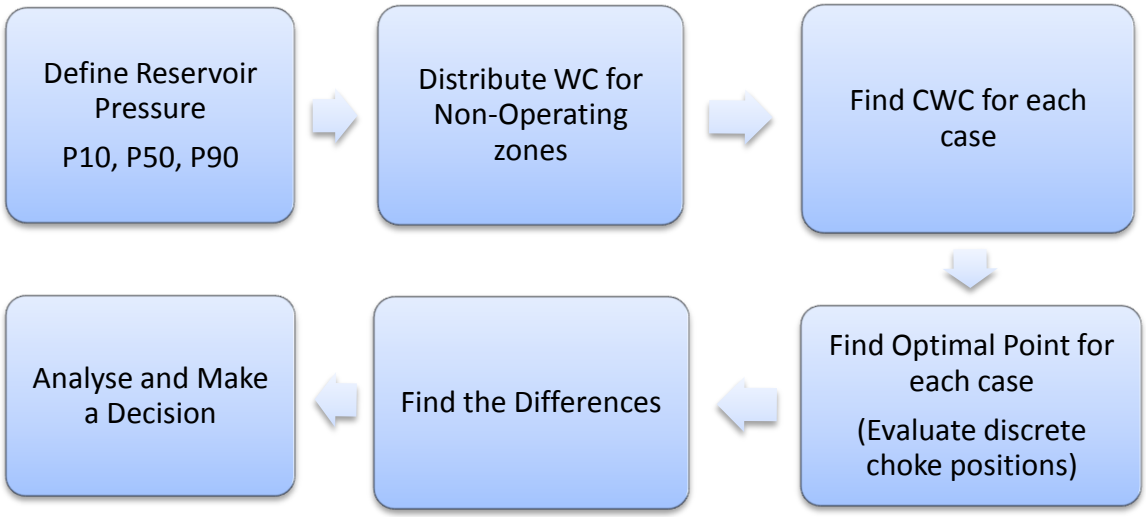


*Figure 8-28 Workflow to find the difference from the optimum at most likely reservoir conditions*

As was noticed previously, the difference from the optimal value reduces if the water cut of the operating zone is not equal CWC. Therefore, the mismatch can be observed in the CWC neighbourhood only (Figure 8-29).

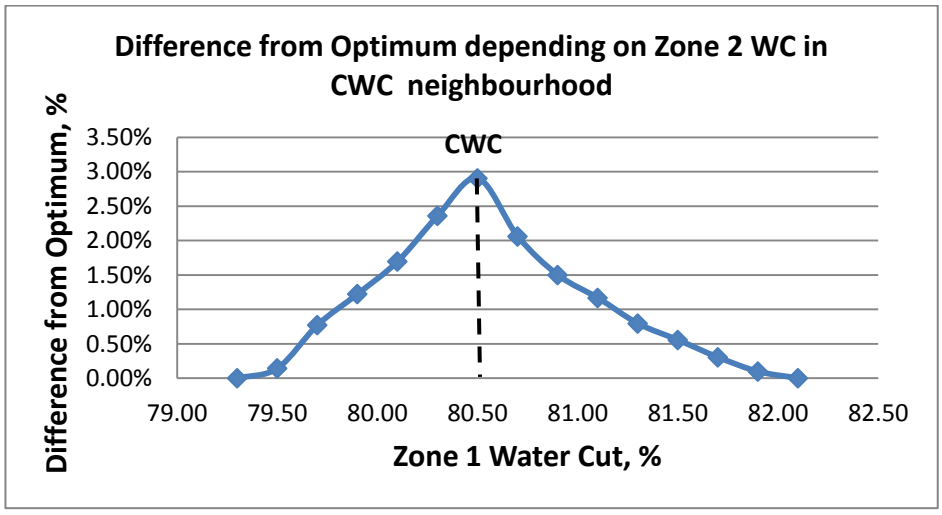


*Figure 8-29 Difference from Optimum depending on Zone 2 WC in CWC neighbourhood*

In Figure 8-30 the difference from maximum oil rate depending on Zone 2 WC in a CWC neighbourhood for P10, P50 and P90 cases is shown. The mismatch rises with increasing WC. However, the difference in the oil rate does not increase because the oil ratio reduces.

These results allow the oil loss of using On/Off valves instead of infinitely variable or discrete position valves to be estimated. It is important to keep in mind that achieving the optimal performance of an ICV with intermediate positions requires that we can

accurately measure the zonal water cut, otherwise the result will be the same as for an On/Off completion.

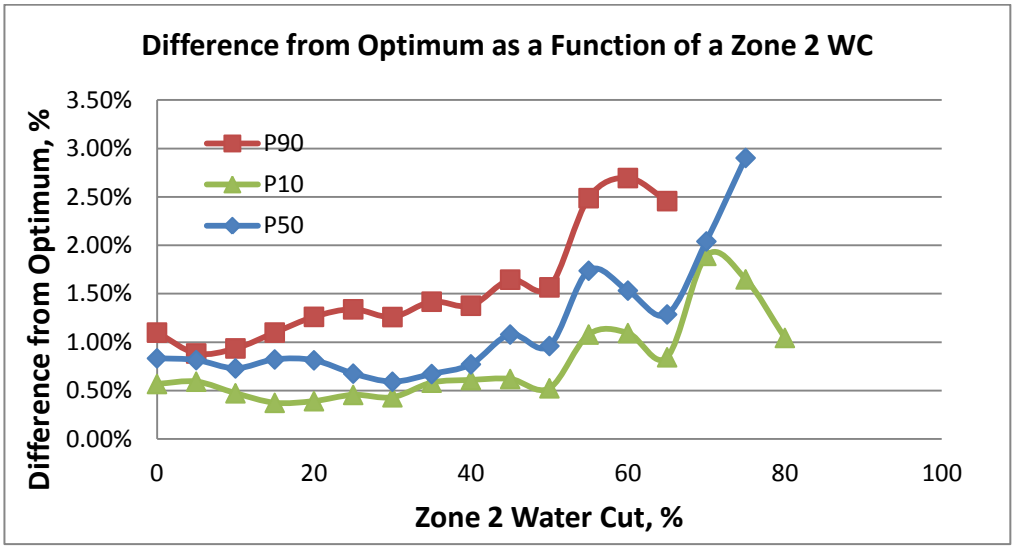


*Figure 8-30 Difference from optimum for P10, P50 and P90 as a function of a zone 2 WC*

## 8.6 Summary

1. A methodology to find the application area for On/Off zonal control strategy has been developed.

2. It was shown that the situation with any number of zones can be described by a 3 zones well. An algorithm for converting any number of zones into an equivalent 3-zone well has been developed.

3. A wide range of input parameters has been investigated:
   - Productivity Index: from 1 to 100 Stb/day/psi
   - WC: from 0 to 100%
   - Reservoir Pressure: from 2200 to 3600 psi
   - GOR: from 50 to 3300 Scf/Stb

   Two scenarios: the natural flow and gas-lift have been analysed. On/Off strategy provided maximum oil rate in about 90% of cases. In about 95% of cases the difference is less than 1%. The ESP scenario has not been analysed, because the optimum ESP and the pump range for each case should be considered in this analysis, which is technically hard and time-consuming task.

4. An On/Off valve may not provide the optimal value when GOR or pressure difference between zones are significant. A probability to have a non optimal value is close to zero when the difference in GOR is less than 400 Stb/Scf.

5. A methodology has been described for finding whether an On/Off ICV is applicable to a particular case.

6. The mismatch with the optimal value is only near the critical water cut value. This mismatch can be ignored in most cases if the accuracy with which the zonal water cut can be determined is less than 0.5%.

In summary, the On/Off control strategy has a wide application area providing a maximum, or very close to maximum, oil production rate. The next chapter will describe the On/Off critical water cut control algorithm and its application for a real field case and uncertainty analysis.

# Chapter 9 – Application of CWC and DS Control Strategies

This chapter demonstrates application of the Critical Water Cut criterion and Direct Search strategy for an ICV optimisation and uncertainty analysis.

## 9.1 Case1: 2 Zones, Vertical Production Well

Our first, relatively simple, case concerns a vertical, gas-lifted well operated at a fixed well head pressure 230 psi while producing from two, separate reservoir intervals (Fig 9-1).

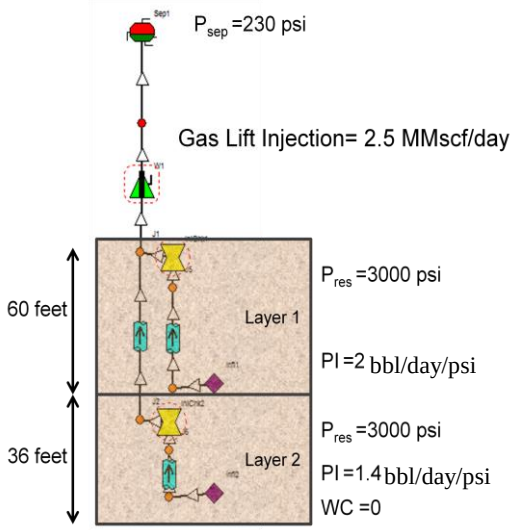


*Figure 9-1 Case 1: Well description*

Zone 2 of this well is producing dry (zero percent WC) oil. Water production is observed from Zone 1 which is completed with an ICV that can select from 11 fixed positions. We wish to calculate the preferred ICV setting at which zone 1 should be operated to maximise the well's total oil production (i.e. identify the optimal position for ICV 1). Nodal analysis was used to calculate the well's operating point for each value of the choke position as a function of the zone 1 WC when it was varied from zero to hundred percent (Fig. 9-2). Artificial lift (gas) lift ensured that the well could flow efficiently from 0% to 100% water cut.

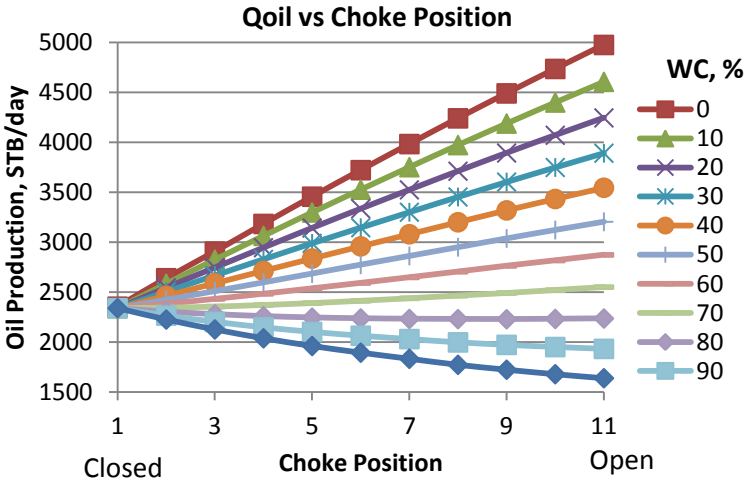


*Figure 9-2 Oil production rate depends on the Zone 1 ICV position*

The well's maximum oil production rate from both zones was achieved with the zone 1 ICV being either fully open for zone 1 WC was less than 74%; or fully closed for all higher WCs. I.e. 74% was the CWC value at which point zone 1 should be fully closed in order to maximise the well's total oil production rate. In other words, the total oil production rate from both zones will be less than that from interval 2 alone if the zone 1 production continued ones its WC exceeds the CWC value. The CWC can be calculated once the operating point of the fully open ICV is known:

$$CWC = (1 - \frac{\Delta P_{BHP} \cdot J_2}{Q_{1,Open}^{Liquid}}) \cdot 100\% \qquad (9\text{-}1)$$

The term $\Delta P_{BHP}$ in equation (9-1) is calculated from the well's Vertical Lift Performance based on the current WC value in each zone. The CWC value varies with the zone 1 WC value (Fig 9-3). The WC equalling the CWC value provides us with the required optimisation criteria for closing the production zone ICV with the highest WC. We calculated the same 74% as was previously found for this example (Fig 9-3).

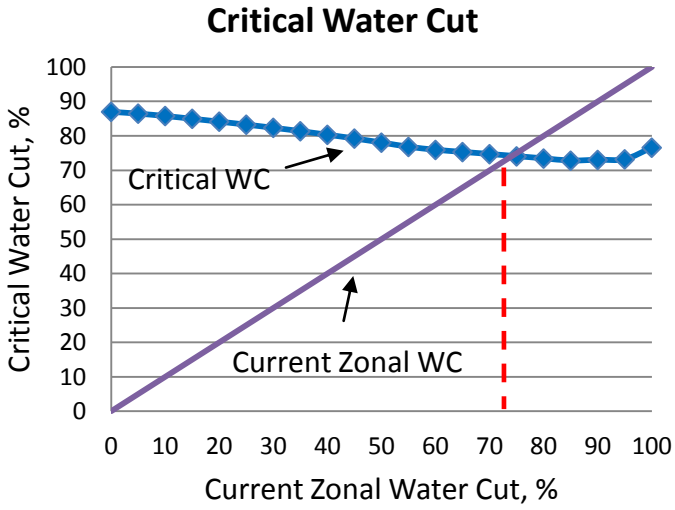


*Figure 9-3 Zonal Critical Water Cut value depends on the zone's current Water Cut*

## 9.2 Case2: 4 Zone, Vertical Production Well

Case 2 represents a more complex well with 4 production zones with different productivity indices, reservoir pressures and water cuts (Fig 9-4).

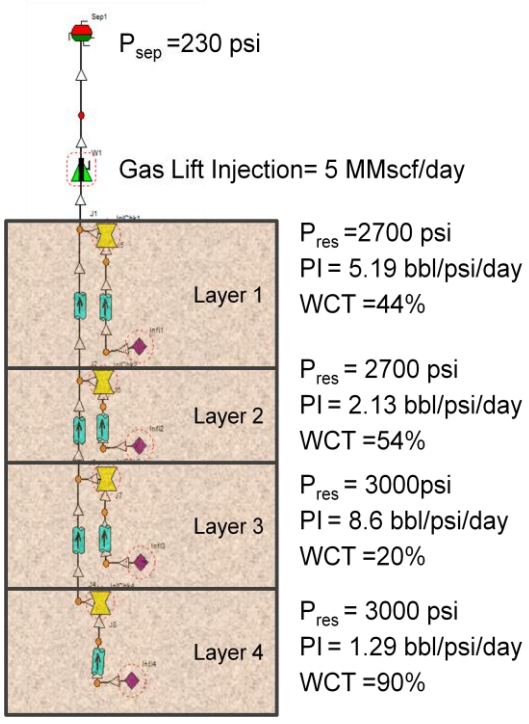


*Figure 9-5 Case 2 well description*

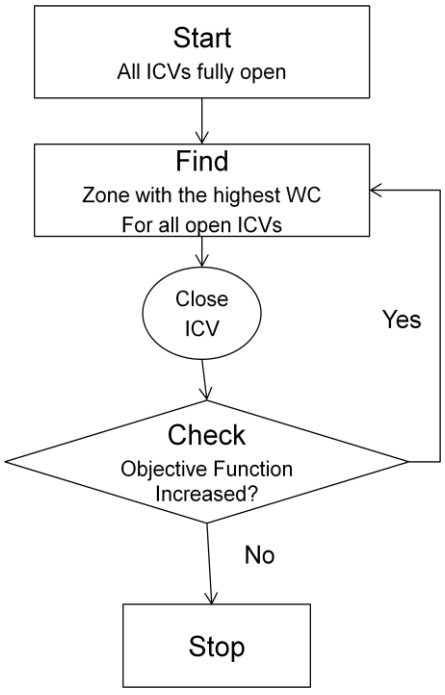


*Figure 9-4 Flow chart for CWC Control algorithm*

The CWC control algorithm (Fig. 9-5) identifies the producing zone with the highest WC for each iteration of the reservoir simulator. It then calculates the CWC for this zone and checks to see if closing this zone improves the well's total oil production from the remaining zones. This "Direct Check" (DC) method allows us to evaluate if the CWC criterion is making the correct decision (Fig. 9-6 and 9-7).

Layer 4 has the highest WC (90%), and is the first one to be tested for closure by the control algorithm. The calculated CWC is 43%; indicating that this zone should be closed. A DC confirms that closing this zone increases the oil production rate from 7,146 to 7,533 stb/day (Fig 9-6).

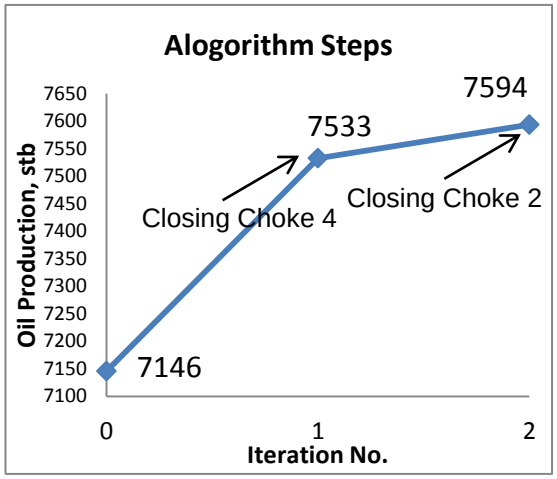


*Figure 9-6 Oil production rate increases with each iteration of the control algorithm*

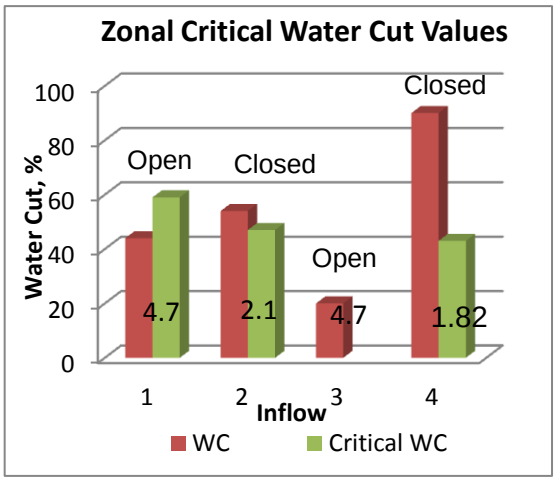


*Figure 9-7 Critical WC values and ICV positions after optimisation with SQP*

The control algorithm next tests whether zone 2, the zone producing the highest WC value, should be closed. Once again, its current WC (54%) is higher than the CWC value (47%); hence its closure will also increase the total oil production rate. Zone 1, the third zone closed for evaluation, produces at 44% WC, a lower value than the CWC of 59%. Zone 1 should thus remain fully open. This was confirmed by DC which indicated that closing this zone reduces the oil production from 7,594 to 7,091 stb/day. We compared the above CWC algorithm results with the values provided by SQP optimisation method as implemented in a commercial, well performance software. Figure 9-7 shows the choke diameters chosen by SQP for each ICV. The initial (fully open) ICV diameter for all zones is 4.7 inches (the same value as the internal diameter of the production tubing). The SQP partially closed zone 2 and 4 ICVs (the same zones as were choked by CWC algorithm). Nevertheless, the SQP algorithm did not close them completely. The resulting production rate of 7,147 stb/day is a marginal improvement on the initial value of 7,146 stb/day and is considerably less than the optimal value of 7,594 stb/day identified by the CWC algorithm.

## 9.3 Case 3: A full-scale, simulation and optimisation study of a real-field with 10 Conventional and 3 Intelligent Wells with 3 or 4 ICVs each

### *9.3.1 Model Description*

The CWC control algorithm has also been tested on a large, complex full-scale field reservoir simulation model. The modelled field contains two main reservoirs which partly overlay each other for a significant fraction of the field area (schematically shown in Fig. 9-8). Each of these layers is further divided into two parts which may or may not be hydraulically connected. The thickness of one of the reservoirs varies from 30 - 60 ft; while the other is significantly thicker at 50 - 150 ft. Both reservoirs are contained within a 15 x 4 km rectangle. The resulting dynamic reservoir simulation model has 200,000 active cells. There is no production history since the field has not yet been developed.

The added complexity to the geological model results from several faults of unknown transmissibility being observed on seismic within the field boundaries. The porosity of both reservoirs is in the range of 15 to 25% with the corresponding permeability of one of the reservoir varying over a relatively small range of 250 - 650 mD; while core analysis of the other one suggested the much greater permeability range of 150 – 1300 mD.

There is currently no evidence for pressure support by an aquifer to the upper layer, though good aquifer pressure support to the lower layer is thought to be highly probable. The fluid properties of both reservoirs are similar, containing a light (40° API) oil with a GOR of approximately 300 scf/bbl. Both reservoirs are normally pressured. A gas cap has not been observed.

It is planned to drill conventional wells in those parts of the field where the two reservoirs do not overlap. The option to install 3 IWs to manage commingled production from both reservoir layers (Fig. 9-8 and 9-9) in the “overlap” reservoir area is to be studied. Therefore, the 21 wells (16 producers and 5 injectors) required in the Base Case scenario can be reduced to 17 wells (13 producers and 4 injectors) in the IW case. All production wells are equipped with gas lift to aid production.

Petex IPM software was used for the integrated production and optimisation modelling of this field. The production and injection systems were modelled in *GAP* (Fig. 9-10) and connected to the *Eclipse*$^{TM}$ reservoir simulation model. The wellhead chokes were optimised with the SQP optimiser implemented in GAP. It also optimised the downhole

chokes when the CWC Algorithm was not being employed. The CWC Algorithm was realised with Excel VBA code.

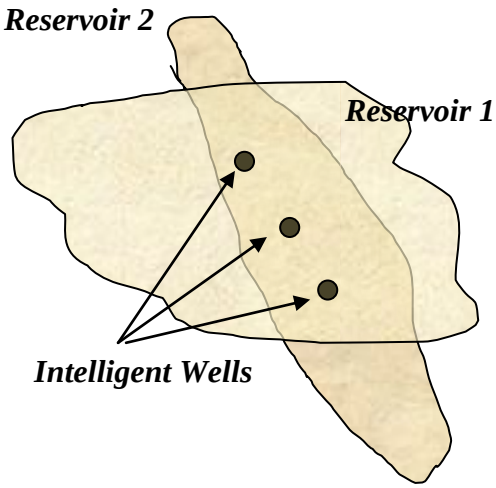


*Figure 9-8 Schematic description of the field area*

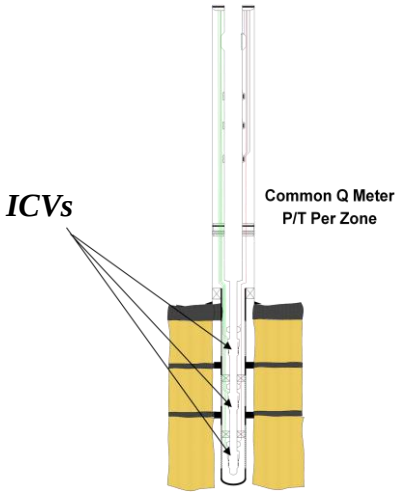


*Figure 9-9 Three or Four Zones with Zonal Isolation Upper and Lower Reservoir*

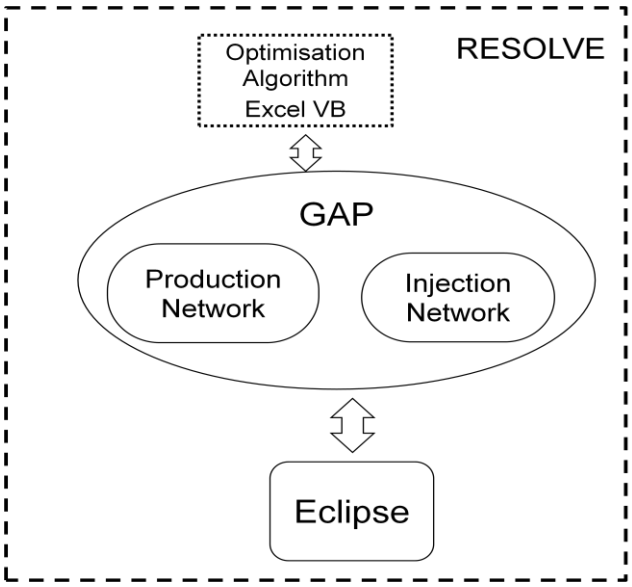


*Figure 9-10 Model Schematic*

### *9.3.2 Control of the Production Wells*

Control of the 11 ICVs installed in the 3 Intelligent Production Wells (Fig.9-8 & 9-9) used the same control philosophy as described for case 2: the ICV inflow showing the highest water cut value in each production well is checked to see if the CWC value calculated for this zone has been exceeded (Fig 9-11). The ICV for this zone is then closed if the zonal WC is higher than the calculated CWC value for this zone.

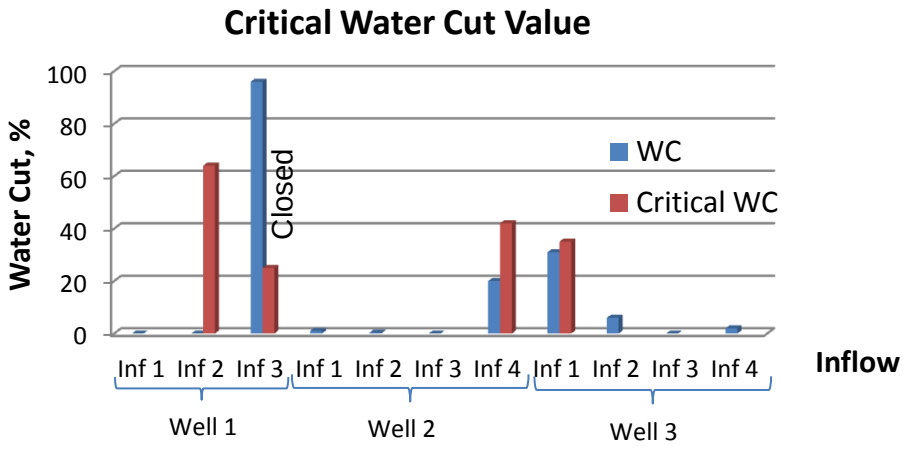


*Figure 9-11 Critical Water Cut Values for all IW inflow Zones*

CWC Control Algorithm showed a higher oil production rate during the decline period, when the field is off-plateau, compared to both the reservoir simulator on its own with all ICVs fully open and the commercial network optimisation software (Table 9-1).

*Table 9-1 Example field production during the decline period when the field is off-plateau*

| Case | Field Oil Production Rate from 13 wells |
|---|---|
| Reservoir simulation with all ICVs fully open | $79.3*10^3$ Stb/day |
| Commercial network optimisation software | $79.6*10^3$ Std/day |
| "Critical-Water-Cut" Control Algorithm | $82.7*10^3$ Stb/day |

This study was repeated a number of times by stopping the simulation and then optimising the "Real-Time" or "Instantaneous" production using either the:

(1) SQP algorithm in GAP for the complete production system (downhole, wellhead and surface network) and

(2) CWC for the downhole chokes and the SQP for the wellhead chokes etc.

In all cases studied the CWC gave a slightly higher oil production rate

### *9.3.3 The Simulation Performance*

The combined reservoir and optimisation model was run for a 30 year period. The On/Off Direct Search algorithm (see chapter 4) was employed to optimise oil rate at every (monthly) time step. In addition, CWC values for the ICVs that were candidates for closure were calculated.

Figure 9-12, the zonal WC for well 1, is a typical example of an IW inflow performance plot over the field's lifetime. It can be seen that zone 3 has the highest WC during the whole production period; hence it was checked for closing at every time step. Fig. 9-13 and 9-14 illustrate that the ICV was open whenever the water cut was less than critical value. It was closed at all other times.

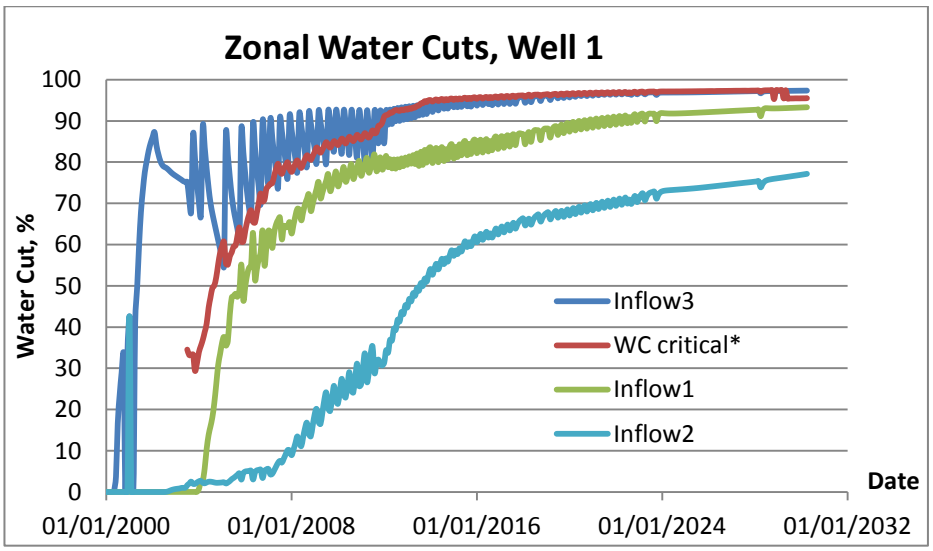


*Figure 9-12 Zonal Water Cuts for I-Well 1 (3 zones)*

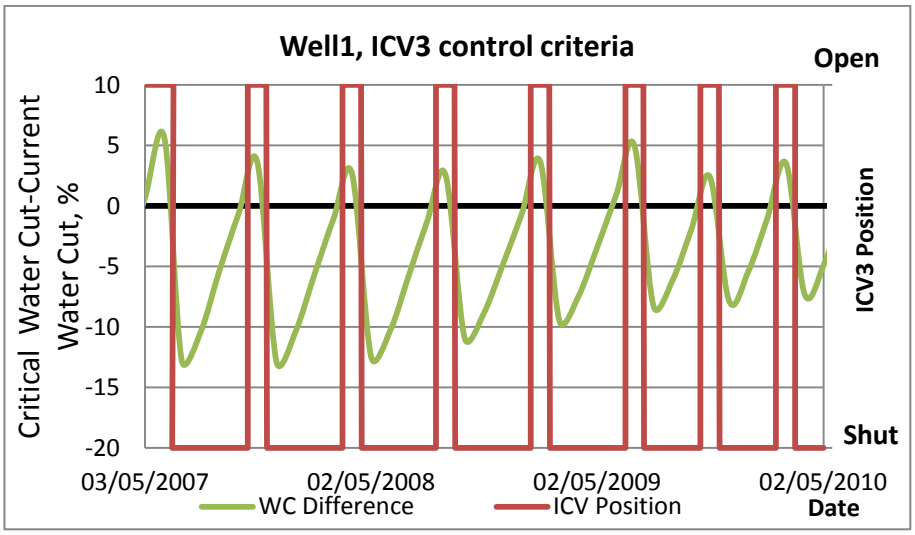


*Figure 9-13 "Critical -Water-Cut" Algorithm closes the ICV when the current WC is higher than the critical value*

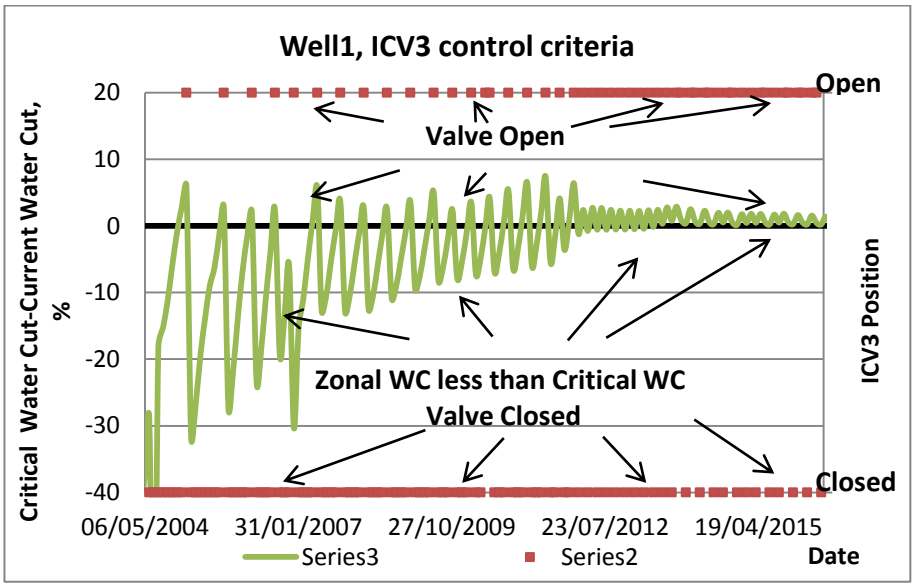


*Figure 9-14 Critical water cut value increases with time, hence the ICV is frequently opened*

CWC criterion suggested a different value from the DS On/Off method in 1.4% of the cases. For all these cases a zonal WC is close to the CWC with the maximum difference less than 3% and less than 1% in 95% of the cases (Fig. 9-15). Moreover, the difference of the NPV from the optimum solution was less than 0.3% in 80% of these cases (Fig. 9-16). The difference can be caused by several reasons, e.g. numerical errors in a production network system at the level of the solver tolerance threshold, changes in the friction and hydrostatic head in the production interval which were simplified in CWC formula, etc.

In summary, the CWC value was within 1% of the correct solution for more than 99% of the cases. The maximum difference of NPV was less than 1.4% in all cases. The two approaches are thus equivalent from a practical point of view, and the CWC criterion can be used for ICV control instead of the Direct Search On/Off method.

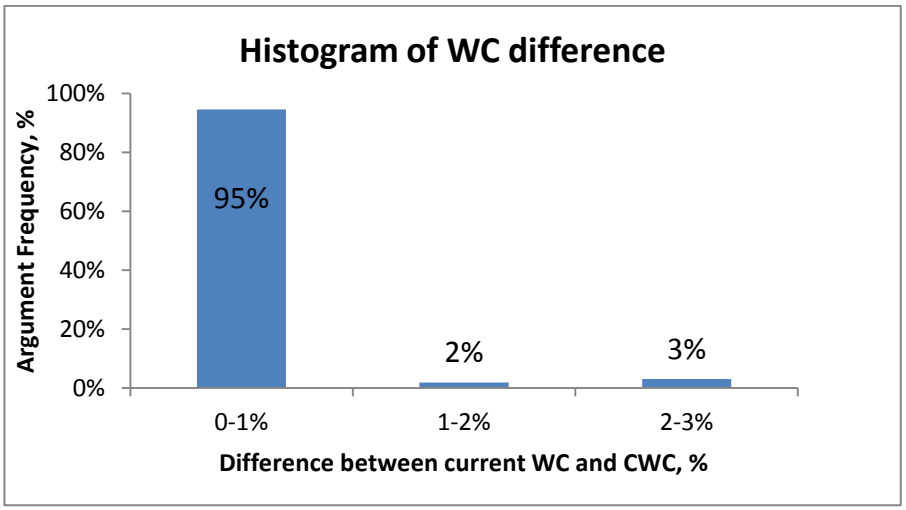


*Figure 9-15 Difference between current WC and CWC in the cases where CWC criterion suggested a different value from the DS On/Off algorithm solution*

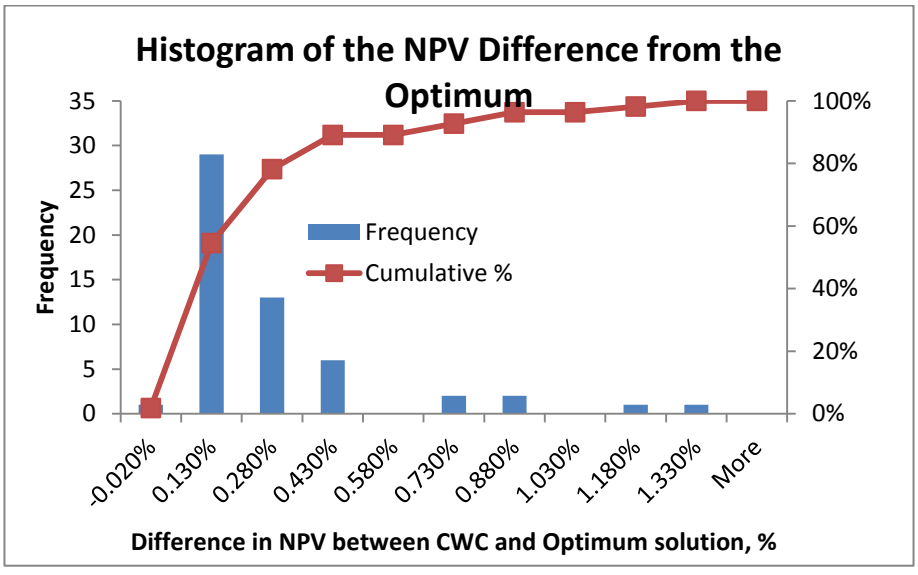


*Figure 9-16 Histogram of the NPV Difference between CWC algorithm and Optimum value*

Table 9-2 summarises the difference in NPV, cumulative oil and water production from the Base Case (16 production wells) and the IW Case (13 production wells) with fully open valves and optimised by commercial software and the DS On/Off method.

*Table 9-2 Changes in Cumulative Oil and Water production for different scenarios*

| Case | Change in Cumulative Oil Production | Change in Cumulative Water Production | Change in NPV |
|---|---|---|---|
| Base Case: Reservoir simulation with conventional wells (16 production wells) | 0% | 0% | 0% |
| No Control: all ICVs fully open (13 production wells) | -1.60% | -0.25% | 1.53% |
| On/Off (CWC) | -0.62% | -6.03% | 4.01% |
| SQP | -0.96% | -8.96% | 3.73% |

The economic parameters used for the NPV calculation were the same as in Chapter 3 (see Tables 3-3 and 3-4).

Oil production in the No Control case is less than in the original Base Case with conventional wells because the number of the production wells has been reduced from 16 to 13. The capital cost is reduced in this case, at the same time, resulting in a higher NPV than for the Base Case.

Both optimisation methods improved the field oil production by approximately 1% and the cumulative NPV by 4%. The DS On/Off optimisation algorithm showed slightly better results than the commercial optimiser, but the difference was not significant.

The run time of On/Off algorithm was approximately the same as for SQP algorithm and 1.8 times longer than for the No Control Case (Table 9-3).

The increase in run-time was 10 times longer for "Box-Shaped" model (see Table 5-7) and 5.4 times for the PUNQS3 model (Table 5-11). Therefore, optimisation of a complex model has relatively less impact on the overall runtime than for a simple model. Note that inclusion of the DS or CWC algorithm within the simulator itself rather than externally via Excel would have resulted in a similar run-time as the Base Case.

*Table 9-3 Running Time for "Fully Open", Commercial Optimiser and CWC algorithm scenarios*

| Case | Reservoir simulation with all ICVs fully open | SQP | On/Off |
|---|---|---|---|
| Run Time, sec | 9,600 | 15,890 | 16,770 |

### *9.3.4 Sensitivity Analysis*

Sensitivity analysis was made for N-Field model for three factors:

- Stressed relative permeability (Fig 9-17);
- Decreased injection capacity;

- Reservoir uncertainty.

The stressed relative permeability case involves increasing the water relative permeability to evaluate a worst scenario with early-time water breakthrough and a considerably higher (total) water production. The impact on the cumulative production and NPV of decreasing the injection capacity by 33% and 66% was also investigated. The reservoir uncertainty was represented by the P10, P50 (original base case) and P90 scenarios summarising the uncertainty of the structure, layer thicknesses and porosity and permeability distribution.

The impact of each parameter on the cumulative production and NPV for the base case is shown in Table 9-4. The stressed relative permeability case showed an increased water production and reduced cumulative oil. The reduced injection capacity significantly decreases water production, but the reservoir pressure also decreases in this case reducing oil production. The reservoir uncertainty has the highest impact on the cumulative production and NPV.

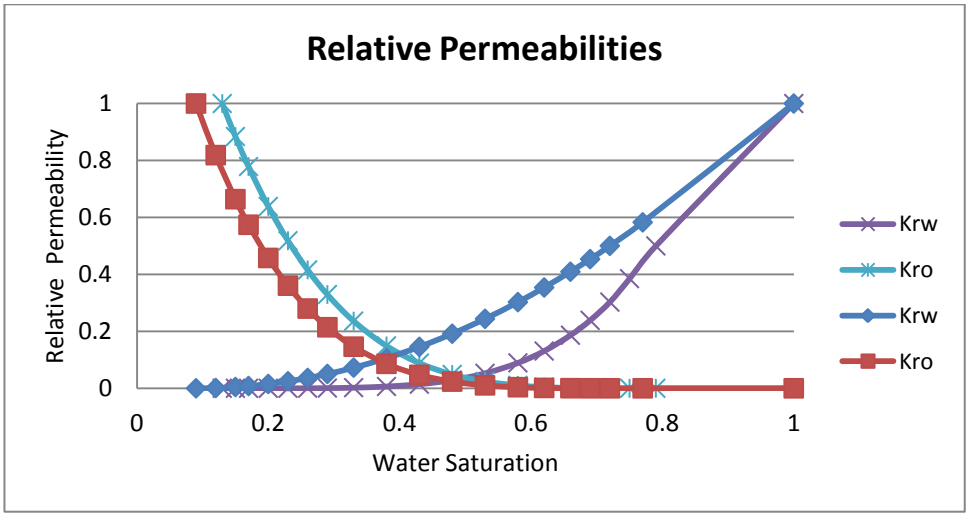


*Figure 9-17 Original and Stressed Relative Permeability Curves as a function of Water Saturation*

*Table 9-4 Impact of Stressed Relative Permeability, Reduced Injection Capacity and Reservoir Uncertainty on the Base Case*

| Scenario | | Difference from the original Base Case | | |
|---|---|---|---|---|
| | | Δ NPV | Δ Cum Oil | Δ Cum Water |
| **Stressed Relative Permeability** | | -7% | -2% | 18% |
| **% of Original Injection Capacity** | **66%** | -9% | -3% | -16% |
| | **33%** | -15% | -9% | -52% |
| **Reservoir Uncertainty** | **P10** | 24% | 26% | 2% |
| | **P50** | 0% | 0% | 0% |
| | **P90** | -35% | -27% | 13% |

Table 9-5 summarises the difference of the cumulative production and NPV of commingled and IW cases from the Base Case for different scenarios.

*Table 9-5 Difference of the Cumulative Production and the NPV compared with the Base Case*

| Scenario | | Method | Difference from the original Base Case=100% | | |
|---|---|---|---|---|---|
| | | | Δ NPV | Δ Cum Oil | Δ Cum Water |
| **Stressed Relative Permeability** | | No Control | -0.41% | -1.27% | 7.60% |
| | | IW | 2.48% | -0.84% | 2.94% |
| **% of Original Injection Capacity** | **66%** | No Control | -1.61% | -5.66% | -28.38% |
| | | IW | 1.14% | -3.68% | -28.29% |
| | **33%** | No Control | -2.74% | -7.25% | -27.96% |
| | | IW | -1.50% | -6.30% | -29.07% |
| **Reservoir Uncertainty** | **P50** | No Control | 1.53% | -1.60% | -0.25% |
| | | IW | 4.01% | -0.62% | -6.03% |
| | **P10** | No Control | 0.35% | -1.43% | 9.18% |
| | | IW | 2.65% | -0.64% | 2.85% |
| | **P90** | No Control | 2.00% | -2.82% | 4.87% |
| | | IW | 3.38% | -2.80% | 0.22% |

The commingled case in the stressed relative permeability scenario showed a lower NPV and cumulative oil production than the Base Case. Employing an intelligent completion for this scenario makes the commingled production more beneficial than separated production with a higher number of wells in the Base Case.

The reduced injection cases do not allow fully maintain the reservoir pressure. An improved result is normally achieved with a greater number of wells when the reservoir pressure is low. However, an intelligent completion is still more profitable than a conventional completion with commingled porduction. Moreover, it is even more profitable than the Base Case if the injection capacity is 66% of the original value.

For the reservoir uncertainties commingled production gives higher NPV than the Base Case for all cases, and intelligent completions further increase the added value and provide the most beneficial scenario.

### *9.3.5 Summary*

The initial reservoir simulation case, employing 16 conventional production wells to separate the production from two reservoirs showed a 0.6% higher cumulative oil production and 6% extra water production than the case when 6 of the conventional wells were replaced by 3 intelligent wells. Nevertheless, an economic analysis showed that latter development scenario for this subsea field in 100 m water depth located in a mature production area had a greater NPV. This has mainly attributed to the reduced capital investment requirement. Sensitivity analyses for stressed formation relative permeabilities and reservoir dynamic and static uncertainty confirmed that the field developement with IWs was the most beneficial economic scenario.

The On/Off algorithm showed similar results with SQP optimisation method (which provides an optimum solution for infinitely variable ICVs). This confirms that an On/Off completion is sufficient for the optimal performance of vertical IWs in a field producing only liquids at the perforations.

The CWC criterion provided the optimal solution in almost 99% of cases. In the rest 1.4% of the cases difference from the optimum is very small. In 90% cases the difference in NPV between Base and IW cases is less than 0.6%. Moreover, for having this difference, a zonal WC resolution should be less than 1%, which is hardly can be achieved in practice. Therefore, CWC criterion can be used for IW's optimisation instead of a Direct Search method.

## 9.4 CWC Algorithm

The critical water cut introduced in chapter 7 depends on the zonal water cuts and pressures (Equation 9-2) which vary during production period. CWC can be calculated for all possible values in advance, i.e. prior to performing the dynamic and production optimisation simulation. The CWC values can then be used as a criterion for either closing or keeping open the ICV during the complete simulation process.

$$CWC = 1 - \frac{\Delta P_{BHP} \sum_{i \neq n}^{N} J_i \cdot (1 - WC_i)}{J_n \cdot dP_n} = 1 - \frac{\Delta P_{BHP}(WC_i, P_{RES,i}) \sum_{i \neq n}^{N} J_i(WC_i) \cdot (1 - WC_i)}{J_n(WC_n) \cdot dP_n(P_{RES,n})} \quad (9\text{-}2)$$

For example, Figures 9-18 and 9-19 show how Critical WC of zone 1 for Case 1 (the 2 Zones, Vertical Production Well case described in Section 9.1) varies with zonal pressure. Fig. 9-18 shows that the minimum CWC for zone 1 is 67% and therefore ICV1 should be open if zonal WC is less than this value. Zone 1 does not need to be optimised at WC below 90% when $WC_2$ has increased to 55%, (Fig. 9-19).

This approach makes runtime of the optimised case similar to the case with no control while the solution does not differ from a Direct Search method. Both solution methods give results close to the optimum value.

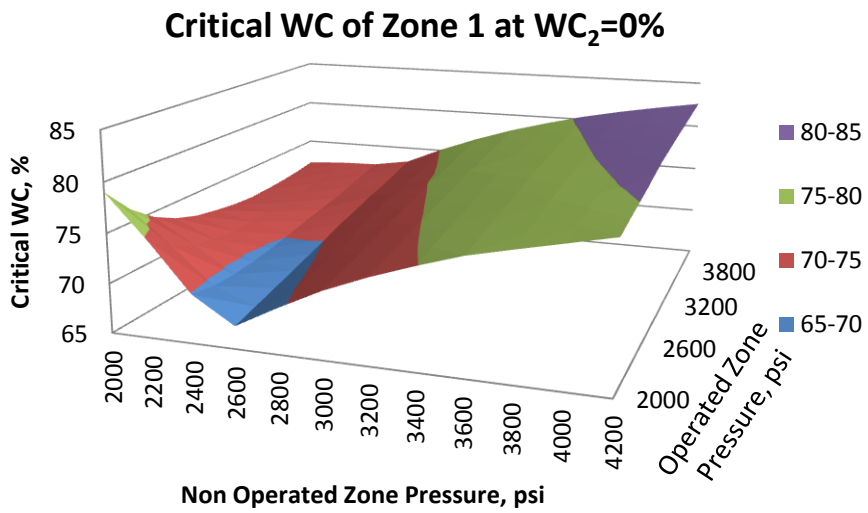


*Figure 9-18 Critical WC of zone 1 at WC=0% for Case 1 depending on zonal reservoir pressure*

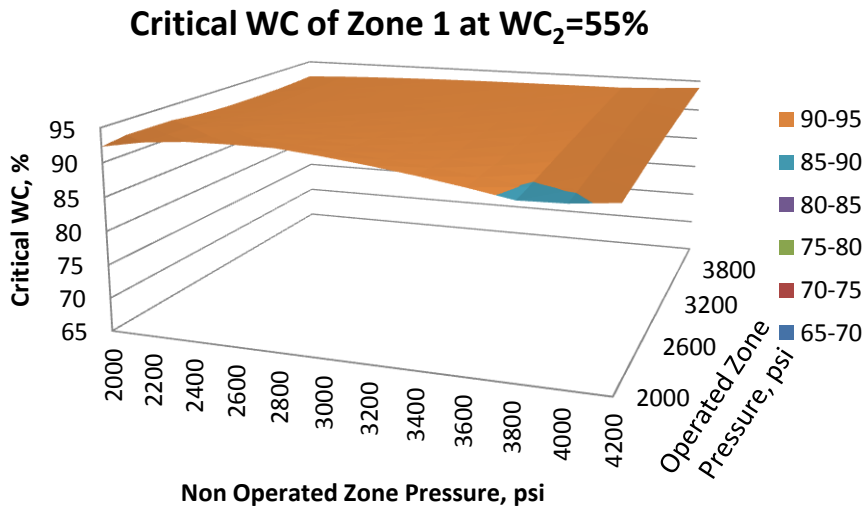


*Figure 9-19 Critical WC of zone 1 at WC=55% for Case 1 depends on zonal reservoir pressure*

## 9.5 Uncertainty Analysis

### *9.5.1 Methodology*

In this section the results of IWs optimised by reactive control methods on the production uncertainty is analysed. Four optimisation methods are included in the analysis: SQP, SLP, Direct search with 10 position valves and On/Off optimisation. PUNQS-3 model with one horizontal producer completed with four ICVs, one water and one gas injection well (see Chapter 2) was used as a reservoir model. The uncertainty was modelled with one hundred realisations of the porosity and permeability, the same as in Chapter 2. The dynamic reservoir model was implemented in *Eclipse* with the production model in *PETEX* software.

### *9.5.2 Results*

The cumulative NPV, oil and water production of each method for the original case are summarised in Table 5-13 of chapter 5. The IW scenarios showed 1.3-2.7% lower cumulative oil production and 0.7-1.2 lower NPV than a Base Case employing a conventional well. The cumulative water production for IW's scenarios reduced up to 20%, which might make these scenarios more attractive for the cases with limited water handling facilities or higher water handling price.

Figure 9-20 shows reserves distribution for 100 realisations. The mean value of the oil in place is 13.14 Million $m^3$ compared to the reserves of the original case are 12.92 Million $m^3$ (decrease of 1.7%). At the same time, the cumulative NPV of the original case is 14% higher than P50 value, the cumulative oil production is 7% greater and the cumulative water production is 8% less (Fig. 9-21, 9-22 and 9-23). This is attributed to the optimal location of the well in the original case.

The optimisation of the wells location in a dynamic model is the common practice in oil industry. However, it often does not consider the reservoir uncertainty. As a result, the production in the specific case is improved and shows better results than other, equally possible, scenarios. Moreover, the potential value of intelligent wells is reduced in this case, because optimal location makes water front more uniform and reduces the difference in the inflow breakthrough times.

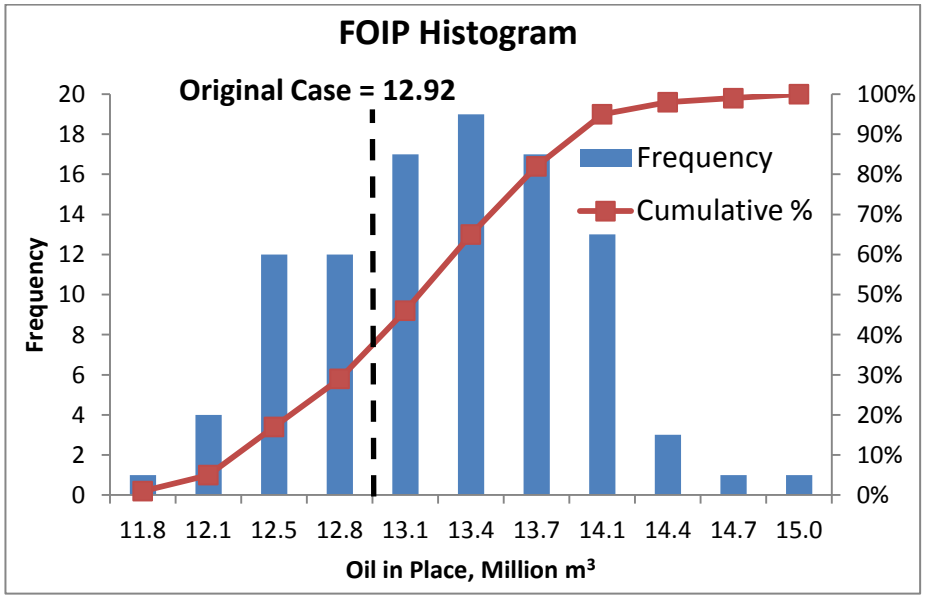


*Figure 9-20 Oil in Place Histogram. Base Case*

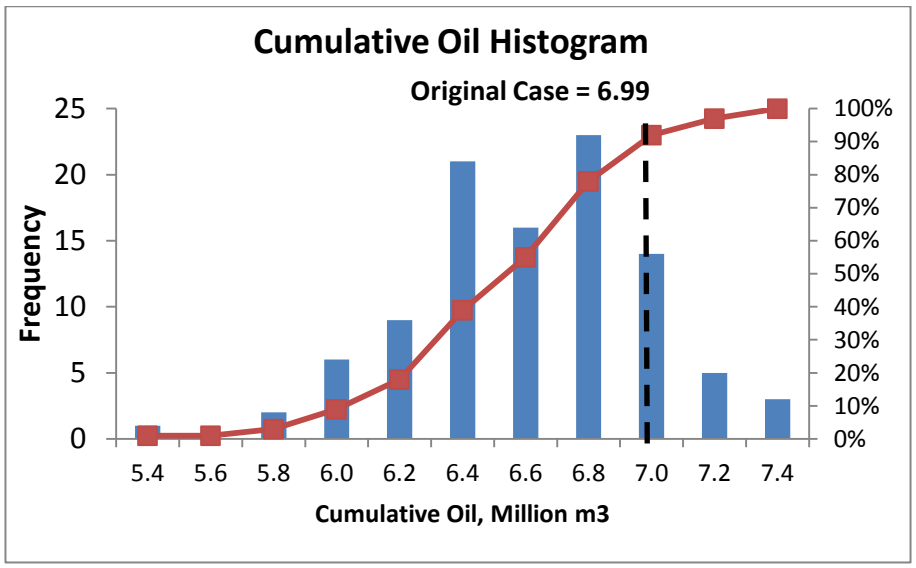


*Figure 9-21 Cumulative Oil Histogram. Base Case*

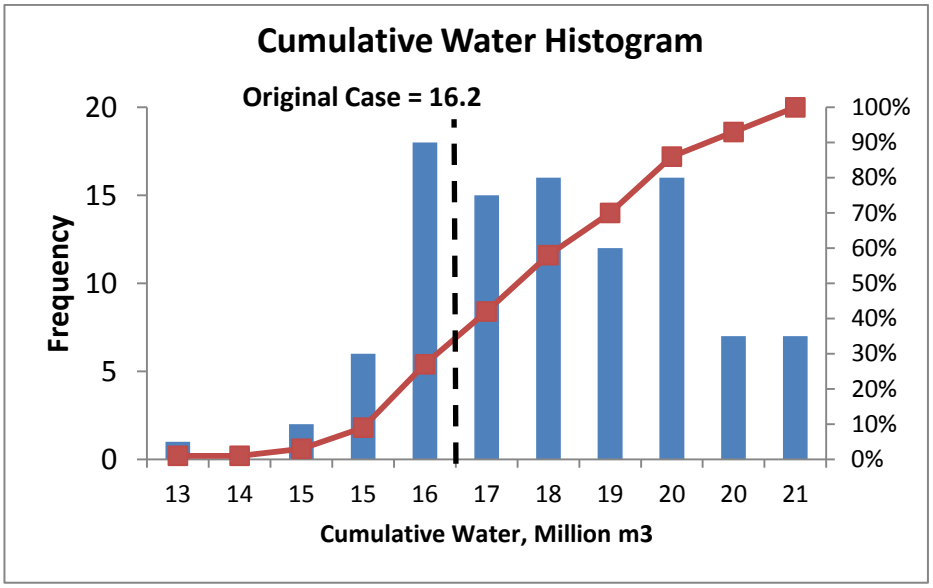


*Figure 9-22 Cumulative Water Histogram. Base Case*

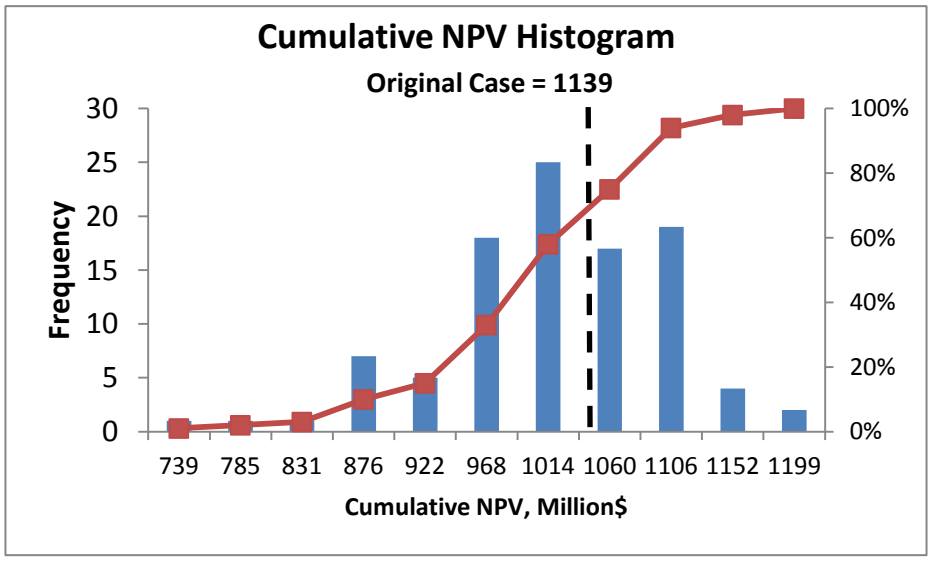


*Figure 9-23 Cumulative NPV Histogram. Base Case*

P10, P50 and P90 of cumulative NPV, oil and water production for Base Case, SQP, SLP, Direct Search (DS) with 10 position valves and On/Off optimisation are summarised in table 9-6.

*Table 9-6 P10, P50 and P90 of Cumulative NPV, Oil and Water Production*

| Case | Cumulative NPV, Million$ | | | Cumulative Oil Production, Million m3 | | | Cumulative Water Production, Million m3 | | |
|---|---|---|---|---|---|---|---|---|---|
| | P10 | P50 | P90 | P10 | P50 | P90 | P10 | P50 | P90 |
| **Base Case** | 1098 | 996 | 878 | 6.93 | 6.53 | 6.10 | 19.65 | 17.61 | 15.51 |
| **IW No Control** | 1097 | 995 | 913 | 6.93 | 6.53 | 6.11 | 19.37 | 17.46 | 15.47 |
| **IW SLP** | 1106 | 1006 | 898 | 6.82 | 6.28 | 5.87 | 14.14 | 12.31 | 10.13 |
| **IW SQP** | 1104 | 1006 | 889 | 6.82 | 6.33 | 5.87 | 16.06 | 14.35 | 12.37 |
| **IW 10 Position** | 1108 | 1009 | 897 | 6.77 | 6.29 | 5.84 | 14.34 | 12.38 | 10.65 |
| **IW On/Off** | 1107 | 1009 | 901 | 6.78 | 6.29 | 5.87 | 14.20 | 12.26 | 10.44 |

Table 9-7 shows that IW increased the cumulative NPV in all scenarios by approximately 1%, though the cumulative oil production is still less than in the Base Case. The optimisation of IW in Eclipse by employing WC threshold (as was described in Chapter 2) demonstrated 4.4% reduction of NPV from the conventional case.

The relative and absolute variance of the cumulative NPV and production for 100 cases was calculated by equation 9-3 and 9-4 summarised in Table 9-8 and 9-9:

$$\text{Relative}\,Variance = \frac{P10 - P90}{P50} \qquad (9\text{-}3)$$

$$\text{Absolute}\,Variance = P10 - P90 \qquad (9\text{-}4)$$

The absolute variance of cumulative NPV has decreased slightly for IW scenarios, thought the difference from the base case is not significant.

*Table 9-7 Added value of IWs for P50*

| Case | Cumulative NPV | | | Cumulative Oil Production | | | Cumulative Water Production | | |
|---|---|---|---|---|---|---|---|---|---|
| | NPV | Difference from Base Case | | Cum Oil | Difference from Base Case | | Cum Water | Difference from Base Case | |
| | Million $ | Million $ | % | Million $m^3$ | Million $m^3$ | % | Million $m^3$ | Million $m^3$ | % |
| **Base Case** | 996 | - | - | 6.53 | - | - | 17.61 | - | - |
| **IW No Control** | 995 | -1 | -0.1% | 6.53 | -0.01 | -0.1% | 17.46 | -0.1 | -0.8% |
| **IW SLP** | 1006 | 10 | 1.0% | 6.28 | -0.25 | -3.8% | 12.31 | -5.3 | -30.1% |
| **IW SQP** | 1006 | 10 | 1.0% | 6.33 | -0.20 | -3.0% | 14.35 | -3.3 | -18.5% |
| **IW 10 Positions** | 1009 | 13 | 1.3% | 6.29 | -0.25 | -3.8% | 12.38 | -5.2 | -29.7% |
| **IW On/Off** | 1009 | 13 | 1.3% | 6.29 | -0.24 | -3.6% | 12.26 | -5.3 | -30.4% |
| **Base Eclipse** | 982 | - | - | 6.51 | - | - | 17.92 | - | - |
| **IW Eclipse** | 939 | -43 | -4.4% | 6.22 | -0.29 | -4.5% | 13.19 | -4.73 | -26.4% |

*Table 9-8 Relative Variance of Cumulative NPV, Oil and Water Production*

| Case | Cumulative NPV | Cumulative Oil Production | Cumulative Water Production |
|---|---|---|---|
| **Base Case** | 22% | 13% | 24% |
| **IW No Control** | 19% | 13% | 22% |
| **IW SLP** | 21% | 15% | 33% |
| **IW SQP** | 21% | 15% | 26% |
| **IW 10 Positions** | 21% | 15% | 30% |
| **IW On/Off** | 20% | 14% | 31% |

*Table 9-9 Absolute Variance of Cumulative NPV, Oil and Water Production*

| Case | Cumulative NPV, Million$ | | Cumulative Oil Production, Million m3 | | Cumulative Water Production, Million m3 | |
|---|---|---|---|---|---|---|
| | Variance | % | Variance | % | Variance | % |
| **Base Case** | 220 | 100% | 0.84 | 100% | 4.14 | 100% |
| **IW No Control** | 185 | 84% | 0.83 | 99% | 3.90 | 94% |
| **IW SLP** | 208 | 95% | 0.95 | 113% | 4.01 | 97% |
| **IW SQP** | 215 | 98% | 0.95 | 113% | 3.69 | 89% |
| **IW 10 Positions** | 210 | 96% | 0.93 | 111% | 3.69 | 89% |
| **IW On/Off** | 207 | 94% | 0.90 | 108% | 3.76 | 91% |

Table 9-10 shows the number of bad cases in which simulation provided unrealistic values or stopped before the production period end. The unrealistically high production rates were observed in SQP scenario when the optimisation stopped because the number of iterations increased the maximum limit. These values were excluded from the analysis and displaced with the interpolated production values in these points.

The earlier stop of the simulation is caused by the problems in production system solving and "freezing" of GAP module. They are not related with optimisation process directly. These cases were excluded from the summary analysis because the cumulative values in them are lower than should be. The number of these cases is not significant; therefore their exclusion should not impact the summary results.

In general, DS demonstrated more stable behaviour than other methods and SQP showed the most unstable

*Table 9-10 Number of bad Cases*

| Case | Number of bad Cases | | |
|---|---|---|---|
| | Unrealistic Values | Early Stopped | Total |
| **Base Case** | 0 | 0 | 0 |
| **IW No Control** | 0 | 0 | 0 |
| **IW SLP** | 0 | 4 | 4 |
| **IW SQP** | 12 | 7 | 19 |
| **IW 10 Positions** | 0 | 3 | 3 |
| **IW On/Off** | 0 | 2 | 2 |

The results of 2 month simulation time step are similar to the adaptive step and summarised in Appendix E.

The cumulative NPV in IW case is higher than in Base Case in 83% realisations. The realisations have been sorted from the smallest to the largest NPV in Base Case. Figure 9-24 shows that the added value of IW is in general higher for poorer reservoir scenarios, reducing the economic risk associated with them.

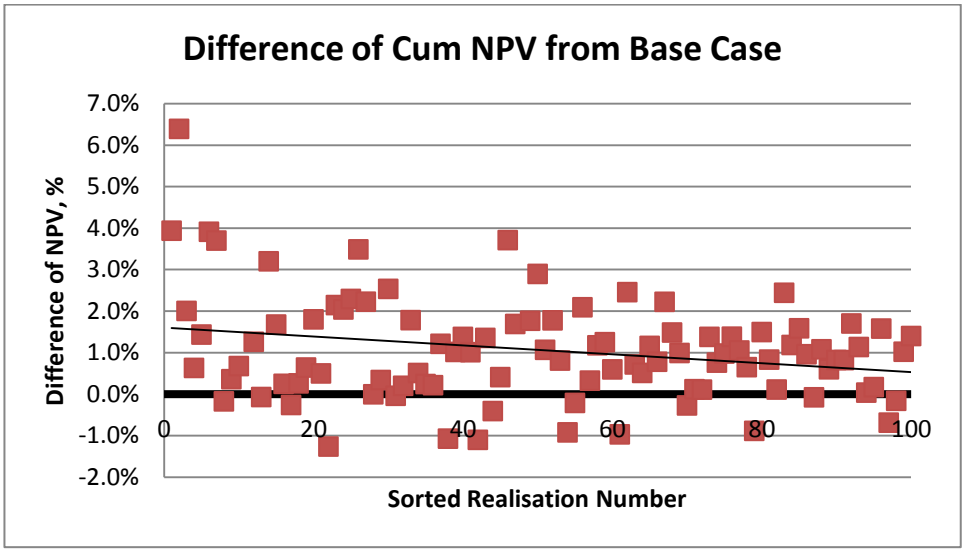


*Figure 9-24 Difference of Cumulative NPV between DS 10 position and Base Case*

## 9.6 Summary

This chapter has demonstrated an application of the novel algorithms for the real field optimisation and uncertainty analysis.

Reactive well control using an algorithm based on the "zonal critical water cuts" was illustrated by optimisation of the production from a:

- Simple and a more complex single well case and
- Large, complex, real field simulation model containing 10 conventional wells and 3 multi-zone intelligent wells over a 30 year time span.

The Direct Search method confirmed that the CWC criterion provided an optimal solution. Both methods gave similar results to commercial production optimisation software employing the SQP algorithm.

The CWC can be calculated before dynamic and production simulation and used as the optimisation criteria. That kind of approach will make runtime of the optimised case similar to the base case if it was included within the reservoir simulator.

The uncertainty analysis has been performed for 100 geological realisation of the PUNQS3 model. Four reactive optimisation methods: SLP, SQP, Direct Search 10 position and On/Off have been employed for IW optimisation. All methods provided

higher value of cumulative NPV for the IW case in comparison with the conventional scenario. The added value of IW is higher for the worse scenarios, which reduces the economical risk for them.

The IW demonstrated cumulative NPV improvement in more than 80% of realisations. The reduced NPV in the original case is caused by the optimal position of the well, which increases production for the base case, but does not consider the reservoir uncertainties.

The results are similar for adaptive and 2 month time steps. Therefore, the larger time step potentially can be used for the uncertainty analysis which significantly reduces the run time, though this can vary from case to case and additional study should be done to investigate that.

The DS optimisation demonstrated more stable performance than the other methods. SQP showed the highest instability and the largest number of inappropriate results.

The On/Off method provided similar results with the other methods. This type of completion is the best for this particular case, because the difference in the IW equipment cost and reliability was not considered in this analysis, while chapter 6 shows that On/Off completion has a higher value if these parameters are taken into account.

The example demonstrates the difference of the conclusion received based on one realisation of the original model and multiple realisations, considering reservoir uncertainty. The intelligent completion provides an extra value by reducing the effect of uncertainty especially for the poorer reservoir scenarios.

The proposed methodology provides more comprehensive analysis than employing only one scenario and is recommended for the comparison of different technologies.

# Chapter 10 - Conclusions and Future Work

## 10.1 Conclusions

This thesis systematized existing and proposed novel methods of intelligent wells optimisation. The methods focus on the production optimisation under reservoir and dynamic parameters uncertainty. The uncertainty analysis requires a fast and robust optimisation method, available for application in multiple realisations without extra tuning for each case.

The thesis not only presents the conclusions of the reservoir uncertainty study but also describes the novel developments achieved in the application area of On/Off ICVs and IW optimisation algorithms.

The main results of this thesis can be grouped into 3 areas:

**1. Optimisation Algorithms and Workflows**

**a.** A novel optimisation strategy is proposed for intelligent wells control. It includes Critical Water Cut (CWC) algorithm and Direct Search method for reactive ICV control and a proactive optimisation algorithm for production optimisation during a plateau period. The strategy is applicable for the cases with THP constraint. It has been tested in several cases, including a real-field model and demonstrated improvement in added value, a stable production, independence from a time step and potentially less time required for optimisation than the other currently available algorithms. In addition, it demonstrated successful results for the uncertainty analysis.

b. A new workflow for ICV reliability analysis was proposed and tested. The methodology quantifies the potential loss due to device failure and allows comparison of the "Value Added" by multiple completion designs employing equipment completions with different reliabilities. This analysis helps to make a decision about a well completion and a further optimisation strategy.

**2. On/Off ICV Application Area**

The On/Off control strategy has been shown to have a wide application area, where the developed Critical Water Cut (CWC) algorithm and On/Off Direct Search method provide an optimal solution:

a. Theoretical analysis shows that the On/Off valves provide the maximum instantaneous oil rate for the reactive control situations satisfying all the following conditions:
    - Reactive control of vertical or slightly deviated wells constrained by wellhead pressure is planned.
    - The oil field has a pressure greater than the bubble point (free gas is absent from the reservoir).
    - Hydrostatic pressure is the dominant cause of the pressure loss across the well's production well tubing.
    - The flowing fluid's friction and acceleration forces are small compared to the hydrostatic head.
    - Production zones are isolated.
b. Stochastic analysis for a wide range of input parameters including both the natural flow and gas-lifted scenarios has demonstrated that the On/Off valve completion strategy provided the maximum oil rate in about 90% of cases with a further 5% of cases having a difference is less than 1%. The On/Off control is not always optimal only in situations where the difference between zonal fluid properties is significant, i.e. the difference in GOR is higher than 400 Stb/Scf. However, the comingled production from such zones is not a common practice. Moreover, the mismatch with the optimal value can be ignored in the most cases, if the ability to measure the zonal water cut has a resolution of less than 0.5%.

A workflow has been developed to determine if the On/Off strategy is applicable in a particular case.

**3. Uncertainty Study**

The uncertainty study demonstrated that more robust evaluation of the preferred well completion design and field development strategy will be achieved if the static and dynamic uncertainty is considered along with the "most likely" realisation:

a. Optimised well location in the "most likely" scenario increases the value of the conventional completion only for one realisation, but the result can be different in a real situation because these uncertainties are not considered.
b. Uncertainty in the "dynamic" parameters gives a comparable (or even larger) variation in the total oil production than the uncertainty associated with the static

reservoir properties distribution. It cannot be ignored and should be analysed at the same time as when evaluating the impact of geological uncertainty.

The developed Direct Search method demonstrated more stable performance and less optimisation time than Sequential Linear Programming and the Sequential Quadratic Programming algorithms.

The intelligent well can potentially reduce the production uncertainty and the risks associated with the worst scenarios, though more detailed study in this area is required.

**Overall Conclusion**

This study demonstrates that an uncertainty analysis is necessary for the correct decision on the well completion design. The workflows described here can be used for a decision making process to:

- Determine if On/Off ICVs are sufficient for the optimal control of an IW;
- Perform a reliability analysis and choose the completion type capable of delivering the greatest "Added Value";
- Run multiple realisations for both CW and IW cases.

The developed optimisation methods can be used for IWs completed with discrete and On/Off valves optimisation. The CWC criterion provides a fast and robust algorithm for control of On/Off valves during multiple realisations of the reservoir model.

The conclusion that On/Off ICVs are sufficient in the most cases indicates that the research in the area of IW optimisation technologies should focus on the potential offered On/Off valves. This conclusion is confirmed by current industry practice where 95% of ICVs installed have an On/Off functionality.

## 10.2 Future Work

Further work is required to fully explore each of the three areas:

**Optimisation Algorithms**

1. Investigate the impact of cross-flow on the results of optimisation and production stability.
2. Investigate how artificial lift impacts on the optimisation strategy. Develop an artificial lift design for IWs.
3. Investigate the impact of optimisation time step on the result. What is the optimal time step and how the value depend on it?

4. Include reservoir reaction to the ICV control into optimisation method. Current optimisation methods consider only instant reservoir conditions at every time step and do not take into account further changes in the reservoir after control is performed. The information about changes in the near well bore area provides more accurate ICV control, may help to avoid unnecessary action and reduce the production oscillation.
5. Theoretical aspects of the proactive strategy convergence can be analysed. The method can be improved and extended, e.g. by adding injection wells.
6. Investigate production optimisation and potential value of intelligent wells for fields with free gas in a reservoir.

**On/Off Application Area**

1. The theoretical analysis of the On/Off ICVs application area can be extended to:
   - Horizontal wells;
   - Connected layers;
   - Reservoirs with gas cap.

   The results of On/Off strategy in this study showed that the value is similar to the infinitely variable and discrete position ICVs even in the cases when the assumption of the theoretical study were not satisfied.
2. Find what the CWC interval value for different scenarios is and when it may exceed the WC resolution. The difference between optimal and On/Off values can be observed only when WC is close to the critical value. The optimal value cannot be achieved in practice if this interval is less than WC resolution. Therefore, the On/Off value is technically optimal in this case, though theoretically the optimum can be located in intermediate point.

**Uncertainty Study**

1. Quantification and ranking of uncertainties is required to specify the most important dynamic and static parameters for experimental design. Comparison of experimental designs and developing methodology which provides the best design for a particular case. This study can provide full range of scenarios covering most of the uncertainties with a minimum number of realisations.
2. Usage of IW gauges and sensors data for reducing uncertainty and improving real-time optimisation.

# Appendix A - Simplex Method and Gradient Projection

## Numerical Estimation of First Derivatives

### *First order finite difference*

Gradient optimisation methods require calculation of the first order derivatives. The simplest method to estimate the first derivative of function ***f*** at point ***x*** is to use the finite difference approximation:

$$f'(x) \approx \frac{f(x+h) - f(x)}{h} \qquad (a\text{-}1)$$

where h is a small value.

This approximation represents a secant in figure A-1 (a). The slope of this secant line can differ from the slope of the tangent line and this approximation is not always accurate. The two-point central approximation calculated by formula a-2:

$$f'(x) \approx \frac{f(x+h) - f(x-h)}{2h} \qquad (a\text{-}2)$$

often provides sufficiently accurate approximation (Fig. A-1 (b)). However, this approximation requires function value in two points for each variable. Therefore, the total number of the calculations is 2·k, if k is a number of variables.

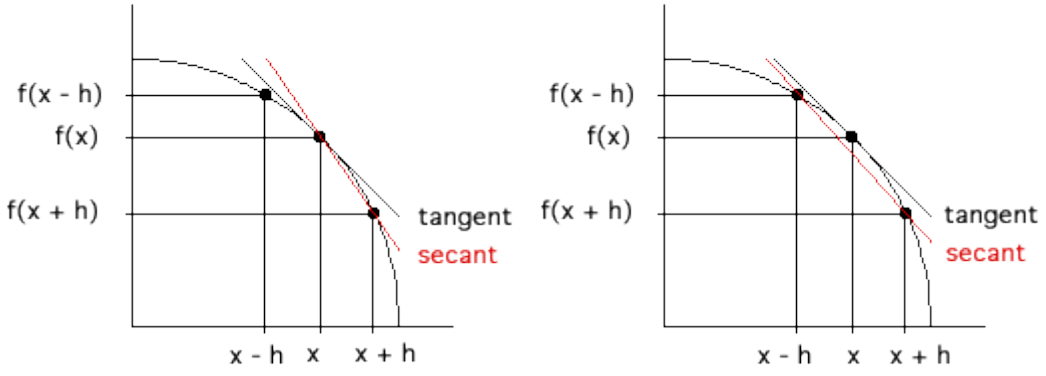


*Figure A-1 Right Side (a) and Central (b) finite difference approximation (after Wattenberg (Wattenberg 1997))*

### *Simplex Method*

Rykov (Rykov 1993) decribed the method which provides the accurate non shifted approximation of the first derivatives in k+1 calculations for k-dimensional optimisation problem. The method uses simplex $S_0$ with a centre in point ***x*** and radius $R_0$ of a circumscribed hypersphere. Figure A-2 shows an example of the simplex for 3 variables.

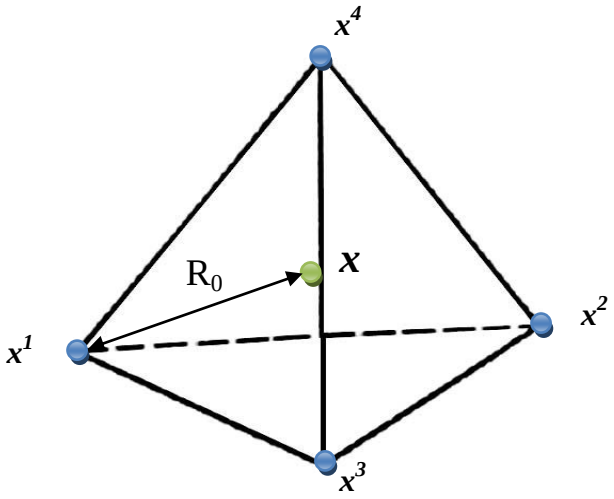


*Figure A-2 Simplex for 3 variables*

The simplex nodes $\boldsymbol{x}^j$ are calculated from the equation a-3:

$$x^j = x + \frac{R_0}{R_k^A} \cdot a^j, \quad \mathrm{j} = \overline{1, \mathrm{k}+1} \tag{a-3}$$

where $a_j$ is a string of the matrix A

$$A = \frac{1}{R_k^A} \left\| \begin{matrix} a^1 \\ a^2 \\ \vdots \\ a^{k+1} \end{matrix} \right\| = \frac{1}{R_k^A} \left\| \begin{matrix} r_1 & r_2 & \cdots & r_{k-1} & r_k \\ -R_1^A & r_2 & \cdots & r_{k-1} & r_k \\ 0 & -R_2^A & \cdots & r_{k-1} & r_k \\ 0 & 0 & \cdots & -R_{k-1}^A & r_k \\ 0 & 0 & \cdots & 0 & -R_k^A \end{matrix} \right\| \tag{a-4}$$

$$R_i^A = \sqrt{\frac{i}{2 \cdot (i+1)}}, \quad r_i = \sqrt{\frac{1}{2i \cdot (i+1)}}, \quad \mathrm{i} = \overline{1, \mathrm{k}}$$

The gradient of the function $\boldsymbol{f}$ in point $\boldsymbol{x}$ is calculated by formula a-5:

$$\nabla f(x) \approx \frac{k}{(k+1) \cdot R_0} \sum_{j=1}^{k+1} \left( f(x^j) - \frac{\sum_{i=1}^{k+1} f(x^i)}{k+1} \right) \cdot e_j \tag{a-5}$$

where

$$e_j = \frac{(x^j - x)}{\left\| x^j - x \right\|} = \frac{1}{R_0} (x^j - x); \tag{a-6}$$

$$\sum_{i=1}^{k+1} e_j = 0; \qquad (e_j, e_i) = -\frac{1}{k} \quad \text{for } i \neq j.$$

More details about the method and the accuracy of the gradient estimation can be found in (Rykov 1993).

**Gradient Projection**

The constraint c2 of equation 5-11 of Chapter 5 is a hyper plane described by the equation a-7:

$$\sum_{i=1}^{n} x_i - Q^0 = 0 \qquad (a\text{-}7)$$

Figure A-3 shows the projection of the gradient $\nabla f$ to this hyper plane which is defined by point:

$$P = X + k \cdot N \qquad (a\text{-}8)$$

where $N = \left( \frac{1}{\sqrt{n}}, ..., \frac{1}{\sqrt{n}} \right)^T$ – is a normal to the hyper plane a-7, while equation a-7 can be replaced with equation a-9:

$$\frac{1}{\sqrt{n}} \sum_{i=1}^{N} x_i - \frac{Q^0}{\sqrt{n}} = 0 \qquad (a\text{-}9)$$

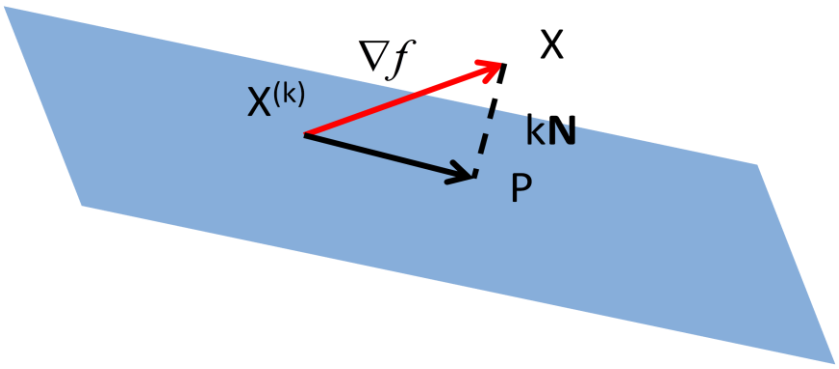


*Figure A-3 Projection of the gradient vector to the hyper plane*

Point **P** lays in the hyper plane and therefore satisfies equation a-9:

$$\frac{1}{\sqrt{n}} \sum_{i=1}^{N} p_i - \frac{Q^0}{\sqrt{n}} = \frac{1}{\sqrt{n}} \sum_{i=1}^{N} (x_i + k \cdot n_i) - \frac{Q^0}{\sqrt{n}} = dot(N, X) + k \cdot dot(N, N) - \frac{Q^0}{\sqrt{n}} = 0 \qquad (a\text{-}10)$$

where ***dot*** – is a scalar multiplication of two vectors.

$dot(N, N)$ =1 because ***N*** is normalised. From equation a-10

$$k = -dot(N, X) + \frac{Q^0}{\sqrt{n}} \qquad (a\text{-}11)$$

Finally, projection ***P*** can be found from equations a-8 and a-11.

# Appendix B – Results of Central Composite Design for Reliability Analysis

*Table b-1 Parameters and results of Central composite Design for a "Box-Shaped" model*

| Variants | CH1 | CH2 | CH3 | CH4 | CH1 | CH2 | CH3 | CH4 | Cum Oil | Cum Water | NPV |
|---|---|---|---|---|---|---|---|---|---|---|---|
| | Failure Date | Failure Date | Failure Date | Failure Date | Failure Parameter | Failure Parameter | Failure Parameter | Failure Parameter | Million $m^3$ | Million $m^3$ | Million$ |
| CCD1 | 01/01/2030 | 01/01/2020 | 01/01/2020 | 01/01/2020 | 1.00 | 0.50 | 0.50 | 0.50 | 6.17 | 9.26 | 1347 |
| CCD2 | 01/01/2010 | 01/01/2020 | 01/01/2020 | 01/01/2020 | 0.00 | 0.50 | 0.50 | 0.50 | 6.16 | 9.13 | 1346 |
| CCD3 | 01/01/2020 | 01/01/2030 | 01/01/2020 | 01/01/2020 | 0.50 | 1.00 | 0.50 | 0.50 | 6.19 | 9.55 | 1349 |
| CCD4 | 01/01/2020 | 01/01/2010 | 01/01/2020 | 01/01/2020 | 0.50 | 0.00 | 0.50 | 0.50 | 6.17 | 9.16 | 1348 |
| CCD5 | 01/01/2020 | 01/01/2020 | 01/01/2030 | 01/01/2010 | 0.50 | 0.50 | 1.00 | 0.00 | 6.45 | 7.59 | 1384 |
| CCD6 | 01/01/2020 | 01/01/2020 | 01/01/2010 | 01/01/2010 | 0.50 | 0.50 | 0.00 | 0.00 | 5.82 | 11.30 | 1192 |
| CCD7 | 01/01/2020 | 01/01/2020 | 01/01/2020 | 01/01/2030 | 0.50 | 0.50 | 0.50 | 1.00 | 6.17 | 9.26 | 1347 |
| CCD8 | 01/01/2020 | 01/01/2020 | 01/01/2020 | 01/01/2010 | 0.50 | 0.50 | 0.50 | 0.00 | 6.16 | 9.30 | 1346 |
| CCD9 | 01/01/2030 | 01/01/2010 | 01/01/2010 | 01/01/2010 | 1.00 | 0.00 | 0.00 | 0.00 | 5.81 | 11.30 | 1192 |
| CCD10 | 01/01/2010 | 01/01/2030 | 01/01/2010 | 01/01/2010 | 0.00 | 1.00 | 0.00 | 0.00 | 5.82 | 11.31 | 1195 |
| CCD11 | 01/01/2010 | 01/01/2010 | 01/01/2030 | 01/01/2010 | 0.00 | 0.00 | 1.00 | 0.00 | 6.45 | 7.59 | 1385 |
| CCD12 | 01/01/2010 | 01/01/2010 | 01/01/2010 | 01/01/2030 | 0.00 | 0.00 | 0.00 | 1.00 | 5.82 | 11.31 | 1195 |
| CCD13 | 01/01/2030 | 01/01/2030 | 01/01/2010 | 01/01/2010 | 1.00 | 1.00 | 0.00 | 0.00 | 5.82 | 11.30 | 1192 |
| CCD14 | 01/01/2030 | 01/01/2010 | 01/01/2030 | 01/01/2010 | 1.00 | 0.00 | 1.00 | 0.00 | 6.45 | 7.57 | 1385 |
| CCD15 | 01/01/2030 | 01/01/2010 | 01/01/2010 | 01/01/2030 | 1.00 | 0.00 | 0.00 | 1.00 | 5.81 | 11.30 | 1192 |
| CCD16 | 01/01/2030 | 01/01/2030 | 01/01/2030 | 01/01/2010 | 1.00 | 1.00 | 1.00 | 0.00 | 6.45 | 7.60 | 1384 |
| CCD17 | 01/01/2030 | 01/01/2010 | 01/01/2030 | 01/01/2030 | 1.00 | 0.00 | 1.00 | 1.00 | 6.48 | 7.44 | 1388 |
| CCD18 | 01/01/2010 | 01/01/2030 | 01/01/2030 | 01/01/2010 | 0.00 | 1.00 | 1.00 | 0.00 | 6.45 | 7.60 | 1385 |
| CCD19 | 01/01/2010 | 01/01/2030 | 01/01/2010 | 01/01/2030 | 0.00 | 1.00 | 0.00 | 1.00 | 5.82 | 11.31 | 1195 |
| CCD20 | 01/01/2010 | 01/01/2030 | 01/01/2030 | 01/01/2030 | 0.00 | 1.00 | 1.00 | 1.00 | 6.47 | 7.42 | 1385 |
| CCD21 | 01/01/2010 | 01/01/2010 | 01/01/2030 | 01/01/2030 | 0.00 | 0.00 | 1.00 | 1.00 | 6.47 | 7.47 | 1385 |
| CCD22 | 01/01/2010 | 01/01/2010 | 01/01/2010 | 01/01/2030 | 0.00 | 0.00 | 0.00 | 1.00 | 5.82 | 11.31 | 1195 |
| CCD23 | 01/01/2020 | 01/01/2020 | 01/01/2020 | 01/01/2020 | 0.50 | 0.50 | 0.50 | 0.50 | 6.17 | 9.26 | 1347 |
| CCD24 | 01/01/2010 | 01/01/2010 | 01/01/2010 | 01/01/2010 | 0.00 | 0.00 | 0.00 | 0.00 | 5.82 | 11.31 | 1195 |
| CCD25 | 01/01/2030 | 01/01/2030 | 01/01/2030 | 01/01/2030 | 1.00 | 1.00 | 1.00 | 1.00 | 6.48 | 7.55 | 1387 |

*Table b-2 NPVs and mismatch of the CCD, Shifted CCD, Shifted CCD + 2 points of ICV3, Shifted CCD + 10 points of ICV3 and ICV 3 designs for CCD scenarios*

| Variants | Cum Oil | Cum Water | NPV | NPV Estim1 | NPV Estim2 | NPV Estim3 | NPV Estim4 | NPV Estim5 | Error1 | Error2 | Error3 | Error4 | Error5 |
|---|---|---|---|---|---|---|---|---|---|---|---|---|---|
| | Million $m^3$ | Million $m^3$ | Million$ | Million$ | Million$ | Million$ | Million$ | Million$ | % | % | % | % | % |
| CCD1 | 6.17 | 9.26 | 1347 | 1346 | 1338 | 1338 | 1338 | 1343 | -0.08% | -0.72% | -0.67% | -0.68% | -0.34% |
| CCD2 | 6.16 | 9.13 | 1346 | 1347 | 1339 | 1338 | 1338 | 1343 | 0.09% | -0.52% | -0.56% | -0.55% | -0.21% |
| CCD3 | 6.19 | 9.55 | 1349 | 1349 | 1339 | 1339 | 1339 | 1343 | -0.01% | -0.75% | -0.70% | -0.70% | -0.44% |
| CCD4 | 6.17 | 9.16 | 1348 | 1349 | 1339 | 1339 | 1339 | 1343 | 0.02% | -0.67% | -0.71% | -0.70% | -0.41% |
| CCD5 | 6.45 | 7.59 | 1384 | 1384 | 1383 | 1383 | 1384 | 1377 | -0.02% | -0.06% | -0.07% | -0.04% | -0.55% |
| CCD6 | 5.82 | 11.30 | 1192 | 1193 | 1192 | 1190 | 1191 | 1202 | 0.03% | -0.06% | -0.16% | -0.13% | 0.78% |
| CCD7 | 6.17 | 9.26 | 1347 | 1347 | 1337 | 1339 | 1338 | 1343 | 0.00% | -0.76% | -0.65% | -0.69% | -0.34% |
| CCD8 | 6.16 | 9.30 | 1346 | 1346 | 1337 | 1337 | 1337 | 1343 | 0.00% | -0.71% | -0.68% | -0.71% | -0.26% |
| CCD9 | 5.81 | 11.30 | 1192 | 1192 | 1192 | 1192 | 1192 | 1202 | -0.04% | -0.01% | -0.05% | -0.03% | 0.78% |
| CCD10 | 5.82 | 11.31 | 1195 | 1195 | 1192 | 1192 | 1192 | 1202 | 0.01% | -0.21% | -0.26% | -0.24% | 0.56% |
| CCD11 | 6.45 | 7.59 | 1385 | 1385 | 1385 | 1389 | 1389 | 1377 | -0.03% | -0.05% | 0.23% | 0.23% | -0.64% |
| CCD12 | 5.82 | 11.31 | 1195 | 1195 | 1192 | 1191 | 1192 | 1202 | -0.04% | -0.27% | -0.30% | -0.29% | 0.56% |
| CCD13 | 5.82 | 11.30 | 1192 | 1192 | 1191 | 1194 | 1195 | 1202 | -0.01% | -0.13% | 0.18% | 0.19% | 0.78% |
| CCD14 | 6.45 | 7.57 | 1385 | 1385 | 1384 | 1383 | 1384 | 1377 | 0.04% | -0.04% | -0.08% | -0.06% | -0.58% |
| CCD15 | 5.81 | 11.30 | 1192 | 1193 | 1191 | 1194 | 1194 | 1202 | 0.08% | -0.12% | 0.17% | 0.19% | 0.80% |
| CCD16 | 6.45 | 7.60 | 1384 | 1385 | 1384 | 1381 | 1381 | 1377 | 0.04% | -0.04% | -0.20% | -0.26% | -0.55% |
| CCD17 | 6.48 | 7.44 | 1388 | 1387 | 1387 | 1384 | 1384 | 1377 | -0.05% | -0.07% | -0.25% | -0.29% | -0.80% |
| CCD18 | 6.45 | 7.60 | 1385 | 1384 | 1384 | 1384 | 1384 | 1377 | -0.04% | -0.05% | -0.08% | -0.07% | -0.61% |
| CCD19 | 5.82 | 11.31 | 1195 | 1195 | 1191 | 1195 | 1195 | 1202 | 0.00% | -0.31% | -0.01% | 0.00% | 0.56% |
| CCD20 | 6.47 | 7.42 | 1385 | 1385 | 1388 | 1385 | 1384 | 1377 | 0.00% | 0.19% | 0.00% | -0.04% | -0.61% |
| CCD21 | 6.47 | 7.47 | 1385 | 1385 | 1387 | 1386 | 1387 | 1377 | 0.03% | 0.16% | 0.12% | 0.14% | -0.60% |
| CCD22 | 5.82 | 11.31 | 1195 | 1195 | 1192 | 1191 | 1192 | 1202 | -0.04% | -0.27% | -0.30% | -0.29% | 0.56% |
| CCD23 | 6.17 | 9.26 | 1347 | 1347 | 1338 | 1338 | 1338 | 1343 | -0.02% | -0.68% | -0.72% | -0.69% | -0.34% |
| CCD24 | 5.82 | 11.31 | 1195 | 1195 | 1194 | 1192 | 1191 | 1202 | 0.01% | -0.08% | -0.25% | -0.32% | 0.56% |
| CCD25 | 6.48 | 7.55 | 1387 | 1387 | 1387 | 1386 | 1383 | 1377 | 0.01% | 0.04% | -0.09% | -0.28% | -0.74% |

*Table b-3 Parameters and results of Random failed cases for a "Box-Shaped" model*

| Variants | CH1 | CH2 | CH3 | CH4 | CH1 | CH2 | CH3 | CH4 | Cum Oil | Cum Water | NPV |
|---|---|---|---|---|---|---|---|---|---|---|---|
| | Failure Date | Failure Date | Failure Date | Failure Date | Failure Parameter | Failure Parameter | Failure Parameter | Failure Parameter | Million $m^3$ | Million $m^3$ | Million$ |
| Random01 | 14/05/2013 | 31/08/2019 | 27/01/2011 | 21/11/2016 | 0.17 | 0.48 | 0.05 | 0.34 | 5.82 | 11.28 | 1192 |
| Random02 | 20/06/2023 | 12/04/2021 | 05/04/2019 | 04/06/2010 | 0.67 | 0.56 | 0.46 | 0.02 | 6.13 | 9.44 | 1340 |
| Random03 | 22/08/2025 | 18/01/2017 | 07/12/2028 | 16/03/2029 | 0.78 | 0.35 | 0.95 | 0.96 | 6.45 | 7.57 | 1385 |
| Random04 | 02/06/2013 | 02/09/2018 | 26/12/2019 | 28/06/2021 | 0.17 | 0.43 | 0.50 | 0.57 | 6.15 | 9.21 | 1345 |
| Random05 | 07/07/2023 | 31/08/2015 | 02/01/2020 | 06/01/2011 | 0.68 | 0.28 | 0.50 | 0.05 | 6.16 | 9.31 | 1347 |
| Random06 | 24/12/2022 | 31/03/2021 | 24/05/2024 | 16/05/2014 | 0.65 | 0.56 | 0.72 | 0.22 | 6.31 | 8.54 | 1370 |
| Random07 | 28/07/2010 | 21/03/2011 | 12/07/2016 | 11/12/2017 | 0.03 | 0.06 | 0.33 | 0.40 | 6.00 | 10.31 | 1293 |
| Random08 | 16/04/2012 | 17/11/2022 | 12/12/2013 | 05/05/2024 | 0.11 | 0.64 | 0.20 | 0.72 | 5.86 | 11.08 | 1220 |
| Random09 | 06/05/2012 | 07/04/2018 | 01/11/2011 | 27/10/2026 | 0.12 | 0.41 | 0.09 | 0.84 | 5.82 | 11.29 | 1192 |
| Random10 | 22/05/2027 | 10/07/2016 | 03/11/2023 | 27/02/2020 | 0.87 | 0.33 | 0.69 | 0.51 | 6.31 | 8.50 | 1371 |
| Random11 | 21/08/2014 | 15/12/2017 | 05/12/2028 | 05/06/2025 | 0.23 | 0.40 | 0.95 | 0.77 | 6.45 | 7.60 | 1383 |
| Random12 | 10/10/2014 | 11/05/2010 | 29/08/2010 | 19/10/2021 | 0.24 | 0.02 | 0.03 | 0.59 | 5.82 | 11.28 | 1192 |
| Random13 | 01/08/2020 | 03/03/2019 | 23/11/2029 | 18/07/2012 | 0.53 | 0.46 | 0.99 | 0.13 | 6.45 | 7.59 | 1384 |
| Random14 | 03/03/2025 | 15/03/2014 | 07/08/2020 | 05/04/2019 | 0.76 | 0.21 | 0.53 | 0.46 | 6.18 | 8.98 | 1352 |
| Random15 | 14/12/2029 | 19/02/2014 | 22/01/2020 | 11/12/2019 | 1.00 | 0.21 | 0.50 | 0.50 | 6.16 | 9.15 | 1346 |
| Random16 | 02/04/2023 | 27/03/2021 | 01/03/2027 | 16/01/2011 | 0.66 | 0.56 | 0.86 | 0.05 | 6.39 | 8.07 | 1379 |
| Random17 | 16/09/2013 | 03/06/2016 | 25/01/2029 | 02/09/2020 | 0.19 | 0.32 | 0.95 | 0.53 | 6.45 | 7.56 | 1386 |
| Random18 | 22/06/2027 | 03/07/2024 | 03/02/2018 | 30/01/2017 | 0.87 | 0.73 | 0.40 | 0.35 | 6.08 | 9.69 | 1327 |
| Random19 | 01/11/2026 | 22/07/2010 | 19/11/2017 | 07/04/2029 | 0.84 | 0.03 | 0.39 | 0.96 | 6.07 | 9.74 | 1322 |
| Random20 | 22/04/2026 | 03/07/2028 | 02/02/2011 | 29/12/2019 | 0.82 | 0.93 | 0.05 | 0.50 | 5.82 | 11.28 | 1192 |

*Table b-4 NPVs and mismatch of the CCD, Corrected CCD, Corrected CCD + 2 points of ICV3, Corrected CCD + 7 points of ICV3 and ICV 3 designs for Random scenarios*

| Variants | Cum Oil | Cum Water | NPV | NPV Estim1 | NPV Estim2 | NPV Estim3 | NPV Estim4 | NPV Estim5 | Error1 | Error2 | Error3 | Error4 | Error5 |
|---|---|---|---|---|---|---|---|---|---|---|---|---|---|
| | Million $m^3$ | Million $m^3$ | Million$ | Million$ | Million$ | Million$ | Million$ | Million$ | % | % | % | % | % |
| Random01 | 5.82 | 11.28 | 1192 | 1216 | 1193 | 1191 | 1191 | 1202 | 2.01% | -0.08% | -0.03% | 0.84% | 0.10% |
| Random02 | 6.13 | 9.44 | 1340 | 1339 | 1326 | 1326 | 1326 | 1332 | -0.12% | -1.07% | -1.09% | -0.58% | -1.10% |
| Random03 | 6.45 | 7.57 | 1385 | 1387 | 1390 | 1388 | 1388 | 1382 | 0.19% | 0.24% | 0.22% | -0.16% | 0.40% |
| Random04 | 6.15 | 9.21 | 1345 | 1347 | 1339 | 1338 | 1338 | 1343 | 0.15% | -0.52% | -0.50% | -0.18% | -0.48% |
| Random05 | 6.16 | 9.31 | 1347 | 1347 | 1337 | 1338 | 1337 | 1343 | -0.02% | -0.68% | -0.71% | -0.29% | -0.71% |
| Random06 | 6.31 | 8.54 | 1370 | 1378 | 1381 | 1381 | 1381 | 1382 | 0.57% | 0.79% | 0.79% | 0.89% | 0.81% |
| Random07 | 6.00 | 10.31 | 1293 | 1308 | 1279 | 1278 | 1278 | 1285 | 1.17% | -1.14% | -1.17% | -0.63% | -1.07% |
| Random08 | 5.86 | 11.08 | 1220 | 1268 | 1217 | 1217 | 1218 | 1226 | 3.94% | -0.27% | -0.20% | 0.51% | -0.23% |
| Random09 | 5.82 | 11.29 | 1192 | 1230 | 1192 | 1191 | 1192 | 1202 | 3.25% | -0.04% | 0.02% | 0.84% | 0.02% |
| Random10 | 6.31 | 8.50 | 1371 | 1375 | 1379 | 1378 | 1378 | 1379 | 0.33% | 0.54% | 0.54% | 0.61% | 0.59% |
| Random11 | 6.45 | 7.60 | 1383 | 1386 | 1391 | 1389 | 1390 | 1382 | 0.24% | 0.45% | 0.50% | -0.03% | 0.56% |
| Random12 | 5.82 | 11.28 | 1192 | 1208 | 1194 | 1192 | 1192 | 1202 | 1.42% | -0.01% | 0.04% | 0.84% | 0.19% |
| Random13 | 6.45 | 7.59 | 1384 | 1384 | 1384 | 1384 | 1384 | 1377 | 0.02% | -0.03% | 0.00% | -0.50% | -0.03% |
| Random14 | 6.18 | 8.98 | 1352 | 1353 | 1347 | 1346 | 1347 | 1350 | 0.10% | -0.38% | -0.36% | -0.08% | -0.35% |
| Random15 | 6.16 | 9.15 | 1346 | 1347 | 1339 | 1339 | 1339 | 1344 | 0.07% | -0.52% | -0.52% | -0.20% | -0.52% |
| Random16 | 6.39 | 8.07 | 1379 | 1385 | 1389 | 1389 | 1389 | 1387 | 0.48% | 0.75% | 0.75% | 0.62% | 0.77% |
| Random17 | 6.45 | 7.56 | 1386 | 1386 | 1390 | 1390 | 1390 | 1382 | 0.03% | 0.29% | 0.35% | -0.28% | 0.31% |
| Random18 | 6.08 | 9.69 | 1327 | 1326 | 1307 | 1308 | 1308 | 1314 | -0.08% | -1.47% | -1.47% | -1.01% | -1.55% |
| Random19 | 6.07 | 9.74 | 1322 | 1325 | 1303 | 1305 | 1305 | 1310 | 0.22% | -1.31% | -1.34% | -0.91% | -1.44% |
| Random20 | 5.82 | 11.28 | 1192 | 1216 | 1192 | 1195 | 1196 | 1202 | 2.04% | 0.27% | 0.34% | 0.84% | 0.01% |

**Estim 1 = CCD**
**Estim 2 = CCD_Corrected**
**Estim 3 = CCD_Corrected +2 points intermediate FT points of ICV3: 01/03/2017 and 01/09/2025**
**Estim 4 = CCD_Corrected +7 points intermediate FT points of ICV3: 15/09/2014, 01/06/2016, 01/02/2018, 15/03/2023/, 01/12/2024, 01/08/2026 and 15/04/2028**
**Estim 5 = 10 FT points of ICV3**

$$\boldsymbol{Error = (NPV_{Estim} - NPV)/NPV}$$

## Appendix C – Theoretical Aspects of a Downhole Production Control

**Statement 7.1**

*In a vertical well with 2 zones if assumptions 1-6 are satisfied zone with the highest water cut should be closed first.*

***Proof***

Assume zone 2 is choked for optimising oil production, while zone 1 should remain fully open:

$$Q_{Added}^{Liquid} = J_1 \cdot \Delta P_{BHP} = Q_{Added}^{Oil} + Q_{Added}^{Water} = J_1 \cdot \Delta P_{BHP} \cdot (1 - WC_1) + J_1 \cdot \Delta P_{BHP} \cdot WC_1 \qquad (c\text{-}1)$$

$$Q_{Choked}^{Liquid} = Q_{Choked}^{Oil} + Q_{Choked}^{Water} = Q_{Choked}^{Liquid} \cdot (1 - WC_2) + Q_{Choked}^{Liquid} \cdot WC_2 \qquad (c\text{-}2)$$

$Q_{Added}^{Oil} \geq Q_{Choked}^{Oil}$ since the valve position is optimal and well produces more oil than initially with both zones fully open

$$Q_{Added}^{Liquid} = J_1 \cdot \Delta P_{BHP} \leq Q_{Choked}^{Liquid} \qquad \text{(from assumption 5)} \qquad (c\text{-}3)$$

Therefore

$$Q_{Add}^{Oil} = J_1 \cdot \Delta P_{BHP} \cdot (1 - WC_1) \geq Q_{Choked}^{Oil} = Q_{Choked}^{Liquid} \cdot (1 - WC_2) \qquad (c\text{-}4)$$

only if $(1 - WC_1) \geq (1 - WC_2)$

*or* $WC_1 \leq WC_2$

■

**Statement 7.2**

*If liquid properties such as water and oil density and GOR in different layers are the same and assumptions 1-6 are satisfied then zone with the highest water cut should be closed first.*

***Proof***

In this case liquid density increases with WC:

$$\rho^{liquid} = \rho^{oil} \cdot (1 - WC) + \rho^{water} \cdot WC \qquad (c\text{-}5)$$

All zones can be reordered to make zone 1 choked for optimisation purposes giving the highest oil production and zone 2 with the highest WC. After zone 1 and zone 2 choking the new liquid rates can be expressed by the following equations:

$$Q_{new,1}^{Liquid} = a \cdot Q_1^{Liquid} + Q_2^{Liquid} + \sum_{i=3}^{N} Q_i^{Liquid} + J_2 \cdot \Delta P_{BHP}^1 + \sum_{i=3}^{N} J_i \cdot \Delta P_{BHP,i}^{ex,1} \qquad (c\text{-}6)$$

$$Q_{new,2}^{Liquid} = Q_1^{Liquid} + b \cdot Q_2^{Liquid} + \sum_{i=3}^{N} Q_i^{Liquid} + J_1 \cdot \Delta P_{BHP}^2 + \sum_{i=3}^{N} J_i \cdot \Delta P_{BHP,i}^{ex,2} \qquad (c\text{-}7)$$

$\Delta P^{ex,1}_{BHP,i}$ is an extra pressure drop in zone ***i*** after choking zone 1. This value is equal to $\Delta P^{1}_{BHP}$ if zone ***i*** is fully open. When zone ***i*** is choked, the extra pressure drop is a function of $\Delta P^{1}_{BHP}$ and choke diameter of ICV ***i***. The situation with partially choked ICVs is described in more details at the end of the chapter 7. At this moment we need to know that if $\Delta P^{1}_{BHP} > \Delta P^{2}_{BHP}$ then $\Delta P^{1,ex}_{BHP,i} > \Delta P^{2,ex}_{BHP,i}$

Let us set

$$\vartheta_1 = a \cdot Q_1^{Liquid} + Q_2^{Liquid} + \sum_{i=3}^{N} Q_i^{Liquid} + J_2 \cdot \Delta P^{1}_{BHP} \qquad (c\text{-}8)$$

$$\vartheta_2 = Q_1^{Liquid} + b \cdot Q_2^{Liquid} + \sum_{i=3}^{N} Q_i^{Liquid} + J_1 \cdot \Delta P^{2}_{BHP} \qquad (c\text{-}9)$$

Therefore, equations c-6 and c-7 can be rewritten as:

$$Q^{Liquid}_{new,1} = \vartheta_1 + \sum_{i=3}^{N} J_i \cdot \Delta P^{ex,1}_{BHP,i} \qquad (c\text{-}10)$$

$$Q^{Liquid}_{new,2} = \vartheta_2 + \sum_{i=3}^{N} J_i \cdot \Delta P^{ex,2}_{BHP,i} \qquad (c\text{-}11)$$

Two situations are possible:

1) There is a $0 \le b \le 1$ that $\vartheta_2 = \vartheta_1$.

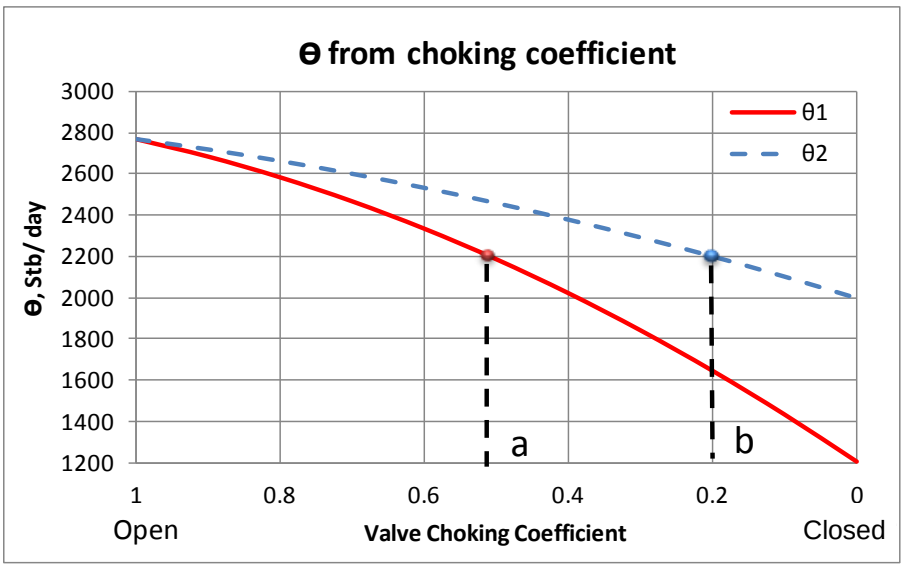


*Figure C-1 θ as a function of coefficients a and b.* $\vartheta_2 = \vartheta_1$

Choking zone 2 with this coefficient ***b*** provides $\Delta P^{2}_{BHP} > \Delta P^{1}_{BHP}$.

Assume that this statement is not correct and $\Delta P^{1}_{BHP} > \Delta P^{2}_{BHP}$.

Then from c-10 and c-11: $Q^{Liquid}_{new,1} > Q^{Liquid}_{new,2}$.

The liquid rate and density increase with a choke opening from *Assumption 5*. Therefore the tubing pressure increases (from A6) and the pressure difference

$$\Delta P_{BHP}(a) = P_{tubing}^{Open} - P_{tubing}^{current}(a) \qquad (c\text{-}12)$$

is a monotonically decreasing function .

Then there is a coefficient $\boldsymbol{a^*} > \boldsymbol{a}$ (Fig. C-2 ) that

$$(Q_{new,1}^{Liquid})^* = a^* \cdot Q_1^{Liquid} + Q_2^{Liquid} + \sum_{i=3}^{N} Q_i^{Liquid} + J_2 \cdot \Delta P_{BHP}^2 + \sum_{i=3}^{N} J_i \cdot \Delta P_{BHP,i}^{ex,2} \qquad (c\text{-}13)$$

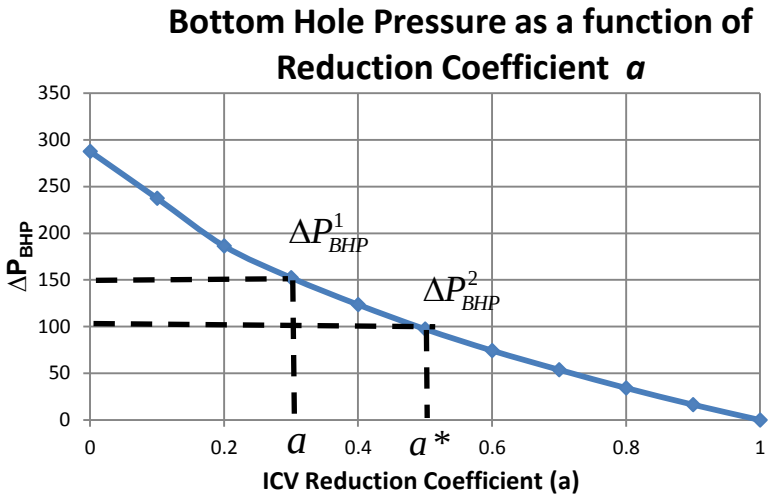


*Figure C-2 The change of the bottom hole pressure as a function of the ICV (or choke) position*

$Q_{new,1}^{Liquid}$(a) is increasing function and $(Q_{new,1}^{Liquid})^* > Q_{new,1}^{Liquid} > Q_{new,2}^{Liquid}$

The liquid density in both situations can also be compared. The relation between these densities does not change if we subtract the same amount of liquid with the same density from both parts:

$$Q_{new,1}^{Liquid}{}_S^* = Q_2^{Liquid} + J_2 \cdot \Delta P_{BHP}^2 - b \cdot Q_2^{Liquid} \qquad (c\text{-}14)$$

$$Q_{new,2}^{Liquid}{}_S = Q_1^{Liquid} + J_1 \cdot \Delta P_{BHP}^2 - a^* \cdot Q_1^{Liquid} \qquad (c\text{-}15)$$

In the first case the liquid is from zone 2 only and in the second case from zone 1.

Therefore, density in the first case is higher and $\rho(Q_{new,1}^{Liquid}{}^*) > \rho(Q_{new,2}^{Liquid})$ which implies $\Delta P_{BHP}^2 > \Delta P_{BHP}^1$ (from A6).

Zone 1 and 2 water cuts are higher than the total water cut of the extra liquid from other zones due to choking. For zone 2 this is because it has the highest water cut. For zone 1, because it provides the optimum solution. Choking zone 1 reduces the wells water production and increases the oil production.

Oil production for both cases can be expressed as:

$$Q_{new,1}^{Oil} = a \cdot Q_1^{Liquid}(1-WC_1) + Q_2^{Liquid}(1-WC_2) + \sum_{i=3}^{N} Q_i^{Liquid}(1-WC_i) + \\ + J_2 \cdot \Delta P_{BHP}^1 (1-WC_2) + \sum_{i=3}^{N} J_i \cdot \Delta P_{BHP,i}^{ex,1}(1-WC_i) \qquad (c\text{-}16)$$

$$Q_{new,2}^{Oil} = Q_1^{Liquid}(1-WC_1) + b \cdot Q_2^{Liquid}(1-WC_2) + \sum_{i=3}^{N} Q_i^{Liquid}(1-WC_i) + \\ + J_1 \cdot \Delta P_{BHP}^2 (1-WC_1) + \sum_{i=3}^{N} J_i \cdot \Delta P_{BHP,i}^{ex,2}(1-WC_i) \qquad (c\text{-}17)$$

We are going to show that choking zone 2 gives more oil: $Q_{new,2}^{oil} > Q_{new,1}^{oil}$

$$Q_{new,2}^{Oil} - Q_{new,1}^{Oil} = (1-a) \cdot Q_1^{Liquid}(1-WC_1) - (1-b) \cdot Q_2^{Liquid}(1-WC_2) + \\ + J_1 \cdot \Delta P_{BHP}^2 (1-WC_1) - J_2 \cdot \Delta P_{BHP}^1 (1-WC_2) + \sum_{i=3}^{N} J_i \cdot (\Delta P_{BHP,i}^{ex,2} - \Delta P_{BHP,i}^{ex,1})(1-WC_i) = \\ = (1-WC_2) \cdot [(1-a) \cdot Q_1^{Liquid} \cdot \frac{1-WC_1}{1-WC_2} - (1-b) \cdot Q_2^{Liquid} + \\ + J_1 \cdot \Delta P_{BHP}^2 \frac{1-WC_1}{1-WC_2} - J_2 \cdot \Delta P_{BHP}^1 (1-WC_2)] + \sum_{i=3}^{N} J_i \cdot (\Delta P_{BHP,i}^{ex,2} - \Delta P_{BHP,i}^{ex,1})(1-WC_i) > \\ > (1-WC_2) \cdot [(1-a) \cdot Q_1^{Liquid} - (1-b) \cdot Q_2^{Liquid} + \\ + J_1 \cdot \Delta P_{BHP}^2 - J_2 \cdot \Delta P_{BHP}^1 (1-WC_2)] + \sum_{i=3}^{N} J_i \cdot (\Delta P_{BHP,i}^{ex,2} - \Delta P_{BHP,i}^{ex,1})(1-WC_i) \qquad (c\text{-}18)$$

The coefficient ***b*** was chosen that

$$(1-a) \cdot Q_1^{Liquid} - (1-b) \cdot Q_2^{Liquid} + J_1 \cdot \Delta P_{BHP}^2 - J_2 \cdot \Delta P_{BHP}^1 (1-WC_2) = 0 \qquad (c\text{-}19)$$

Therefore $Q_{new,2}^{Oil} - Q_{new,1}^{Oil} > \sum_{i=3}^{N} J_i \cdot (\Delta P_{BHP,i}^{ex,2} - \Delta P_{BHP,i}^{ex,1})(1-WC_i) > 0$ and choking zone 2 provides greater oil production.

2) At any $0 \le b \le 1$ $\vartheta_2 \ne \vartheta_1$.

This situation is possible only if $\vartheta_2(0) > \vartheta_1(a)$ (Figure C-3).

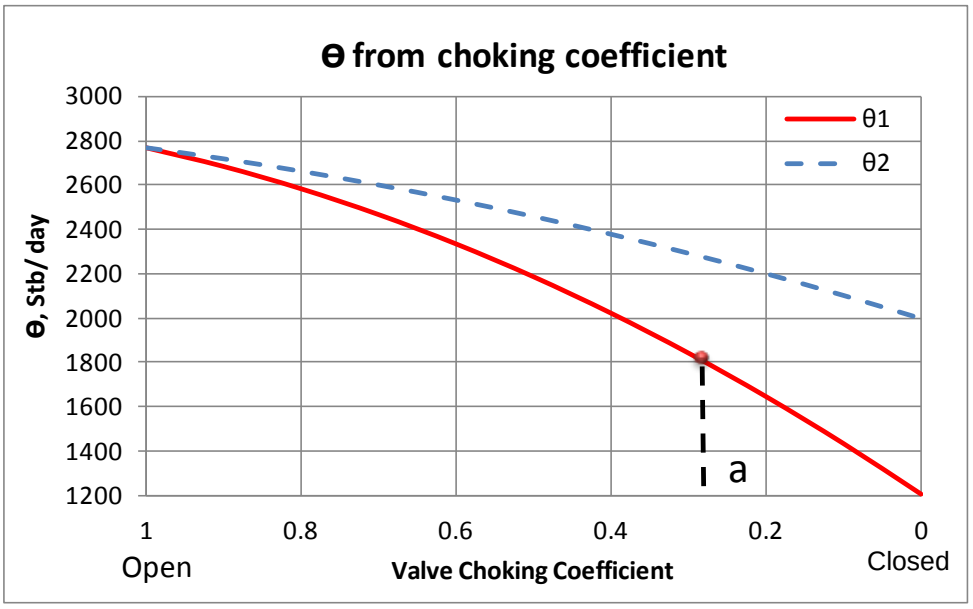


*Figure C-3 θ as a function of coefficients a and b.* At any $0 \le \boldsymbol{b} \le 1$ $\vartheta_2 \neq \vartheta_1$.

Therefore, zone 2 should be fully closed and $\vartheta_2$ can be reduced further by choking zone1 with coefficient $\boldsymbol{c} < \boldsymbol{a}$ until $\vartheta_2 = \vartheta_1$:

$$\vartheta_2 = c \cdot Q_1^{Liquid} + \sum_{i=3}^{N} Q_i^{Liquid} + J_1 \cdot \Delta P_{BHP,1}^{ex,2} \qquad (c\text{-}20)$$

$$Q_{new,2}^{Liquid} = c \cdot Q_1^{Liquid} + \sum_{i=3}^{N} Q_i^{Liquid} + J_1 \cdot \Delta P_{BHP,1}^{ex,2} + \sum_{i=3}^{N} J_i \cdot \Delta P_{BHP,i}^{ex,2} = \vartheta_2 + \sum_{i=3}^{N} J_i \cdot \Delta P_{BHP,i}^{ex,2} \qquad (c\text{-}21)$$

The same technique as previously can be used to prove that $Q_{new,2}^{oil} > Q_{new,1}^{oil}$.

Firstly, it can be proved that $\Delta P_{BHP}^2 > \Delta P_{BHP}^1$.

Assume that that this statement is not correct and $\Delta P_{BHP}^1 > \Delta P_{BHP}^2$.

Then from c-10 and c-21 $Q_{new,1}^{Liquid} > Q_{new,2}^{Liquid}$.

Then there is a coefficient $\boldsymbol{a^*} > \boldsymbol{a}$ that

$$(Q_{new,1}^{Liquid})^* = a^* \cdot Q_1^{Liquid} + Q_2^{Liquid} + \sum_{i=3}^{N} Q_i^{Liquid} + J_2 \cdot \Delta P_{BHP}^2 + \sum_{i=3}^{N} J_i \cdot \Delta P_{BHP,i}^{ex,2} \qquad (c\text{-}22)$$

$Q_{new,1}^{Liquid}(a)$ is increasing function and $(Q_{new,1}^{Liquid})^* > Q_{new,1}^{Liquid} > Q_{new,2}^{Liquid}$

The liquid density in both situations can also be compared. The relation between densities will be unchanged if we subtract the same volume of liquid with the same density from both parts:

$$Q_{new,1}^{Liquid}{}^*{}_S = Q_2^{Liquid} + J_2 \cdot \Delta P_{BHP}^2 \qquad (c\text{-}23)$$

$$Q_{new,2}^{Liquid}{}_S = c \cdot Q_1^{Liquid} + J_1 \cdot \Delta P_{BHP}^2 - a^* \cdot Q_1^{Liquid} \qquad (c\text{-}24)$$

In the first case the liquid is from zone 2 only and in the second case from zone 1.

Therefore, density in the first case is higher and $\rho(Q_{new,1}^{Liquid}*) > \rho(Q_{new,2}^{Liquid})$ which imply $\Delta P_{BHP}^{2} > \Delta P_{BHP}^{1}$.

Oil production for both cases can be expressed as

$$Q_{new,1}^{Oil} = a \cdot Q_1^{Liquid}(1-WC_1) + Q_2^{Liquid}(1-WC_2) + \sum_{i=3}^{N} Q_i^{Liquid}(1-WC_i) + \\ + J_2 \cdot \Delta P_{BHP}^{1}(1-WC_2) + \sum_{i=3}^{N} J_i \cdot \Delta P_{BHP,i}^{ex,1}(1-WC_i) \qquad (c\text{-}25)$$

$$Q_{new,2}^{Oil} = c \cdot Q_1^{Liquid}(1-WC_1) + \sum_{i=3}^{N} Q_i^{Liquid}(1-WC_i) + \\ + J_1 \cdot \Delta P_{BHP,1}^{ex,2}(1-WC_1) + \sum_{i=3}^{N} J_i \cdot \Delta P_{BHP,i}^{ex,2}(1-WC_i) \qquad (c\text{-}26)$$

We will now show that choking zone 2 gives more oil: $Q_{new,2}^{oil} > Q_{new,1}^{oil}$

$$Q_{new,2}^{Oil} - Q_{new,1}^{Oil} = (c-a) \cdot Q_1^{Liquid}(1-WC_1) - Q_2^{Liquid}(1-WC_2) + \\ + J_1 \cdot \Delta P_{BHP,1}^{ex,2}(1-WC_1) - J_2 \cdot \Delta P_{BHP}^{1}(1-WC_2) + \sum_{i=3}^{N} J_i \cdot (\Delta P_{BHP,i}^{ex,2} - \Delta P_{BHP,i}^{ex,1})(1-WC_i) = \\ = (1-WC_2) \cdot [(c-a) \cdot Q_1^{Liquid} \cdot \frac{1-WC_1}{1-WC_2} - Q_2^{Liquid} + \\ + J_1 \cdot \Delta P_{BHP,1}^{ex,2} \frac{1-WC_1}{1-WC_2} - J_2 \cdot \Delta P_{BHP}^{1}(1-WC_2)] + \sum_{i=3}^{N} J_i \cdot (\Delta P_{BHP,i}^{ex,2} - \Delta P_{BHP,i}^{ex,1})(1-WC_i) > \\ > (1-WC_2) \cdot [(c-a) \cdot Q_1^{Liquid} - Q_2^{Liquid} + J_1 \cdot \Delta P_{BHP,1}^{ex,2} - J_2 \cdot \Delta P_{BHP}^{1}(1-WC_2)] + \\ + \sum_{i=3}^{N} J_i \cdot (\Delta P_{BHP,i}^{ex,2} - \Delta P_{BHP,i}^{ex,1})(1-WC_i) \qquad (c\text{-}27)$$

The coefficient ***c*** was chosen so that

$$(c-a) \cdot Q_1^{Liquid} - Q_2^{Liquid} + J_1 \cdot \Delta P_{BHP,1}^{ex,2} - J_2 \cdot \Delta P_{BHP}^{1}(1-WC_2) = 0 \qquad (c\text{-}28)$$

Therefore $Q_{new,2}^{Oil} - Q_{new,1}^{Oil} > \sum_{i=3}^{N} J_i \cdot (\Delta P_{BHP,i}^{ex,2} - \Delta P_{BHP,i}^{ex,1})(1-WC_i) > 0$ and choking zone 2 provides higher oil production.

■

**Statement 7.3**

*The well's fluid density increases while opening the valve of operating zone.*

***Proof***

The liquid production rate of a well after setting the operating valve to a position ***i*** can be expressed by equation 7-10 of Chapter 7.

The fluid density in this case is

$$\rho^i = \frac{i \cdot \Delta Q \cdot \rho_n + \sum_{j \neq n}^{N} Q_j^{Liquid} \rho_j + \Delta P_{BHP}^i \cdot \sum_{j \neq n}^{N} J_j \rho_j}{Q^i} \qquad (c\text{-}29)$$

The liquid production rate and density for the next position i+1 can be expressed by equations:

$$Q^{i+1} = (i+1) \cdot \Delta Q + \sum_{j \neq n}^{N} Q_j^{Liquid} + \Delta P_{BHP}^{i+1} \cdot \sum_{j \neq n}^{N} J_j \qquad (c\text{-}30)$$

$$\rho^{i+1} = \frac{(i+1) \cdot \Delta Q \cdot \rho_n + \sum_{j \neq n}^{N} Q_j^{Liquid} \rho_j + \Delta P_{BHP}^{i+1} \cdot \sum_{j \neq n}^{N} J_j \rho_j}{Q^{i+1}} \qquad (c\text{-}31)$$

Let us denote $\alpha$, $d_1$ and $d_2$:

$$\alpha = i \cdot \Delta Q \cdot \rho_n + \sum_{j \neq n}^{N} Q_j^{Liquid} \rho_j + \Delta P_{BHP}^i \cdot \sum_{j \neq n}^{N} J_j \rho_j \qquad (c\text{-}32)$$

$$\begin{aligned} d_1 &= (i+1) \cdot \Delta Q \cdot \rho_n + \sum_{j \neq n}^{N} Q_j^{Liquid} \rho_j + \Delta P_{BHP}^{i+1} \cdot \sum_{j \neq n}^{N} J_j \rho_j - \\ &- (i \cdot \Delta Q \cdot \rho_n + \sum_{j \neq n}^{N} Q_j^{Liquid} \rho_j + \Delta P_{BHP}^i \cdot \sum_{j \neq n}^{N} J_j \rho_j) = \\ &= \Delta Q \cdot \rho_n - (\Delta P_{BHP}^i - \Delta P_{BHP}^{i+1}) \cdot \sum_{j \neq n}^{N} J_j \rho_j \end{aligned} \qquad (c\text{-}33)$$

$$\begin{aligned} d_2 &= Q^{i+1} - Q^i = (i+1) \cdot \Delta Q + \sum_{j \neq n}^{N} Q_j^{Liquid} + \Delta P_{BHP}^{i+1} \cdot \sum_{j \neq n}^{N} J_j - \\ &- (i \cdot \Delta Q + \sum_{j \neq n}^{N} Q_j^{Liquid} + \Delta P_{BHP}^i \cdot \sum_{j \neq n}^{N} J_j) = \\ &= \Delta Q - (\Delta P_{BHP}^i - \Delta P_{BHP}^{i+1}) \cdot \sum_{j \neq n}^{N} J_j \end{aligned} \qquad (c\text{-}34)$$

Then the densities can be rewritten as:

$$\rho^i = \frac{\alpha}{Q^i} \quad and \quad \rho^{i+1} = \frac{\alpha + d_1}{Q^i + d_2}$$

$$\rho^{i+1} = \frac{\alpha + d_1}{Q^i + d_2} > \rho^i = \frac{\alpha}{Q^i} \quad <=> \qquad (c\text{-}35)$$

$$\alpha \cdot Q^i + d_1 \cdot Q^i > \alpha \cdot Q^i + \alpha \cdot d_2 \quad <=> \qquad (c\text{-}36)$$

$$d_1 > \frac{\alpha}{Q^i} \cdot d_2 = \rho^i \cdot d_2 \qquad (c\text{-}37)$$

The fluid density of the operating zone is higher than the density of the fluid from the other zones:

$$\rho_n > \sum_{j\neq n}^{N} \rho_j J_j / \sum_{j\neq n}^{N} J_j \qquad \textit{(c-38)}$$

From equations c-33, c-34 and c-38:

$$d_1 = \Delta Q \cdot \rho_n - (\Delta P_{BHP}^{i} - \Delta P_{BHP}^{i+1}) \cdot \sum_{j\neq n}^{N} J_j \rho_j > \Delta Q \cdot \rho_n - (\Delta P_{BHP}^{i} - \Delta P_{BHP}^{i+1}) \cdot \sum_{j\neq n}^{N} J_j \rho_n = d_2 \cdot \rho_n \qquad \textit{(c-39)}$$

Therefore, the inequality c-37 is also satisfied, which proves the statement.

■

**Statement 7.4**

*The change in Δρ decreases as the ICV is opened for the operating zone.*

To prove this statement first of all two intermediate statements will be proved.

**Statement 7.4a**

1) Adding higher volume of heavier liquid increases the density higher:

$V_1 > V_2$, $\rho^* > \rho$ $\quad\Rightarrow\quad$ $\rho_1 = \dfrac{V_1\rho^* + V\rho}{V_1 + V} > \rho_2 = \dfrac{V_2\rho^* + V\rho}{V_2 + V}$ *(c-40)*

2) Adding higher volume of lighter liquid decreases the density higher:

$V_1 > V_2$, $\rho^* < \rho$ $\quad\Rightarrow\quad$ $\rho_1 = \dfrac{V_1\rho^* + V\rho}{V_1 + V} < \rho_2 = \dfrac{V_2\rho^* + V\rho}{V_2 + V}$ *(c-41)*

***Proof***

$$\rho_1 - \rho_2 = \frac{V_1\rho^* + V\rho}{V_1 + V} - \frac{V_2\rho^* + V\rho}{V_2 + V} =$$

$$= \frac{\rho^* V_1 V_2 + \rho^* V_1 V + \rho V_2 V + \rho V^2 - (\rho^* V_1 V_2 + \rho^* V_2 V + \rho V_1 V + \rho V^2)}{(V_1 + V)\cdot(V_2 + V)} =$$

$$= \frac{\rho^* V(V_1 - V_2) - \rho V(V_1 - V_2)}{(V_1 + V)\cdot(V_2 + V)} = \frac{(\rho^* - \rho)V(V_1 - V_2)}{(V_1 + V)\cdot(V_2 + V)} \qquad \textit{(c-42)}$$

Therefore $\rho_1 - \rho_2 > 0 \Leftrightarrow \rho^* - \rho > 0$

■

**Statement 7.4b**

*There are two volumes of liquid with volume $V_1 > V_2$ and density $\rho_1 > \rho_2$. The same volume $V$ with density $\rho > \rho_1 > \rho_2$ is added to these two volumes. Then the difference of density in the first case is less than the difference in the second:*

$$\rho_1^{new} - \rho_1 < \rho_2^{new} - \rho_2 \qquad \textit{(c-43)}$$

***Proof***

$$\rho_1^{new} = \frac{V_1\rho_1 + V\rho}{V_1 + V} \qquad \textit{(c-44)}$$

$$\rho_2^{new} = \frac{V_2\rho_2 + V\rho}{V_2 + V} \quad (c\text{-}45)$$

$$\rho_1^{new} - \rho_1 = \frac{V_1\rho_1 + V\rho}{V_1 + V} - \rho_1 = \frac{V(\rho - \rho_1)}{V_1 + V} < \frac{V(\rho - \rho_2)}{V_1 + V} < \frac{V(\rho - \rho_2)}{V_2 + V} = \rho_2^{new} - \rho_2 \quad (c\text{-}46)$$

■

***Proof of Statement 7.4***

$$Q^{i+1} = (i+1)\cdot\Delta Q + \sum_{j\neq n}^{N} Q_j^{Liquid} + \Delta P_{BHP}^{i+1}\cdot\sum_{j\neq n}^{N} J_j = Q^i + \Delta Q - (\Delta P_{BHP}^i - \Delta P_{BHP}^{i+1})\sum_{j\neq n}^{N} J_j \quad (c\text{-}47)$$

$$Q^i = Q^{i-1} + \Delta Q - (\Delta P_{BHP}^{i-1} - \Delta P_{BHP}^i)\sum_{j\neq n}^{N} J_j \quad (c\text{-}48)$$

Two situations are possible:

1) $\Delta P_{BHP}^i - \Delta P_{BHP}^{i+1} > \Delta P_{BHP}^{i-1} - \Delta P_{BHP}^i$ *(c-49)*

Then $\Delta P_{BHP}^i - \Delta P_{BHP}^{i+1} = \Delta P_{BHP}^{i-1} - \Delta P_{BHP}^i$ +X, where X>0

***Let's assign:***

$$V = \Delta Q - (\Delta P_{BHP}^i - \Delta P_{BHP}^{i+1})\sum_{j\neq n}^{N} J_j \quad (c\text{-}50)$$

$V_1 = Q^i,\ V_2 = Q^{i-1} + X$

$Q^{i+1} > Q^i \Rightarrow Q^i > Q^{i-1} + X$

Desity($Q^i$)> Desity($Q^{i-1}$) from Statement 7.3

$$Density(X) = \sum_{j\neq n}^{N} \rho_j J_j \Big/ \sum_{j\neq n}^{N} J_j < Density(Q^{i-1}) \quad (c\text{-}51)$$

Therefore, according **Statement 7.4a** $Density(Q^{i-1} + X) < Density(Q^{i-1})$.

Conditions of the **Statement 7.4b** are satisfied and

$$\Delta\rho^{i+1} = \rho^{i+1} - \rho^i < \Delta\rho^i = \rho^i - \rho^{i-1} \quad (c\text{-}52)$$

2) $\Delta P_{BHP}^i - \Delta P_{BHP}^{i+1} < \Delta P_{BHP}^{i-1} - \Delta P_{BHP}^i$ *(c-53)*

Then $\Delta P_{BHP}^{i-1} - \Delta P_{BHP}^i = \Delta P_{BHP}^i - \Delta P_{BHP}^{i+1}$ +X, where X>0

Let's assign:

$$V = \Delta Q - (\Delta P_{BHP}^{i-1} - \Delta P_{BHP}^i)\sum_{j\neq n}^{N} J_j \quad (c\text{-}54)$$

$V_1 = Q^i + X,\ V_2 = Q^{i-1}$

$Q^i > Q^{i-1} \Rightarrow Q^i + X > Q^{i-1}$

$$X < (\Delta P_{BHP}^{i-1} - \Delta P_{BHP}^i)\sum_{j\neq n}^{N} J_j$$

Therefore, according Statement 7.4a

$$Density(Q^i + X) > Density(Q^i + (\Delta P_{BHP}^{i-1} - \Delta P_{BHP}^{i}) \sum_{j \neq n}^{N} J_j) \qquad (c\text{-}55)$$

On the other side

$$Density(Q^i + (\Delta P_{BHP}^{i-1} - \Delta P_{BHP}^{i}) \sum_{j \neq n}^{N} J_j) = Density(Q^{i-1} + \Delta Q) > Density(Q^{i-1}) \qquad (c\text{-}56)$$

Conditions of the **Statement 7.4b** are satisfied and

$$\Delta\rho^{i+1} = \rho^{i+1} - \rho^i < \Delta\rho^i = \rho^i - \rho^{i-1} \qquad (c\text{-}57)$$

■

**Statement 7.5**

*If the oil production increases when the ICV is opened, then it will continue to increase if the choke is opened further.*

***Proof***

The statement will be proved by employing the mathematical induction method (Kolmogorov and Fomin 1975). The concept of this method is as follows:

If statements 1 and 2 can be proved:

1. The **Inductive Basis:** shows that the statement holds when *n* is equal to the **lowest** value that *n* is given in the question. Usually, *n* = 0 or *n* = 1.
2. The **Inductive Step**: shows that ***if*** the statement holds for some *n*, ***then*** the statement also holds when *n* + 1 is substituted for *n.*

Then the statement is correct for any n.

From equation c-30:

$$Q^{oil,i} = i \cdot \Delta Q \cdot (1 - WC_n) + \sum_{j \neq n}^{N} Q_j^{Liquid} (1 - WC_j) + \Delta P_{BHP}^{i} \cdot \sum_{j \neq n}^{N} J_j (1 - WC_j) \qquad (c\text{-}58)$$

***Inductive Basis***

The point ***B*** where oil production started to increase can be chosen as the basis:

$$Q^{oil,B} = B \cdot \Delta Q \cdot (1 - WC_n) + \sum_{j \neq n}^{N} Q_j^{Liquid} (1 - WC_j) + \Delta P_{BHP}^{B} \cdot \sum_{j \neq n}^{N} J_j (1 - WC_j) \qquad (c\text{-}59)$$

$$Q^{oil,B} \geq Q^{oil,B-1} \qquad \Leftrightarrow \Delta Q \cdot (1 - WC_n) > (\Delta P_{BHP}^{B-1} - \Delta P_{BHP}^{B}) \cdot \sum_{j \neq n}^{N} J_j (1 - WC_j) \qquad (c\text{-}60)$$

***Inductive Step***

Assume that for i > B the oil production increases $Q^{oil,i} \geq Q^{oil,i-1}$.

Then $$\Delta Q \cdot (1 - WC_n) > (\Delta P_{BHP}^{i-1} - \Delta P_{BHP}^{i}) \cdot \sum_{j \neq n}^{N} J_j (1 - WC_j) \qquad (c\text{-}61)$$

From **Assumption 8** $\Delta P_{BHP}^{i-1} - \Delta P_{BHP}^{i} > \Delta P_{BHP}^{i} - \Delta P_{BHP}^{i+1}$, therefore

$$\Delta Q \cdot (1 - WC_n) > (\Delta P_{BHP}^{i} - \Delta P_{BHP}^{i+1}) \cdot \sum_{j \neq n}^{N} J_j (1 - WC_j) \qquad (c\text{-}62)$$

Which proves that $Q^{oil,i+1} \geq Q^{oil,i}$.

■

# Appendix D – Auxiliary Statements of On/Off Application Area Analysis

**Converting from choked zones to fully open**

**Statement 8.1**

*If the maximum oil rate is achieved at partially choked positions for several valves, there is a corresponding case, were all valves are fully open except one valve which should be partially choked.*

***Proof***

Based on the Equation 7-4 of Chapter 7 the maximum oil rate can be described as:

$$Q_{\max}^{Oil} = \sum_{i \in Ch} a_i \cdot Q_i^{Liquid}(1-WC_i) + \sum_{j \notin Ch} Q_j^{Liquid}(1-WC_j) + \Delta P_{BHP} \cdot \sum_{j \notin Ch} J_j(1-WC_j) \quad (d\text{-}1)$$

where $0 < \boldsymbol{a_i} < 1$– reducing coefficients which correspond certain valve positions and provide maximum oil rate.

**3 Zones**

First of all lets show that the statement is correct for 3 zones.

The equation d-1 in this case can be written as

$$Q_{\max}^{Oil} = a_1 \cdot Q_1^{Liquid}(1-WC_1) + a_2 \cdot Q_2^{Liquid}(1-WC_2) + Q_3^{Liquid}(1-WC_3) + \Delta P_{BHP} \cdot J_3(1-WC_3) \quad (d\text{-}2)$$

If $a_1 = a_2$ then zones 1 and 2 can be replaced with one zone:

$$\begin{aligned} Q_{\max}^{Oil} &= a_1 \cdot (J_1 \cdot dP_1 \cdot (1-WC_1) + J_2 \cdot dP_2 \cdot (1-WC_2)) + \\ &+ Q_3^{Liquid}(1-WC_3) + \Delta P_{BHP} \cdot J_3(1-WC_3) = \\ &= a_1 \cdot J^* \cdot dP^* \cdot (1-WC^*) + Q_3^{Liquid}(1-WC_3) + \Delta P_{BHP} \cdot J_3(1-WC_3) \end{aligned} \quad (d\text{-}3)$$

Where

$$J^* = J_1 + J_2 \quad (d\text{-}4)$$

$$dP^* = \frac{J_1 \cdot dP_1 + J_2 \cdot dP_2}{J_1 + J_2} \quad (d\text{-}5)$$

$$WC^* = \frac{J_1 \cdot dP_1 \cdot WC_1 + J_2 \cdot dP_2 \cdot WC_2}{J_1 \cdot dP_1 + J_2 \cdot dP_2} \quad (d\text{-}6)$$

$$GOR^* = \frac{J_1 \cdot dP_1 \cdot GOR_1 + J_2 \cdot dP_2 \cdot GOR_2}{J_1 \cdot dP_1 + J_2 \cdot dP_2} \quad (d\text{-}7)$$

Suggest that $a_1 < a_2$, then from the Equation d-3:

$$Q_{\max}^{Oil} = a_1 \cdot (J_1 \cdot dP_1 \cdot (1 - WC_1) + J_2 \cdot dP_2 \cdot (1 - WC_2)) + (a_2 - a_1) \cdot J_2 \cdot dP_2 \cdot (1 - WC_2) + \\ + Q_3^{Liquid}(1 - WC_3) + \Delta P_{BHP} \cdot J_3(1 - WC_3)$$

*(d-8)*

The first term of the equation d-8 can be described by fully open zone with

$$J^* = a_1(J_1 + J_2) \qquad (d\text{-}9)$$

and the other parameters defined by equations d-5, d-6 and d-7.

Zone 2 is operated with reducing coefficient ***b*** which changes from 0 to $1\text{-}a_1\text{-}\Delta$. The value of term Δ will be explained further.

The oil rate is therefore:

$$Q_b^{Oil} = J^* \cdot dP^* \cdot (1 - WC^*) + \Delta P_{BHP}^{b} \cdot J^* \cdot (1 - WC^*) + b \cdot J_2 \cdot dP_2 \cdot (1 - WC_2) + \\ + Q_3^{Liquid}(1 - WC_3) + (\Delta P_{BHP} + \Delta P_{BHP}^{b,3}) \cdot J_3(1 - WC_3) \qquad (d\text{-}10)$$

If $b = a_2 - a_1$ then $Q_b^{Oil} = Q_{\max}^{Oil}$

We need to show that this intermediate position of $0 < b = a_2 - a_1 < 1\text{-}a_1\text{-}\Delta$ is still optimal for this case.

From Equations d-5, d-6 and d-9:

$$J^* \cdot (1 - WC^*) \cdot \Delta P_{BHP}^{b} = a_1 \cdot (J_1 + J_2) \cdot \frac{J_1 \cdot dP_1 \cdot (1 - WC_1) + J_2 \cdot dP_2 \cdot (1 - WC_2)}{J_1 \cdot dP_1 + J_2 \cdot dP_2} \cdot \Delta P_{BHP}^{b} = \\ = a_1 \cdot (J_1 \cdot dP_1 \cdot (1 - WC_1) + J_2 \cdot dP_2 \cdot (1 - WC_2)) \cdot \frac{\Delta P_{BHP}^{b}}{dP^*}$$

*(d-11)*

Therefore Equation d-10 becomes

$$Q^{Oil} = a_1 \cdot J_1 \cdot (1 + \frac{\Delta P_{BHP}^{b}}{dP^*}) \cdot dP_1 \cdot (1 - WC_1) + J_2 \cdot (a_1 \cdot \frac{\Delta P_{BHP}^{b}}{dP^*} + b) \cdot dP_2 \cdot (1 - WC_2) + \\ + Q_3^{Liquid}(1 - WC_3) + \Delta P_{BHP}^{b} \cdot J_3(1 - WC_3)$$

*(d-12)*

In the original case the coefficient ***b*** varies from 0 to $1\text{-}a_1$. However, if we choose this upper boundary for our modified case, the reducing coefficient for zone 2 becomes:

$$1 - a_1 + a_1 \cdot \frac{\Delta P_{BHP}^{b}}{dP^*} \qquad (d\text{-}13)$$

Therefore, we need to reduce the upper boundary for a value $\Delta = a_1 \cdot \frac{\Delta P_{BHP}^{\Delta}}{dP^*}$ if we want to stay in the boundaries of the original case.

Equation d-12 describes original case with the optimal position at $b = a_2 - a_1$ which proves the statement.

**N Zones**

A case with multiple zones can be reordered as $a_1 < a_2 < ... < a_{N-1}$.

The equation d-8 for this situation can be written as:

$$Q_{\max}^{Oil} = a_1 \cdot \sum_{i=1}^{N-1} J_i \cdot dP_i \cdot (1 - WC_i) + a_2 \cdot \sum_{i=2}^{N-1} J_i \cdot dP_i \cdot (1 - WC_i) + ... +$$
$$+ a_{N-2} \cdot \sum_{i=N-2}^{N-1} J_i \cdot dP_i \cdot (1 - WC_i) + (a_{N-1} - a_{N-2}) \cdot J_{N-1} \cdot dP_{N-1} \cdot (1 - WC_{N-1}) + \qquad (d\text{-}14)$$
$$+ Q_N^{Liquid}(1 - WC_N) + \Delta P_{BHP} \cdot J_N (1 - WC_N)$$

The first N-2 terms can be modelled with fully open zones. It can be shown that N-1$^{th}$ choke has the optimal position at intermediate point with reducing coefficient $b = a_{N-1} - a_{N-2}$ similar to the previous case.

■

**Converting from any number of zones into three zones**

***Problem formulation***

$$Q_{new}^{Liquid} = a\ Q_1^{Liquid} + \sum_{i=2}^{N} dP_i \cdot J_i + \sum_{i=2}^{N} J_i \cdot \Delta P_{BHP} \qquad (d\text{-}15)$$

Assume that $dP_i \geq 0$.

Find $J_2^*$, $J_3^*$, $dP_2^*$, $dP_3^*$, $WC_2^*$, $WC_3^*$, $GOR_2^*$, $GOR_3^*$, $\rho_2^*$ and $\rho_3^*$ that the following system of equations is satisfied:

$$\begin{cases} J_2^* + J_3^* = \sum_{i=2}^{N} J_i & (d\text{ - }16) \\ J_2^* \cdot dP_2^* + J_3^* \cdot dP_3^* = \sum_{i=2}^{N} J_i \cdot dP_i & (d\text{ - }17) \\ J_2^* \cdot WC_2^* + J_3^* \cdot WC_3^* = \sum_{i=2}^{N} J_i \cdot WC_i & (d\text{ - }18) \\ J_2^* \cdot dP_2^* \cdot WC_2^* + J_3^* \cdot dP_3^* \cdot WC_3^* = \sum_{i=2}^{N} J_i \cdot dP_i \cdot WC_i & (d\text{ - }19) \\ J_2^* \cdot GOR_2^* + J_3^* \cdot GOR_3^* = \sum_{i=2}^{N} J_i \cdot GOR_i & (d\text{ - }20) \\ J_2^* \cdot dP_2^* \cdot GOR_2^* + J_3^* \cdot dP_3^* \cdot GOR_3^* = \sum_{i=2}^{N} J_i \cdot dP_i \cdot GOR_i & (d\text{ - }21) \\ J_2^* \cdot \rho_2^* + J_3^* \cdot \rho_3^* = \sum_{i=2}^{N} J_i \cdot \rho_i & (d\text{ - }22) \\ J_2^* \cdot dP_2^* \cdot \rho_2^* + J_3^* \cdot dP_3^* \cdot \rho_3^* = \sum_{i=2}^{N} J_i \cdot dP_i \cdot \rho_i & (d\text{ - }23) \end{cases}$$

**Solution**

There are 10 parameters and 8 equations in total. Therefore 2 parameters are free and can have any values. Suggest that $J_3^*$ *and* $dP_3^*$ are free parameters. All the other parameters can be expressed from these 2.

From Equation d-16: $J_2^* = \sum_{i=2}^{N} J_i - J_3^*$ *(d-24)*

From Equation d-17: $dP_2^* = \dfrac{\sum_{i=2}^{N} J_i \cdot dP_i - J_3^* \cdot dP_3^*}{\sum_{i=2}^{N} J_i - J_3^*}$ *(d-25)*

From Equation d-18: $WC_2^* = \dfrac{\sum_{i=2}^{N} J_i \cdot WC_i - J_3^* \cdot WC_3^*}{J_2^*} = \dfrac{\sum_{i=2}^{N} J_i \cdot WC_i - J_3^* \cdot WC_3^*}{\sum_{i=2}^{N} J_i - J_3^*}$ *(d-26)*

Placing the values of d-24 and d-25 in equation d-19 we have

$$\frac{(\sum_{i=2}^{N} J_i \cdot dP_i - J_3^* \cdot dP_3^*) \cdot (\sum_{i=2}^{N} J_i \cdot WC_i - J_3^* \cdot WC_3^*)}{\sum_{i=2}^{N} J_i - J_3^*} + J_3^* \cdot dP_3^* \cdot WC_3^* = \sum_{i=2}^{N} J_i \cdot dP_i \cdot WC_i \qquad \textit{(d-27)}$$

After multiplying the equation on $\sum_{i=2}^{N} J_i - J_3^*$ an assembling coefficient before $WC_3^*$

$$\begin{aligned} &(J_3^* \cdot dP_3^* \cdot (\sum_{i=2}^{N} J_i - J_3^*) - J_3^* \cdot (\sum_{i=2}^{N} J_i \cdot dP_i - J_3^* \cdot dP_3^*)) \cdot WC_3^* = \\ &= \sum_{i=2}^{N} J_i \cdot dP_i \cdot WC_i \cdot (\sum_{i=2}^{N} J_i - J_3^*) - \sum_{i=2}^{N} J_i \cdot WC_i \cdot (\sum_{i=2}^{N} J_i \cdot dP_i - J_3^* \cdot dP_3^*) \end{aligned} \qquad \textit{(d-28)}$$

After simplifying the left part of the equation:

$$\begin{aligned} &J_3^* \cdot (dP_3^* \cdot \sum_{i=2}^{N} J_i - \sum_{i=2}^{N} J_i \cdot dP_i) \cdot WC_3^* = \\ &= \sum_{i=2}^{N} J_i \cdot dP_i \cdot WC_i \cdot (\sum_{i=2}^{N} J_i - J_3^*) - \sum_{i=2}^{N} J_i \cdot WC_i \cdot (\sum_{i=2}^{N} J_i \cdot dP_i - J_3^* \cdot dP_3^*) \end{aligned} \qquad \textit{(d-29)}$$

And finally

$$WC_3^* = \frac{\sum_{i=2}^{N} J_i \cdot dP_i \cdot WC_i \cdot (\sum_{i=2}^{N} J_i - J_3^*) - \sum_{i=2}^{N} J_i \cdot WC_i \cdot (\sum_{i=2}^{N} J_i \cdot dP_i - J_3^* \cdot dP_3^*)}{J_3^* \cdot (dP_3^* \cdot \sum_{i=2}^{N} J_i - \sum_{i=2}^{N} J_i \cdot dP_i)} \qquad \textit{(d-30)}$$

It can be found using the same technique that:

$$GOR_3^* = \frac{\sum_{i=2}^{N} J_i \cdot dP_i \cdot GOR_i \cdot (\sum_{i=2}^{N} J_i - J_3^*) - \sum_{i=2}^{N} J_i \cdot GOR_i \cdot (\sum_{i=2}^{N} J_i \cdot dP_i - J_3^* \cdot dP_3^*)}{J_3^* \cdot (dP_3^* \cdot \sum_{i=2}^{N} J_i - \sum_{i=2}^{N} J_i \cdot dP_i)} \qquad \textit{(d-31)}$$

$$\rho_3^* = \frac{\sum_{i=2}^{N} J_i \cdot dP_i \cdot \rho_i \cdot (\sum_{i=2}^{N} J_i - J_3^*) - \sum_{i=2}^{N} J_i \cdot \rho_i \cdot (\sum_{i=2}^{N} J_i \cdot dP_i - J_3^* \cdot dP_3^*)}{J_3^* \cdot (dP_3^* \cdot \sum_{i=2}^{N} J_i - \sum_{i=2}^{N} J_i \cdot dP_i)} \qquad \textit{(d-32)}$$

And finally $GOR_2^*$ and $\rho_2^*$ can be calculated from the equations:

$$GOR_2^* = \frac{\sum_{i=2}^{N} J_i \cdot GOR_i - J_3^* \cdot GOR_3^*}{\sum_{i=2}^{N} J_i - J_3^*} \qquad \textit{(d-33)}$$

$$\rho_2^* = \frac{\sum_{i=2}^{N} J_i \cdot \rho_i - J_3^* \cdot \rho_3^*}{\sum_{i=2}^{N} J_i - J_3^*} \qquad \textit{(d-34)}$$

All necessary parameters may thus be calculated.

# Appendix E – Uncertainty Analysis Results for 2 Month Optimisation Time Step

*Table e-1 P10, P50 and P90 of Cumulative NPV, Oil and Water Production for 2Month time step*

| Case | Cumulative NPV, Million$ | | | Cumulative Oil Production, Million m3 | | | Cumulative Water Production, Million m3 | | |
|---|---|---|---|---|---|---|---|---|---|
| | P10 | P50 | P90 | P10 | P50 | P90 | P10 | P50 | P90 |
| **Base Case** | 1110 | 1008 | 902 | 6.94 | 6.55 | 6.14 | 19.60 | 17.56 | 15.47 |
| **IW No Control** | 1102 | 1003 | 895 | 6.94 | 6.55 | 6.14 | 19.35 | 17.42 | 15.17 |
| **IW SLP** | 1119 | 1021 | 915 | 6.81 | 6.36 | 5.94 | 14.42 | 12.48 | 10.06 |
| **IW SQP** | 1116 | 1018 | 913 | 6.88 | 6.46 | 6.11 | 16.30 | 14.58 | 13.01 |
| **IW 10 Positions** | 1115 | 1017 | 911 | 6.78 | 6.36 | 5.90 | 14.49 | 12.43 | 10.56 |
| **IW On/Off** | 1121 | 1022 | 907 | 6.85 | 6.42 | 5.92 | 14.18 | 12.30 | 10.51 |

*Table e-2 Added value of IWs for P50 for 2Month time step*

| Case | Cumulative NPV | | | Cumulative Oil Production | | | Cumulative Water Production | | |
|---|---|---|---|---|---|---|---|---|---|
| | NPV | Difference from Base Case | | Cum Oil | Difference from Base Case | | Cum Water | Difference from Base Case | |
| | Million $ | Million $ | % | Million $m^3$ | Million $m^3$ | % | Million $m^3$ | Million $m^3$ | % |
| **Base Case** | 1008 | - | - | 6.55 | - | - | 17.56 | - | - |
| **IW No Control** | 1003 | -5 | -0.5% | 6.55 | 0.00 | 0.0% | 17.42 | -0.1 | -0.8% |
| **IW SLP** | 1021 | 14 | 1.4% | 6.36 | -0.19 | -2.9% | 12.48 | -5.1 | -28.9% |
| **IW SQP** | 1018 | 10 | 1.0% | 6.46 | -0.10 | -1.5% | 14.58 | -3.0 | -17.0% |
| **IW 10 Positions** | 1017 | 9 | 0.9% | 6.36 | -0.20 | -3.0% | 12.43 | -5.1 | -29.2% |
| **IW On/Off** | 1022 | 14 | 1.4% | 6.42 | -0.13 | -2.1% | 12.30 | -5.3 | -29.9% |

*Table e-3 Relative Variance of Cumulative NPV, Oil and Water Production for 2Month time step*

| Case | Cumulative NPV | Cumulative Oil Production | Cumulative Water Production |
|---|---|---|---|
| **Base Case** | 21% | 12% | 23% |
| **IW No Control** | 21% | 12% | 24% |
| **IW SLP** | 20% | 14% | 35% |
| **IW SQP** | 20% | 12% | 23% |
| **IW 10 Positions** | 20% | 14% | 32% |
| **IW On/Off** | 21% | 14% | 30% |

*Table e-4 Absolute Variance of Cumulative NPV, Oil and Water Production for 2Month time step*

| Case | Cumulative NPV, Million$ | | Cumulative Oil Production, Million m3 | | Cumulative Water Production, Million m3 | |
|---|---|---|---|---|---|---|
| | Variance | % | Variance | % | Variance | % |
| **Base Case** | 208 | 100% | 0.81 | 100% | 4.12 | 100% |
| **IW No Control** | 207 | 99% | 0.80 | 99% | 4.18 | 101% |
| **IW SLP** | 204 | 98% | 0.87 | 108% | 4.35 | 106% |
| **IW SQP** | 203 | 98% | 0.77 | 95% | 3.29 | 80% |
| **IW 10 Positions** | 203 | 98% | 0.89 | 110% | 3.92 | 95% |
| **IW On/Off** | 214 | 103% | 0.93 | 115% | 3.67 | 89% |

# Appendix F - Papers

## SPE 136335

# Analysis of the Impact of an Intelligent Well Completion on the Oil Production Uncertainty

I.M. Grebenkin and D.R Davies, Heriot-Watt University



This paper was prepared for presentation at the 2010 SPE Russian Oil & Gas Technical Conference and Exhibition held in Moscow, Russia, 26–28 October 2010.



### Abstract

Oil production is influenced by many parameters, for example the distribution of the petrophysical properties, fluid contacts, relative permeabilities, faults, aquifer strength etc. These parameters influence the production production process in different manners, with every parameter displaying its own, unique, level of uncertainty. This is one reason why the probabilistic approach, which takes into account the major uncertaintiesin the reservoir description and production processes, has developed into an important tool for the prediction of a field's hydrocarbon recovery. This is especially important in the case of heterogeneous reservoirs and horizontal wells. Here, unexpected early water or gas breakthrough into one of the zones will reduce the oil production by preventing oil inflow from other parts of the well.

Intelligent Well (IW) Technology has ability to identify and control the inflow rate at a zone level, preventing the breakthrough of unwanted gas or water. Previous work examined the impact of choking by an IW's Interval Control Valves (ICVs) on the geological uncertainty attributed to the statistical distribution of the formation's properties[1].

This paper extends this study to the "dynamic" parameters (fluid contacts, relative permeabilities, aquifer strength and zonal skin). Each of these parameters exhibit its own uncertainty; with each, individual uncertainty being combined to generate an accurate estimation of overall risk associated with the reservoir's development. The workflow employed will be demonstrated for two cases. This will be followed by an analysis to identify which of the above factors allow the flow control ability of an IW to reduce the production uncertainty in general as well as in specific cases.

The results emphasize the importance of the probabilistic approach for production prediction and illustrate its use as a tool to justify the installation of IW Technology in a particular well. This method will be used for both estimating, as well as reducing, the risks associated with the initial uncertainty of a planned development.

### Introduction

Horizontal wells have become quite popular in oil industry. They can deliver an increased oil production while reducing the field development time and costs by reducing the required number of wells. This is especially relevant for offshore fields where the incremental cost per well is high. But long horizontal wells also cause production management problems, e.g. reservoirs are not homogeneous, allowing water or gas to breakthrough into different parts of the well at different times. These unwanted fluids with a higher mobility reduce the inflow from the oil bearing zones. The result is a non-uniform displacement of the oil, a reduced sweep efficiency and an increased cost due to water and gas recycling. All these factors will increase the field's operating cost and reduce its recovery and profitability.

Intelligent (or smart) well completion can help to solve these problems. IWs are equipped with downhole sensors; allowing monitoring of the inflow from the various well zones. Moreover, advanced control equipment may be used for managing the inflow into each zone. This combination of monitoring and control can give a significant improvement in the oil recovery while reducing the field's processing cost. There are two main types of flow control completions: "passive" Inflow Control Devices (ICDs) and "active" ICVs.

ICDs are used for equalising the inflow rate per unit length of completion along the horizontal well's length. Such inflow heterogeneity in different parts of the well can be caused by, for example, differences in the reservoir's permeability or the horizontal well's "heel-toe" effect. ICDs employ a fixed flow restriction installed in each completion joint that restricts the inflow from high-permeability zones of the reservoir into the well. By contrast, ICVs are controlled from the surface by an operator in order to restrict the inflow into specific intervals. Al-Khelaiwi and Birchenko have made a detailed analysis comparing the application area for both devices [2, 3]. "Passive" control has a low installation cost and risk, but "active" control devices are often prefered in heterogeneous reservoirs due to the higher levels of uncertainty in this type of reservoir.

The flexibility of "active" IW control allows changes to be made at any time to the well's production strategy, reducing the risk caused by reservoir uncertainty.
However, choice of an efficient control strategy is a difficult problem. There are two main types of optimization strategy: "proactive" and "reactive" [4]. "Reactive" optimization requires the IW to respond to the current inflow into the well; WCT or GOR in our case. The simplest approach is using a two position choke which can be open or closed according to a water-cut threshold. A more flexible policy is to employ ICVs with several valve positions that can be used together with a water cut threshold which increases with time [5].
Sequential linear programming (SLP) is a more complex approach to production optimisation. The initial task is non-linear [6], hence it requires linearization after which the simplex method can be applied to find the optimum value. The individual calculation steps are fast, but this method suffers from convergence problems caused by non-linearities and oscillations. Emerick and Portella [7] used a direct search method in their work. It does not have problems with convergence and has proved to be a good technique for optimising discreet position ICVs. However, the results achieved with this method depend on the sequence in which the valves are selected for optimisation. Altering this order may lead to quite different results from the global optimum value. Gradient methods are also widely used for the optimisation of non-linear tasks, e.g. Yeten used a conjugant gradient method for production optimisation [8]. It proved capable of finding a local optimum value, similar to the other gradient methods.
In summary, a reactive strategy may prevent inflow of a limited amount of unwanted fluid, but it does little to change the global position of the water or gas front that is advancing across the reservoir. By contrast, a "proactive" strategy can change the invading front's behaviour; delaying the breakthrough and increasing the sweep efficiency. Sarma and Aziz used an adjoint algorithm for controlling the IW and increasing the value of the recovered hydrocarbons [9]. Doublet et al showed that an augmented Lagrangian function method can find approximately the same NPV value as the ajoint method, but less computational effort is required [10]. A "proactive" strategy can thus be more beneficial than a "reactive" one, giving an increased total oil production. However, most published reports on the use of proactive strategies refer to it being employed in the optimisation of a synthetic reservoir model rather than it being used on a real, full-field model. This is not surprising since the computational time required for a "proactive" method is much higher than their "reactive" equivalent, making them difficult to use when analysing reservoir simulation models that are either big or very detailed.
Reservoir uncertainty is a second challenge for the "proactive" optimisation strategy. This strategy requires selective choking of some intervals to start early in a well's or field's productive life. If effective, this choking will delay the breakthrough time of unwanted fluids; but it will also, of necessity, lead to a decreased early oil production unless the well has a higher zonal flow capacity than the well's allowable production rate.
The accuracy of the initial reservoir simulation model will also strongly influence the total oil production achieved. For example, an inappropriate (early) choking strategy based on an inaccurate model can lead to a decreased oil production and an earlier breakthrough of an (unwanted) fluid front. A control strategy based on a model which is different from the real field will give a non-optimum production strategy for the real case. Some authors overcome this problem by periodically updating their models based on "real-time", measured well data [11]. However the initial control strategy still has, of necessity, a high degree of uncertainty associated with it. It is not possible to precisely predict the breakthrough time or the initial water and/or gas production profile of a real field during this early production period since the well is usually producing 100% oil at this time. By contrast, this information is always available from a reservoir simulation model. Hence it can be actively used even during early times by "proactive" optimisation methods.
In this paper we have chosen to use a simple "reactive" control strategy to avoid such problems as are always present in a real case, i.e. the scale of the computational effort required and the uncertainty associated with the optimum production strategy prior to breakthrough. Our production strategy will be based on reducing the ICV choke diameter as a function of the current water cut and GOR values. We will evaluate where application of this control strategy to an IW will generate greater benefit than that achieved by a conventional well. If this proves to be the case, it can be used as an argument to support installing an IW completion.
A previous paper showed that an IW is able to reduce the impact of geological uncertainty on the production forecast [1]. This paper considered the uncertainty associated with the distribution of porosity and permeability values. However, other parameters, such as relative permeabilities, oil-water and gas-oil contacts, aquifer strength and the zonal formation damage skins are also uncertain; especially at the early stages of field development. In this work we will analyse whether the use of an IW completion can impact the production uncertainty compared to a conventional well.

## Intelligent completion model

We simulated the performance of an IW using the commercial reservoir simulator *Eclipse 100*$^{TM}$ [12]. The multi-segment option was used for modeling the fluid flow from the reservoir grid to the tubing via the ICVs (Fig. 1). Flow is allowed to move freely between certain annulus segments and then passes into the tubing via the ICV.

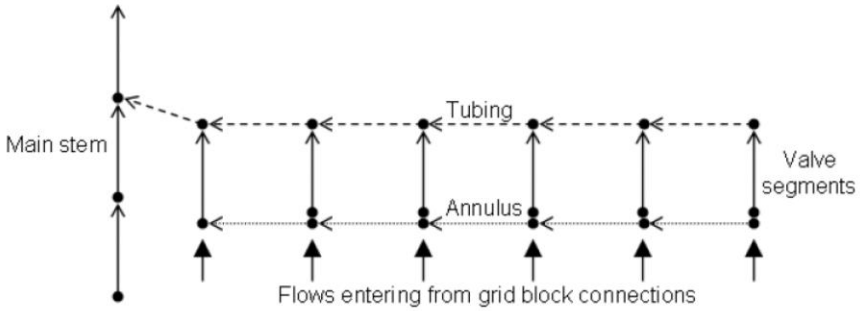


**Fig 1 – Schematic of a multi-segmented well (after Schlumberger [12])**

The total liquid production of each zone can be written as:

$$Q_{liq}^{i} = \frac{B_o + (GOR^i - Rs)B_g}{1 - B_w \cdot WCT^i} Q_{oil}^{i}$$

where i is the interval number. A lower value of :

$$a^i = \frac{B_o + (GOR^i - Rs)B_g}{1 - B_w \cdot WCT^i}$$

allows more oil to be produced from that interval.

The water cut and gas-oil ratio parameters are calculated by *Eclipse*$^{TM}$ for each well interval at every time step. The appropriate, normalised $a^i$ coefficient may then be used as a criterion for controlling the extent of choking applied by each ICV.

## Case 1: PUNQ-S3 Reservoir model

The PUNQS3 reservoir model is a publically available synthetic model [13] that was originally built by Elf Exploration Production based on real field data from 6 vertical wells. It has an aquifer, an impermeable fault at the east and south side of the field and relatively weak gas cap at the centre of the model (Fig 2). The 3.2 x 5 km model is quite coarse, the cell size being 150 x 150 x 5 m. Its 1761 active cells result in a fast simulation time. The model is also quite heterogeneous. These two aspects make it popular with reservoir engineers when investigating the role of uncertainty.

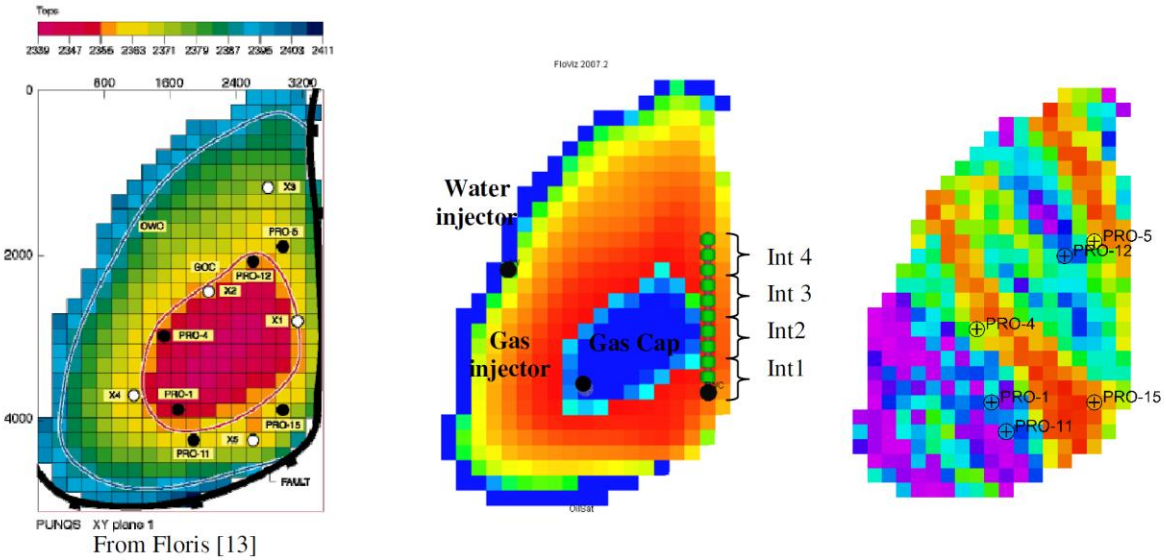


From Floris [13]

**Fig 2– Structure, wells location and permeability distribution of the PUNQS3 model**

Our development strategy for the PUNQ-S3 model called for production from a single horizontal well of 1800 m. length combined with two vertical injectors. The water injector helps support the reservoir pressure in cases where the aquifer strength is insufficient to compensate for the volume of production while the gas injector returns any produced gas to the reservoir crest. The horizontal production well was drilled with a 8½" open hole for the base case. This was converted to an IW by installing 4 ICVs connected by a 3½" tubing installed in the 8. ½" open hole. The well production limits were a Liquid

Rate ≤ 600 $m^3$/day and a BHP > 120 bar. This production limit equals the maximum total liquid rate of the six vertical wells in the original model. The injection wells are operated under BHP control at 300 bar.
The horizontal well was placed in the thickest oil bearing zone as far from water and gas sources as possible (Fig 3). This optimal well location allows a delayed water and gas breakthrough and an increased recovery factor compared to all other, alternative locations tested.

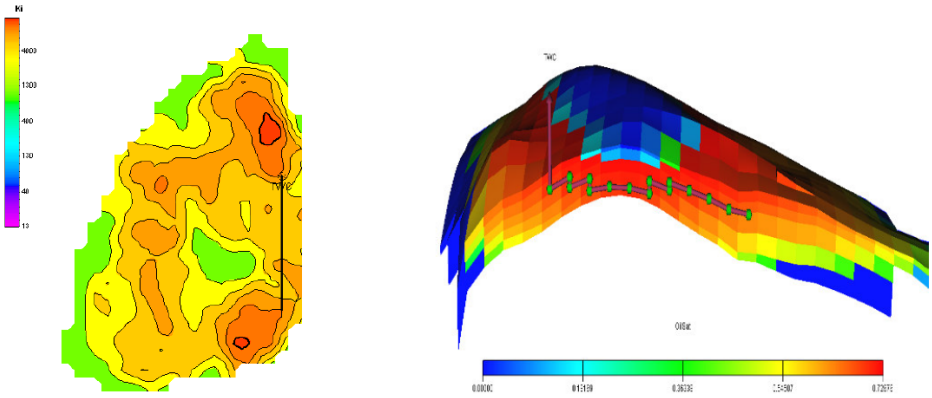

**Fig 3– Optimum horizontal well location**

## Case 2: AINSA II Reservoir model

The AINSA II model is based on the outcrop description [14]. A very detailed description of the facia location was available (Fig 4). The cell dimensions of the original model are 20 x 20 x 0.5 m. which were then upscaled to 60 x 60 x 2 m. This level of upscaling retained a detailed description of the reservoir while limiting the model complexity to 43750 active cells.

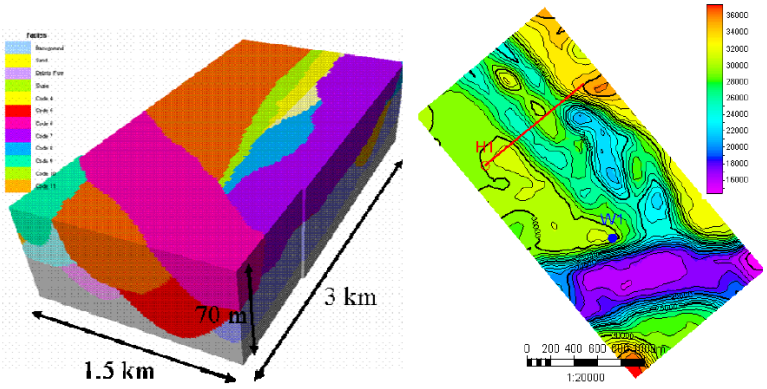


**Fig 4 – AINSA II model facies and well locations**

A 1200 m. long horizontal production well and a vertical injection well complete the dynamic model. The production well was also restricted to a liquid production rate less 1200 $m^3$/day while the injection pressure was also limited a BHP of 300 bar.

## Geological parameter variation

One hundred realisations of the porosity and permeability distribution for the PUNQS3 model were made with a sequential Gaussian simulation algorithm based on data from the six original wells. The correlation length values and anisotropy in the orientation of each layer were randomly generated based on the parameters listed in Table 1.
The AINSA II geological model was originally built based on an outcrop description. Thirteen turbidity channels were carefully correlated and included in the initial model. A stochastic, object modelling method based on the variation of original channel parameters such as width, thickness and orientation was used to build one hundred realisations for this case.

Table 1. Geological parameter variation

| | Range along | | Range across | | Angle | |
|---|---|---|---|---|---|---|
| Layer | Lower limit | Upper limit | Lower limit | Upper limit | Lower limit | Upper limit |
| 1 | 2000 | 5000 | 700 | 900 | 100 | 160 |
| 2 | 700 | 1300 | 700 | 1300 | -10 | 10 |
| 3 | 2000 | 5000 | 700 | 1300 | 100 | 160 |
| 4 | 500 | 5000 | 500 | 5000 | -10 | 10 |
| 5 | 2000 | 5000 | 700 | 900 | 100 | 160 |

## Variation of the "Dynamic" parameters

Variation of the "dynamic" parameters relative permeability, oil-water contact, gas-oil contact, aquifer strength and the formation damage skin for each interval summarised in Fig 5 and Table 2:

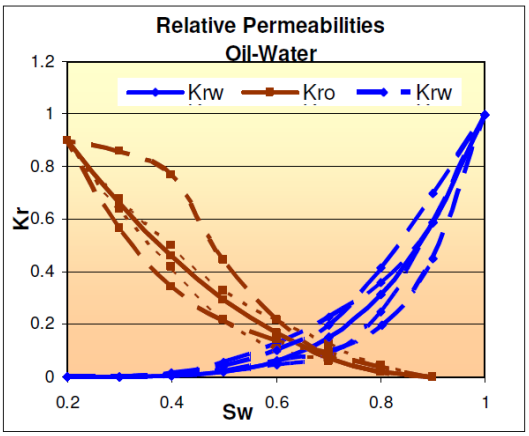


Fig 5-Relative permeability variation

Table 2. Dynamic parameters variation

| Model | PUNQS3 | | | Ainsa II | | | Distribution |
|---|---|---|---|---|---|---|---|
| Parameter | min | max | original | min | max | original | |
| AQUIPerm, mD | 1 | 300 | 137.5 | 1 | 1000 | 200 | lognormal |
| AQUIPoro, % | 10 | 30 | 20 | 10 | 40 | 25 | normal |
| GOC, m | 2352.5 | 2357.5 | 2355 | - | - | - | normal |
| OWC, m | 2392.5 | 2497.5 | 2395 | 2425 | 2435 | 2430 | normal |
| Skin effect Intervals 1-4 | 0 | 10 | 1 | 0 | 10 | 1 | triangular |

We changed the shape, intersection and critical points for the oil and water relative permeabilities when modelling their variation (Fig.5). Aquifer porosity, OWC and GOC have a normal distribution with a mean value equal to that of the original case. The aquifer response usually has a large uncertainty associated with it, especially during the early stage of the field development. We therefore used a lognormal distribution for the aquifer permeability to allow for a high aquifer strength.

A skin is often observed in wells due to drilling and completion formation damage. Its severity can be different in the various parts of the well; hence we decided to vary the skin value at the zone level in our model. It was assumed that an effective, well clean-up procedure had been employed to minimise this skin value; hence the minimum skin value was set to 0 and the maximum value was 10, with a triangular distribution between these values and the most probable value skin value of 1.

Sensitivity analysis to variation of the "dynamic" parameters for both models was performed with using the *Cougar*™ software's ability to select from a large number of experimental design methods [15]. The "Small Face Centred Composite Design" (SFCCD) was used for analysing the impact of the above uncertainties on the production. This technique was recommended [15] as the best quadratic experimental design method for variation of our selected parameters. This recommendation was confirmed by comparing the predictive quality of SFCCD with the "Latin Hypercube Design" (LHCD). LHCD employes many more realisations (1000) than the 51 realisations required by SFCCD for 9 independent parameters. The parameter values for the 1000 LHCD realisations were randomly selected according to their probability distribution; while the final distribution for SFCCD was derived using 1000 realisations based on the 51 experimental calculated results and a Monte-Carlo type selection of the input parameter's probability distribution.

Table 3 shows that the results for both methods are similar; SFCCD gave equally accurate results with a more than 95% reduction in the calculation time. Further, comparison of the Response Surface built for the SFCCD results gave almost perfect fit to the actual values.

**Table 3. Comparison of the oil production for "Small Face Centred Composite Design" and "Latin Hypercube Design"**

| Case | Mean, $m^3$ | Standard Deviation, $m^3$ | Variation | Calculation time, hours:minutes:seconds |
|---|---|---|---|---|
| "Small Face Centred Composite Design" | 4474000 | 383200 | 8.6% | 00:27:07 |
| "Latin Hypercube Design" | 4394000 | 366700 | 8.3% | 09:28:07 |
| Difference | 1.8% | 4.5% | 0.3% | 09:01:00 or 95% |

## Results and Discussion

The results of the oil water production distribution for PUNQS3 and AINSA II model are shown in Figs. 6 and 7 and Table 3.

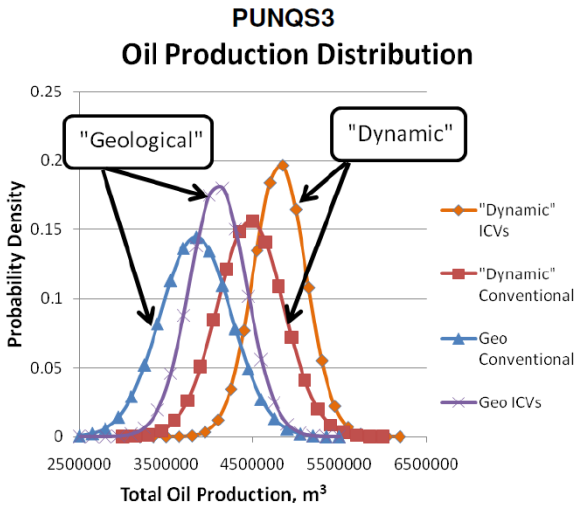


**Fig 6 - Total oil production distribution for the conventional and IW cases, PUNQS3**

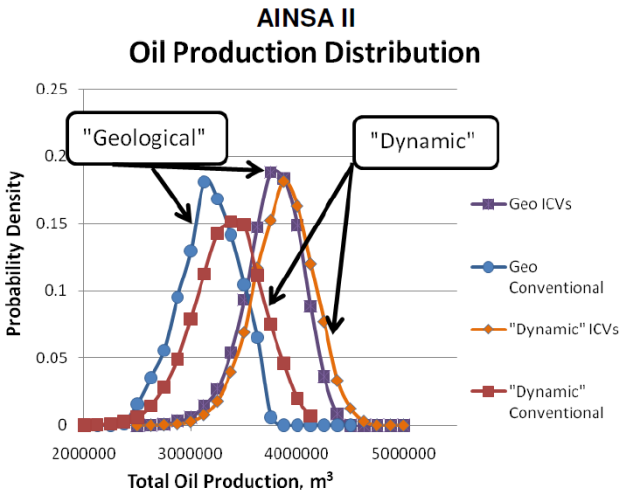


**Fig.7 Total oil production distribution for the conventional and IW cases, AINSA II**

**Table 4. Total oil and water production (MM $m^3$) variation for conventional and IW cases**

| | Model | | PUNQS3 | | | | Ainsa II | | | |
|---|---|---|---|---|---|---|---|---|---|---|
| | Case | Uncertainty | P50 | P90 | P10 | Variation | P50 | P90 | P10 | Variation |
| Oil Production | Base Case | Geological | 3.91 | 3.31 | 4.35 | 10.8% | 3.12 | 2.73 | 3.46 | 8.7% |
| | | Dynamic | 4.55 | 3.9 | 4.92 | 8.6% | 3.14 | 2.63 | 3.59 | 15.2% |
| | ICV | Geological | 4.16 | 3.66 | 4.52 | 8.0% | 3.73 | 3.37 | 4.04 | 7.1% |
| | | Dynamic | 4.87 | 4.42 | 5.15 | 6.3% | 3.81 | 3.44 | 4.16 | 9.4% |
| Water Production | Base Case | Geological | 2.57 | 3.17 | 2.13 | 20.2% | 9.75 | 10.1 | 9.41 | 3.7% |
| | | Dynamic | 1.93 | 2.58 | 1.56 | 26.4% | 9.73 | 10.2 | 9.278 | 4.9% |
| | ICV | Geological | 2.32 | 2.82 | 1.96 | 18.5% | 9.14 | 9.5 | 8.83 | 3.7% |
| | | Dynamic | 1.61 | 2.06 | 1.33 | 22.7% | 9.06 | 9.43 | 8.71 | 4.0% |

IW achieves a reduction in both cases for the oil production variation caused by geological and dynamic uncertainty. Moreover, for this development strategy, IW increases the average oil production by approximately 6% for PUNQS3 and 20% for the AINSA II model when compared with the conventional case. Additionally, it decreases the absolute value of the average water production as well as its variation. This is also important because it reduces both the uncertainty in the required size of the surface facilities (reduced capital cost) as well as the operational cost of water recycling.

It is significant that the mean value of the total oil production is larger for the dynamic rather than the geological uncertainty cases for the PUNQS3 model. This occurs because the production well has been located in an optimum position in the original

model. Therefore, any changes in the geological properties tend to reduce the oil production. This example shows importance of employing an uncertainty investigation when analysing for the optimum well location and development strategy.
The next question to be answered was to try and understand when an IW completion is capable of reducing the impact of uncertainty on the volume of hydrocarbon produced.

### IW efficiency for reducing the impact of uncertainty

Variation of the productivity index (PI) was analysed and compared for the PUNQS3 model for both the IW and conventional cases. Firstly, the PI multipliers were changed from 0.3 to 3 for each of the 4 intervals of the horizontal well (Fig 8a). In a second study, this PI variation was only implemented in the 4th interval. This interval has the highest water cut and is the most regulated (choked) by the IW completion.

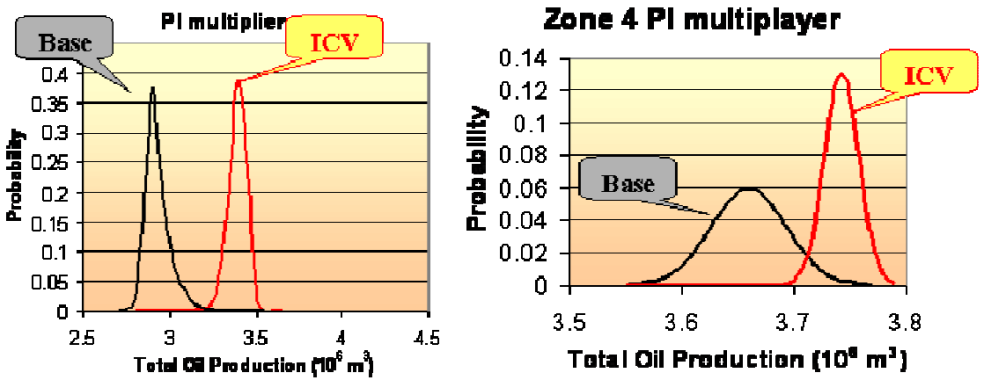


a b

**Fig.8 Comparison of the impact of the uncertainty in the PI multiplayer on the oil production a) for all intervals and b) for the 4th interval only, PUNQS3**

Fig.8 shows that the intelligent well increases the production compared to the conventional well, but has little impact on the associated uncertainty when it is evenly distributed across the well. The result changes dramatically if the uncertainty is concentrated in one part of the well (Fig. 8b).
The impact of different levels of uncertainty can also be illustrated for the geological uncertainty analysis. The toe area of the horizontal well becomes more uncertain than the heel if wells PRO-5 and PRO-12 are excluded from the geological model building process (Fig. 9, Table 5). Both the average volume of oil and the uncertainty associated with it hardly changes for an IW completed with an ICV, while the the conventional well shows a reduced recovery with an increase in the impact of uncertainty of a factor 2 (Table 5).

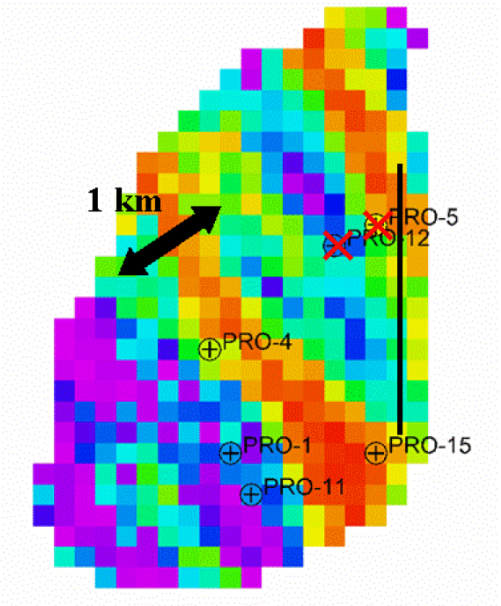


**Fig.9 Well data location for the geological parameters distribution. PUNQS3 model.**

**Table 5. Total oil production variation for geological parameters distribution with and without well's information from near the toe of the horizontal well**

| Total Production, MM $m^3$ | | | | | | | | |
|---|---|---|---|---|---|---|---|---|
| | With wells data from near the horizontal well's toe (original model) | | | | Without welldata from near the horizontal well's toe | | | |
| **Case** | P50 | P90 | P10 | Variation | P50 | P90 | P10 | Variation |
| **Base Case** | 3.91 | 3.31 | 4.35 | 10.8% | 3.79 | 3.11 | 4.47 | 18.0% |
| **ICV** | 4.16 | 3.66 | 4.52 | 8.0% | 4.22 | 3.84 | 4.59 | 8.9% |

Another situation where different levels of uncertainty within the reservoir impact the production is water or gas coning. A horizontal well designed for oil production is normally drilled above the water contact, below the gas cap or within the oil rim. Water and gas inflow into such a well can be affected by several forms of heterogeneity, e.g. a varying productivity in different parts of the well caused by formation damage skin, reservoir permeability or the heel-toe effect. This latter problem may be solved by vompleting the well with ICDs.

A second reason for heterogeneity in the breakthroughtime of unwanted fluids is a variable distribution of thin shale layers (or baffles) which are preventing / hindering vertical flow in different parts of the reservoir. This problem is often only discovered after production has commenced. A well intervention for preventing production of an unwanted fluid at this time is normally expensive (at least in terms of lost oil production).

In our example there was a shale barrier below the third interval in AINSA II model (Fig10). In the original model it had zero vertical permeability, i.e. it was a barrier. However, such thin shaly layers often allow some vertical fluid flow, i.e. they behave as a baffle rather than an absolute barrier. Hence we analysed the impact of variation of the vertical permeability of this (originally shale) layer on the oil and water production.

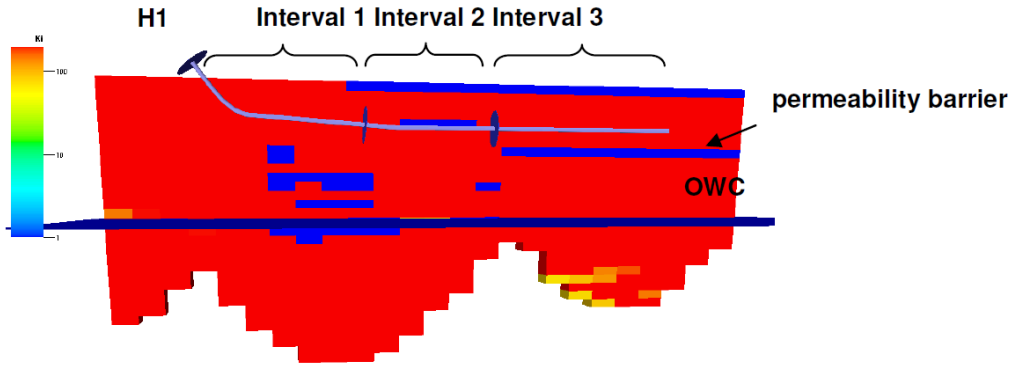


**Fig.10 Horizontal well location and permeability barrier below third interval. AINSA II model.**

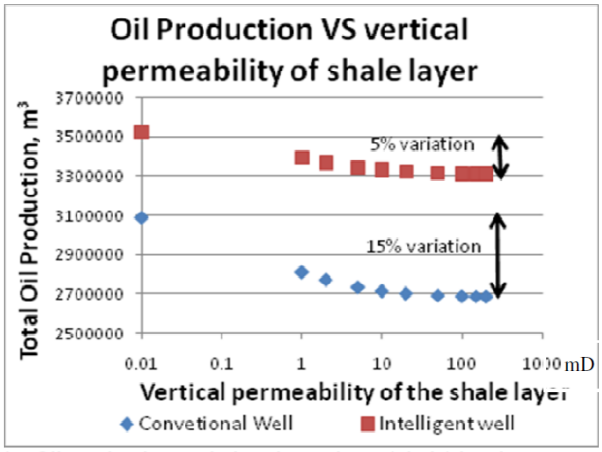


**Fig.11 – Oil production variation depends on (shale) barrier permeability**

Fig. 11 shows that even a relatively limited vertical permeability across the shale layer has a dramatic impact on the produced oil volume and the time when the water breaks through into the well. For instance, a change of vertical permeability from 0.01 mD to 1 mD reduces the oil production by 9% for conventional well and by only 3 % for the IW. In addition, the accompanying uncertainty of the IW case is reduced to 33% of that shown by the conventional completion.

## Conclusion

The impact of intelligent well with active inflow control valves to the geological and "dynamic" parameters uncertainty was investigated in this work.

1. Uncertainty of the "dynamic" parameters gives a comparable (or even larger) variation in the total oil production than uncertainty associated with the reservoir properties distribution. It cannot be ignored and must be analysed at the same time as when evaluating the impact of geological uncertainty.
2. The liquid production limit strategy application of IWT gave an increased volume of oil production coupled with decrease in its variation. In addition, the total volume of water production and its variation was decreased.
3. The IW's ability to reduce the oil and water production variation increases if different levels of uncertainty are shown within the various completion zones. The impact of local variations in parameters such as (barrier) shale transmissibility, fault transmissibility, inflated OWC or GOC can be mitigated by the installation of completions employing IW.

## Acknowledgements

One of the authors would like to thank the sponsors of the "Added Value from Intelligent Field & Well system Technology" Joint Industry Project at Heriot-Watt University for funding. Also, Schlumberger Information System's provision of the software used in this study is gratefully acknowledged.

## Nomenclature

*AQUIPerm* - average aquifer permeability
*AQUIPoro* – average aquifer porosity
$B_g$ – gas formation volume factor
$B_o$ – oil formation volume factor
$B_w$ – water formation volume factor
*GOC* – gas-oil contact
*GOR* – gas oil ratio
*ICDs* – inflow control devices
*ICVs* –interval control valves
*IW* –intelligent well
*OWC* – oil-water contact
$Q_{liq}$ – liquid production rate
$Q_{oil}$ – oil production rate
$R_s$ – dissolved gas oil ratio
*PI* – productivity index
*SFCCD* - Small Face Centred Composite Design
*SLP* – sequential linear programming
*WCT* – water cut

## References

1.Birchenko, V.M., et al., *Impact of Reservoir Uncertainty on Selection of Advanced Completion Type*, in *SPE Annual Technical Conference and Exhibition*. 2008, Society of Petroleum Engineers: Denver, Colorado, USA.

2.Al-Khelaiwi, F.T., et al., *Advanced Wells: A Comprehensive Approach to the Selection between Passive and Active Inflow Control Completions*, in *International Petroleum Technology Conference*. 2008, International Petroleum Technology Conference: Kuala Lumpur, Malaysia.

3.Birchenko, V.M., et al., *Advanced Wells: How To Make a Choice Between Passive and Active Inflow-Control Completions*, in *SPE Annual Technical Conference and Exhibition*. 2008, Society of Petroleum Engineers: Denver, Colorado, USA.

4.F. Ebadi, S., and D.R. Davies, SPE, Heriot-Watt U. , *Should "Proactive" or "Reactive" Control Be Chosen for Intelligent Well Management?* , in *Intelligent Energy Conference and Exhibition*. 2006: Amsterdam, The Netherlands.

5.Cullick, A.S. and T. Sukkestad, *Smart Operations with Intelligent Well Systems*, in *SPE Intelligent Energy Conference and Exhibition*. 2010, Society of Petroleum Engineers: Utrecht, The Netherlands.

6.M.M.J.J. Naus, D.U.o.T.D.N.D., Shell International Exploration and Production (SIEP); J.D. Jansen, DUT and SIEP, *Optimization of Commingled Production Using Infinitely Variable Inflow Control Valves* in *SPE Annual Technical Conference and Exhibition*. 2004: Houston, Texas.

7.Emerick, A.A. and R.C.M. Portella, *Production Optimization With Intelligent Wells*, in *Latin American & Caribbean Petroleum Engineering Conference*. 2007, Society of Petroleum Engineers: Buenos Aires, Argentina.

8.Yeten, B., L.J. Durlofsky, and K. Aziz, *Optimization of Smart Well Control*, in *SPE International Thermal Operations and Heavy Oil Symposium and International Horizontal Well Technology Conference*. 2002, Copyright 2002,SPE/PS-CIM/CHOA International Thermal Operations and Heavy Oil Symposium and International Horizontal Well Technology Conference: Calgary, Alberta, Canada.

9.Sarma, P., K. Aziz, and L.J. Durlofsky, *Implementation of Adjoint Solution for Optimal Control of Smart Wells*, in *SPE Reservoir Simulation Symposium*. 2005, 2005,. Society of Petroleum Engineers Inc.: The Woodlands, Texas.

10.Doublet, D.C., S.I. Aanonsen, and X.C. Tai, *An efficient method for smart well production optimisation.* Journal of Petroleum Science and Engineering, 2009. **69**(1-2): p. 25-39.
11.Aitokhuehi, I. and L.J. Durlofsky, *Optimizing the performance of smart wells in complex reservoirs using continuously updated geological models.* Journal of Petroleum Science and Engineering, 2005. **48**(3-4): p. 254-264.
12.Schlumberger, *ECLIPSE Reference Manual 2009.1.* 2009.
13.Floris, F.J.T., et al., *Methods for quantifying the uncertainty of production forecasts: a comparative study.* Petroleum Geoscience, 2001. **7**(S): p. S87-96.
14.Stephen, K.D., J.D. Clark, and G.E. Pickup, *Modeling and Flow Simulations of a North Sea Turbidite Reservoir: Sensitivities and Upscaling*, in *European Petroleum Conference*. 2002, Copyright 2002, Society of Petroleum Engineers Inc.: Aberdeen, United Kingdom.
15.Schlumberger, *Reference Manual - COUGAR Version 2009.1.* 2009.


# SPE 154472

# A Novel Optimisation Algorithm for Inflow Control Valve Management

Ivan M. Grebenkin and David R. Davies, Heriot-Watt University



This paper was prepared for presentation at the EAGE Annual Conference & Exhibition incorporating SPE Europec held in Copenhagen, Denmark, 4–7 June 2012.



## Abstract

Intelligent Wells are distinguished from conventional wells by being equipped with downhole sensors to monitor the Inflow Control Valves (ICVs) to control the (multiple) zonal flow rates. The data from the downhole sensors monitors the properties of the fluid flowing into the well from the reservoir at a zonal or a well level. The sensor data is analysed to provide the necessary information for the ICVs to be operated in the optimum manner i.e. to increase the hydrocarbon recovery and prevent unwanted fluid production.

This objective is simply stated, but the optimisation calculations required to identify the optimum ICV settings necessitates the repetitive solution of a complex, non-linear problem. Several commercial software providers have made such optimisation algorithms available to the industry to perform this task. However, experience has shown that challenges still arise when they are applied to large, complex models even though these algorithms work well on many simple cases. This is especially true when the optimisation algorithm is combined with a large, multi-well simulation model of multiple reservoirs with a complex, surface production network that is typical of those used today by operators to study real-field cases prior to field development.

Inclusion of the optimisation algorithm not only dramatically increases the calculation time (up to 50 times when compared with the equivalent run without such optimisation); but also stability and convergence problems give additional increases in the running time. More importantly, the combined software will sometimes simply stop, due to erroneous control parameters being provided by the optimisation algorithm. The optimisation algorithm may also return unrealistic results at random time intervals, a problem that can lead to unnecessary complications as it may not be immediately recognised. Such problems are particularly acute if the software is performing multiple realisations, for example when it is being applied to analyse the impact of a multiple field development scenarios or when studying how uncertainty in the reservoir's dynamic and static properties affect the field's production performance.

This paper will present a novel method based on the direct search algorithm for implementing an ICV control strategy. This method was chosen since it is not affected by the convergence problems which have caused many of the difficulties associated with previous efforts to solve our non-linear optimisation problem. Our control strategy will use the current, zonal inflow rate and water cut data to identify the optimal ICV choke positions. The availability of this data reduces the number of possible choke positions that have to be evaluated at each time step by the simulator. Run times similar to the base case are potentially possible while, equally importantly, the optimal value identified is similar to the value returned by the other published optimisation methods referred to above.

This paper outlines the assumptions made and, after exploring the method's use in two single well models for reactive control of oil production from intelligent wells completed with discrete ICVs, its application to a large, reservoir simulation model will be illustrated. The latter application could be implemented rapidly, unlike some other optimisation software, because "tuning" of the model and/or the method was not required; the control algorithm being always convergent, fast and stable.

The proposed approach is particularly valuable for the analysis of the impact of uncertainty of the reservoir's dynamic a static parameters. This arises because the modified direct search method employed here, being convergent and independent of the initial point, ensures that the result from the multiple realisations are directly comparable because "tuning" of the algorithm's parameters are not required in the middle of the calculation procedure.

## 1. Introduction

Intelligent wells have become a popular well completion option. Such wells are equipped with various kinds of sensors that allow a better understanding of the zonal reservoir properties and help to reduce uncertainty. Passive Inflow Control Devices allow equalization of the production from different zones, reduce horizontal well's "heel-toe" effect and, as a result, increase

the sweep efficiency (Birchenko et al 2009). By contrast, "active" devices – Inflow Control Valves (ICVs) - are controlled from the surface in order to reduce undesired fluid production, improve the recovery factor, avoid costly well interventions and reduce production uncertainty (Grebenkin and Davies, 2010). However, many oil companies today still do not feel confident in investing in the latter, more expensive, technology. For example, verbal reports at industry gatherings have indicated that, even when this technology has been installed in the wells, it is not always being fully utilised because field operators do not have an "easy to use" tool that allows them to determine when, and how much, the setting of a particular ICV should be changed.

A further difficulty is that the benefit of Intelligent Well (IW) technology is still not always clear at the Field Development Design stage. Partly this is because the standard simulation tools and workflows used by reservoir engineers only identify some of the IW benefits. They do not have an "easy-to-use" tool that allows them to consider the full range of possible uncertainties present in the field. Further, the standard reservoir development strategy is to place the wells in their optimal location within a chosen reservoir model. This reduces the potential benefit of IWs in that model, making them less, or even, un-profitable. However, the real reservoir will always differ from this chosen model since high levels of uncertainty always exists in the reservoir properties. This is especially true during the initial field development stages when there is insufficient information to identify the full range of Uncertainties in the reservoir data. In practice these difficulties result in wells being drilled in non-optimum locations, followed by water or gas unexpectedly coning into the well. Such problems can be solved employing the capabilities of IWs, if they have been installed. By contrast, the production performance of a lower cost conventional well (CW) option would have been disappointing with the actual production possibly being far below the expected value.

Another major difficulty is to find the optimal positions for all the many ICVs installed in the intelligent field. The optimisation problem is complex and non-linear, with the computational time required for solving this type of task increasing exponentially with the number of variables involved. Previous work has shown that there are two main types of optimisation strategy: "proactive" and "reactive"(Ebadi and Davies 2006). The "reactive" optimisation optimization strategy calls for the IW to respond to the current inflow into the well; normally the water cut (WC) or Gas Oil Ratio (GOR), in order to improve the objective function (total oil production) instantly. By contrast, a "proactive" strategy aims to change the invading front's behaviour, delay the breakthrough of any unwanted fluid and hence increase the sweep efficiency. This can be the most effective manner to optimise the cumulative production over the long-term, but it frequently involves reducing the production rate over the short-term. Hence it is not always applied.

"Proactive" methods are more complex and require even greater computational time than their "reactive" counterpart. Moreover, "proactive" strategies require reservoir data from the space between the wells if they are to identify the optimal valve settings that will delay arrival of the unwanted fluid at the wellbore. Therefore the accuracy of the initial simulation model will also strongly influence the total oil production achieved. For example, an inappropriate (early) choking strategy based on an inaccurate model can lead to a decreased oil production and an earlier breakthrough of the (unwanted) fluid front. A control strategy based on a model which is different from the real field will usually not give an optimum production strategy for the real (or truth) case. A sensitivity analysis should be carried out to reduce the impact of such uncertainty on the resulting optimisation strategy. This additional, but necessary, procedure increases even further the complexity of the optimisation task and calculation time required to solve it.

Several optimisation methods have been described in the literature. Some of them have even been realised in commercial petroleum engineering software. The simplest approach for "reactive" control is to use a two position valve which can be either open or closed according to a water-cut threshold. A more flexible policy is to employ ICVs with several valve positions that are used with such a water cut threshold which increases with time (Cullick and Sukkestad 2010). The advantage of this approach is that it is very fast and can be easily implemented. It can be used when the well is restricted by total liquid production; but the choke performance may not be optimal and there is even risk of reducing the total oil production.

Sequential linear programming is a more complex approach to production optimisation. The initial task is non-linear (Naus and Jansen 2004); hence it requires linearization after which the simplex method can be applied to find the optimum value. The individual calculation steps are fast, but this method suffers from convergence problems caused by non-linearities and oscillations. The sequential quadratic programming method employs a more accurate approximation to the Lagrangian function (Lorentzen, Shafieirad et al. 2009). However, it requires a value for the second derivative which cannot always be calculated accurately. Moreover, instability and convergence problem are still observed; especially for the cases with high number of constraints.

Gradient methods are also widely used for the optimisation of non-linear tasks, e.g. Yeten used a conjugate gradient method for production optimisation (Yeten et al. 2002). Gradient methods often have difficulties when solving constrained tasks and the solution is very dependent on the initial starting point of the calculation. The methods often provide different solutions when the calculation is started at different initial points.

This problem with algorithm convergence results in the large scale use of currently available optimisation methods often not being possible for real-field cases. The program run time often increases dramatically, the optimisation may deliver unrealistic solutions, or the calculation may be interrupted in the middle of the process. These problems become especially important when multiple-realisations are being run on a common basis, as required for production uncertainty analysis.

(Emerick and Portella 2007) used a direct search method in their work. The advantage of this method is that it does not show convergence problems. Moreover it is a good technique for optimising discreet position ICVs, a capability that is not possible when employing the standard gradient-based algorithms. However, the results achieved with this method depend on the

sequence in which the valves are selected for optimisation, resulting in the solution not always being optimal. Moreover it may take a long time to run all intermediate steps required in this algorithm before it finds the output solution. This paper uses the direct search method to develop a "reactive" control algorithm. Thealgorithm will employ the current production data, zonal liquid production and water cut, to reduce the required number of iterations. Moreover we have discovered that, with a few extra assumptions which are usually satisfied for most real field cases, the optimisation algorithm becomes fast simple and reliable.

## 2. The Algorithm's Application area

Consider a production well with N zones completed with ICVs that is controlled by a constant well head pressure (WHP). A gas cap (or free gas) is absent from the reservoir. The new liquid production rate, or operating point, after choking one of the ICVs is given by:

$$Q_{new}^{Liquid} = Q_{Open}^{Liquid} - \Delta Q_{choked}^{Liquid} + \Delta Q_{BHP}^{Liquid} + \Delta Q_{friction}^{Liquid} + \Delta Q_{gravity}^{Liquid} \quad (1)$$

Where $Q_{Open}^{Liquid}$ – is the liquid rate when all chokes are fully open.

$$\Delta Q_{choked}^{Liquid} = \sum_{i=1}^{N} a_i Q_i^{Liquid}$$

Where $\Delta Q_{choked}^{Liquid}$ is the change in the liquid rate of zone $i$ due to the additional pressure drop across the ICV and $a_i$ is a coefficient varying from 0 (when the ICV is fully open) to 1 (the ICV is fully closed). $N$ is the number of zones, each of which is separately controlled by an ICV.

$$\Delta Q_{BHP}^{Liquid} = \sum_{i=1}^{N} J_i \cdot \Delta P_{bhp}$$

Where $\Delta P_{bhp}$ is the change in the bottom hole pressure and $J_i$ is the productivity index of zone ***i***.

$$\Delta Q_{friction}^{Liquid} = \sum_{i=1}^{N} J_i \cdot \Delta P_{friction,i}$$

Where $\Delta P_{friction,i}$ is the change in the frictional pressure drop across the downhole completion area at the production interval $i$.

$$\Delta Q_{gravity}^{Liquid} = \sum_{i=1}^{N} J_i \cdot \Delta P_{gravity,i}$$

Where $\Delta P_{gravity,i}$ is the change in the pressure drop due to changes in the fluid density in the downhole completion area of the production interval $i$.

The objective function to be maximised during this particular time step is the well's current oil production rate. The objective function will be recalculated at the multiple time steps employed by the reservoir simulator. It will, at the end of the calculation, be summed to give the total field production followed by conversion to Net Present Value.

### 2.1 Assumptions Made

***Assumption 1 (A1)***

*Choking (or closing) of an ICV will always decrease the well's liquid production rate.*

This assumption implies that well's tubing is large enough to be able to produce at the maximum possible liquid production rate. Friction across the length of the tubing usually has a lower value than the hydrostatic head in liquid producing wells. I.e. the friction has a smaller influence on the well's outflow performance than the hydrostatic pressure. This situation applies in oil fields which are producing a crude oil with either a reasonably low viscosity or a high water cut. This is a reasonable assumption since the tubing diameter is normally optimised to achieve the maximum production rate from the well.

One situation where ICV closure can increase the liquid production is when there is a large difference in oil density between the various layers. Here, reducing production from a layer containing a dense oil might reduce the hydrostatic pressure sufficiently to cause an increase in the production rate. This would be an unusual case since reservoirs with very different fluid properties are not normally considered to be candidates for commingled development. ICV choking will not increase the

liquid production if the difference in oil density for various production zones is less than 100g/m$^3$. *Assumption 1* is thus satisfied.

**Assumption 2 (A2)**
*The change in the hydrostatic pressure across the completion interval due to a change in the fluid density across the completion is small compared to the total hydrostatic pressure across the length of the well is small in comparison to the other components and the term* $\Delta Q_{gravity}^{Liquid}$ *can be ignored.*

This condition is usually satisfied if the thickness of the production interval is much smaller than the depth of the reservoir. For example, a naturally flowing well with a 200 ft thick production interval at a vertical depth of 8,000 ft below the surface, shows a change in (hydrostatic) pressure across the production interval of only 2.5% compared to the total (hydrostatic) pressure to the surface. This assumption is equally valid when the well employs artificial lift.
It should be noted that this assumption is purely employed to simplify the equations and the mathematical proof of the following statements. It is not a limitation in the sense that it restricts the practical application of our approach.

**Assumption 3 (A3)**
*Changes in the acceleration pressure are small and can be ignored.*

This assumption is also used in order to simplify the mathematical proof. Nevertheless, it is true in most oil fields and applies to virtually all wells apart from low pressure gas wells.

**Assumption 4 (A4)**
*Changes in the friction pressure due to fluid flow across the production interval are small and can be ignored.*

This assumption is normally satisfied in wells that are either vertical or deviated at a low angle.
Assumptions A1 - A4 allow equation 1 to be rewritten as follows:

$$Q_{new}^{Liquid} = Q_{Open}^{Liquid} - \Delta Q_{choked}^{Liquid} + \Delta Q_{BHP}^{Liquid} \quad (2)$$

**2.2 Assumptions Reviewed**
These four assumptions indicate that our method is applicable:

1. To oil fields at pressures greater than the bubble point (free gas is absent from the reservoir).
2. For reactive control of vertical or slightly deviated wells constrained by wellhead pressure.
3. If the hydrostatic pressure is the dominant cause of the pressure loss across the well's production well tubing.
4. When friction and acceleration forces are small compared to the hydrostatic head. This allows changes in the bottom hole pressure due to operation of the ICVs to be correlated with changes in the density of the inflowing liquid.

It can be checked that assumptions A1 - A3 apply to a particular case by using nodal analysis to test all possible scenarios during production life of the well: water cut, zonal pressures, wellhead pressure, changes in artificial lift control, etc.

## 3. Methodology

The above four assumptions allow a mathematical proof to be developed for the following statements. The full mathematical proof, together with a more detailed analysis of their application area, will be published separately (Grebenkin 2012). It has not been provided here since this paper concentrates on an initial application of these assumptions to illustrate how our approach advances the field production optimisation.

### *3.1 Statement 1*

*The Zone with the highest water cut should be choked first.*

This statement specifies a unique, initial start point for the control algorithm's calculations. The algorithm will always start by examining the optimization of the ICV producing with the highest water cut. The statement also implies that choking of a zone with a lower water cut will not be beneficial if the highest water cut zone has not been fully closed.

### *3.2 Statement 2*

*The change in* $\Delta P_{BHP}$ *decreases as the ICV is opened for the Zone with the highest water cut.*

We assume that the ICV controlling zone n, the zone with the highest water cut, should be closed first. The ICVs controlling the well's inflows from all other zones remain fully open. Assumption A1 implies that the liquid rate:

$$Q^{Liquid}(\alpha) = \sum_{i \neq n}^{N} Q^{Liquid}_{i,previous} + \alpha \cdot Q^{Liquid}_{n,previous} + \sum_{i \neq n}^{N} J_i \cdot \Delta P_{BHP}(\alpha)$$

will be a monotonously increasing function (Fig 1) where $0 \leq \alpha < 1$. $\alpha = 0$ for a completely closed ICV while $\alpha = 1$ if it is fully open. The required flowing bottom hole pressure also increases as the the produced fluid's water fraction increases; increasing the hydrostatic head of the fluid column in the tubing. Fig 2 illustrates how $\Delta P_{BHP}(\alpha)$ reduces as the ICV is opened. Moreover, it can be shown that the rate of change bottom hole pressure $\{\Delta P_{BHP}(\alpha)\}$ decreases as $\alpha$ increases.

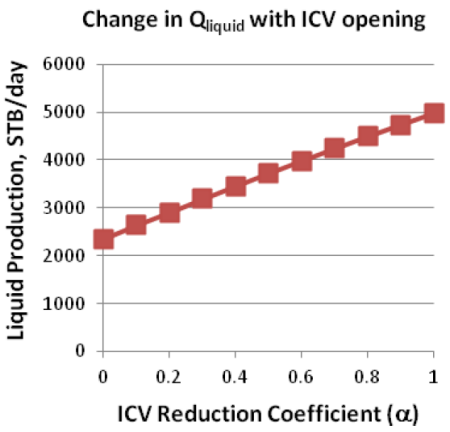


Fig 1 . Liquid production as a function of the ICV (or choke) position

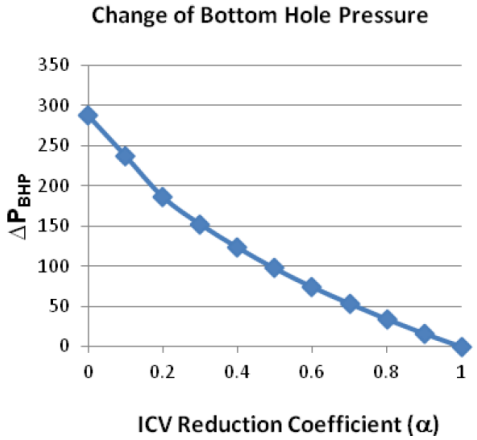


Fig 2 . The rate of change of the bottom hole pressure decreases as the ICV is progressively opened

### *3.3 Statement 3*

*If the oil production increases when the ICV is opened, then it will continue to increase if the choke is opened further.*

This statement excludes the situation where oil production starts to reduce at large ICV openings having initially increased when the ICV was first opened (Fig 3a and 3b).

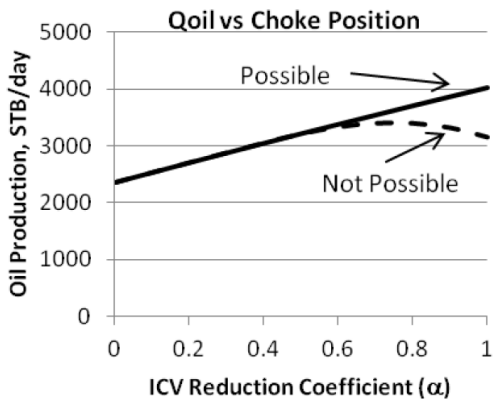


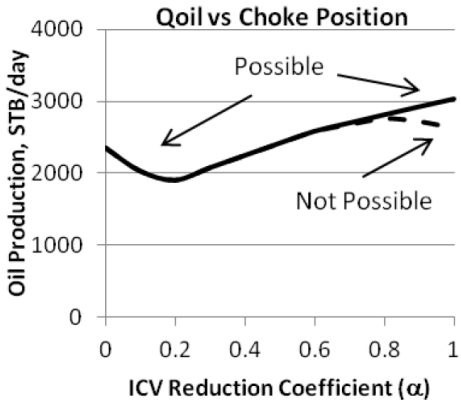


Fig3. a, b Oil production continuously increases at larger ICV openings once it begins to increase on opening the ICV

The consequence of this last statement is that the maximum oil production can be achieved only at the end points; i.e. the fully open or fully closed ICV positions. On/Off chokes should thus be installed in well which is planned to use "reactive" optimal well control and assumptions A1 - A4 are satisfied.

## 4. The Critical Water Cut Criterion

We will now examine in more detail the conditions required when need to shut zone producing water to increase the well's oil production by closing the zone with the highest water production.
The production rate from a well producing from N zones is:

$$Q_{initial}^{Liquid} = \sum_{i=1}^{N} Q_i^{Liquid}$$

$$Q_{initial}^{Oil} = \sum_{i=1}^{N} Q_i^{Liquid}(1-WC_i) = \sum_{i\neq n}^{N} Q_i^{Liquid}(1-WC_i) + Q_n(1-WC_n)$$

with the highest water cut (WC) being observed in zone ***n***. The new production rate on closing this zone is:

$$Q_{New}^{Liquid} = \sum_{i\neq n}^{N} Q_i^{Liquid} + \Delta P_{BHP} \sum_{i\neq n}^{N} J_i$$

$$Q_{New}^{Oil} = \sum_{i\neq n}^{N} Q_i^{Liquid}(1-WC_i) + \Delta P_{BHP} \sum_{i\neq n}^{N} J_i(1-WC_i)$$

$$Q_{New}^{Oil} \geq Q_{initial}^{Oil} \Leftrightarrow \Delta P_{BHP} \sum_{i\neq n}^{N} J_i(1-WC_i) \geq Q_n(1-WC_n) \Leftrightarrow$$

$$WC_n \geq 1 - \frac{\Delta P_{BHP} \sum_{i\neq n}^{N} J_i(1-WC_i)}{J_n \cdot dP_n}$$

where $dP_n$ is a drawdown of zone ***n***.

The value of the term $1 - \frac{\Delta P_{BHP} \sum_{i\neq n}^{N} J_i(1-WC_i)}{J_n \cdot dP_n}$ provides the objective function criterion for the optimisation algorithm.

We will call this value the *Critical Water Cut* (CWC) for zone n: $WC_n^{Critical}$. The ICV should be closed if the current WC exceeds this value, otherwise it should remain open.

## 5. Case Study

### 5.1 Case1: 2 Zones, Vertical Production Well

Our first, relatively simple, case concerns a vertical, gas-lifted well operated at a fixed well head pressure 230 psi while producing from two, separate reservoir intervals (Fig 4).

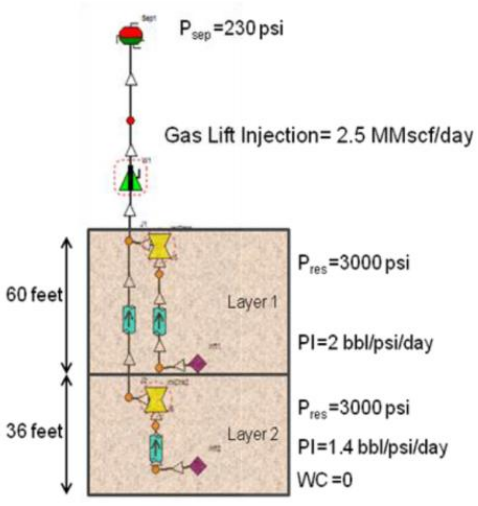


**Fig 4 . Case 1: Well description**

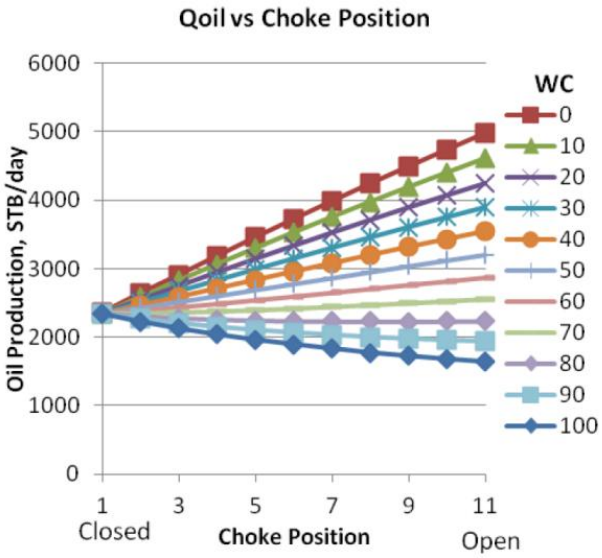


**Fig 5 . Oil production rate depends on the Zone 1 ICV position**

Zone 2 of this well is producing dry (or zero percent WC) oil. Water production is observed from Zone 1 which is completed

with an ICV that can select from 11 fixed positions. We wish to calculate the preferred ICV setting at which zone 1 should be operated to maximise the well's total oil production {i.e. identify the optimal position for ICV 1}. Nodal analysis was used to calculate the well's operating point for each value of the choke position as a function of the zone 1 WC when it was varied from zero to hundred percent (Fig. 5). The well's maximum oil production rate from both zones was achieved with the zone 1 ICV being either fully open for zone 1 WCs being less than 74%; or fully closed for all higher WCs. I.e. 74% water cut was the CWC value at which zone 1 should be fully closed in order to maximise the well's total oil production rate. In other words, the total oil production rate from both zones will be less than that from interval 2 alone if the zone 1 WC exceeds the CWC and zone 1 is allowed to continue to produce.
The CWC can be calculated once the operating point of the fully open ICV is known:

$$WC^{Critical} = 1 - \frac{\Delta P_{BHP} \cdot J_2}{Q_{1,Open}^{Liquid}}$$

The term $\Delta P_{BHP}$ in this equation can be found from well's Vertical Lift Performance based on the current WC in each zone. The CWC value will vary with the current WC of zone 1. The WC equalling the CWC value equals provides us with the required optimisation criteria to close the production zone ICV with the highest WC. In this example we calculate exactly the same 74% as was previously found (Fig 6).

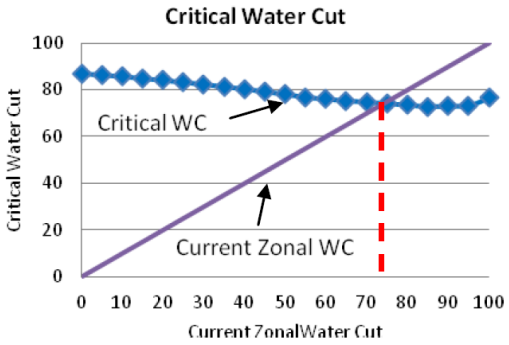


**Fig 6 . Critical Water Cut value depends on the current, zonal Water Cut**

### 5.2 Case2: A 4 Zone, Vertical Production Well

Our case 2 is a more complex single well study. The well has 4 production zones with different productivity indices, reservoir pressures and water cuts (Fig 7).
The control algorithm identifies the zone with the highest WC for each iteration of the reservoir simulator. It then calculates the CWC for this zone and checks to see if closing this zone improves the well's total oil production from the remaining zones. This "Direct Check" (DC) method allows us to evaluate if the CWC criterion is making the correct decision (Fig. 9 and 10).
Layer 4 has the highest WC (90%), and hence will be the first one to be closed. The CWC is calculated to be equal to 43%, indicating that this zone should be closed. A DC confirms that closing this zone increases the oil production rate from 7,146 to 7,533 Stb/day (Fig 9).

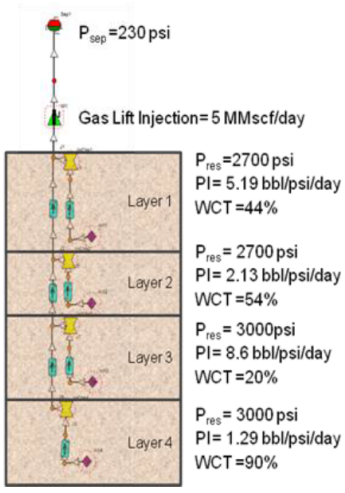


**Fig 7. Case 2 well description**

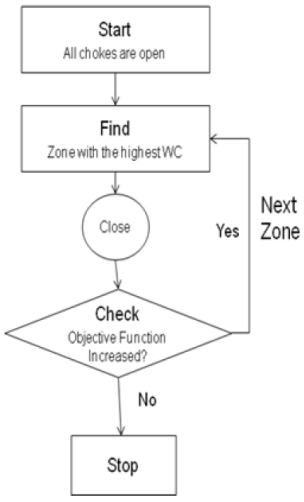


**Fig 8. Control algorithm flow chart**

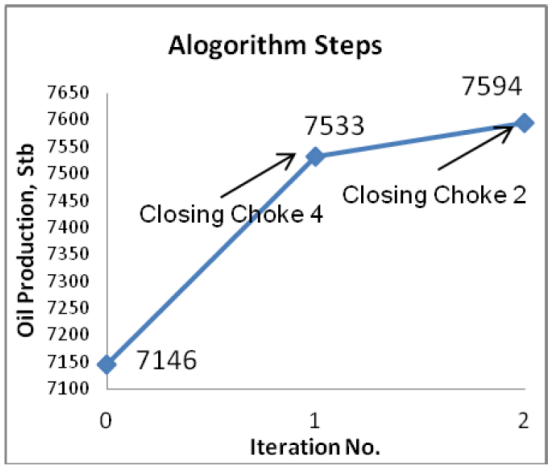


Fig 9. Oil production rate increases with each iteration of the algorithm

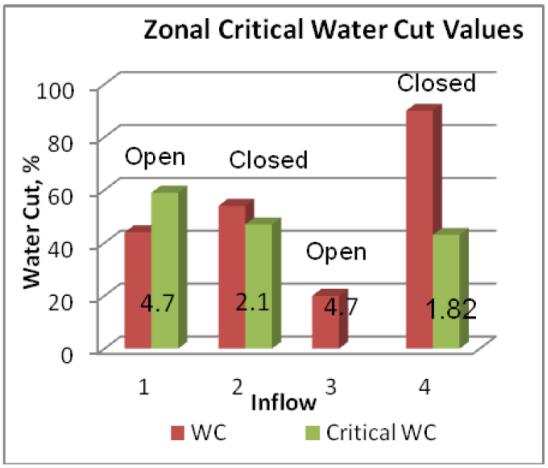


Fig 10. Critical Water Cut values and ICV positions after optimisation with commercial, network optimisation software

The process (or algorithm) was repeated for zone 2 which has a current WC value of 54%. Once again, the current WC is higher than the critical value; hence closing this zone will also increase the total oil production rate. Zone 1, the next zone to be evaluated, is producing at 44% WC, which is lower than the critical value of 59%. Closing this zone leads to the oil production reducing from 7,594 to 7,091 Stb/day; confirming that only inflows with a current water cut higher than the critical value should be closed.

We compared the above CWC algorithm results with the values provided by a commercial, network optimisation software. Fig. 10 shows the choke diameters chosen by this commercial software for each ICV. The initial (fully open) ICV diameter for all zones is 4.7 inches (i.e. the fully open ICV does not restrict the inflow into the 4.7 inch diameter tubing). The commercial software reduced the ICV diameters for zones 2 and 4. This is in agreement with part of our conclusion, that these ICVs are the ones which should be choked. Nevertheless, the commercial software's optimisation algorithm does not close them completely, resulting in a production rate of 7,147 Stb/day. This marginal improvement on the initial value of 7,146 Stb/day is considerably less than the optimal value of 7,594 Stb/day identified by the CWC algorithm.

### 5.3 Case 3: A full-scale, simulation and optimisation study of a real-field with 10 Conventional and 3 Intelligent Wells with 3 or 4 ICVs each

#### *5.3.1 Model Description*

The control algorithm has also been tested on a large, complex full-scale field reservoir simulation model. The modelled field contains two main reservoirs which partly overlay each other for a significant fraction part of the field area (schematically shown in Fig. 11). Each of these layers is further divided into two parts which may or may not be hydraulically connected. The thickness of one of the reservoirs varies from 30 - 60 ft; while the other is significantly thicker at 50 - 150 ft. Both reservoirs are contained within a 15 x 4 km rectangle. The resulting dynamic reservoir simulation model has 200,000 active cells. There is no production history since the field has not yet been developed.

Added complexity to the geological model results from several faults of unknown transmissibility being observed on seismic within the field boundaries. The porosity of both reservoirs is in the range of 15 to 25% with the corresponding permeability of one of the reservoir varying over a relatively small range of 250 - 650 mD; while core analysis of the other one suggested the much greater permeability range of 150 – 1300 mD.

There is currently no evidence for pressure support by an aquifer to the upper layer, though good aquifer pressure support to the lower layer is judged to have a high probability. The fluid properties of both reservoirs are similar, containing a light (40° API) oil with a GOR of approximately 300 scf/bbl. Both reservoirs are normally pressured. A gas cap has not been observed.

It is planned to drill CWs in those parts of the field where the two reservoirs do not overlap. IWs to manage commingled production from both reservoir layers (Fig. 11 and 12) can be installed in the "overlap" reservoir area. Both the CWs and the IWs will be equipped with gas lift to aid production. The production and injection systems were modelled in a commercial network management and optimisation software. This was connected to the above reservoir simulation model which had been prepared using software from a second, commercial provider. The network management and optimisation software was also used to control and optimise the wellhead chokes. It also optimised the downhole chokes when and the CWC Algorithm was not being employed.

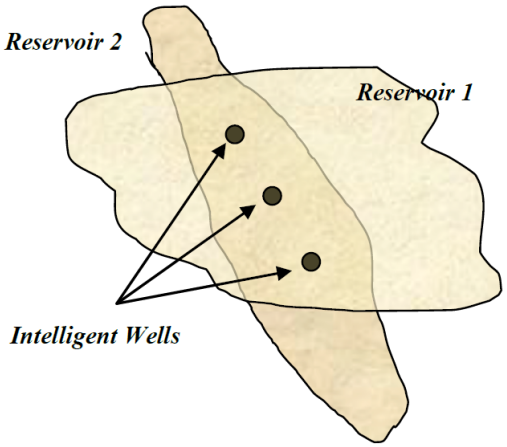


Fig 11 . Schematic description of the field area

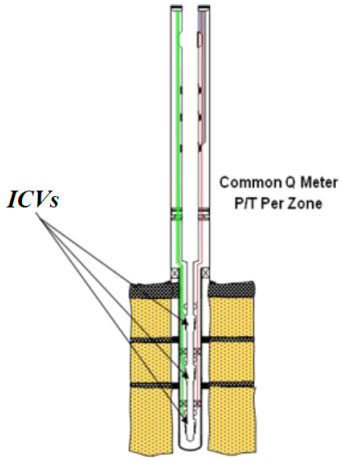


Fig 12 . Three or Four Zones With Zonal Isolation Upper and Lower Reservoir

### *5.3.2 Instant Production Control*

Control of the 11 ICVs installed in the 3 Intelligent Production Wells (Fig.11 & 12) used the same control philosophy as described for case 2: the ICV inflow showing the highest water cut value in each production well is checked to see if the CWC value calculated for this zone has been exceeded (Fig 13). The ICV for this zone is then closed if the zonal WC is higher than the calculated CWC value for this zone.

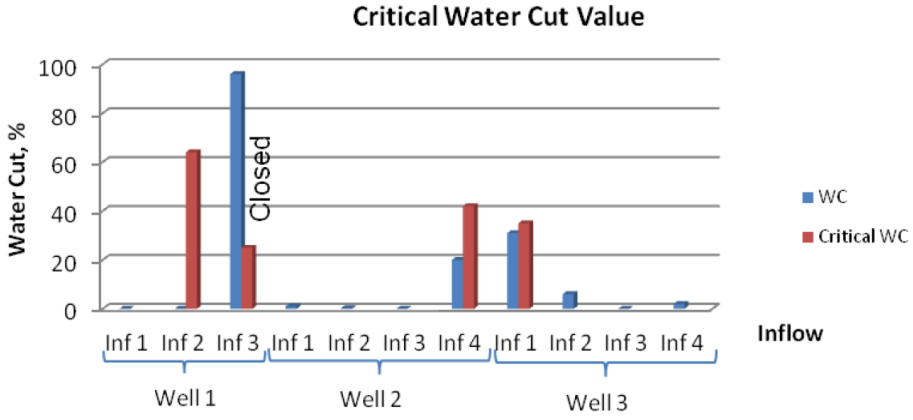


Fig 13 . Critical Water Cut Values for all IW inflow Zones

Our CWC Control Algorithm showed a higher oil production rate during the decline period, when the field is off-plateau, compared to both the reservoir simulator on its own with all ICVs fully open and the commercial network optimisation software (Table 1).

| Case | Field Oil Production Rate from 13 wells |
|---|---|
| Reservoir simulation with all ICVs fully open | $79.3*10^3$ Stb/day |
| Commercial network optimisation software | $79.6*10^3$ Std/day |
| "Critical-Water-Cut" Control Algorithm | $82.7*10^3$ Stb/day |

Table 1. Example field production during the decline period when the field is off-plateau

This study was repeated a number of times by stopping the simulation and then optimising the "Real-Time" or "Instantaneous" production using either the:

(1) Commercial network optimisation software for the complete production system (downhole, wellhead and surface network) and

(2) CWC for the downhole chokes and the commercial software for the wellhead chokes etc.
In all cases studied the CWC gave a slightly higher oil production rate

### *5.3.3 Simulation Run in Time*

The combined reservoir and optimisation model was run for a 30 year period. The above control philosophy, appliyng the DC algorithm at every (monthly) time step was performed. The CWC values for the ICVs that were candidats for closure were then calculated.

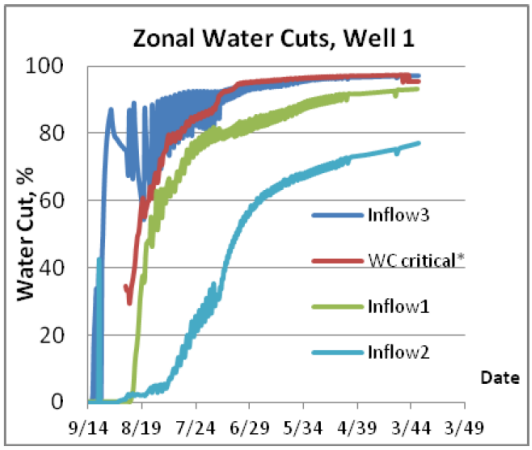


**Fig 14 . Zonal Water Cuts for I-Well 1 (3 zones)**

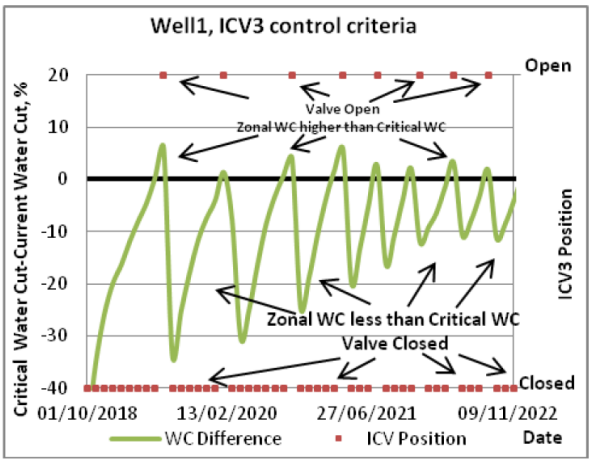


**Fig 15 a . "Critical -Water-Cut" Algorithm closes the ICV when the current WC is higher than the critical value**

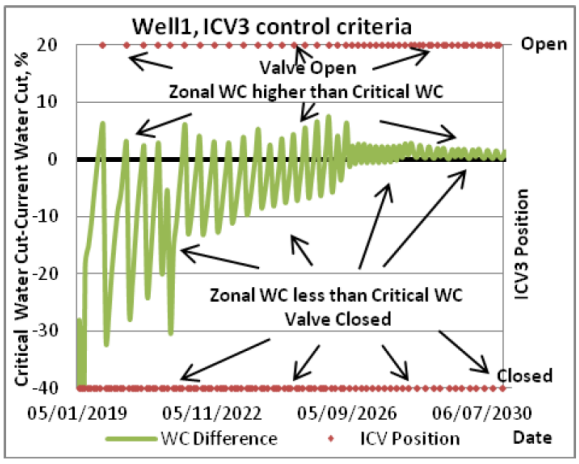


**Fig 15 b . The critical water cut value increases with time, hence the ICV is frequently opened**

Fig 14, the zonal WC for well 1, is a typical example of an IW inflow performance plot over the field's lifetime. It can be seen that zone 3 has the highest WC during whole production period; hence it was checked for closing at every time step. Fig. 15a & 15b illustrate that the ICV was open whenever the water cut was less than critical value. It was closed at all other times.

| Case | Change in Cumulative Oil Production | Change in Cumulative Water Production |
|---|---|---|
| Base Case Reservoir simulator only with all ICVs fully open | 100% | 100% |
| Commercial network optimisation software | 101.44% (+1.44%) | 98.47% (- 1.63%) |
| "Critical-Water-Cut" Control Algorithm | 101.25% (+1.25%) | 97.93% (-2.07%) |
| Reservoir simulation with conventional wells (16 producers) | 102.11% (+2.11%) | 101.01% (+1.01%) |

**Table 2. Changes in Cumulative Oil and Water production for different scenarios**

The normalized production rates and the corresponding cumulative oil and water production are shown in Fig. 16 and 17 with the results being summarised in Table 2.

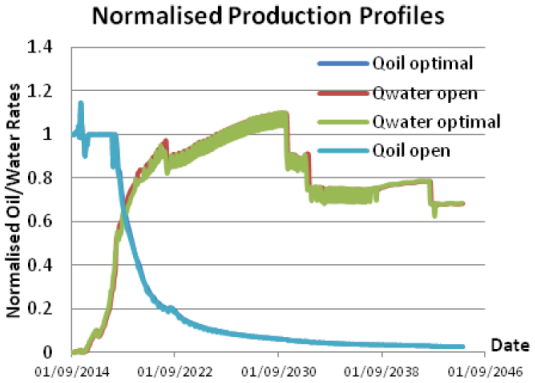


**Fig 16 . Normalised Oil and Water Rates for (1) Fully Open ICVs and (2) ICVs Optimised with the "Critical Water Cut" Algorithm**

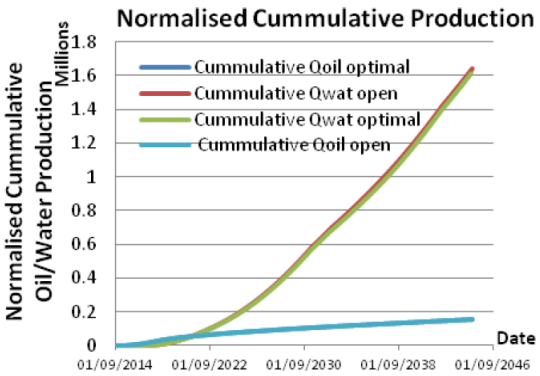


**Fig 17 . Normalised Cumulative Oil and Water Production for (1) Fully Open ICVs and (2) ICVs Optimised with the "Critical Water Cut" Algorithm**

Both optimisation methods improved the field oil production by more than 1%. Surprisingly the optimisation algorithm based on the CWC shows better "instantaneous" results than the commercial optimiser at each time step, while the cumulative oil production was slightly less.

This could be caused by several reasons, the most likely being that the reservoir pressure behaviour for the two cases is different (Fig. 18). The water injection was controlled to maintain the regional pressures over several of the reservoir's regions. The necessary changes in the injection well rates proceeded as a reaction to the current pressure conditions, but only after some delay. The target reservoir pressures are not achieved during periods of high or rapidly changing production when there is a lag in pressure compensation. The CWC case achieved a constant pressure of 3,250 ± 40 psi considerably earlier that the commercial software. The drawdown of the CWC case's production wells during the period when the commercial optimiser had a significantly higher reservoir pressure would have been significantly lower.

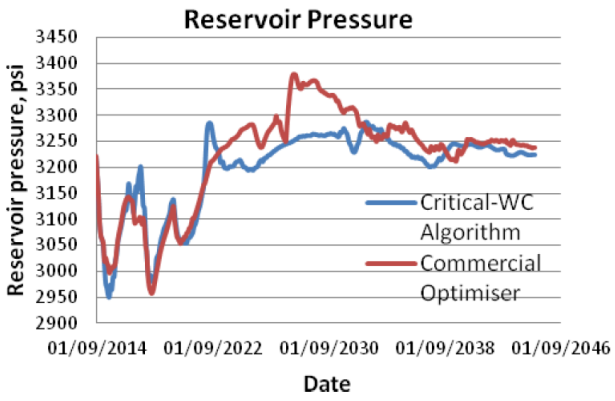


**Fig 18 . Reservoir Pressure for Commercial Optimisation and "Critical –Water-Cut" Algorithm Cases**

Another reason may be a difference in network optimiser performance for the two cases. Nevertheless, the total oil productions for both approaches are very similar.

The two approaches differ in terms of the running time for the simulation. The CWC algorithm's runtime was 1.4 times longer than in the base case without downhole optimisation (Table 3); while the commercial optimiser increased the runtime by a factor of 1.8.The number of iterations required by CWC algorithm are much required compared to this commercial optimiser. The CWC optimisation was realised with a Visual Basic script in Excel which was connected to the production system. Data exchange between these two modules was required at every optimisation iteration. This is a slow process which has significantly increased the running time. Based on the number of iterations required, it is reasonable to expect that the CWC algorithm will require only a 10% increase in the run time (~1,000 s) once it has been built in into commercial module.

| Case | Reservoir simulation with all ICVs fully open | Commercial network optimisation software | "Critical-Water-Cut" Control Algorithm |
|---|---|---|---|
| Running Time, sec | 9,600 s | 17,000 s | 13,500 s |

**Table 3.Running Time for "Fully Open", Commercial Optimiser and CWC algorithm scenarios**

The initial reservoir simulation case with separate production of two reservoirs using 16 CWs shows a 0.9% higher cumulative oil production and 2.5% extra water production than the (10 CWs + 3 IWs) case. Nevertheless, economic analysis shows that latter development option for this subsea field in 100 m water depth located in a mature area had a greater NPV, mainly due to the reduced capital investment required. Moreover, as shown previously by (Grebenkin and Davies 2010), the operational flexibility of the intelligent completion can reduce the impact of unexpected events (e.g. fast water breakthrough) and reduce production uncertainty.

## 6. Conclusion

1. The critical water cut criterion has been developed for the optimal "reactive" control of vertical wells producing with a well head pressure constraint. The four, basic assumptions required for the criterions application have been defined, explored, tested and shown to be applicable to many, if not the majority, of practical cases.
2. The critical water cut criterion's applicability for a particular case can always be checked by nodal analysis combined with sensitivity analysis for possible scenarios during the well's production life.
3. It was shown an On/Off valve ICV completion is sufficient for optimal reactive production performance once the above assumptions have been satisfied.
4. The critical water cut method is a modified version of the direct search optimisation method. It is fast, stable and convergent while providing a well defined, initial starting point for the iterative, optimisation, calculation process.
5. "Reactive" well control using an algorithm based on the "zonal critical water cuts" was illustrated by optimisation of the production from a :
    a. Simple and a more complex single well case and
    b. Large, complex, real field simulation model containing 10 conventional wells and 3 multi-zone intelligent wells over a 30 year time span.
6. The latter case confirmed that the algorithm is fast, simple to implement, did not have convergence problem while achieving similar results to a commercially available optimizer. In addition, it reduced the computer run time.
7. This initial study is promising, but further work is required to investigate and extend its application area. However, it may already be concluded that it is a prime candidate for the:
    a. Prediction of the optimised oil production from well number, location and completion scenarios during Field Development Planning. It is particularly useful for the investigation of the impact of an intelligent completion on the production uncertainty since the algorithm is fast, stable and convergent while providing a single-valued solution which is independent on the initial point of optimisation.
    b. Real Time optimisation of the downhole ICV settings for optimal "reactive" control of vertical wells producing with a well head pressure constraint.

## 7. Acknowledgements

The authors wish to acknowledge funding provided by the sponsors of the "Added Value from Intelligent Field & Wells system Technology" Joint Industry Project at Heriot-Watt University, Edinburgh, U.K. Schlumberger Information Systems, Weatherford EPS and Petroleum Experts are gratefully acknowledged for their generous provision of software. In addition, the latter's contribution of a high-level support contributed greatly to the success of the project.

## 8. Nomenclature

*CWC* – critical water cut
*CWs*- conventional wells
*DC*-Direct Check
*GOR* – gas oil ratio
*ICVs* –interval control valves
*IW* –intelligent well
*Ji* –productivity index of zone i
$\Delta PBHP$ –bottom hole pressure change
*PI*–productivity index
*Pres* – reservoir pressure
*Q* - production rate
*WC* – water cut

## 9. References

Birchenko, V.M. Usnich A. I. B., A.V., Davies D.R. (2009). "Application of Inow Control Devices to Heterogeneous Reservoirs." Journal of Petroleum Science and Engineering.

Cullick, A. S. and Sukkestad T. (2010). Smart Operations with Intelligent Well Systems. SPE Intelligent Energy Conference and Exhibition. Utrecht, The Netherlands, Society of Petroleum Engineers.

Emerick, A. A. and Portella R. C. M. (2007). Production Optimization With Intelligent Wells. Latin American & Caribbean Petroleum Engineering Conference. Buenos Aires, Argentina, Society of Petroleum Engineers.

Ebadi, F. and Davies D.R. (2006). Should "Proactive" or "Reactive" Control Be Chosen for Intelligent Well Management? . Intelligent Energy Conference and Exhibition. Amsterdam, The Netherlands.

Grebenkin, I. (2012). Added Value of IWFsT from Uncertainty Influence. Reduction. PhD Thesis , Heriot-Watt University, Edinburgh, U.K. (in preparation)

Grebenkin, I. and Davies D. R. (2010). Analysis of the Impact of an Intelligent Well Completion on the Oil Production Uncertainty. SPE Russian Oil and Gas Conference and Exhibition. Moscow, Russia, Society of Petroleum Engineers.

Lorentzen, R. J., Shafieirad A., et al. (2009). Closed Loop Reservoir Management Using the Ensemble Kalman Filter and Sequential Quadratic Programming. SPE Reservoir Simulation Symposium. The Woodlands, Texas, Society of Petroleum Engineers.

Naus, M.M.J.J.and Jansen J.D., (2004). Optimization of Commingled Production Using Infinitely Variable Inflow Control Valves SPE Annual Technical Conference and Exhibition. Houston, Texas.

Yeten, B., Durlofsky L. J., et al. (2002). Optimization of Smart Well Control. SPE International Thermal Operations and Heavy Oil Symposium and International Horizontal Well Technology Conference. Calgary, Alberta, Canada, Copyright 2002,SPE/PS-CIM/CHOA International Thermal Operations and Heavy Oil Symposium and International Horizontal Well Technology Conference.

# References


Abduldayem M. A., Shafiq M., et al. (2007). Intelligent Completions Technology Offers Solutions to Optimize Production and Improve Recovery in Quad–Lateral Wells in a Mature Field. SPE 110960, SPE Saudi Arabia Section Technical Symposium, Dhahran, Saudi Arabia, Society of Petroleum Engineers.

Addiego-Guevara E., Jackson M. D., et al. (2008). Insurance Value of Intelligent Well Technology Against Reservoir Uncertainty. SPE 113918, SPE/DOE Symposium on Improved Oil Recovery, Tulsa, Oklahoma, USA, Society of Petroleum Engineers.

Aitokhuehi I. and Durlofsky L. J. (2005). "Optimizing the performance of smart wells in complex reservoirs using continuously updated geological models." Journal of Petroleum Science and Engineering **48**(3-4): 254-264.

Ajayi A. A. and Konopczynski A. A. (2007). Theory and Application of Probabilistic Method of Designing Customized Interval Control Valves Choke Trim for Multizone Intelligent Well Systems. SPE 110600, SPE Annual Technical Conference and Exhibition, Anaheim, California, U.S.A., Society of Petroleum Engineers.

Ajayi A. A., Mathieson D., et al. (2005). An Innovative Way of Integrating Reliability of Intelligent Well Completion System with Reservoir Modelling. SPE 94400, Offshore Europe, Aberdeen, United Kingdom, Society of Petroleum Engineers.

Akram N., Hicking S., et al. (2001). Intelligent Well Technology in Mature Assets. SPE 71822, Offshore Europe, Aberdeen, United Kingdom, Society of Petroleum Engineers Inc.

Al-Khelaiwi F. T., Birchenko V. M., et al. (2008). Advanced Wells: A Comprehensive Approach to the Selection between Passive and Active Inflow Control Completions. IPTC 12145, International Petroleum Technology Conference, Kuala Lumpur, Malaysia, International Petroleum Technology Conference.

Al-Khelaiwi F. T., Davies D. R., et al. (2007). Successful Application of a Robust Link to Automatically Optimise Reservoir Management of a Real Field. SPE 107171, EUROPEC/EAGE Conference and Exhibition, London, U.K., Society of Petroleum Engineers.

Alghareeb Z., Horne Z., et al. (2009). Proactive Optimization of Oil Recovery in Multilateral Wells Using Real Time Production Data. SPE 124999, SPE Annual Technical Conference and Exhibition, New Orleans, Louisiana, Society of Petroleum Engineers.

Alhuthali A. H. H., Datta-Gupta A., et al. (2008). Optimal Rate Control Under Geologic Uncertainty. SPE 113628, SPE/DOE Symposium on Improved Oil Recovery, Tulsa, Oklahoma, USA, Society of Petroleum Engineers.

Almeida L. F., Tupac Y. J., et al. (2007). Evolutionary Optimization of Smart-Wells Control Under Technical Uncertainties. SPE 107872 Latin American & Caribbean Petroleum Engineering Conference, Buenos Aires, Argentina, Society of Petroleum Engineers.

Arenas E. and Dolle N. (2003). Smart Waterflooding Tight Fractured Reservoirs Using Inflow Control Valves. SPE 84193, SPE Annual Technical Conference and Exhibition, Denver, Colorado, Society of Petroleum Engineers.

Batocchio M. A. P., Triques A. L. C., et al. (2010). Case History - Steam Injection Monitoring with Optical Fiber Distributed Temperature Sensing. SPE 127937, SPE Intelligent Energy Conference and Exhibition, Utrecht, The Netherlands, Society of Petroleum Engineers.

Beggs H. D. (1991). Production optimization using NODAL analysis.

Beggs H. D. and Brill J. P. (1973). "A Study of Two Phase Flow in Inclined Pipe." *JPT*: 606-617.

Berg F. G. V. D., Perrons R. K., et al. (2010). Business Value From Intelligent Fields. 128245, SPE Intelligent Energy Conference and Exhibition, Utrecht, The Netherlands, Society of Petroleum Engineers.

Birchenko V. M., Al-Khelaiwi F. T., et al. (2008). Advanced Wells: How To Make a Choice Between Passive and Active Inflow-Control Completions. SPE 115742, SPE Annual Technical Conference and Exhibition, Denver, Colorado, USA, Society of Petroleum Engineers.

Birchenko V. M., Bejan A. I., et al. (2011). "Application of inflow control devices to heterogeneous reservoirs." Journal of Petroleum Science and Engineering **78**(2): 534-541.

Birchenko V. M., Demyanov V., et al. (2008). Impact of Reservoir Uncertainty on Selection of Advanced Completion Type. SPE 115744, SPE Annual Technical Conference and Exhibition, Denver, Colorado, USA, Society of Petroleum Engineers.

Brouwer D. R. and Jansen J. D. (2002). Dynamic Optimization of Water Flooding with Smart Wells Using Optimal Control Theory. SPE 78278, European Petroleum Conference, Aberdeen, United Kingdom, Society of Petroleum Engineers Inc.

Brown G. A., Kennedy B., et al. (2000). Using Fibre-Optic Distributed Temperature Measurements to Provide Real-Time Reservoir Surveillance Data on Wytch Farm Field Horizontal Extended-Reach Wells. SPE 62952, SPE Annual Technical Conference and Exhibition, Dallas, Texas, Society of Petroleum Engineers Inc.

Bryan D. (2006). The Weibull Analysis Handbook, ASQ Quality Press.

Burda B., Crompton J., et al. (2007). Information Architecture Strategy for the Digital Oil Field. SPE 106687, Digital Energy Conference and Exhibition, Houston, Texas, U.S.A., Society of Petroleum Engineers.

Chen Y., Oliver D. S., et al. (2009). "Efficient Ensemble-Based Closed-Loop Production Optimization." SPE Journal **14**(4): 634-645.

Cramer H. (1946). Mathematical Methods of Statistics, Princeton University Press.

Cullick A. S. and Sukkestad T. (2010). Smart Operations with Intelligent Well Systems. SPE 126246, SPE Intelligent Energy Conference and Exhibition, Utrecht, The Netherlands, Society of Petroleum Engineers.

Davidson J. E. and Beckner B. L. (2003). "Integrated Optimization for Rate Allocation in Reservoir Simulation." SPE Reservoir Evaluation & Engineering **6**(6): 426-432.

Davies D. R. and Aggrey G. H. (2007). A Rigorous Stochastic Coupling of Reliability and Reservoir Performance When Defining the Value of Intelligent Wells. SPE 107197, Offshore Europe, Aberdeen, Scotland, U.K., Society of Petroleum Engineers.

Dehdari V. and Oliver D. S. (2011). Sequential Quadratic Programming (SQP) for Solving Constrained Production Optimization --- Case Study from Brugge field. SPE 141589, SPE Reservoir Simulation Symposium, The Woodlands, Texas, USA.

Dezen F. and Morooka C. (2001). Field Development Decision Making Under Uncertainty: A Real Option Valuation Approach. SPE 69595, SPE Latin American and Caribbean Petroleum Engineering Conference, Buenos Aires, Argentina, Society of Petroleum Engineers Inc.

Dezen F. and Morooka C. (2002). Alternatives for Deepwater Field Developments: A Real Option Approach. OTC 14205, Offshore Technology Conference, Houston, Texas, USA.

Dilib F. A. and Jackson M. D. (2012). Closed-loop Feedback Control for Production Optimization of Intelligent Wells under Uncertainty. SPE 150096, SPE Intelligent Energy International, Utrecht, The Netherlands, Society of Petroleum Engineers.

Doublet D. C., Aanonsen S. I., et al. (2009). "An efficient method for smart well production optimisation." Journal of Petroleum Science and Engineering **69**(1-2): 25-39.

Drakeley B. K., Douglas N. I., et al. (2003). "Application of Reliability Analysis Techniques to Intelligent Wells." SPE Drilling & Completion **18**(2): 159-168.

Duns H. and Ros N. C. J. (1963). Vertical flow of gas and liquid mixtures in wells. WPC 10132, World Petroleum Congress.

Ebadi F. and Davies D. R. (2006). Should "Proactive" or "Reactive" Control Be Chosen for Intelligent Well Management? . SPE 99929, Intelligent Energy Conference and Exhibition, Amsterdam, The Netherlands.

Elmsallati S. M. and Davies D. R. (2005). Automatic Optimisation of Infinite Variable Control Valves. SPE 10319, International Petroleum Technology Conference, Doha, Qatar, International Petroleum Technology Conference.

Emerick A. A. and Portella R. C. M. (2007). Production Optimization With Intelligent Wells. SPE 107261, Latin American & Caribbean Petroleum Engineering Conference, Buenos Aires, Argentina, Society of Petroleum Engineers.

Emerick A. A. and Reynolds A. C. (2010). EnKF-MCMC. SPE 131375, SPE EUROPEC/EAGE Annual Conference and Exhibition, Barcelona, Spain, Society of Petroleum Engineers.

Evensen G. (2003). "The Ensemble Kalman Filter: theoretical formulation and practical implementation." Ocean Dynamics **53**(4): 343-367.

Evensen G., Hove J., et al. (2007). Using the EnKF for Assisted History Matching of a North Sea Reservoir Model. SPE 106184, SPE Reservoir Simulation Symposium, Houston, Texas, U.S.A., Society of Petroleum Engineers.

Faiz S. (2001). "Real-Options Application: From Successes in Asset Valuation to Challenges for an Enterprisewide Approach." Journal of Petroleum Technology **53**(1): 42-47, 74.

Fancher. G. H. and Brown K. E. (1963). Prediction of Pressure Gradients for Multiphase Flow in Tubing.

Floris F. J. T., Bush M. D., et al. (2001). "Methods for quantifying the uncertainty of production forecasts: a comparative study." Petroleum Geoscience **7**(S): 87-96.

Gai H. (2002). A Method to Assess the Value of Intelligent Wells. SPE 77941, SPE Asia Pacific Oil and Gas Conference and Exhibition, Melbourne, Australia, Society of Petroleum Engineers Inc.

Gao C., Rajeswaran T., et al. (2007). A Literature Review on Smart Well Technology. SPE 106011, Production and Operations Symposium, Oklahoma City, Oklahoma, U.S.A., Society of Petroleum Engineers.

Glandt C. A. (2005). "Reservoir Management Employing Smart Wells: A Review." SPE Drilling & Completion **20**(4): 281-288.

Grebenkin I. M. and Davies D. R. (2010). Analysis of the Impact of an Intelligent Well Completion on the Oil Production Uncertainty. SPE 136335, SPE Russian Oil and Gas Conference and Exhibition, Moscow, Russia, Society of Petroleum Engineers.

Hagedorn A. R. and Brown K. E. (1965). Experimental Study of Pressure Gradients Occurring During Continuous Two-Phase Flow in Small-Diameter Vertical Conduits.

Han J. T. (2003). There is Value in Operational Flexibility: An Intelligent Well Application. SPE 82018, SPE Hydrocarbon Economics and Evaluation Symposium, Dallas, Texas, Society of Petroleum Engineers.

Han J. T., Rajagopalan S., et al. (2002). SMARTWELL® VALUATION USING REAL OPTIONS ANALYSIS. WPC 32151, Rio de Janeiro, Brazil, World Petroleum Congress.

Hasan A. I., Ciaurri D. E., et al. (2009). Discrete Optimization of Oil Production in Thin Oil Rim Reservoir under Geological Uncertainty. SPE 123989, SPE.

Hauser M. K. and Gilman H. (2008). Evolution of Decision Environments: Lessons Learned From Global Implementations and Future Direction of Decision Environments. SPE 112215, Intelligent Energy Conference and Exhibition, Amsterdam, The Netherlands, Society of Petroleum Engineers.

He J., Sarma P., et al. (2011). Use of Reduced-order Models for Improved Data Assimilation within an EnKF Context. SPE 141967, SPE Reservoir Simulation Symposium, The Woodlands, Texas, USA, Society of Petroleum Engineers.

Hother J. (2003). The First Year's Achievements of the Intelligent Well Reliability Group. OTC 15192, Offshore Technology Conference, Houston, Texas, USA.

Jackson-Nielsen V. B., Piedras J., et al. (2001). Aconcagua, Camden Hills, and King's Peak Fields, Gulf of Mexico Employ Intelligent Completion Technology in Unique Field Development Scenario. SPE 71675, SPE Annual Technical Conference and Exhibition, New Orleans, Louisiana, Society of Petroleum Engineers.

Jansen J. D., Wagenvoort A. M., et al. (2002). Smart Well Solutions for Thin Oil Rims: Inflow Switching and the Smart Stinger Completion. SPE 77942, SPE Asia Pacific Oil and Gas Conference and Exhibition, Melbourne, Australia, 2002,. Society of Petroleum Engineers Inc.

Khrulenko A. A. and Zolotukhin A. B. (2011). Approach for Full Field Scale Smart Well Modeling and Optimization. SPE 149926, SPE Arctic and Extreme Environments Conference and Exhibition, Moscow, Russia, Society of Petroleum Engineers.

Kolda T., Lewis R., et al. (2003). "Optimization by Direct Search: New Perspectives on Some Classical and Modern Methods." SIAM Review **45**(3): 385-482.

Kolmogorov A. and Fomin S. (1975). Introductory Real Analysis, New York: Dover.

Konopczynski M. and Ajayi A. (2004). Design of Intelligent Well Downhole Valves for Adjustable Flow Control. SPE 90664, SPE Annual Technical Conference and Exhibition, Houston, Texas, Society of Petroleum Engineers.

Konopczynski M. R. and Ajayi A. A. (2008). Reservoir Surveillance, Production Optimisation and Smart Workflows for Smart Fields - a Guide for Developing and Implementing Reservoir Management Philosophies and Operating Guidelines in Next Generation Fields. SPE 112244, Intelligent Energy Conference and Exhibition, Amsterdam, The Netherlands, Society of Petroleum Engineers.

Kuznetsov A. G. (1992). Nonlinear optimization toolbox. Report OUEL 1936. University of Oxford, Oxford, UK. **1936/92:** 82.

Lau H. C., Deutman R., et al. (2001). Intelligent Internal Gas Injection Wells Revitalise Mature S.W. Ampa Field. SPE 72108, SPE Asia Pacific Improved Oil Recovery Conference, Kuala Lumpur, Malaysia, Society of Petroleum Engineers Inc.

Lima G. A., Suslick S. B., et al. (2007). The Real-Options Approach To Analyze Sequential Investments in Oil and Gas Projects: An Application to Heavy-Oil Production Projects. SPE 108105, Latin American & Caribbean Petroleum Engineering Conference, Buenos Aires, Argentina, Society of Petroleum Engineers.

Lorentzen R. J., Shafieirad A., et al. (2009). Closed Loop Reservoir Management Using the Ensemble Kalman Filter and Sequential Quadratic Programming. SPE 119101, SPE Reservoir Simulation Symposium, The Woodlands, Texas, Society of Petroleum Engineers.

Manceau E., Mezghani M., et al. (2001). Combination of Experimental Design and Joint Modeling Methods for Quantifying the Risk Associated With Deterministic and Stochastic Uncertainties - An Integrated Test Study. SPE 71620, SPE Annual Technical Conference and Exhibition, New Orleans, Louisiana, 2001,. Society of Petroleum Engineers Inc.

Mazerov K. (2012). "Industry maps smarter way to build wellbores." from http://www.drillingcontractor.org/industry-maps-smarter-way-to-build-wellbores-16754.

Mubarak S., Dawood N., et al. (2009). Lessons Learned from 100 Intelligent Wells Equipped with Multiple Downhole Valves. SPE 126089, SPE Saudi Arabia Section Technical Symposium, AlKhobar, Saudi Arabia, Society of Petroleum Engineers.

Nagib M., Ezuka I., et al. (2011). "Economic Comparison of Intelligent Wells in Simultaneous Production of Oil and Gas Reserves From Single Wellbore." SPE Production & Operations **26**(2): 203-210.

Naus M., Dolle N., et al. (2006). "Optimization of Commingled Production Using Infinitely Variable Inflow Control Valves." SPE Production & Operations **21**(2): 293-301.

Omolev O. A., Saputelli L. A., et al. (2011). Real-time Production Optimization in the Okume Complex Field, Offshore Equatorial Guinea. SPE 144195, SPE Digital Energy Conference and Exhibition, The Woodlands, Texas, USA.

Peringod C., Al-Ruheili M. S., et al. (2011). Successful Auto Gaslift using Intelligent Completion Boosted Oil Production – A Case History from Petroleum Development Oman. SPE 148474, SPE/IADC Middle East Drilling Technology Conference and Exhibition, Muscat, Oman, SPE/IADC Middle East Drilling Technology Conference and Exhibition.

Peters L., Arts R., et al. (2010). "Results of the Brugge Benchmark Study for Flooding Optimization and History Matching." SPE Reservoir Evaluation & Engineering **13**(3): 391-405.

PETEX (2012). Petroleum Experts IPM 8.0 User Guides.

PETEX (2012). PROSPER Manual.

Pinto M. A. S., Barreto C. E., et al. (2012). Optimization of Proactive Control Valves of Producer and Injector Smart Wells under Economic Uncertainty. SPE 154511, SPE Europec/EAGE Annual Conference, Copenhagen, Denmark, Society of Petroleum Engineers.

Qing Y. and Davies D. (2011). "Generalized Predictive Control Applied to Intelligent Production of an Oil Well." 2011 6th Ieee Conference on Industrial Electronics and Applications (Iciea): 2033-2038.

Robinson M. (2003). "Intelligent Well Completions." SPE Journal of Petroleum Technology **55**(8): 57-59.

Rykov A. S. (1993). Search Optimization. Moscow, Physmatlit.

Sakowski S. A., Anderson A. B., et al. (2005). Impact of Intelligent Well Systems on Total Economics of Field Developments. SPE 94672, SPE Hydrocarbon Economics and Evaluation Symposium, Dallas, Texas, Society of Petroleum Engineers.

Sankaran S., Olise M. O., et al. (2010). Realizing Value From Implementing i-field$^{TM}$ in a Deepwater Greenfield in Offshore Nigeria Development. SPE 127691, SPE

Intelligent Energy Conference and Exhibition, Utrecht, The Netherlands, Society of Petroleum Engineers.

Sarma P., Chen W. H., et al. (2008). "Production Optimization With Adjoint Models Under Nonlinear Control-State Path Inequality Constraints." SPE Reservoir Evaluation & Engineering **11**(2): 326-339.

Schlumberger (2009). "ECLIPSE Reference Manual 2009.1."

Schlumberger (2009). Reference Manual - COUGAR Version 2009.1.

Schulze-Riegert R. W., Krosche M., et al. (2009). Hybrid Optimization Coupling EnKF and Evolutionary Algorithms for History Matching: A Case Example. SPE 121965, EUROPEC/EAGE Conference and Exhibition, Amsterdam, The Netherlands, Society of Petroleum Engineers.

Sharma A. K., Chorn L. G., et al. (2002). Quantifying Value Creation from Intelligent Completion Technology Implementation. SPE 78277, European Petroleum Conference, Aberdeen, United Kingdom, Society of Petroleum Engineers Inc.

Sigurd M. E. (2000). Production Experience From Smart Wells in the Oseberg Field. SPE 62953, SPE Annual Technical Conference and Exhibition, Dallas, Texas, Society of Petroleum Engineers Inc.

Silva M. F. D., Muradov K. M., et al. (2012). Review, Analysis and Comparison of Intelligent Well Monitoring Systems. SPE 150195, SPE Intelligent Energy International, Utrecht, The Netherlands, Society of Petroleum Engineers.

Sinha S., Kumar R., et al. (2001). Flow Equilibration Towards Horizontal Wells Using Downhole Valves. SPE 68635, SPE Asia Pacific Oil and Gas Conference and Exhibition, Jakarta, Indonesia, Society of Petroleum Engineers Inc.

Skarsholt L. T., Mitchell A. F., et al. (2005). Use of Advanced Completion Solutions to Maximise Reservoir Potential - Experiences in The Snorre Field. SPE 92255, SPE/IADC Drilling Conference, Amsterdam, Netherlands, SPE/IADC Drilling Conference.

Skilbrei O., Chia R., et al. (2003). Case History Of A 5 Zone Multi-Drop Hydraulic Control Intelligent Offshore Completion In Brunei. OTC 15191, Offshore Technology Conference, Houston, Texas.

Stephen K. D., Clark J. D., et al. (2002). Modeling and Flow Simulations of a North Sea Turbidite Reservoir: Sensitivities and Upscaling. SPE 78292, European Petroleum Conference, Aberdeen, United Kingdom, Society of Petroleum Engineers Inc.

Su H.-J. and Oliver D. S. (2010). "Smart Well Production Optimization Using An Ensemble-Based Method." SPE Reservoir Evaluation & Engineering **13**(6): 884-892.

Sun K., Constantine J., et al. (2009). Intelligent Well Systems—Providing Value or Just Another Completion? SPE 124916, SPE Annual Technical Conference and Exhibition, New Orleans, Louisiana, Society of Petroleum Engineers.

Talavera A. G., Tupac Y. J., et al. (2010). Controlling Oil Production in Smart Wells by MPC Strategy with Reinforcement Learning. SPE 139299, SPE Latin American and Caribbean Petroleum Engineering Conference, Lima, Peru, Society of Petroleum Engineers.

Tirado R. A. (2009). Hydraulic Intelligent Well Systems in Subsea Applications: Options for Dealing with Limited Control Line Penetrations. SPE 124705, SPE Annual Technical Conference and Exhibition, New Orleans, Louisiana, Society of Petroleum Engineers.

Vilanova J. and Alvarez J. A. (2010). Delivering Value by Continuous and Automated Production Monitoring and Optimization. SPE 127915, SPE Intelligent Energy Conference and Exhibition, Utrecht, The Netherlands, Society of Petroleum Engineers.

Wang C., Li G., et al. (2009). "Production Optimization in Closed-Loop Reservoir Management." SPE Journal **14**(3): 506-523.

Wattenberg F. (1997). "http://www.math.montana.edu/frankw/ccp/modeling/continuous/heatflow2/firstder.htm."

WellDynamics and Halliburton (2009). November 2009 Reliability Assurance Newsletter.

Williamson J. R., Bouldin B., et al. (2000). An Infinitely Variable Choke for Multi-Zone Intelligent Well Completions. SPE 64280, SPE Asia Pacific Oil and Gas Conference and Exhibition, Brisbane, Australia, Society of Petroleum Engineers Inc.

Wright P. J. and Womack W. (2006). Fiber-Optic Downhole Sensing: A Discussion on Applications and Enabling Wellhead Connection Technology. OTC 18121, Offshore Technology Conference, Houston, Texas, USA.

Yadav V. and Surya N. (2012). Evaluating the Performance of Intelligent Completions. SPE 150408, SPE Intelligent Energy International, Utrecht, The Netherlands, Society of Petroleum Engineers.

Yeten B., Castellini A., et al. (2005). A Comparison Study on Experimental Design and Response Surface Methodologies. SPE 93347, SPE Reservoir Simulation Symposium, The Woodlands, Texas, 2005,. Society of Petroleum Engineers Inc.

Yeten B., Durlofsky L. J., et al. (2002). Optimization of Smart Well Control. SPE 79031, SPE International Thermal Operations and Heavy Oil Symposium and International Horizontal Well Technology Conference, Calgary, Alberta, Canada, SPE/PS-CIM/CHOA International Thermal Operations and Heavy Oil Symposium and International Horizontal Well Technology Conference.

Zakirov I. S., Aanonsen S. I., et al. (1996). Optimization of reservoir performance by automatic allocation of well rates. 5th European Conference on the Mathematics of Oil Recovery, Leoben, Austria.

Zandvliet M. J. (2008). Model-based lifecycle optimization of well locations and production settings in petroleum reservoirs, Delft University of Technology.

Zandvliet M. J., Bosgra O. H., et al. (2007). "Bang-bang control and singular arcs in reservoir flooding." Journal of Petroleum Science and Engineering **58**(1-2): 186-200.